

Process Capability Management for Selective Laser Melting



By

Paul O'Regan

A Thesis Submitted for the Degree of

Doctor of Philosophy (Ph.D.)

September 2019

**Supervisors:
Mr Paul Prickett
Professor Rossi Setchi**

Acknowledgements

The author would like to thank a few people for all the encouragement and support provided throughout the length of the research period.

First of all the author would like to thank and acknowledge all the help Mr. Paul Prickett provided throughout these four years. His guidance, helpful comments and suggestions were invaluable. The author would also like to thank Professor Rossi Setchi for also providing support throughout the research period.

Special thanks must go to Renishaw and more precisely Mr. Nick Jones who provided this unique research opportunity and the ability to complete it.

Furthermore, the author would like to thank his parents Thomas and Brigid and his brother Andrew for all the moral support they provided during the last four years.

Lastly, the author would like to express his most genuine thanks to his girlfriend Daniella and to all his friends and extended family for being there when needed.

To all of you my most sincere thanks.

Abstract

This research was undertaken to improve the understanding of the selective laser melting (SLM) manufacturing process. It engineers an approach that can provide quantitative evidence of SLM process integrity. This was needed to underpin the acceptance of SLM components. The research established an assessment technique that can be applied to manage the process capability of SLM machines. This will enable more effective process set-up and control. This in turn will enable improvements in process capability and provides a basis for a more informed product design for manufacture.

This research investigated the application of the established Renishaw productive process pyramid (PPP) to the SLM manufacturing process. The resulting SLM-PPP can be applied to enable a better understanding of the quality control and management of the SLM process. Ishikawa fishbone diagrams have been provided for each of the four layers of the SLM-PPP. These diagrams provide researchers and original equipment manufacturers a foundation that can be used to understand the variables that affect builds. This framework can be further developed in the future.

An arrangement of 12 artefacts on an SLM build plate was specifically engineered for this project to enable direct comparisons and assessments of each build. A co-ordinate measuring machine (CMM) was used to measure the artefacts. The suitability of the CMM was evaluated to ensure it could provide repeatable and reproducible data. The gauge evaluation was investigated and the specified measurement process was validated and assured. The gauge evaluation process was engineered, developed and tested. The CMM was shown to provide the accuracy and precision required in the context of the measurement of the test piece features, this had not been previously proven.

An accumulative quality ranking matrix was developed, providing a novel method for combining the various feature measurements into a visually appealing format, which is easier to understand and evaluate. This method was engineered and tested, and then adopted to inform the remaining research undertaken. The artefacts can be combined with the quality matrix approach to assure process quality. SLM specific parts can be produced in set locations and evaluated after each build. Data from these parts can feed back into the process setting stage to improve precision and/or accuracy. The individual artefact can be used to understand that the process used to make the artefact has been enacted correctly.

List of Abbreviations

AIAG	Automotive Industry Action Group
ALM	Additive layer manufacturing
AM	Additive manufacturing
AMF	Additive Manufacturing File
AV	Appraiser Variation
BJ	Binder Jetting
BS	British Standards Institution
CAD	Computer-aided design
CCD	Charge-coupled device
CMM	Co-ordinate measuring machine
CMOS	Complementary metal oxide semiconductor
CNC	Computer numerical controlled
DMIS	Dimensional measuring interface standard
EBM	Electron beam melting
EDM	Electrical discharge machine
EV	Equipment Variation
FDM	Fused deposition modelling
FMEA	Failure Mode Effect Analysis
GR&R	Gauge Repeatability and Reproducibility
HIP	Hot isotropic pressure
IR	Infrared
ISO	The International Organization for Standardization
LCL	Lower control limit
LOM	Laminated object manufacturing

MCH	Hot cutter machine
MMP	Micro machining process
OEM	Original equipment manufacturers
PBF	Powder bed fusion
PCS	Part Co-ordinate System
PG	Photogrammetry
PLC	Programmable logic control log
PPP	Productive process pyramid
PV	Part variation
RF	Reference figure
RFT	Right first time
R&R	Repeatability and Reproducibility
SAW	Surface acoustic wave
SGC	Solid ground curing
SLM	Selective laser melting
SLS	Selective laser sintering
SRAS	Spatially resolved acoustic spectroscopy
STL	Stereolithography
T	Specified tolerance
TOL	Total representative deviation
TV	Total variation
UCL	Upper control limit
UV	Ultraviolet light
XCT	X-ray computer tomography

Contents

Acknowledgements.....	i
Abstract	ii
List of Abbreviations.....	iii
Contents	v
List of Figures	ix
List of Tables.....	xiv
Chapter 1: Introduction.....	1
1.1 Introduction	1
1.2 Research aim and objectives.....	3
1.3 Structure of thesis.....	4
Chapter 2: SLM Process Control State of the Art.....	5
2.1 Chapter Overview	5
2.2 Brief History.....	5
2.3 Additive layer manufacturing	8
2.4 Current SLM challenges.....	9
2.5 Current SLM Process capability research	12
2.6 Consideration of a Test Artefact.....	13
2.7 The current state of SLM process monitoring and control.....	16
2.8 Quality appraisal (In-process monitoring state-of-the-art)	19
2.9 The use of metrology in SLM.....	20
2.10 Measurement uncertainty	22
2.11 Summary.....	22
Chapter 3: The Productive Process Pyramid Approach for SLM.....	24
3.1 Chapter Overview	24
3.2 The Productive Process Pyramid Approach.....	24
3.3 SLM process overview	26

3.4	Known process problems	27
3.5	SLM Work Flow Analysis	35
3.6	SLM Process Cycle Variables	41
3.7	Process Foundation layer	45
3.7.1	CAD Data.....	47
3.7.2	Material (Feed Stock)	47
3.7.3	SLM machine.....	49
3.7.4	Maintenance	51
3.7.5	Human	51
3.8	Process Setting Layer	52
3.8.1	Material (Feed stock).....	55
3.8.2	Digital information	56
3.8.3	SLM machine.....	57
3.9	In-Process Control	58
3.9.1	Operator.....	58
3.9.2	SLM Machine.....	61
3.9.3	In-process Monitoring: Quality appraisal.	61
3.10	Post-process Monitoring: Informative inspection	63
3.10.1	Quality Appraisal.....	65
3.10.2	Material	65
3.10.3	Post-Processing.....	66
3.11	Summary	67
Chapter 4: <i>Establishing the validity to the approach of measurement</i>		
	68
4.1	Chapter Overview	68
4.2	Feature measurements	68
4.3	Gauge Repeatability and Reproducibility	71
4.3.1	GR&R using the Average and Range method	72
4.3.2	Development and use of a SLM test piece.....	73
4.3.3	SLM top-hat manufacturing settings.....	75
4.4	Measurement process	77
4.4.1	Set up and alignment.....	77
4.4.2	Measurement of features.....	79
4.4.3	Measurement output.....	81

4.5	Conducting the GR&R.....	83
4.5.1	Average and Range method for GR&R	85
4.5.2	GR&R Results and Analysis	88
4.5.3	Measurement analysis X-bar R charts process capability	90
4.6	GR&R discussion	94
4.7	Chapter summary	96
Chapter 5: Artefact appraisal and use in process assessment.....		98
5.1	Chapter Overview	98
5.2	Artefact Condition	98
5.3	Variation in artefact condition	103
5.4	Discussion	118
5.5	Summary	119
Chapter 6: Artefact evaluation and its use in process foundation..		120
6.1	Artefacts and the process foundation fishbone.....	120
6.2	Build plate evaluation and analysis	120
6.3	Comparing build sections across builds	133
6.4	Artefact diameter adjustment	138
6.5	Cylindricity investigation	142
6.6	A quantitative approach.....	144
6.7	Discussion	149
6.8	Summary	152
Chapter 7: Discussion; of the use of the artefact across all four layers of the process pyramid.....		153
7.1	The use of the artefact in process foundation.....	153
7.2	The use of the artefact in process setting	156
7.3	The use of the artefact in-process control.....	163
7.4	The use of the artefact in post-process monitoring.....	169
7.5	Summary	177
Chapter 8: Conclusions, Research Contributions and Future work		179

8.1	Conclusion	179
8.2	Research contributions	181
8.3	Future Work.....	182
	List of Appendices.....	183
	References	184

List of Figures

Figure 2-1 Additive manufacturing categories	7
Figure 2-2 Structure of ALM standards reproduced from (International Organization for Standardization 2016)	11
Figure 2-3 AM Emission Spectrum amended from (Eriksson et al. 2010)	17
Figure 2-4 Build indicating hot-spots in part (A) Renishaw InfiniAM Spectral (B)	19
Figure 3-1 Renishaw “Productive process pyramid” adapted from (Renishaw Plc 2011)	25
Figure 3-2 AM250 build chamber reproduced from (O’Regan et al. 2018)	26
Figure 3-3 Scan hatch types A. Meander, B. Stripe, C. Chessboard, and D. Total fill	28
Figure 3-4 Large surface area created with meander scanning strategy which has caused over-melt and damaged the rubber re-coater	29
Figure 3-5 Reconstruction of part with un-supported overhang facing re-coater spreading direction showing powder packing under lead edge of part	29
Figure 3-6 Overhang downward facing surface created with no supports showing over-melting due to higher heat concentrations	30
Figure 3-7 Inadequate part supports manufactured perpendicular to the re-coater blade movement	31
Figure 3-8 Build chamber out of powder with process continuing to build and over-melting part	32
Figure 3-9 Evidence of short feeding with part evidencing depression	32
Figure 3-10 Part with fracture and peeling away from build plate	33
Figure 3-11 Part designed with radii to decrease stress concentration	34
Figure 3-12 Work flow diagram for SLM. Physical workflow diagram from design (concept) to finished product.	36
Figure 3-13 Representative 3D CAD model (left) and developed .STL file (right)	38
Figure 3-14 High level SLM process variable Ishikawa fishbone diagram	43
Figure 3-15 Ishikawa fishbone diagram of Process Foundation Layer expanded from Figure 3-14	46
Figure 3-16 Process setting Ishikawa fishbone diagram derived from Figure 3-14	54
Figure 3-17 In-process control Ishikawa fishbone diagram	60
Figure 3-18 Post-process monitoring Ishikawa fishbone diagram	64

Figure 4-1 Wrong results because of A. Number of points used and B. Measuring strategy. Reproduced from (Chajda et al. 2008)	69
Figure 4-2 A. Six uniformly spaced points (*) with failure to identify lobbing. B. Seven uniformly spaced points (*) with 79% of the lobbing detected. Reproduced from (Flack 2001)	70
Figure 4-3 Measurement system variability Ishikawa diagram	72
Figure 4-4 (A): A bridge made up of seven top hats (artefact) which has been removed from build plate, (B): CAD drawing of the bridge (artefact/test piece)	74
Figure 4-5 12 stainless steel top-hat assemblies on build plate	75
Figure 4-6 Planes defined with touch points on the top surface and bottom of cylinder	79
Figure 4-7 Cylinder defined with touch points	80
Figure 4-8 Cylinder defined with three circular scans and corresponding DMIS instructions for one of the three heights	80
Figure 4-9 Cylinder defined with helix scan	81
Figure 4-10 X-bar R chart for the top-hat diameters derived from helix scan, circular scans and point measurements. Made up of 60x7 subgroups (produced using Minitab17)	90
Figure 4-11 X-bar R chart for the top-hat cylindricity derived from helix scan, circular scans and point measurements. Made up of 60x7 subgroups (produced using Minitab17)	91
Figure 4-12 I-MR charts showing the top-hat depths across a bridge for: (A.) top-hat one (B.) top-hat two (C.) top-hat three (D.) top-hat four (E.) top-hat five (F.) top-hat six (G.) top-hat seven	93
Figure 5-1 Screen shot of furnace program with tracked temperature read out.	103
Figure 5-2 A. Run chart of all hole diameters from all top hats on plate 8 pre heat treatment (left) Histogram of all hole diameters on plate 8 with a fitted normal distribution curve pre heat treatment (right) B. Run chart of all hole diameters from all top hats on plate 8 post heat treatment (left) Histogram of all hole diameters on plate 8 with a fitted normal distribution curve post heat treatment (right) C. Run chart of all hole diameters from all top hats on plate 8 cut off build plate (left) Histogram of all hole diameters on plate 8 with a fitted normal distribution curve cut off build plate (right)	104

Figure 5-3 Histograms of all hole diameters for pre post and off with normal distribution curve fitted.	105
Figure 5-4 Interval plot of plate 8 mean diameters pre, post, and off.	106
Figure 5-5 Interval plot of all mean diameters for all plates pre, post and off.	107
Figure 5-6 Plate 3 before removal from furnace showing excessive oxidisation	110
Figure 5-7 Interval plot of all mean cylindricity measurements for all plates pre, post and off.	111
Figure 5-8 Interval plot of all mean true positions of cylinders measurements for all plates pre, post and off.	113
Figure 5-9 Interval plot of all mean top plane measurements for all top hats pre, post and off.	115
Figure 5-10 Interval plot of all mean top hat hole depths for pre, post and off.	117
Figure 6-1 I-MR run chart for all top hat diameters on plate 8	121
Figure 6-2 I-MR-R/S (Between/Within) for all bridge diameter measurements on plate 8	122
Figure 6-3 Top hat diameter plot for bridges manufactured on the outside edge of the build plate. (The legend indicates the bridge number where a bridge is made up of seven top hats.)	123
Figure 6-4 Top hat diameter plot for bridges manufactured near to the centre of the build plate. (The legend indicates the bridge number where a bridge is made up of seven top hats.)	124
Figure 6-5 A. Build quality matrix for plate 8 presenting a quality ranking based on average bridge diameter measurements and variance of measurements. B. Bridge location and numbering convention.	Error! Bookmark not defined.
Figure 6-6 Top hat diameter plot for bridges 5 and 9.	127
Figure 6-7 Build quality matrix for plate 8 presenting a quality ranking for; A. Average cylindricity measurements and variance, B. Average true position measurements and variance, C. Average top plane measurements and variance, and D. Average depth measurements and variance across the build plate.	128
Figure 6-8 Line plots showing the best and worst bridges for A. Cylindricity, B. True position, C. Top plane variation, and D. Depth variation.	129
Figure 6-9 Build quality ranking matrix for all attributes on plate 8, indicating best region.	131
Figure 6-10 line graph showing regional comparisons for plates 8-11	134

Figure 6-11 line graph showing regional comparisons for plates 8-11	134
Figure 6-12 Combined attributes ranking for each individual build plate (top), build plate accumulative ranked average (bottom)	135
Figure 6-13 build plates 1-11 combined ranking (shown on top row) and build plate accumulative average ranking (bottom row)	137
Figure 6-14 build plates 1-12 combined ranking (shown on top row) and build plate accumulative average ranking (bottom row)	139
Figure 6-15 Line plot of diameter bias average for plates 1-3 and 8-12	140
Figure 6-16 Top hat diameter plot for all bridges manufactured on build plate 13. (The legend indicates the bridge number where a bridge is made up of seven top hats.)	141
Figure 6-17 Top hat diameter plot for bridges 7 and 10	142
Figure 6-18 Cylindricity measurements for all top hat on plates 12 and 13	143
Figure 6-19 Cylindricity measurements for all top hat on plates 12 – 14	144
Figure 6-20 Normal distributions for the "Best" and "Worst" areas on the build plate	145
Figure 7-1 line graph showing regional comparisons for plates 1-3, 8-11, and 12	154
Figure 7-2 line graph showing regional comparisons for plates 1-3, 8-11, and 12	155
Figure 7-3 Combined attributes ranking for plate 12 (top) and build plate accumulative ranked average (bottom)	156
Figure 7-4 Amended CAD drawing of the bridge with and increased inner diameter	160
Figure 7-5 Amended CAD drawing of the bridge with and increased inner diameter and external cylinder diameter	161
Figure 7-6 line graph showing layer duration (Green) and layer number (Blue) for plate 1	164
Figure 7-7 Line graph showing elevator temperature and Layer number for plate 1	165
Figure 7-8 Line graph showing top and bottom oxygen levels and layer number for plate 1	166
Figure 7-9 Line graph showing oxygen levels and layer number for plate 12	167
Figure 7-10 (A.) Specialist stainless steel vice jaws made using AL250 machine after post processing, (B.) Machine vice with stainless steel vice jaws fitted holding top hat, (C.) Machine vice with stainless steel jaws fitted	169

Figure 7-11 Interval plot for plates 12, 13, and 14 for mean diameters for post and off	171
Figure 7-12 Interval plot for plates 12, 13, and 14 for cylindricity measurements for post and off	171
Figure 7-13 Interval plot for plates 12, 13, and 14 for true position for post and off	172
Figure 7-14 Interval plot for plates 12, 13, and 14 for top plane measurements for post and off	173
Figure 7-15 Interval plot for plates 12, 13, and 14 for mean depths for post and off	174
Figure 7-16 Matrices for post heat treatment on the build plate (top) and top hats cut of off the build plate (bottom) plates 12-13	175

List of Tables

Table 3-1 Part of the AM250 process Log (PLC log) from a build cycle	62
Table 4-1 AM250 fixed manufacturing settings for the production of a top-hat	76
Table 4-2 Prerequisite GR&R data for top-hat helix scan diameters for Appraiser 1 (A1) and A&R values for Appraisers 2 and 3 (A2, A3)	84
Table 4-3 The results of the average and range method for all the scan strategies mentioned in Section 4.3 in relation to the tolerance	89
Table 5-1 Build plate layout and process observations.	100
Table 5-2 Mean and standard deviation results for diameter distributions.	108
Table 5-3 P-values for diameter equal variance test comparison.	109
Table 5-4 Two-sample T-test results for sample means	109
Table 5-5 Mean and standard deviation results for cylindricity distributions.	112
Table 5-6 Two-sample T-test results for cylindricity sample means	112
Table 5-7 Two-sample T-test results for true position mean measurements	114
Table 5-8 Mean and standard deviation results for top plane measurements.	115
Table 5-9 Two-sample T-test results for top plane mean measurements	116
Table 5-10 Mean and standard deviation results for all top hat hole depths for pre, post, and off.	117
Table 6-1 Plate 8 statistical outliers from Figure 6-1 run chart	122
Table 6-2 All attributes and combined attribute ranks for all bridges on plate 8.	130
Table 6-3 Section sum comparisons for Plate 8	131
Table 6-4 Section sum comparisons for plates 8-11	133
Table 6-5 Average standard deviations for all attributes per bridge	146
Table 6-6 Build tolerance analysis	147
Table 6-7 Build tolerance analysis showing new tolerances	148
Table 7-1 Sum comparisons for plates 1-3, 8-11, and 12	153
Table 7-2 Summary of key process parameters in AM250 machine	157
Table 7-3 One-way ANOVA results for plates 12-14 for all attributes measured	174

Chapter 1: Introduction

1.1 Introduction

This PhD has been undertaken in collaboration with Renishaw plc. The motivation was to investigate the role advanced metrology can play in the establishment and enhancement of the process capability of selective laser melting (SLM). The exciting and rapid growth in the adoption of SLM is related to the capability to produce complex geometrical shapes and innovative weight reducing parts. Currently there is a need, however, to confirm that the individual parts being produced are acceptable because the enactment of the SLM process cannot be fully assured. The associated testing and measurement of individual parts is time consuming and difficult.

Renishaw plc introduced the Productive Process Pyramid (PPP) in 2011 to represent, evaluate, adjust and control reductive manufacturing processes. It did so by controlling the variation within the elements that combine to form the process. This research will demonstrate the benefits of adapting the PPP to the SLM process. In doing so it will outline the structure needed to develop the SLM-PPP. To start this work it was necessary to define and represent all of the variables that can contribute towards the reliable and repeatable enactment of the SLM process. A convenient way of presenting this information using Ishikawa diagrams was identified and used in this thesis. These diagrams are informative and can be continuously enhanced as greater understanding of the relationship between variables is acquired. Their use will be the basis for the work going forward in future research.

To try to bring the SLM process under control is a very challenging undertaking. In order to assist this process the variables have been broken down into the levels of the SLM-PPP. It must be noted that variables may affect the process on different levels and that each variable needs to be considered individually as well as in combination. The scope and volume of the work required to complete this task is beyond the scope of this work, but researchers, users and original equipment manufacturers (OEM) will need to be aware and take ownership of these requirements if this manufacturing process is to be fully adopted.

It was sensible to use an existing SLM artefact, supplied by Renishaw plc, to support this research. The artefact was developed by Renishaw in support of its dental SLM applications. There was, therefore, an element of know-how available relating to the manufacture and assessment of the artefact. It must be noted that the use of an

individual artefact was not sufficient to meet the aims of this research, so consideration was needed to decide how to best use it. For this research project it was therefore decided to deploy the artefact within the build chamber across the build plate in order to indicate the nature of the variations arising from the enactment of the process. In this thesis, twelve artefacts were located in different positions and orientations across the build plate to investigate the nature of variations arising within SLM.

There are critical stages in the SLM process which extend beyond the production of the artefact. It has to be recognised that each artefact or part that is manufactured using SLM will need to be post processed in some way. The minimum form of post processing applied will include shot peening and/or heat treatment and the part must obviously be removed from the build plate. Within this thesis the manufactured artefact will be used to assess the effects arising from these post-processes and add these into the SLM-PPP. It will also make the judgement at what stage in the process the most effective measurements may be made.

Based upon the number and range of existing applications it may be anticipated that part measurement using a co-ordinate measuring machine (CMM) can support this investigation into SLM process capability. This research considered why it is important to show that one must validate the use of the CMM and the associated approach used to measure the artefacts. There are standards currently emerging related to all aspects of SLM, including part measurement requirements. In this case, it is important to understand repeatability and reproducibility of the measurement method, which has not previously been reported in detail. Where it has been discussed it has only been in a small study comparing manufacturing processes. This research will therefore consider the use of CMM and the measurements techniques available to enable more effective process set-up and control. This will allow for improved process capability and provide a basis for more informed product design for manufacture.

The current problem with SLM and the continuous growth in process monitoring is the volume of digital data that is generated. Bringing all of this data together and being able to assess it is a huge challenge. This thesis considers the problem of resolving the information generated and presents a relatively straight forward two-dimensional representation of the build performance across the build plate. This can be used to support subsequent improvements in the build process which would be reflected in improved products. Once the SLM machine has been evaluated with the

accumulative sum matrix and a 'finger print' of the SLM machine established, an individual artefact can be utilised. Building a series of artefacts each time is not a sustainable option for manufactures so building an individual artefact has been considered. The individual artefact would need to be built in the same location as previous artefacts so that measurements can be related back to the established 'finger print' of the machine. The use of a test piece in a complex build can also be considered, though it is outside of the scope of this research, but is discussed at the end of this thesis.

1.2 Research aim and objectives

The overall aim of the research is to establish an assessment technique that can be applied to the process capability of an SLM machine to enable more effective process set-up and control. This will allow for improvements in process capability and provide a basis for more informed product design for manufacture.

In planning this research it was established that there was a need for a test piece that could be deployed within an SLM build cycle to assure the quality of all stages of the build process. To fully utilise the planned deployment of this test piece there was an associated requirement to establish and test a measurement methodology that could be repeatedly and reliably applied. The combination of a specially designed test piece and measurement methodology was not currently deployed within the SLM sector.

In order to achieve this aim the following objectives were identified:

- To review the state-of-the-art in SLM process, standards, and technology to identify the current gaps in the management and assessment of the process.
- To produce fishbone diagrams to enable the identification and analysis of process variables that can influence the parts being produced in the SLM process and to provide a way of communicating where and when these variables occur.
- To undertake a sequence of SLM builds based upon the deployment of combinations of a designed test piece. The adoption of the test piece and the associated approach will enable users to better manage the application of the SLM process.
- To develop an assessment tool that can be used to verify the SLM process. This will be used to identify how and when metal SLM parts should be measured and assessed. The research will demonstrate how this

measurement data can be used to assess the effectiveness of the manufacturing process being utilised.

- To engineer a system to represent the outcome of the enacted SLM process that may be applied by users to better manage SLM processes.

1.3 Structure of thesis

The remainder of the thesis is organised as follows:

Chapter 2: SLM Process Control State-of-the-art; is a review of ALM capability and how it is currently established. The research focusses on SLM and in particular the challenges facing SLM OEM as well as the evaluation of parts being produced.

Chapter 3: The productive process pyramid approach for SLM; this chapter will introduce the PPP approach and will acknowledge known SLM related process problems and variations. Ishikawa fishbone diagrams are used to identify the variables that interact to affect product quality at each level of the PPP.

Chapter 4: Establishing the validity to the approach of measurement; a gauge repeatability and reproducibility (GR&R) study is carried out to validate that the specified CMM measurement approaches are suitable to measure the artefacts manufactured using SLM.

Chapter 5: Artefact appraisal and use in process assessment; this chapter evaluates at which stage of production the artefact should be measured.

Chapter 6: Artefact evaluation and its use in process foundation; explores and analyses the artefact with relation to build location, orientation, position, and depth.

Chapter 7: Discussion; of the use of the artefact across all four layers of the process pyramid; discusses the use of the artefact in relation to each level of the PPP and identifies that the artefacts can be used post or off the build plate. It discusses the use of the artefacts for calibration and for process integrity. Consideration is also given to how information can be combined to produce a “fingerprint” for a SLM machine.

Chapter 8: Conclusions, research contributions and future work; this chapter provides the conclusions to the research completed, research contributions and suggestions for further work.

Chapter 2: SLM Process Control State of the Art

2.1 Chapter Overview

This chapter is not intended to be an in-depth review of additive layer manufacturing (ALM) technology, but a review of ALM process capability and how it is currently established. However, before being able to consider fully the capability of the process, it is necessary to understand how the technology originated and to briefly review potential future directions. The first section of this chapter provides a concise history of ALM and presents an overview of the direction society is taking within this area.

The research is then narrowed to focus on selective laser melting (SLM). In particular, the work explores the current challenges facing SLM original equipment manufacturers (OEMs). One of these challenges is the evaluation of parts produced using SLM. Evaluation is currently carried out by destructive and non-destructive testing and after examining the findings reported in current research, the measurement of parts using tactile metrology is identified as the preferred tool for part evaluation and hence adopted in this work.

2.2 Brief History

ALM as we know it today was conceived in the 1960's. It first emerged in a commercial capacity in 1987 with the stereolithography (SL) process from 3D Systems (3D Systems 2019). The process entailed solidifying thin layers of liquid polymer, which is light-sensitive to ultraviolet (UV) light, by using a laser to initiate the reaction so that solid parts could be produced. The SLA-1 machine was the first commercially available ALM system utilising this manufacturing process (Wohlers and Gornet 2014). ALM was only possible after the integrated development of processes based upon advances in computers, lasers, and controllers in the early 1980's (Gibson et al. 2015). These systems were complemented by the development of computer-aided design (CAD) (Gardan 2016). In 1991, three new ALM technologies were commercialised; fused deposition modelling (FDM), solid ground curing (SGC) and laminated object manufacturing (LOM). FDM extrudes a thermoplastic material in rod form to produce parts made layer-by-layer. SGC uses UV-sensitive liquid polymer, solidifying full layers by flooding UV light through masks created using

electrostatic toner on a glass plate. LOM bonds and cuts sheet material using a digitally guided laser to create a 3D shape. In 1992, selective laser sintering (SLS) was commercialised by the DTM Corporation (now 3D Systems). SLS fused powder materials which at that time were mainly plastics. In the late 1990's /early 2000's, some metals were fused with the inclusion of binding agents and metal based ALM was introduced (Tapia and Elwany 2014). In the early 2000's, MTT (now Renishaw) released a commercial selective laser-melting (SLM) machine. The machine utilised a technique designed to use the power of a laser to melt and fuse metallic powders together to form a 3D product. A company, Arcam, at this time produced the first commercial electron beam melting (EBM) machine which melted electrically conductive powder layer-by-layer with an electric beam.

The technologies may be divided into seven standard categories, illustrated in Figure 2-1. This categorisation enables consideration of the technology and the processes to be standardised (ASTM International 2013; British Standards Institution 2015a). Such classification uses the manufacturing process and consideration of how the materials are bonded to distinguish the categories. Presently, a range of materials is used to create 3D parts; polymers, metals, ceramics and composites (Huang et al. 2015). The raw materials utilised will vary depending on the ALM process, for example, the raw material may consist of powder, liquid, wire/rod, or sheet/film as outlined in the previous section. The generic term powder bed fusion (PBF) is used to refer to some of the most common metal ALM process (Tapia and Elwany 2014). The work carried out in this thesis focuses on the PBF technology of SLM.

Additive manufacturing categories

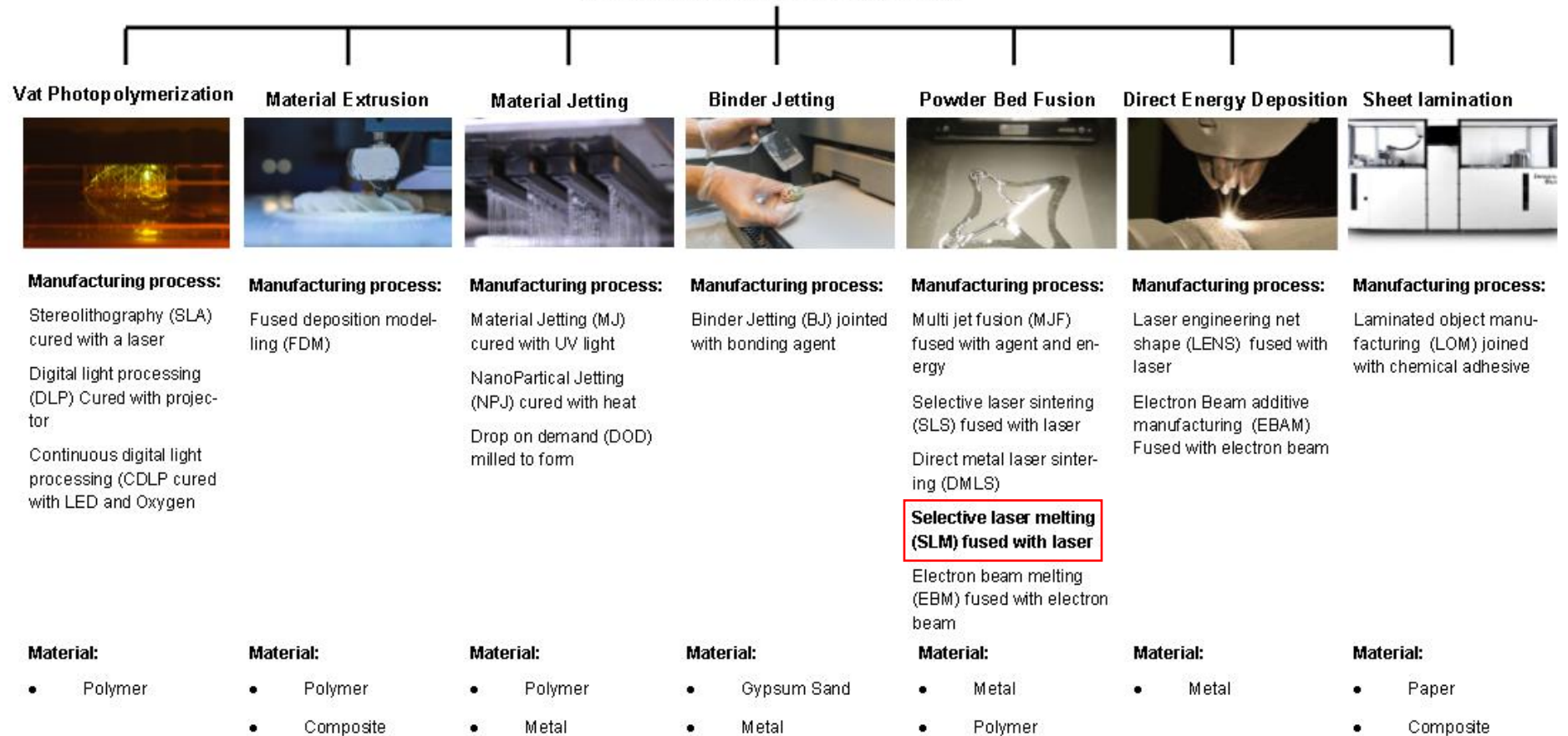


Figure 2-1 Additive manufacturing categories

2.3 Additive layer manufacturing

Traditionally ALM has been applied in industry for prototyping and producing concept visual designs. In the last few years and with some refinements, ALM processes have switched towards end-use parts. A report produced in 2018 revealed that the ALM market for end-use parts grew by 21% in the previous twelve-months and that the ALM market now exceeds \$7.4 billion (Campbell et al. 2018). The same report suggests there was a 79.8% increase of metal ALM machines sold; 983 in 2016 to 1,768 in 2017. This increase was identified as being due mainly to the enhanced capabilities of the processes, which allow improved geometric designs. These improvements include, for example, features allowing the development of internal lattices that reduce component weight and increase strength. It is predicted that, based on historical growth within ALM, by 2025 the UK gross value added will be £3,500 million with the associated requirement for a work force of some 60,000 (Smith and Maier 2017).

Research reflects the market place trend, showing a sharp increase of published papers centred around different facets of ALM (Ryan and Eyers 2016). Much of this research has been supported by the long-term planning of the UK government and other global institutions. It has also been supported by OEMs and other private research and development groups (Hague et al. 2016). In 2016, it was recorded that the UK ALM research fund was approximately £55 million (Jing et al. 2016) and that 41% of the research in the UK focuses on the underpinning science of ALM, such as material characterisation and software tools (Hague et al. 2016). The remaining research covers the development of new ALM technology; process development, validation of the ALM processes and the optimisation of products for manufacture using ALM technology. Due to the high value and large market for metal ALM parts an estimated 66% of this research has been directed towards the metal ALM area, currently worth \$1 billion (Campbell et al. 2018).

The potential application of SLM to manufacture end-use parts in metal materials is providing opportunities for the development of the aerospace, tool making, dental and medical markets. To meet this demand, research is being continuously undertaken to improve the process. It is also evident that, in order to underpin the acceptance of SLM components, manufacturers will need to provide quantitative evidence of SLM process integrity.

Until recently, the market impression of the metal SLM process was one of high variability in the dimensional accuracy of a part (Spears and Gold 2016). The

emerging market has led to consumers making increased demands for improvement to the quality of the parts being produced (Koester et al. 2016), requiring the OEMs of SLM systems to address their concerns. The SLM OEM sector has reacted in a quick and positive manner by engineering a new generation of machines capable of reliable and repeatable production. There can be no doubt that this sector will continue to develop with very important and valuable consequences.

2.4 Current SLM challenges

SLM may be considered to represent the state of the art in ALM, but there are still problems to be solved before it can be deployed as a consistent manufacturing production tool. Reports and research have identified a number of challenges that need to be addressed to make ALM processes more reliable and traceable (UK Additive Manufacturing Steering Group 2016; Barneveld van and Jansson 2017; Smith and Maier 2017). These studies show that work is needed in design, IP security, materials, processes, skills/education, standards, certification, testing and validation.

The International Organization for Standardization (ISO) have started to provide standards and guidelines so that the materials, products and process can be made fit for purpose. There are currently six ALM specific standards in use with ten more under development. Two standards have been withdrawn because they have been superseded. The standards released in the UK by BSI, in close co-operation with the ISO and ASTM, include:

- BS ISO 17296-1, Additive manufacturing. General principles. Part 1: Terminology (To be published)
- BS ISO 17296-2:2015 Additive manufacturing. General principles. Overview of process categories and feedstock (British Standards Institution 2015b)
- BS ISO 17296-3:2014 Additive manufacturing. General principles. Main characteristics and corresponding test methods (British Standards Institution 2014b)
- BS ISO 17296-4:2014 Additive manufacturing. General principles. Overview of data processing (British Standards Institution 2014c)
- BS ISO/ASTM 52910:2018 Additive manufacturing Design Requirements, guidelines and recommendations (British Standards Institution 2018).
- BS ISO/ASTM 52915:2017 Standard specification for additive manufacturing file format (AMF) version 1.2 (British Standards Institution 2017)

- BS ISO/ASTM 52921:2013 Standard terminology for additive manufacturing, Coordinate systems and test methodologies (British Standards Institution 2013)

Current ISO 17296-3 (British Standards Institution 2014b) specifies the main quality characteristics of parts fabricated using AM and specifies appropriate test procedures for these characteristics. Surface texture, size, dimensional and geometric tolerances are among the part characteristics specified. However, ISO 17296-3 does not provide any AM-specific test procedures; it provides relevant generic standards used for all manufacturing applications. ISO and ASTM have issued a draft standard providing general descriptions of benchmarking test piece geometries along with quantitative and qualitative measurements to be taken to assess the performance of AM systems ISO/ASTM 52902 (2018) (International Organization for Standardization 2018). This thesis can be used to inform these standards as it provides a novel way of assessing an artefact in a qualitative and quantitative which can be used to inform the manufacturing process.

The ISO/TC 261 committee are currently creating 25 more standards (International Organization for Standardization 2011b). The work in this thesis could help inform:

- ISO/ASTM 52900:2015 Additive manufacturing, General principles. Terminology (British Standards Institution 2015a)
- ISO/ASTM FDIS 52902 Additive manufacturing -- Test artefacts -- Geometric capability assessment of additive manufacturing systems (Approval stage)
- ISO/ASTM FDIS 52904 Additive manufacturing -- Process characteristics and performance -- Practice for metal powder bed fusion process to meet critical applications (Approval stage)
- ISO/ASTM DTR 52905 Additive manufacturing -- General principles -- Non-destructive testing of additive manufactured products (Committee stage)
- ISO/ASTM AWI 52909 Additive manufacturing -- Finished part properties -- Orientation and location dependence of mechanical properties for metal powder bed fusion (Preparatory stage)
- ISO/ASTM CD 52921 Standard terminology for additive manufacturing -- Coordinate systems and test methodologies (Committee stage)

ISO have created a road map for the development of these standards. It categorises standards into three groups:

General Standards: standards that specify general concepts, common requirements or are applicable to most types of ALM materials, processes and applications.

Category Standards: standards that specify requirements specific to a material category or process category.

Specialised Standards: standards that specify requirements that are specific to a material, process or application. This structure, thus formed, is shown in Figure 2-2.

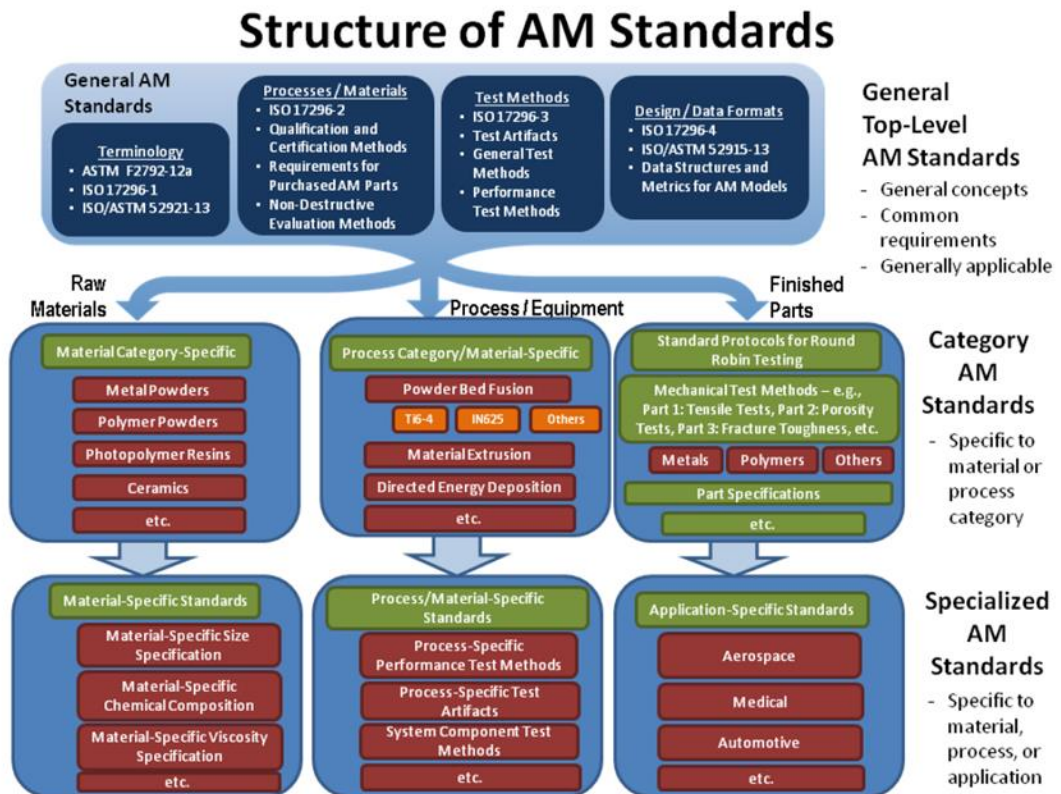


Figure 2-2 Structure of ALM standards reproduced from (International Organization for Standardization 2016)

The BS ISO/ASTM 52910:2018 Additive Manufacturing Design Requirements, Guidelines and Recommendations (British Standards Institution 2018) provides guidance for ALM users, however, in reality it provides only a very high level overview of design elements. It does cover all ALM technologies providing an overview of when to use ALM and how the design should be considered. More detailed and specific design suggestions have been produced (Thomas 2009; Kranz et al. 2015; Renishaw Plc 2018; Peels 2019). Although some effort has been made in the amalgamation of design information, there is still no definitive guide.

Some design packages have utilised the available information to be at the forefront of the market and form the 'go-to' choice for manufacturing companies. There are a number of ALM predictive software programs, both being developed and available on the market, produced by companies including; Netfabb (Autodesk 2016), Virfac (Geonx and LPT 2016), Amphon (Additiveworks 2016), exaSIM (3DSIM 2016), Simufact Additive (Simufact 2016) and QuantAM (Renishaw Plc 2015). These programs can help operators and designers design for manufacture and maximise the advantages of using ALM to produce parts or prototypes. Using these programs, users can calculate the deformation of the final part and reduce and/or avoid distortion and minimise residual stress. The programs can optimise the build-up orientation and the support structure and can also be used to predict the micro-structure as well as indicate criteria-based part failure. They enable the conditioning of the part after heat treatment, base plate and support structure removal. Overall, the programs can be shown to reduce material and energy consumption cost and increase machine and manpower productivity whilst reducing unnecessary costs by replacing tests with simulations.

2.5 Current SLM Process capability research

The exciting and rapid growth in the adoption of SLM is related to the capability to produce complex geometrical shapes and innovative weight reducing parts. Currently, however, there is a need to confirm that the individual parts being produced are acceptable because the process cannot be fully assured. This represents a potential barrier to the wider exploitation of SLM as a production process, particularly in the context of many applications where product dimension and integrity may challenge current process capabilities. SLM OEMs are leading research into process control, monitoring and management procedures that can be used to provide process-based quality assurance in order to reduce this barrier (Renishaw PLC 2018).

The generic capabilities of the SLM process are becoming more understood and defined, as in BS ISO/ASTM 52910:2018 (British Standards Institution 2018). OEMs are very supportive of the needs of their customers and user networks are growing to allow shared experiences. It will, however, remain the case that the specific capabilities of a particular SLM machine need to be established so that the machine set-up can be optimised to produce accurate parts. In the context of the building of production parts, the use of a test piece to provide an ongoing supportive function each time a build is completed is important, particularly so on SLM machines that do not contain in-process monitoring equipment. It will continue to be the case even on

those that do, because the development of SLM process monitoring technology is still at an early stage. Indeed, its further development can be complemented by the manufacture of known artefacts. Until precise and repeatable in-process confirmation can be obtained and accepted as showing the actual part being constructed as correct, it will be necessary to rely on the manufactured test piece. Thus the ongoing use of such a test piece is not only to explore its capabilities of creating different shapes, but also to confirm how repeatable and reproducible the enactment of the individual manufacturing process is.

2.6 Consideration of a Test Artefact

An interim stage in this procedure is to consider the design and application of a representative test piece that can be used to assure the enactment of the required process. If correctly applied this could, in effect, be deployed to replace the part by part measurement of often complicated individual components on an SLM build plate. The advantages of such an approach can be directly aligned with those cited to support conventional reductive manufacturing (Renishaw Plc 2016). An important part of this procedure is to identify how metal SLM parts are going to be measured and assessed. Once this question is answered the measurement data can be used to assess the process capability of the manufacturing process being utilised.

There has been a body of research looking at the geometric capability of SLM processes and two in-depth benchmarking reviews were carried out recently (Rebaioli and Fassi 2017; Toguem et al. 2018). Initial research within this area has been focused on either the capability of a single metal ALM process or comparing the capability of different metal ALM manufacturing processes. In this context, Kruth et.al. created an artefact to benchmark five commercial systems which included SLS and SLM processes (Kruth et al. 2005). The machines were benchmarked in respect of the dimensional accuracy, surface roughness, mechanical properties, speed and repeatability on subsequent parts. The artefact allowed SLS and SLM process resolutions to be tested by means of creating cylinders of reduced diameter as both extrusions and inclusions (0.5mm-5mm diameter). Wall thicknesses were also evaluated (0.25mm -1mm thickness).

Castillo designed an artefact to investigate the geometric and dimensional performance for BJ and SLM systems (Castillo 2005). As well as looking at cylinders and thickness of material, the author investigated the capability of such systems to create unsupported overhangs, inclines and curved surfaces. The SLM process has been considered in detail for dental implants (Kruth et al. 2007; Vandenbroucke and

Kruth 2007), using two differently designed artefacts. The artefacts were designed to evaluate the accuracy and the process capability of fine details. The first SLM part was employed to evaluate the process accuracy along X, Y and Z axes, as well as the accuracy of cylinders and angled features (Kruth et al. 2007). The second part was used to evaluate the process resolution with regards to cylinder diameters (0.5-3mm), slots (0.5-3mm thickness), cylinders (1-5mm) and thin walls (0.5-3mm) (Vandenbroucke and Kruth 2007).

Instead of producing a new test artefact for SLM or EBM, researchers have investigated process accuracy using NAS 979 circle-diamond-square with an inverted cone (Cooke and Soons 2010). This was adapted from the Aerospace Industries Association (AIA) BS ISO 10791-7:2014 (British Standards Institution 2014a). A number of artefacts were produced on different ALM machines and the process capability of each manufacturing process was compared. The circle-diamond-square with inverted cone is a well-known and established test artefact for reductive manufacturing processes such as CNC milling machines. It was developed to evaluate size, flatness, squareness, parallelism, surface finish and angular deviation. The cylinder is measured for diameter, circularity and surface finish. Although the circle-diamond-square with inverted cone was not designed for ALM system evaluation it was used in this study as an experimental and exploratory sample to obtain information on geometric errors. In this research the circle-diamond-square with inverted cone was evaluated using a CMM and recorded an uncertainty of $\pm 5\mu\text{m}$. It was found that the circle-diamond-square with inverted cone produced using different AM processes could not be directly compared because they were produced from different materials. The circle-diamond-square with inverted cone was also manufactured hollow so that a seventh measurement could be assessed. The hollow artefact allowed for the assessment of thin walls without the need for creating a new feature. The circle-diamond-square with inverted cone was removed from the build plate without post-processing (Cooke and Soons 2010). It was noted that the artefact walls showed evidence of buckling when the form was evaluated. It was concluded that this was caused by residual stresses in the artefact due to a lack of post-processing.

Subsequent studies all introduce different and more intricate ALM designed artefacts to assess dimensional accuracy and surface finish (Moylan et al. 2014; Yasa et al. 2014; Teeter et al. 2015; Kniepkamp et al. 2016). However, they still evaluate the same geometrical forms as their predecessors; size, flatness, squareness, parallelism, surface finish, angular deviation, diameter, cylindricity, and circularity or

combinations of these. The use of the artefacts tends towards benchmarking the machine's build capability rather than the capability of the ALM machine. More recent work has been carried out considering how ALM artefacts are measured and what these measurements are revealing about the manufacturing process (Calignano et al. 2017; O'Regan et al. 2018; Rivas Santos et al. 2018; Schoeters et al. 2018). These artefacts are designed for metrology and are linked to objects that may be produced on the ALM machine in a manufacturing environment. Though it is important to evaluate the manufacturing capability of each ALM machine, knowing whether a part is fit-for-purpose is critical when producing parts that have to function outside of the laboratory. While earlier work (Cooke and Soons 2010) reported an uncertainty of $\pm 5\mu\text{m}$, recent studies indicate that $\pm 50\text{-}70\mu\text{m}$ is more typical. The cause of the discrepancy between the studies could not be determined. The most recent research shows that measurement understanding has improved and the uncertainty increase over time is due to the surface roughness of the ALM parts being produced. Such uncertainty has been shown to occur whether it be through tactile measurements, non-contact photogrammetry systems (PG), X-ray computed tomography systems (XCT), or electron beam microscopes (Leach et al. 2019a).

It is not always evident from studies whether the measurement systems used have undergone a gauge repeatability and reproducibility study carried out in accordance with ISO-TR12888:2011 (International Organization for Standardization 2011a) or developed guidelines (Flack 2001). This may be taken as indicating that the variation in the measurements of the test piece used could include variation associated with the gauge measurement process. If that is the case, then the measurements may not provide a complete assessment of the process related information.

Measurement can lead to improvement and post-process monitoring can provide valuable information to the research regarding aspects of the capability of the SLM process. There are numerous factors to be considered in this context, the effect of some are, at present, largely unknown. Dimensional accuracy in metal SLM manufacturing can be taken to relate to the geometrical differences between the three-dimensional CAD model and the physical part after the build process and after post-processing. Due to the enactment of the SLM production technique, there are a number of effects that can influence dimensional accuracy; some, but not all, have been previously considered (Mani et al. 2015; O'Regan et al. 2016; Spears and Gold 2016).

It is useful to bring together important elements for consideration, particularly in the context of the test artefact design. For example, current research has shown that orientation, build direction and support structures are important elements that need to be considered when trying to manufacture dimensionally accurate parts (Strano et al. 2013; Renishaw Plc 2018). On upward facing surfaces, the finish is highly influenced by the stability of the melt pool and the distance of each hatching vector (Han 2017; Hitzler et al. 2017). Vertical facing surfaces and downward facing surfaces are regularly rough due to particles being drawn into the melt pool but not fully melting because of the insufficient energy at the melt pool boundary. In these locations, particles can be found partially melted. The main causes of this are the process parameters laser energy and scan speed (Mumtaz and Hopkinson 2010). Another effect on dimensional accuracy is the distortion of parts caused by residual stress and the production of an anisotropic grain structure due to the production method (Spears and Gold 2016; Hitzler et al. 2017). This occurs due to the large change in temperature gradient. Though the material is pre-heated, the temperature change can be as much as 900°C (depending on the make of production machine and material being processed) taking the material from a solid to a liquid then back to a solid, creating large residual stresses within the component which need to be relieved (Carter et al. 2014).

With all these potential variations arising within the process, it is important that the test piece is measured accurately using a specific gauge before the performance of the production technique can be assessed. In the majority of benchmarking research, CMMs have been used to assess the artefacts being produced because they are traceable.

2.7 The current state of SLM process monitoring and control

The objective of monitoring any process is to improve its reproducibility and to assure reliability and quality. In this context, reliability relates to a single manufacturing cycle and reproducibility to several cycles. One of the main areas hindering the full adoption of ALM and in particular SLM is the limited control and monitoring processes currently in place. This was mentioned in Section 2.5, but not reviewed in detail. The aim of introducing in-process monitoring equipment is to produce a manufacturing process which is completely closed-loop. This is the next step of evolution for SLM machines. Different OEM's have approached this challenge in different ways, but they are still

not at a place where the SLM machines being produced are completely closed-loop. Many manufactures are generating in-process data, but are unable to analyse it in real-time due to the volume and therefore have not been able to extrapolate it so that closed-loop feedback can occur.

The development of in-process monitoring has been targeted since the first metal SLM, EBM and SLS machines were produced. In 1994, researchers developed an infrared light thermal sensor control laser to improve the power distribution for the sintering process (Benda 1994). Later, others divided the thermal detectors into three groups; diode, camera and light stripe systems (Bollig et al. 2005) The optical systems are either active (using external illumination) or passive (no external illumination) (Boillot et al. 1985). The passive optical systems can be further divided into reflective or emissive. Many authors classify these again into spatially resolved, which are vision systems like charge-coupled device (CCD) and complementary metal oxide semiconductor (CMOS) cameras; spatially integrated, which include photodiodes, and; spectrally resolved, which refer to spectrometers (Vallejo 2014). It is important to note that the emissions within the build chamber have different wave lengths and different information can be inferred or recorded from each of the windows; plasma emissions (300–1000nm), melt-pool thermal emissions (1100-3000nm) and laser emission (1070nm) in the case of Renishaw AM250 machine, Figure 2-3. Looking at all three wavelengths identifies process defects such as laser energy fluctuations and part defects such as over-melting and porosity.

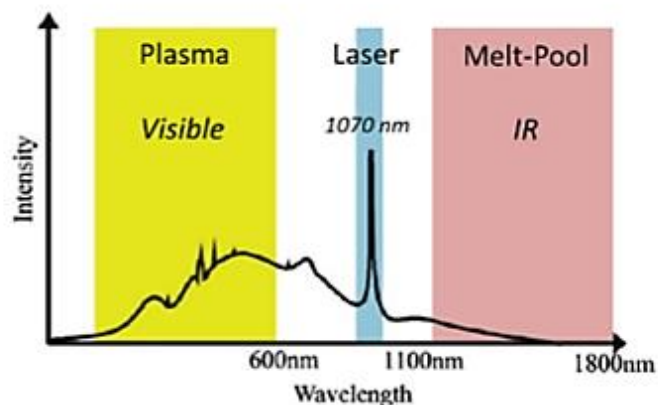


Figure 2-3 AM Emission Spectrum amended from (Eriksson et al. 2010)

An in-depth review on thermal modelling methods was completed for SLS and SLM production techniques (Zeng et al. 2012). Emphasis was given to uniform temperature distribution when processing the powder as this led to better part and/or track quality. To implement thermal models, a temperature monitoring system using

pyrometers and thermocouples was suggested and used to monitor the melt pool temperature. Thermocouples require contact with the surface or fluid to provide accurate readings, therefore pyrometers have been the dominant choice for monitoring the melt pool. The use of thermocouples to monitor six different builds which utilised different metallic powders has been considered (Shishkovsky et al. 2008). The thermocouples were set up to provide a temperature reading of the powder bed. Most modern SLM machines have thermocouples linked to the heater plate which sits under the build plate to monitor the build plate temperature. These sensors have been used in conjunction with strain gauges to record residual stress which builds up during production of the part (Van Belle et al. 2013). Thermocouples in this position have also been utilised to monitor energy absorption and thermal conductivity so that researchers can better understand the transfer of heat in the powder and the consolidated material (Taylor and Childs 2001).

To improve the information being collected, a control system using thermocouples and an infrared (IR) sensor was designed and patented (Low and Ake 2004). IR sensors or cameras can be used to measure the temperature when completing the hatch, contour, or when pre-heating the material or part. Researchers used a coaxial optical monitoring system consisting of a CCD camera to measure the brightness in the laser irradiation zone (Yadroitsev et al. 2014). The resulting monitoring system was deployed to identify that laser power affected the melt pool size greater than exposure time when using Ti_6Al_4V alloy.

Continuous data capture methods have been developed using IR to demonstrate that it is feasible to detect porosities inside materials and evaluate thermal phenomenon, such as those that happen between beam and powder (Dinwiddie et al. 2013). However, it has been suggested that a number of non-contact temperature monitoring methods lack accuracy due to the build chamber environment (Köhler et al. 2013). It was thought that the inert gas that is used to prevent oxidation and the dust/soot that is produced when the laser melted the powder attenuated the temperature signals in the optical path. Despite the promise that such solutions can offer, they are currently far from being deployed. It is also likely that such systems will require careful development which will inevitably be linked to the use of a test artefact.

2.8 Quality appraisal (In-process monitoring state-of-the-art)

There is an ongoing drive to integrate in-situ defect monitoring methods into new SLM machines. Doing so provides many challenges due to the large amount of data which will be required to be processed in real-time. The digital information that needs to be processed to complete this task will be at the terabyte level. Processing this in real-time is therefore a huge challenge. InfiniAM Spectral (Renishaw PLC 2018) is an example of integrated thermal hardware and software. Developed by Renishaw Plc, InfiniAM Spectral detects the interaction of the ytterbium fibre laser interacting with the metal powder. The reaction results in a melt pool, plasma, sparks and small droplets of molten metal. Plasma predominately emits in the visible spectrum whilst the melt pool emits in the near-infrared spectrum (Figure 2-4). Radiation is emitted in all directions with a proportion propagating back up the laser beam path into an optical module. Plasma and melt pool emissions pass into the module and are filtered. This data is then displayed in a 2D or 3D real-time stream on a PC with InfiniAM Spectral software. Current implementations can provide the operator with the capability to review the process as it is proceeding but more work is needed if this system is to operate as a truly in-process monitoring function. This needs to be assessed by an operator in real-time or after the build is completed. Figure 2-4 shows a visual example of the information an operator would be able to access. The image on the left shows an area on a part that has been overheated. This could be due to a problem with the laser, short feeding or power. The image on the right shows the hot-spot in a 2D image which can then be evaluated with other information to identify the cause of this phenomenon (Renishaw PLC 2018).

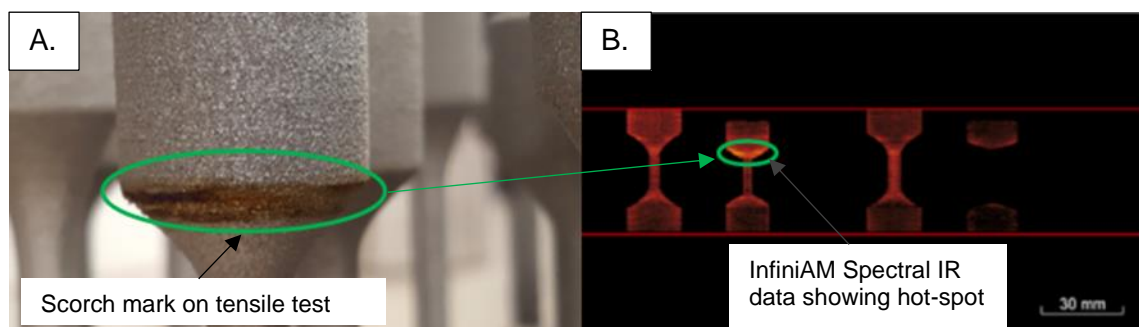


Figure 2-4 Build indicating hot-spots in part (A) Renishaw InfiniAM Spectral (B)

Running concurrently with thermal emission monitoring are visual digital cameras. Researchers and OEMs have added digital cameras to complete a slightly more basic, but important, evaluation of the build area (Craeghs et al. 2011). Standard

digital cameras are used to take pictures after each laser exposure and after the wiper blade spreads a new powder layer over the build plate. An automated picture recognition process would then evaluate each image taken to identify errors in the process (Krauss et al. 2014). The picture recognition software would identify short feeding, wiper blade damage, part curling, over melting and part movement including separation from the build plate. Developments in this software use the CAD model to identify regions of interest to reduce the computational load, improving the speed of analysis (Tobergte and Curtis 2015).

The use of acoustic emission evaluation for SLM has not been as well researched as that of thermal emissions, but some research has been focused in this area. OEMs have also invested time and money to determine if the data generated from acoustic emissions can be used in conjunction with thermal monitoring processes to improve part quality and defect detection. Spatially resolved acoustic spectroscopy (SRAS) has been applied to determine the surface and sub-surface features, further research is ongoing (Hirsch et al. 2017). Research using SRAS has indicated that the operator can obtain surface defect information and grain information on rough surfaces (Achamfuo-Yeboah et al. 2015). This technology has been used in the past to scan over optically smooth surfaces to identify microstructure and grain orientation for metals for high value applications. This is accomplished by identifying changes in the surface acoustic wave (SAW) velocity or signal dropout. SRAS has been utilised on SLM parts with the intention of developing the technology into an in-situ investigation tool (Smith et al. 2016). Another approach introduced a microphone into the build chamber of an SLM machine and identified three uniquely different acoustic emissions that can link with three manufacturing processes; balling, normal process and overheating (Ye et al. 2018). This study is limited to single track scans, but provides enough evidence that acoustic emissions could be used in conjunction with other monitoring techniques to identify and cross reference defects.

2.9 The use of metrology in SLM

Form metrology is critical for quality control of SLM products. SLM machine manufacturers require form metrology to successfully characterise and optimise their SLM processes when new materials and part geometries are developed. Deformation of form is one of the most noticeable effects following most metal SLM processes due to the relaxation of thermal stresses (Roberts 2012; Moylan et al. 2013). It is therefore important that detailed in-situ monitoring using metrology and post-process characterisation methods are used to understand these effects and analysis can then

provide possible techniques to avoid the effects. There are other considerations that need to be assessed before an SLM product can be classed as being suitable to consistently produce a functional component. These other considerations vary depending on the application. The part will need to conform to a set of tolerances that refer to internal part defects and surface texture, both of which are all critical to its long term functionality (Todorov et al. 2014; Triantaphyllou et al. 2015).

Dimensional tolerances vary from industry to industry, as does the part's mechanical properties (Savio et al. 2007). Most examples use tactile systems to evaluate this form such as mechanical probe-based CMM's. These machines have been widely and successfully used in the aerospace and automotive industries for many years (Hocken and Pereira 2011) and can measure to a high accuracy. They may be classed, however, as being relatively slow and may not be ideal for in-line inspection applications (Hammett et al. 2005). They will continue to be very effective and important tools in their intended domain as they are more accurate than current non-contact systems (Leach et al. 2019a). The non-contact systems that have been identified as having potential include photogrammetry (PG), x-ray computer tomography (XCT) or electron beam microscope. Currently, the use of these methods raises the question of resolution, traceability and accuracy, meaning few in-depth analyses have been carried out.

Non-contact metrology has improved and is still being actively developed. With the improvements in computing power, algorithms and hardware, measurements using this technology can be carried out in real-time which can provide many advantages when improving in-process monitoring systems. Though these measurement techniques could be used to assess the SLM process, in this work it was decided that as tactile CMM measurements are still preferred by industry and researchers as the golden standard for taking measurements and assessing form, the focus will be on the use of tactile probing.

A CMM is an extremely powerful metrological instrument. It measures the geometry of physical objects by sensing discrete points on the surface of the object using a tactile probe, though there are non-contact options available for modern CMM's. A CMM uses a co-ordinate system, invented by Rene Descartes in the 1600's which allows location of features relative to other features on a work piece. The CMM typically specifies a probe's position in terms of displacement from a reference point in a three dimensional Cartesian co-ordinate system (using X,Y and Z axis). The two types of coordinate systems are machine co-ordinate systems and part co-ordinate

systems. Machines co-ordinate systems are all relative to the machine's measurement bed, so the X direction would be defined across the bed of the machine left to right from a point the machine manufacturer would have coded into the software. The Y direction would be from the front to the back of the machine and Z would run perpendicular to those two vertically up from the machine's measurement bed. The part co-ordinate system relates to the machine's coordinates (X, Y, and Z) being the three axes to the datum or features of the work piece.

2.10 Measurement uncertainty

There is also an identified need to address the potential level of uncertainty that is associated with the measurement process. In particular, the assessment of the effects of the relatively poor surface finishes currently associated with SLM parts. The topic is subject to ongoing research which suggests that the typical surface finish achieved using SLM can vary between 20 and 70 μm affecting the component measurements acquired using CMM (Schild et al. 2018). The nature of the uncertainty arising due to surface roughness, therefore, needs to be further considered (Rivas Santos et al. 2018; Leach et al. 2019b). Uncertainty may also be associated with the enactment of the measurement process. It is possible that the "same" measurement cycle may actually be subject to minor changes as the algorithm applied by the CMM controller calculates the measurement procedure each time. Thus a scan based sequence can vary each time it is undertaken, depending upon the acquisition of an initial touch point, which may vary. The nature of such variations will depend upon how the parameters are set within the software. Some of the measurement functions applicable to the CMM allow the operator to explicitly define via the program where points are to be taken on a part. The application of restrictions may be considered as a means to ensure that the data is collected in the same position each time. It should be the case that, by explicitly defining where points are taken, the repeatability will improve. The scan function can also be set up with minimal restrictions thus allowing the machine to commence with the same reference point before completing the scanning data acquisition process independently.

2.11 Summary

This chapter has reviewed the current state-of-the-art for the SLM manufacturing process. It has identified the need to show how process variables influence the parts being manufactured. It is clear from the number of benchmarking exercises that have been undertaken, that researchers have identified a need to assess the capabilities

and the process management of SLM machines to assure and support the ongoing viability of SLM as a production process. It is also clear that an awareness of the manufacturing process is required, as well as an understanding of fundamental metrology techniques, before the capability of an SLM process can be assessed. The tools used to measure the test piece must be evaluated so that the measurement process is valid and assured. In this context, it is important that the test piece reflects the process and is designed for measurement traceability.

Chapter 3: The Productive Process Pyramid Approach for SLM

3.1 Chapter Overview

This chapter presents an overview of the challenges associated with the effective deployment and management of SLM. The work considers how it is possible to modify, extend and apply the Productive Process Pyramid (PPP) approach to support process management functions in the context of SLM based manufacturing. The PPP was originally developed by Renishaw for application to reductive manufacturing processes, it is a well-established tool that has been adopted by numerous people and organisations. The use of Ishikawa fishbone diagrams was developed through the course of this chapter and are the most suitable mechanism for presenting SLM process information.

3.2 The Productive Process Pyramid Approach

The representation used to define the PPP comprises of four layers, shown in Figure 3-1. The layers build upon each other to deliver consistently conforming parts within a manufacturing process. The pyramid has been used to represent, evaluate, adjust and bring reductive manufacturing processes under control by controlling the variation within the elements that combine to form the process. The four layers of the PPP are;

- Process Foundation, which relates to assessing the condition of the machining environment and adjusting it so that a stable manufacturing environment is provided. These adjustments can be viewed as being preventative controls introduced to reduce the sources of variation prior to the start of manufacturing.
- Process Setting, which addresses the control of the predictable sources of variation.
- In-process Control, which focusses on the identification and eventual elimination of the sources of variation that are inherent to the manufacturing process. These in-process controls are also known as active controls because they can be changed during the process.
- Post-process Monitoring which assesses the qualities of the final produced part to advise the enactment of subsequent processes. The post-process approach is currently used by many manufacturing companies to confirm the

integrity of the process based upon the quality of the product. In general, it assesses the process by comparing the parts against their respective specifications. Post process monitoring can also be used to inform other layers of the PPP, also known as informative controls.

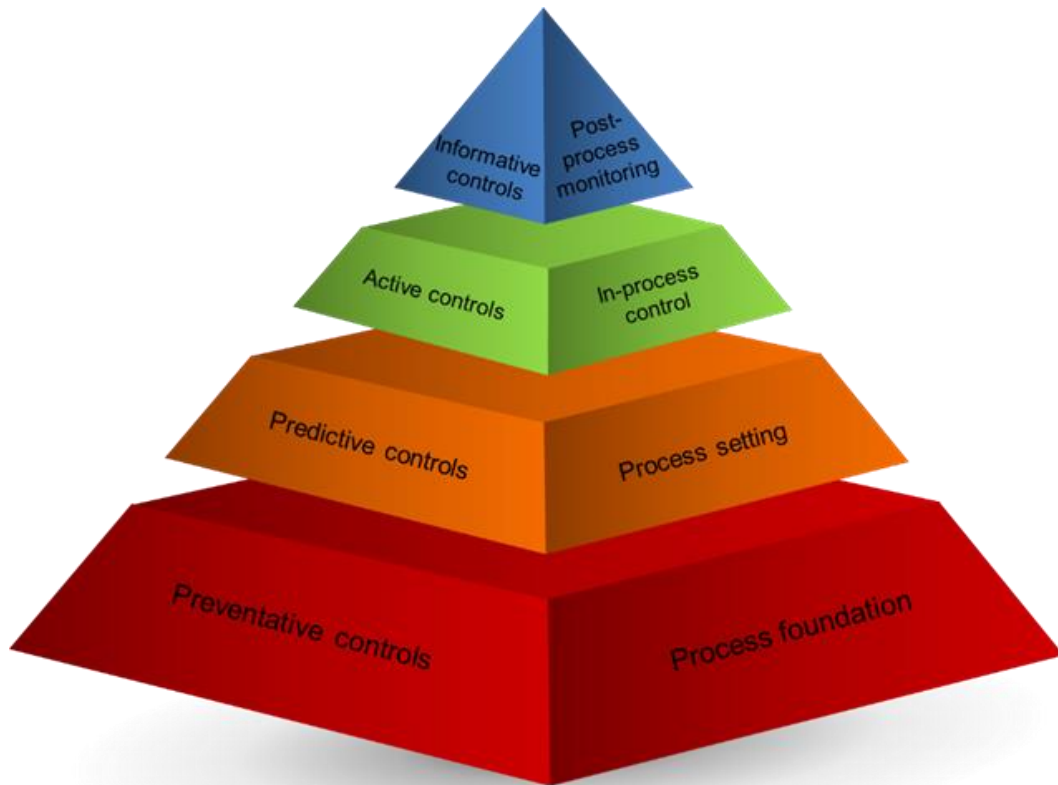


Figure 3-1 Renishaw “Productive process pyramid” adapted from (Renishaw Plc 2011)

The four layers are to be populated and used in this chapter in order to create an SLM-PPP. To enhance the information presented in each layer it is necessary to bring together current research and practice to formulate a representation of the factors that need to be managed within the enactment and control of the SLM process. To aid understanding these are associated with each layer of the PPP. The basis of this approach is to identify the important decisions that need to be made regarding each input into the SLM part processing cycle, at each layer in the SLM-PPP. For example, in this way the true importance of decisions made at the data preparation stage can be traced through each of the four layers of the SLM-PPP. It is also possible to consider inputs into the layers of the SLM-PPP that relate to external considerations which lie outside of the SLM manufacturing cycle, these could include economic and environmental considerations.

3.3 SLM process overview

The Renishaw ALM250 machine used in this work is shown in Figure 3-2. This is a third generation SLM machine which is capable of processing parts using a range of materials. This is made possible by the inclusion of a safe-change filter and removable powder hopper system that enables users to switch between materials. The ALM250 can produce fully dense metal parts directly from 3D CAD data.

The SLM part processing cycle is conducted within the build chamber, within which there is a 250 mm (X-axis) x 250 mm (Y-axis) x 300-360 mm (Z-axis) build envelope. To commence a build, the build chamber atmosphere is made inert with a gas (in this case Argon). The level of oxygen in the chamber is thus maintained at less than 50 parts per million, which allows the safe processing of reactive powders. The heated build plate is utilised to initiate a heat soak cycle before the raw material being used for the build is deposited on the build plate. The inert atmosphere is recirculated through a filter during the build to remove any impurities that are produced when melting the metal powder material. The metal powder being used in the build chamber is stored in a hopper which is typically situated above the build plate within the machine. The powder is fed into the chamber in such a way that it is deposited in front of the re-coater blade (via the powder dose). The re-coater blade then spreads the metal powder over the build plate, typically moving from the back of the chamber to the front. The powder is layered onto the build with thicknesses varying from 20-100µm. Any excess powder from the recoating procedure is deposited in two overflow hoppers for re-use in subsequent builds.



Figure 3-2 AM250 build chamber reproduced from (O'Regan et al. 2018)

The X-Y galvanometer mirrors above the build chamber are controlled to guide the laser beam around the build plate to create geometry onto each powder layer. This laser beam passes through the f- θ lens which reduced the spot variation. Required parts within each layer can be melted by continuous exposure or by discrete point exposures. The energy from the laser is absorbed through radiation by the powder and the heat transfer produces a phase transformation. The powder changes from a solid to a liquid, forming a melt pool. Once the laser moves, this melt pool solidifies to produce a consolidated layer. When the scan finishes the geometry for the layer, the build bed is lowered in the Z-axis and a fresh layer of powder deposited. The process will be repeated until the part is finished.

When the build is complete, the solid metal part will be embedded in powder. Once removed from the build chamber, the un-sintered powder is then sieved and put back into the machine to produce a new part. When the part has been removed from the SLM machine it will need one, if not more, secondary machining process to finish the part. Post-processing the part to manage its geometric shape, surface finish or mechanical properties may be necessary.

3.4 Known process problems

Despite current developments in machine control, the use of SLM production is still subject to known modes of failure. A set of the most common of these failures and their resolution are presented here. This work was undertaken by the author in collaboration with Renishaw engineers to provide an initial understanding of these failure modes and thus build evidence of the need for the type of process control considerations made possible with the application of the SLM PPP. Figure 3-4 to Figure 3-11 illustrate aspects of these failure modes and their effects provided by this collaborative work.

Scan path induced over-melting: Large areas that are scanned using a “meander” laser path can incur irregular residual heat concentrations. Figure 3-3 shows the different scan hatch types.

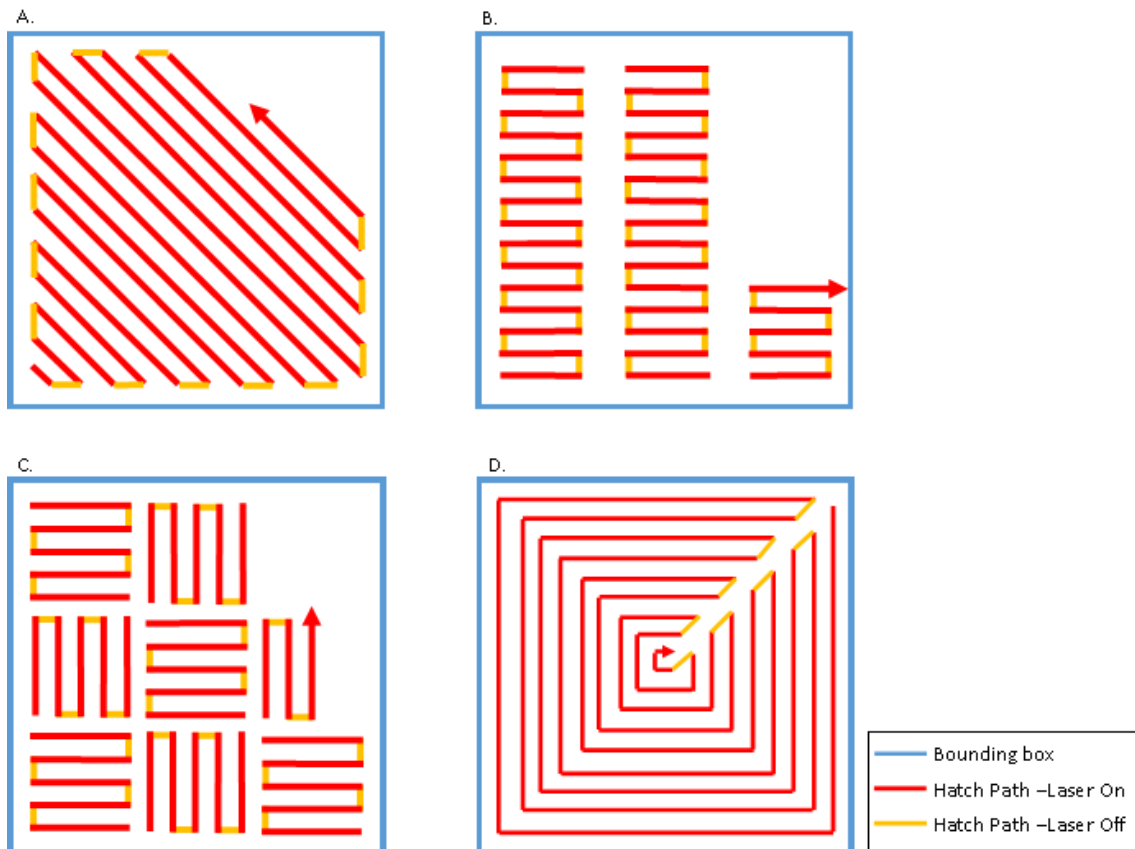


Figure 3-3 Scan hatch types A. Meander, B. Stripe, C. Chessboard, and D. Total fill

The powder over-melts, producing a surface that is very irregular and rough (Figure 3-4). Such a surface will damage the re-coater blade and lead to the wearing of ridges in the soft rubber. This damage leads to a change in the powder distribution which then exacerbates the problem further, potentially causing the top surface to become rougher and out of specification. The problem can be mitigated by using “chess board” or “stripe scan” strategies to create a more even heat distribution.

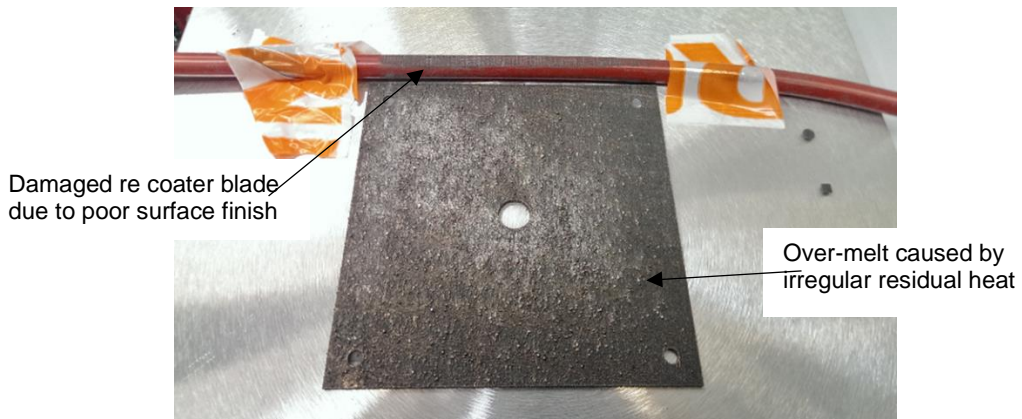


Figure 3-4 Large surface area created with meander scanning strategy which has caused over-melt and damaged the rubber re-coater

Surface form related over-melting: Unsupported overhanging surfaces that are angled towards the re-coater can cause powder to be packed under leading edges, as shown in Figure 3-5. The increase in powder can lead to over-melting because the part is unable to cool quickly enough. As well as the supports securing parts to the build plate they act as a “heatsink” by transmitting heat away from the part, similar to a “heatsink”. This helps reduce the chance of “hot spots” and the reduction in “hot-spots” prevents the chance of over-melt.

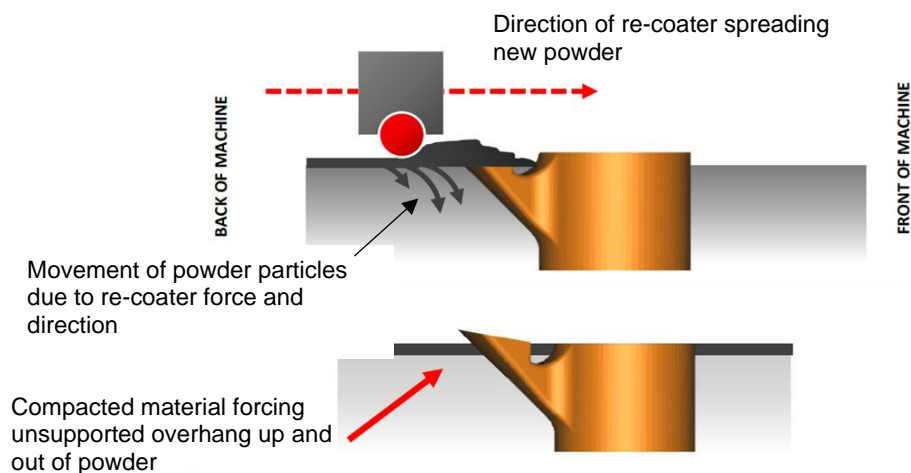


Figure 3-5 Reconstruction of part with un-supported overhang facing re-coater spreading direction showing powder packing under lead edge of part

Surface form related re-coater blade damage: Powder packing under the leading edge can also lift the part out of the powder, as illustrated in Figure 3-5. Once this happens the re-coater blade will catch and wear in that location, affecting the smooth distribution of powder. It is also possible that such a feature will cause the process to

stop once the protruding section of the part reaches the degree that prevents the recoater from running. Unsupported overhangs angled away from the wiper direction, where possible, will obviate this happening. Where this is not possible, the overhang should be designed with a supporting structure to restrain the surface so as to stop it from moving. The supporting structure will also help to dissipate heat. Figure 3-6 shows where an overhang which is not supported has produced over-melt on the downward facing skin because of high heat concentrations.

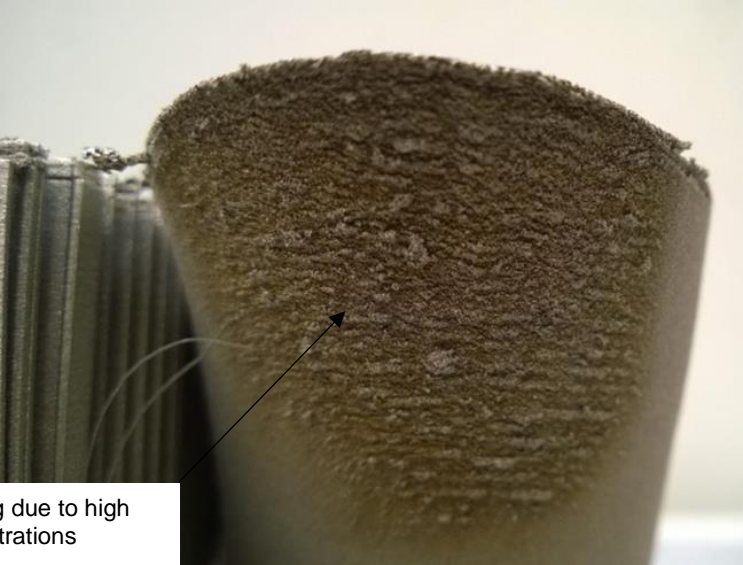


Figure 3-6 Overhang downward facing surface created with no supports showing over-melting due to higher heat concentrations

Support structure element bending: occurs when a support’s geometry is too tall and/or thin. This problem is further emphasised if the thin section of the support is located perpendicular to the wiper direction. Locating the supports in this way means that the supports can bend or distort during the build if the wiper blade catches the top surface. If the support moves during the build process the consecutive melted layers will be out of alignment. The effect of such a failure is shown in Figure 3-7.



Figure 3-7 Inadequate part supports manufactured perpendicular to the re-coater blade movement

Experience has shown that increasing the thickness of the supports or interconnecting them will minimise or mitigate the bending due to the force exerted by the re-coater. This solution should only be used if the orientation of the part cannot be altered due to build restriction. Orientating the part so that the supports are not perpendicular to the re-coater will prevent the bending from occurring and, where possible, gusset supports should be used.

Powder level: SLM machines can run out of powder and although the “low powder level” alarm acts as a warning, some machines will continue to build. If a build continues with an insufficient amount of powder then the part will be over melted and its intended height not achieved, as shown in Figure 3-8. Though a relatively simple procedure, checking that the hopper contains enough powder to complete the build is critical.

Lack of powder,
but build continued



Figure 3-8 Build chamber out of powder with process continuing to build and over-melting part

Short feeding: The addition of lower than required levels of powder can result in a problem known as “short feeding”. The dosing amount needs to be set so that powder covers the whole build plate in an even fashion. Care should be taken when setting the re-coater height and blade. If the blade is over tightened the rubber can be pinched and an uneven distribution can occur. If the blade is set too tight to the build bed then minimal powder will be distributed onto the build bed and if it is too far away from the build bed the layer thickness will be incorrect and can exacerbate the chances of short feeding. The effect of this can be seen on the front edge of the part shown in Figure 3-9. It has a depression caused by short feeding which has resulted in over-melting. Some new SLM machines use cameras to assess the powder coverage highlighting to the operator through visual or audio alarms that more powder is needed so that the build area is fully covered.

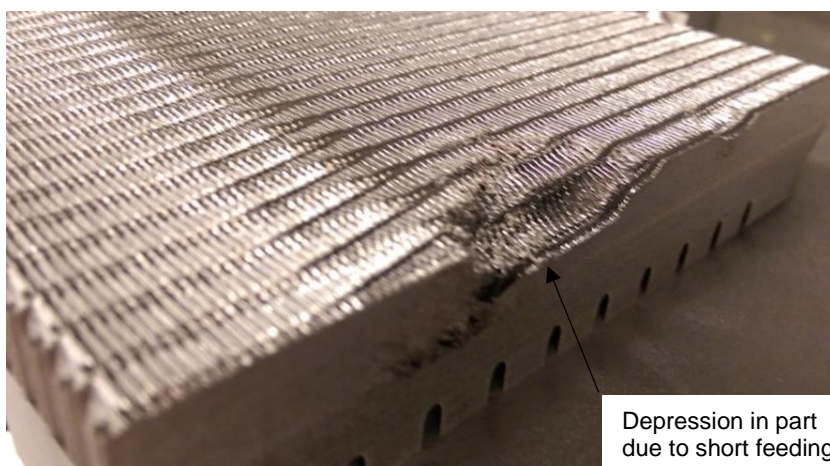


Figure 3-9 Evidence of short feeding with part evidencing depression

Residual stress: Parts can peel away from supports during a build causing fracture lines, as illustrated in Figure 3-10. This failure is most common in materials associated with high residual stresses such as titanium and other materials that contain a high carbon content.

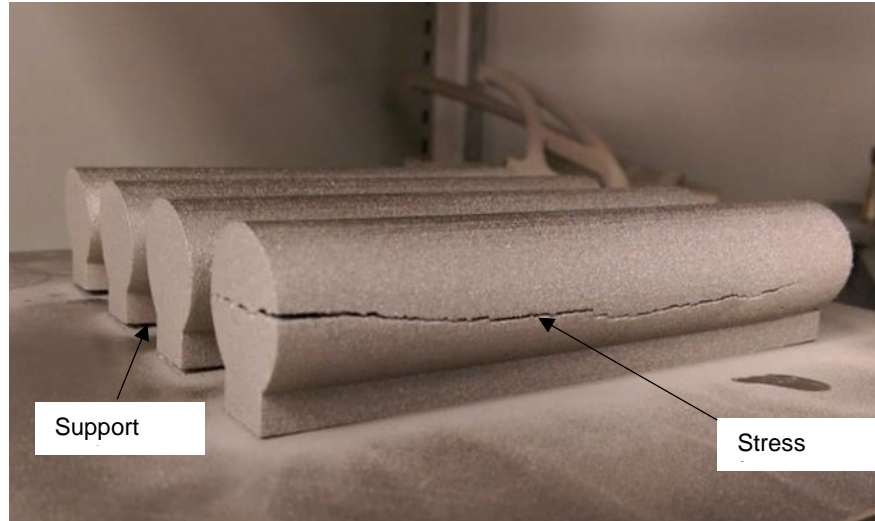


Figure 3-10 Part with fracture and peeling away from build plate

Resolving the issues highlighted in this section is not straight forward and relies upon a mixture of process know-how and machine management. It is, for example, difficult to identify the influence of only one individual process parameter which develops residual stresses in a part during the build process. This is because multiple process parameters influence other important mechanical factors, such as part density. Researchers over time have identified that scan speed, laser power, hatch spacing and layer thickness all influence the part's residual stress. It is also the case that changing any one of these parameters can have an adverse effect on the manufactured part's mechanical properties.

To illustrate the complicated nature of the SLM process the following issues can be cited. It is known that lowering the speed of the scan can reduce the residual stress in a part (Brückner et al. 2007) as it reduces the temperature (Vasinonta et al. 2007) and therefore reduces the cooling rate (Manvatkar et al. 2015). This was shown to reduce the deformation in bridge shaped builds (Kruth et al. 2012; Vrancken 2016). If the laser power is reduced the maximum temperature of the melt pool is reduced (Alimardani et al. 2009; Manvatkar et al. 2015). With less energy melting the powder, the melt pool will be smaller but there is an increase in the cooling rate (Manvatkar et al. 2015). Lower scan speed with higher laser power also reduces deformation in parts (Kruth et al. 2012; Wu et al. 2014; Vrancken 2016).

By increasing the hatch spacing there is a reduction in hot spots, but there can be an issue if the spacing between tracks prevent melt pools overlapping in some way. If there is no overlap in melt pools, parts will not be fully dense and powder or voids will be present in the part being produced. Increasing the layer thickness produced a reduction in deformation for parts that contained bridges, thin plates and cantilever parts (Zaeh and Branner 2010; Kruth et al. 2012; Van Belle et al. 2013). Each researcher noted a decrease in cooling rates due to the increased energy input when using thicker layers.

Finally, the design of the part can also be a major influence. Changing the geometries can also reduce areas of high stress concentration. As in conventional components the specified radii can be used to reduce the stress concentrations between two planes, as shown in Figure 3-11. This can also be completed for parts that are built directly on the build plate.

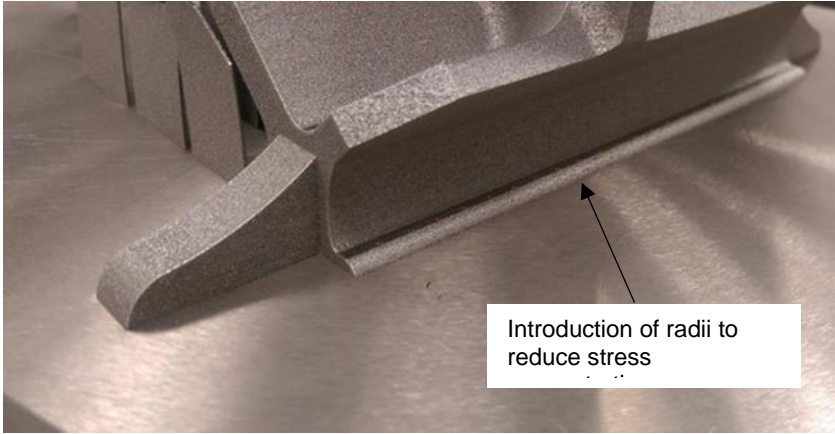


Figure 3-11 Part designed with radii to decrease stress concentration

There are multiple causes and potentially many combinations of causes which can result in these failures. Consideration by the author of the implications of such failures indicated that a more defined representation of their cause and associated prevention was needed. In this way the author was aiming to bring together the existing case by case expertise embedded within the knowledge of the engineers who operated these processes to form a coherent basis for subsequent process improvement. It is therefore necessary to break down the SLM process more closely and identify ways and means by which this can then be incorporated to formulate the PPP which can actually contribute towards stopping these failures from occurring.

3.5 SLM Work Flow Analysis

The work flow progression in SLM developed during this research by the author is represented in Figure 3-12. This represents the steps enacted to take a product idea conceived through the SLM process to production. At the initial stage this information will inform the Process Foundation layer so that any variables that are known to occur can be controlled. Variables that cannot be fully controlled must be managed and/or compensated for within the remaining SLM-PPP layers. Completing this task means that steps may be taken to make sure that the process can be brought under control and made repeatable.

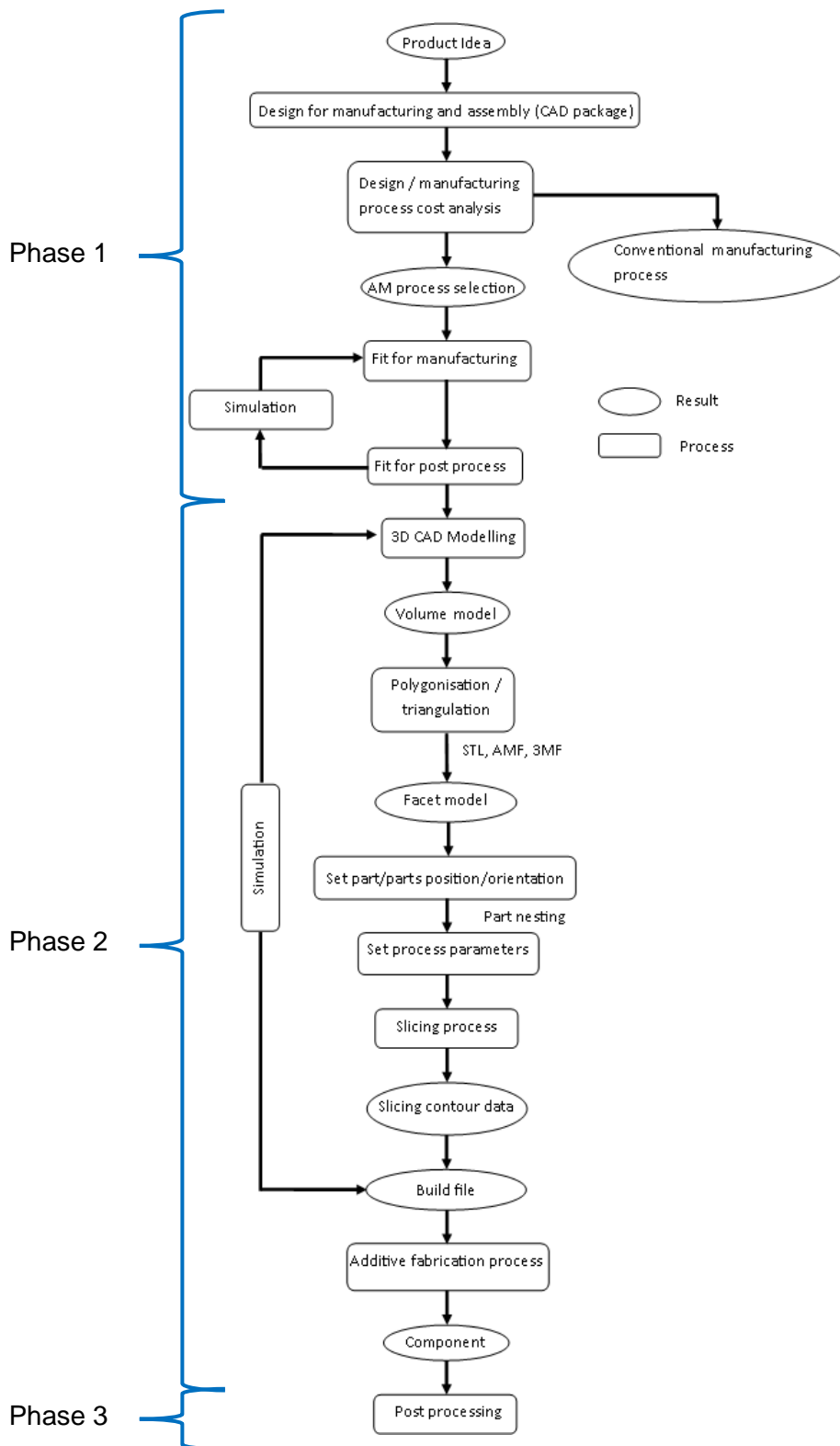


Figure 3-12 Work flow diagram for SLM. Physical workflow diagram from design (concept) to finished product.

The process usually starts with the design of a part based on a new **product idea** (phase 1). The enactment of an SLM process requires that a 3D model of the part must be produced, normally using a computer aided design (**CAD**) **package**. At present, there are no SLM-specific design standards available for engineers to follow

(design for manufacture process cost analysis). A draft BS ISO 20195 Standard Practice Guide for Design for Additive Manufacturing is available (British Standards Institution 2015). This and any related emerging standards will aim to provide guidance and promote best practice when using AM in product designs. It will not however include specific design solutions, process specific or material specific data. Until this standard is finalised only people that have a detailed understanding of the SLM process will be able to maximise product designs and exploit their full potential.

The designer will initially use best judgment to produce a design which can then be improved by using **simulation** and/or modelling software. To optimise the production process, it is important that the product is designed to be “**fit for manufacture**” and “**fit for post process**”. This requires extensive knowledge of the manufacturing technique. In this case information relating to the specific SLM process being employed must be introduced and prepared. To acquire some of this understanding designers can of course refer to work completed by other researchers for guidance.

Proprietary (OEM specific) modelling software can be used to maximise strength in the appropriate planes of the part and to minimise material usage, but a compromise on the design may be required to suit the manufacturing technique. As such, a designer cannot solely rely on one evaluation tool (**simulation**), i.e. structural analysis, but may need to consider also other factors including thermal conductivity within the part and fluid flow. One example of this problem is the creation of thin walls, without suitable wall thicknesses the heat being transferred from the part to the build bed may not be uniform or high enough to prevent warping. The wall or surface could change shape or even fail due to the stress introduced by the speed of heating and cooling of the material each time the laser passes over.

In the context of the SLM work flow progression (Figure 3-12) once the design has been finalised the **3D CAD** file must be transformed into a machine compatible format (Phase 2). This is usually configured as either a Stereolithography (.STL) or Additive Manufacturing File (.AMF) format (**polygonisation / triangulation**) which is a **facet model**. Figure 3-13 shows a 3D CAD rendering converted into the STL format; this is the rendering for the bridge test piece used in this research. In the STL format each intersection on the model indicates a node. At this stage understanding the resolution of the SLM machine that is being used is critical. It has been found that tessellation resolution improves surface finish when producing parts using SLM. Increasing the resolution affects a part’s geometry but has little impact on surface roughness, which means that post processing time will decrease, but pre-process times will increase

due to the increased time required to complete a high resolution image. To create the best finish on the part possible, the tessellation must be smaller than the resolution on the SLM machine; this will reduce the roughness on curved surfaces and create more defined changes in plane angles. The drawback in decreasing the size of the tessellation of the model is increased processing time when converting the 3D model in to an STL or AMF file.



Figure 3-13 Representative 3D CAD model (left) and developed .STL file (right)

The part is then manipulated so that critical surfaces are built in the best build orientation. This may be completed so that build supports are minimised or critical build features are put in the best orientation to give best results, this is completed with OEM specific software. Implicit in these procedures is the need for input(s) from the expert(s) at each stage, which currently may be provided in a rather ad-hoc fashion. Understanding process design factors is critical for all SLM designers and maybe complicated further as every machine is slightly different. Currently these differences are not recorded in the design software, meaning that the predictive model produced differs from the final part that is produced on any one machine.

Part proximity and part density (**nesting**) (how many parts are being manufactured on the build plate at any one time) are two variables that will always be different when discussing SLM builds, except when the machine is being used for the production of a series of parts. Part proximity will have an effect on temperature distribution as well as the number of parts within the build envelope. Sometimes builds may have sacrificial parts manufactured on the build plate to help control the thermal distribution, reducing or eliminating warping. The sacrificial parts are introduced to the build to act as a heat-sink to dissipate the heat uniformly to prevent warping. Heat transfer occurs mainly in the solidified material because the powder has a very low thermal coefficient making it an insulator due to the small air gaps within the powder and the reduced

surface area of touching powder particles. If the parts are produced close enough together the insulating properties of the powder are reduced and a higher heat transfer rate can occur.

The parts can also be orientated for optimum geometrical form. This allows operators to maximise build bed volume. Maximizing the build plate usually means that parts are orientated to minimize their footprint on the build bed. Care is required because build orientation is a key factor in build quality due to the characteristics of the process which produce resolutions that are different in the X, Y and Z axes. Part orientation can also be used to optimise the use of support structures; these are temporary features that prevent layers from collapsing during the SLM build process. Minimising these supports means that less time is required during the post processing of the part.

Once the build bed has been assembled in the virtual build software the composite 3D model containing all the parts at their specific location is itself **sliced** into multiple two-dimensional cross-sections. The number of slices is dictated by the layer thickness. Each layer contains geometric information. The process information, material information, and machine information are stored in the build file. Each layer also includes the laser path and related information providing process parameters such as; build bed temperature, laser power, laser speed, and chamber pressure.

When the 3D model has been sliced and the scanning strategy has been set (i.e. chessboard see Figure 3-3) the laser path is set. The SLM operator sets the exposure strategy for the part production. Currently, selection is based on the operator's knowledge of the machine. An example of this type of knowledge is part orientation and the production of holes, if holes are manufactured parallel to the build bed their circumferential measurement is more accurate than those produced perpendicular to the build plate. Build orientation and overhangs are another design consideration. Each metal has a different overhang capability due to the material properties. Knowing this capability is key to minimise the use of supports. If a part can be produced with a minimum of support structures, time can be saved later on during the post processing stage.

The part is then sliced in layers appropriate to the resolution required. This produces a list of instructions (machine code) for the machine to follow and is usually completed using software developed by the OEM. The resulting machine code will include processing parameters, which are either set by the operator or pre-set in the software produced by the machine manufacturer.

At the slicing stage the laser path is also defined. The two dimensional slices are converted into laser path scan lines. Each layer contains three different hatching paths:

“Up skin” paths are layers that are not covered by another layer.

“Down skin” is a path which makes up a surface which faces down without any melted material below it.

“Volume” is the inner core of the part which is not on any edges.

Each hatching path can be split into three further parts, “borders”, “fill contours”, and “fill hatch”. “Borders” is the scan that outline the two dimensional areas of each layer. They improve the surface structure and finish. “Fill contours” are similar to borders, their purpose is to reduce porosity and strengthen the bond between the fill hatch and the border. “Fill hatch” is the remainder of the laser path that fills the remaining volume and can be set to one of four different styles; meander, strip, chessboard, or total fill as explained in 3.4. Laser power, speed, point distance, build plate temperature and chamber oxygen level are pre-set by the manufacturer based on their knowledge of what works best for their machine for a particular material. The operator has the ability to change these settings if alternative settings improve characteristics important to the part being produced.

To minimize the occurrence of embedded errors in the part it is important to evaluate the STL model before initiating the slicing stage. Problems with incomplete form definition that can arise in the CAD models are usually identified when attempting to convert the file into slices. If this process cannot be completed there is evidence that the model itself is not fully defined. If the model is created and it is not fully defined, processing errors will appear later on during the manufacture of the part. These processing errors can manifest themselves in different ways; holes can appear in surfaces or over-melting may occur and lead to the key holing effect. Designers can either use repair software such as MAGICS (Materialise 2017) or manufacturer specific software that comes with their SLM machine. This procedure is represented by the simulation process loop in Figure 3-12 (in phase 2). Geometry editing methods such as noise reduction or hole filling are often necessary to provide an SLM model that can be processed (Botsch et al. 2010). At this stage compensation for material shrinkage is also required. If the shrinkage ratio is not correctly set the parts being produced will have a constant dimensional error.

When the STL/AMF file has been fully checked it is compiled as a **build file**. The resulting parts may then be added to the build bed, initially within a virtual environment. As well as modelling software, SLM companies provide their own software that can be used to slice the 3D model and position the parts on the build bed. This provides the designer and operator with further information such as the path of the laser and the settings for processing the material. These programs may have been developed by an individual manufacturer to work best with their machine. The program relies on the operator knowing best practice, for instance part position on the build bed can affect the geometrical shape of the part because of the change in laser shape and energy distribution. These in turn can affect the build bed temperature, creating uneven bed temperature distributions which can cause fractures, cracking, de-lamination and warping in the part being manufactured, as discussed in the known problems section 3.4.

The final stage required to produce a finished part is **post processing** (phase 3). Once the parts have been removed from the build plate the minimum work required would usually be to shot peen the part to remove excess and/or un-melted powder. Shot peening is a cold work process used to finish metal parts to prevent fatigue and stress corrosion failures, for work hardening to improve wear characteristics, straightening distortions and surface texturing. A range of post process heat treatments can be used to reduce residual stresses in the part. If required, density of the part can be improved with the application of hot isostatic pressing. Parts usually need to be removed from the build plate, using a range of potential processes, following which some finishing operations may be performed to complete the manufacture of the part.

3.6 SLM Process Cycle Variables

The quality of a part produced using SLM can vary and the nature of this variation will depend upon many interrelated process, environmental and operational factors. Bringing these factors together to enable further consideration is a challenging task. Taking as a frame of reference the influence that these factors can have on process quality, a series of interconnected Ishikawa or “fishbone diagrams” were developed by the author. The use of fishbone diagrams to provide a comprehensive overview of the interlinked stages in the SLM process is innovative and was developed by the author in this research. The basis of this information was acquired by the author during the enactment of a sequence of SLM processes both in-house and in Renishaw. The expertise thus acquired was a critical element in the enactment of this research and

due acknowledgment is given where appropriate to the sources used. The fishbone diagrams that form the basis of this approach are being utilised within Renishaw by the engineers with whom the author collaborated. Whilst developed in regard to the specific SLM used in this research the approach used and the parameters identified on the fishbone diagrams will be more widely applicable. Both users and manufactures of such equipment can thus adapt and utilise the information provided in the following sections.

The highest level diagram is shown in Figure 3-14. The output of this diagram was set to: "Process Quality". This is taken in this thesis to refer to the overall performance, reliability and repeatability of the process used to manufacture a part. Control of process inputs may involve the use of Failure Mode Effect Analysis (FMEA) and similar techniques to understand and control all the upstream factors that can affect machining process outcomes. This chapter identifies over 175 sources of variation which exist in the SLM process which can affect part quality. These are considered in the context of their importance of influence within the process in the following sections.

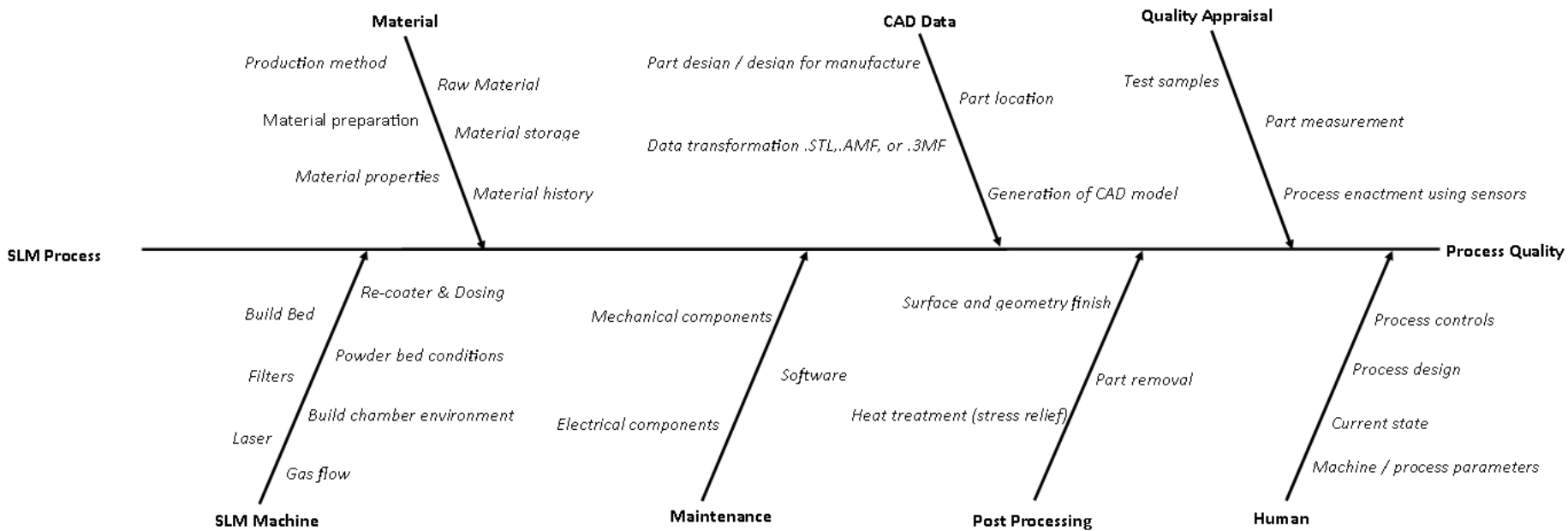


Figure 3-14 High level SLM process variable Ishikawa fishbone diagram

Figure 3-14 is the starting point for analysis of the factors affecting the process quality and will be developed further. For SLM **Process Quality**, consideration of the following would be typical; the qualities of the **material** being used in the process, including its specification, properties, production method, handling, preparation and storage. It is often critical that full traceability of this information should be demonstrated, particularly in some safety-critical sectors. The state of the **SLM machine**, including confirmation that the laser optics are clean, focused and aligned. The condition of the powder bed, recoating and dosing functions must be known; the heating element is functional and able to uniformly heat the build bed area. Knowing that the filters for the circulation of inert gas are clean, dry and in place, this means that the build chambers gas flow will be optimised for the duration of the build. The inert gas level would need to be checked prior to the build starting to ensure there is a sufficient amount to complete a build. If these conditions are consistent at the start of the process, it is assumed that they are most likely to be consistent and predictable during the build cycle.

Machine **maintenance** and regular monitoring of the condition of the electrical and mechanical elements in the machine is essential for the reliable and repeatable enactment of a process. An inaccurate machine cannot make consistently accurate parts and therefore cannot complete parts right first time (RFT). When applying these measures to the SLM machine a company can assure increased machine availability, increase process capability, improved quality and reduced overheads by focusing on proactive tasks. Software may also need to be maintained.

In addition to these machine and process-based considerations, the confirmation of process quality will reflect how the design attributes are met. The attributes are most likely to be represented by the various inputs included in the **CAD Data** used to describe the product required. These will be set by the (human) designer and will include the design of the part for manufacture, the interfacing to the required machine format and the arrangement of parts on the build plate. **Quality Appraisal** will require the measurement of parts, testing of samples and increasingly the confirmation of the appropriate enactment of the process, using sensors. This can be based upon the measurement of part characteristics and their comparison with the CAD model, however, when this is not possible the use of a test piece can be considered to provide a viable quality appraisal process.

The final stage of the SLM procedure is **Post-Processing**. This relates to the treatment of the parts to improve their qualities and typical processes applied include heat and surface treatments. Inevitably, this stage also includes the removal of the parts from the build plate.

As indicated there is always a **human** element of user know-how, which, is often implicit in the design and management of the SLM manufacturing cycle. The operator will influence the specification and control of the process parameters and support changes needed to enable an acceptable manufacturing cycle. In so doing, it is assumed that the human operator can access information regarding the current state of the machine and/or process being enacted.

Many of these process parameters can be identified in different stages of the SLM PPP processes depending upon the point at which variables are fixed and can no longer be controlled or changed. Knowing when a variable can be fixed is important as it can improve the accuracy of any developed modelling software. It also means that the process can be checked at certain points during the operation to see if the process is within the manufacturing specification.

For comprehensive assessment, within this thesis, these variables have been divided into the four layers defined in the SLM-PPP, to identify which variables influence which point in the process. Section 3.7 considers the process foundation layer of the PPP in more detail. The same procedure is followed for the other layers: Section 3.8 details the Process Setting layer; specifying the variables that can be set during the process and illustrated in Figure 3-16, Section 3.9 covers the In-Process layer; providing an indication of the information relating to in-process control (Figure 3-17), and Section 3.10 consider the Post-Process layer; which indicates the information needed to enable post process monitoring (Figure 3-18).

3.7 Process Foundation layer

The Process Foundation layer must provide the basis upon which an automated, capable process can be built. This relates to the machining environment, which involves assessing its condition and adjusting it so that a stable manufacturing environment is provided, thus ensuring preventative controls are introduced to reduce the number of sources of variance before manufacturing starts. Figure 3-15 provides a high-level Ishikawa fishbone diagram that can be used to address preventative controls within the SLM process.

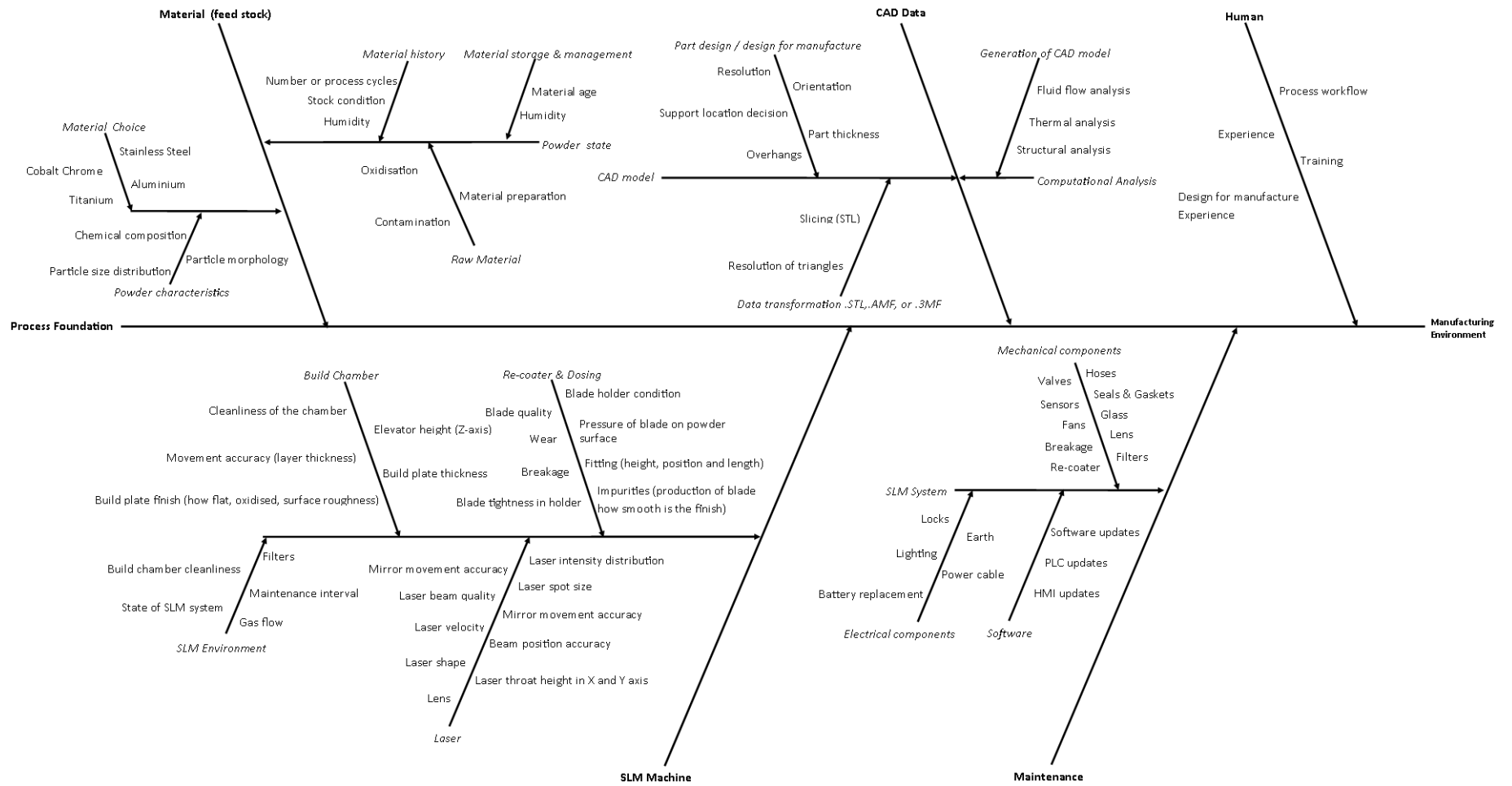


Figure 3-15 Ishikawa fishbone diagram of Process Foundation Layer expanded from Figure 3-14

3.7.1 CAD Data

The process by which a design is transformed into SLM machine ready information was outlined in phases 1 and 2 of the SLM workflow, shown in Figure 3-12. The resulting part design information will be transformed into the build and SLM machine specific form that must correctly represent an acceptable manufacturing process. In a typical production cycle, it is likely that several parts will be positioned within the build plate. Each part must be carefully located and orientated and all related parts requirements considered. It could be argued that for effective manufacture the compiled build plate must be considered as a single **CAD model**, allowing gas flow and mechanically related (thermal and structural) analysis to be applied. This will normally require the application of appropriate **computational analysis** tools. The above procedure will ultimately produce the inputs into the machine controller required to undertake the build. This will then require specific process setting actions, which will be considered in the appropriate sections of the next PPP layer.

3.7.2 Material (Feed Stock)

The correct **material choice** should be made by designers based on the requirements of the part being manufactured. Consideration should also be given to the specific properties of the particular feed stock being used. A challenging and hugely involved topic which is the subject of ongoing research and as such the detailed consideration of each of the parameters indicated on the **Powder State** branch in Figure 3.14 is not attempted here-in. It will be assumed that an appropriate consideration of the suitability of the powder material has been applied and that an acceptable material has been sourced and the required SLM process has been engineered.

Given this assumed starting point, it must be stated that process variation can occur due to differences in the **raw material** supplied. The metal powder used in SLM can be produced using a number of different material preparation techniques which can produce different particle morphology. For instance, a powder which is produced using ball milling creates extremely irregular particles and would have completely different flow characteristic to gas atomised powder where the particles are spherical. Clearly, if the morphology of the powder changes from build to build or because of oxidation and/or contamination and no compensation is made, then the parts produced will be subject to variation mechanically or geometrically.

One factor that influences the final part density is the ability to melt thin uniform layers that are accurately deposited by the feeding device. In this context homogeneous powder distribution over the build area is one of the most important requirements.

Powder flow and distribution is difficult to relate to any one given parameter of a powder, but there are some rules which can be applied. In general, particles which are spherical flow better than irregular particles and larger particles are freer flowing than smaller particles. It has also been found that powders with a higher packing density are less free flowing than those of a lower packing density. Moisture in powders has been shown to reduce flow due to capillary forces acting between particles. Finally, attractive forces such as Van der Waals and electrostatic forces can adversely affect powder flow (Angelo and Subramanian 2008). These points are included to illustrate the considerations that must be made in relation to **material storage and management**.

The difference in material composition can directly affect the material absorption rates as well as the flow characteristics (Sainte-Catherine 1991). So it is important to maintain continuity in the material source. **Material history** is another important consideration; if the powder being used is virgin, then it is possible to assume the characteristics of the material will be within the manufacturer's tolerances and partial size distribution (PSD) consistent. If recycled material is introduced, the morphology of the powder is changed therefore affecting the flow ability of the material and tap density (tap density refers to the ratio of the mass to the volume including the voids between particles). In some cases, material is continuously recycled to very good effect, suggesting that a mix of virgin and used powder may be recommended.

SLM machines that can process multiple metals are in danger of increased contamination from external influences even though machines may be set up in "clean" environments. Unless the SLM machine is set up in a clean room environment the powder can be exposed to a number of potential contaminants such as oils, dust and grease. The humidity of the metal powder is a known factor and it should be stored in a cool dry place which is hermetically sealed. If the material is exposed to high humidity it can oxidise and the material properties can be affected. Material storage and material preparation should occur in similar room conditions eliminating the chance that the material could be contaminated. For SLM machines that are used in research cross-contamination can be a common occurrence, especially if the machine can be utilised to run different materials. Cross contamination of metal powders can become common if the machine is not stripped down and thoroughly cleaned. New production focused machines that only deal with single metal powders will not have these issues, but they are restricted to only one powder. It can be assumed that their internal powder handling units reduce the human factor affecting powder recycling and powder handling.

3.7.3 SLM machine

Build chamber cleanliness is fundamental to the **SLM environment** input into the process foundation layer. As discussed in Section 3.7.2 if the machine is not fully cleaned there can be material contamination. Re-circulation filters are another area of potential process variation; the more saturated they become the less effective they will be at cleaning the environment. As a result, the flow of Argon will reduce due to the increased impedance of clogged filters denoting more soot lying on the build bed. The increased soot can embed itself into a layer of a build if the velocity of the Argon is not high enough to move it into the air stream and to a filter. This can cause a void to appear as the soot is burnt off when it is re-hit with the laser or micro cracks can appear due to the lack of fusion during solidification. Problems may also be caused by the different thermal properties of the metal powder and the soot.

Machine calibration is a critical input into process foundation. In the case of the Renishaw AM250 machine used in this research, each new machine is put through a dry set-up/calibration process. The calibration process is then repeated once the machine is in operation every twelve months to prevent loss of performance. Apart from the very first calibration, all calibrations include the build chamber being fully cleaned. The dry commissioning/calibration process is broken up into four parts; build chamber elevator, laser power, laser spot size and scan field configuration. These are further broken down on the fishbone diagram, Figure 3-15. Full details of this calibration process are provided in Appendix 1. The elements of the calibration process included here relate to the inputs into the process foundation layer, identified on the fishbone.

The build chamber elevator height is checked by attaching a build plate and driving the elevator a set distance and taking four measurements, one at each corner. Using several steps, it is possible to determine how level the build platform is as it moves up. It is then possible to identify if there are any issues with the encoders used to control the elevator height. If a problem is found the machine “Z” position can be re-calibrated using the on-board PC. The condition of the build plate, including thickness and surface properties must also be considered. This is of particular relevance when build plates are re-used following machining and finishing to remove previous parts.

There are several **laser**-related parameters that may be managed and/or controlled using the steps described in Appendix 1. These include the power of the laser, which can be assessed and mapped against the specification provided by the OEM during calibration. Once the power has been mapped correctly, the beam focus may be

checked and adjusted if needed. The laser spot size (and shape) can be evaluated in both the X and Y axis and the power distribution for the laser checked. The scan field calibration process is used to assess the laser position across the whole of the build plate. Implicit in this is the assessment of the operation of the mirrors controlling laser movement, it is important to establish the link between mirror movement; laser accuracy and beam quality. A consideration critical to the accurate delivery of energy into the powder is the cleanliness of the laser lens. The build-up of soot particles on the lens will cause diffraction and deflection of the beam. This will alter some of the focused energy onto other parts of the build bed and will change the energy at the focus point of the bed. This change will depend on the amount of soot, however, any amount can cause parts to not melt fully and therefore produce parts that are less dense than required.

These operations must be carried out every time the machine is moved, calibrated or serviced. This calibration procedure does not fully cover every processing variable, but it does allow a user to produce a part within the OEM's specified tolerance. The resulting machine set-up is applicable to the process for as long as the trained technician is there running the machine calibration. During these scheduled visits general maintenance is carried out on all the SLM mechanical, electrical and software components. As soon as the technician leaves, there is no ongoing process that evaluates the build process until the next OEM's scheduled visit.

In addition to controlled factors linked to the operation of the machine, environmental stability addresses those external sources of non-conformance that cannot be eliminated in advance, but which are inherent to the operating environment. These include changes in powder temperature within the elevator while parts are being produced, laser life management and gas flow velocity.

The final "mechanical" function in the SLM machine is the **re-coater and dosing** system that controls the distribution of powder across the build plate. It usually consists of a wiper blade assembly which is drawn across the chamber between each layer. Parameters that affect its performance include the condition and quality of the blade. These can be affected by wear, misalignment or breakage. Compensation to blade position and pressure may be applied by adjusting the blade manually within the holder assembly. At process foundation layer it is possible to set-up this assembly in an acceptable configuration to support the production of parts, however, as most of the parameters in this section, these settings cannot be taken for granted and they must be monitored during use. The effects of increasing levels of impurities into the

powder must be assessed and managed. Such monitoring can be direct or indirect, and thus can be linked to part quality, or to assessments made using test pieces.

3.7.4 Maintenance

The maintenance schedule provided by the manufacturer explains best practice for keeping the SLM machine in peak condition. Included is a cleaning schedule so that the occurrence of foreign particles is minimised and the best processing atmosphere can be achieved. Within the maintenance schedule is a document providing the operator with clear instructions on minor maintenance procedures which can be carried out on a daily, weekly or monthly basis. Minor maintenance would include visual inspections, functional safety device checks, cleaning the build chamber, cleaning the SLM machine and working room, changing filters, topping up coolant levels and other non-technical checks. For convenience these tasks are identified in Figure 3-15 with the inputs under two categories: **mechanical components** and **electrical components**.

Annual and biannual maintenance checks are usually more onerous and are carried out by the manufacturer trained or approved technician. The highly skilled technician will carry out more in-depth analysis on the health of the **SLM machine systems**. This would include any **software updates** required to run the SLM machine. The laser power, accuracy and spot size / power distribution will be evaluated as well as the movement in the build elevator. If any part has degraded an associated function it will be brought back into conformance. The technicians require access to embedded software to which the everyday operator currently does not have access. These same operations need to be carried out when the SLM machine is first installed or if it is relocated during its working life.

3.7.5 Human

The final major variation in the process foundation layer is the operator. Currently the SLM process is not fully automated, meaning that operator interaction has a considerable impact on the quality of the parts being produced. The operator, using the OEM's software is able to change the laser power, speed, and point distance when creating the build file. All of which can affect the quality of the parts directly. The operator can also use the control panel on the machine to alter the build plate temperature, chamber oxygen level, pause and start the build, and change powder dosing levels during the manufacturing process. Lastly the operator cleans and maintains the machine, the quality of this work impacts indirectly on the parts being manufactured as discussed in Section 3.7.3.

Some of these operations can result in interaction and/or conflict between parameters and their settings. The resolution of these operator interactions will rely on the knowledge of the operator who can provide the needed inputs when attempting to design and engineer a procedure in a set way. In terms of process foundation clearly the intention should be to deploy a manufacturing cycle that is robust and repeatable and will need to rely on the investigation into each parameter and the effect of any variation for each parameter that can be controlled. **Training and experience** currently are the best way of fortifying the process foundation layer in this area. With the development of machines that carry out all the powder handling and with software engineers producing better modelling packages the expertise and knowledge currently required by an SLM operator will lessen.

3.8 Process Setting Layer

Process setting manages the preparation and programming of the SLM machine to produce parts. This implies it is possible to mitigate against predictable causes of variation that are known to present challenges to robust manufacturing. It relates to the fixed settings the operator programs into the SLM machine so that a part is produced. The intention is that these settings can be engineered and applied to mitigate or restrict the effects of sources of error in the set-up of the machine. Figure 3-16 provides the Ishikawa fishbone diagram for the process setting layer of the PPP. Many of these parameters overlap with the Process Foundation section and will have been considered in Section 3.7. This is typical in the development of any manufacturing process as the process foundation layer establishes generic rules that can be applied to facilitate manufacture and these rules are then adapted and applied to establish process setting information enabling the production of specific parts.

To illustrate this, when developing a program to manufacture a part using a standard milling machine, the engineer will be able to consult guidelines regarding the relationship between important parameters and the process to be enacted. In effect these guidelines represent the knowledge that needs to be provided in the process foundation layer. Then, to achieve a required tolerance or surface finish for a specific part, it will be possible to set specific machining feeds and speeds. These will depend upon many factors, such as machine, material and tool properties. Once they are set then specific operations can be defined. Depending upon the actual milling machine used this program may need to be adapted, and the process setting parameters changed. Similar considerations can arise with changes in material properties and/or cutters. However, at this level in the PPP, it is assumed that once set for a specific

process, these parameters are capable of enabling the manufacture of the required part to the required quality specification. These assumptions are based upon the very well established knowledge that is formulated in the milling-process process foundation layer so that any adjustments needed, due to any identified variations, can be engineered in the process setting layer. It is possible that the settings applied can be checked with pre-production procedures before manufacturing commences. This procedure depends upon the manufacture of a test artefact that can be assessed to produce the information required to set tool offsets etc. before production starts. A mechanical probe can be used to measure a “slave” artefact to establish the effects of any wear on the cutter or changes in material hardness, before it attempts the manufacture of the final product. It is interesting to note that, as discussed in the next section, such a procedure can also be enacted “in-process” thus contributing vital in-process information to the next layer of the PPP.

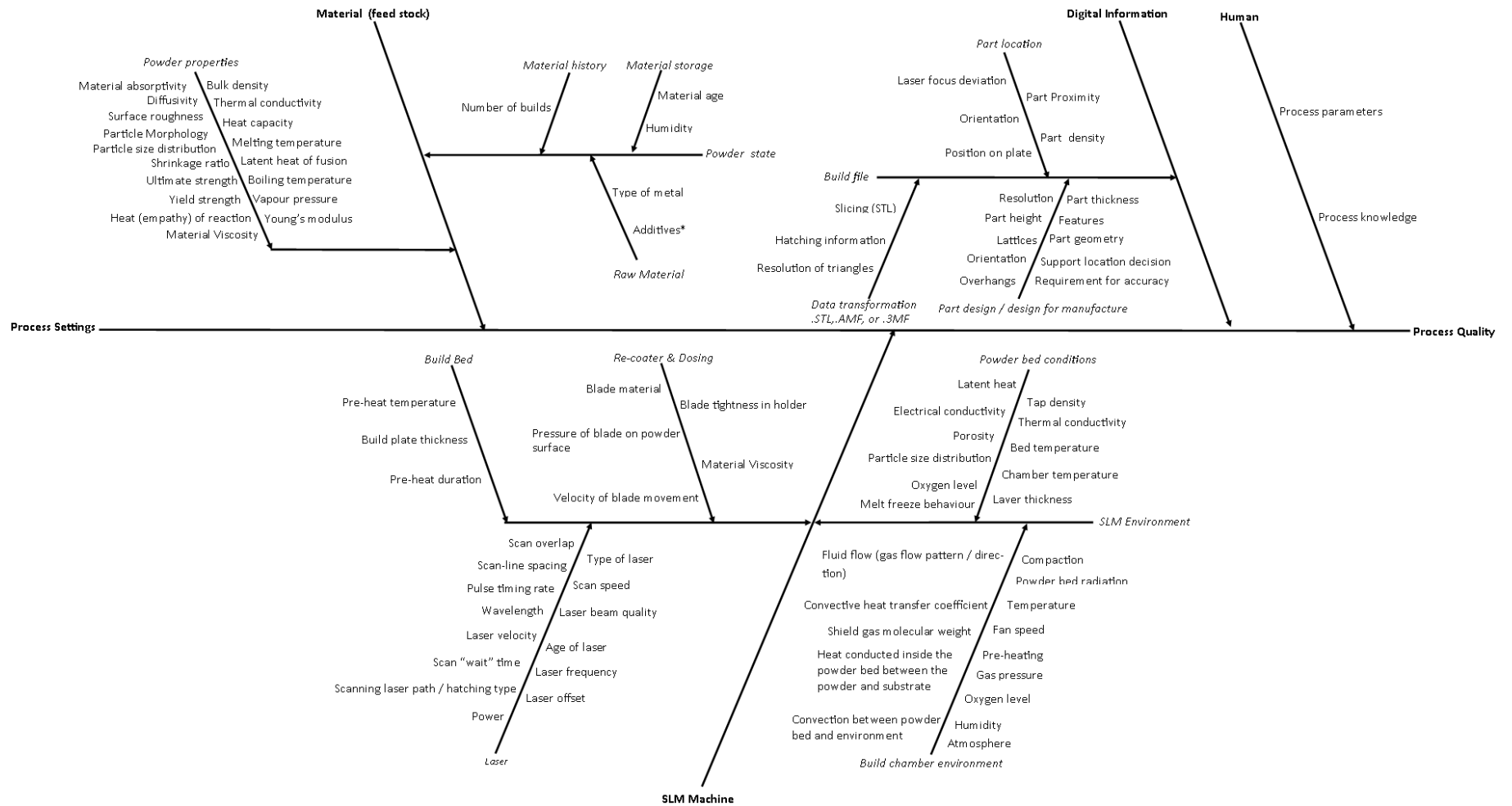


Figure 3-16 Process setting Ishikawa fishbone diagram derived from Figure 3-14

Due to the relative lack of current knowledge regarding the way SLM processes can be enacted, standard techniques developed for reductive manufacture cannot be utilised. As the SLM process creates parts layer on layer from powder, the traditional pre-process setting up procedures previously mentioned, cannot be applied. What is required at this level is the setting of a part specific process that can utilise the SLM facility to produce a part with the required characteristics. The aim of this research was thus to establish and demonstrate a viable PPP-based approach that can be utilised for SLM. Whilst the PPP approach has been widely applied to conventional manufacturing its application to SLM has not been previously considered and represents a novel contribution in this research. This is further enhanced by the integration of the knowledge represented by the fishbone diagrams into the appropriate levels of the PPP.

3.8.1 Material (Feed stock)

The considerations related to the properties of the material used in SLM falls into both the Process Foundation and Process Setting layers of the PPP. To distinguish between these inputs, it is helpful to assert that, when the designer has selected the material, using for example its mechanical properties, it is then “set”. The material used in the process is now restricted to only one material. Clearly care must be taken to the provision of the specified material, and it is necessary to carefully manage the procurement process. It is clearly possible for different versions of the “same” material to exist and critical parameters must be established in all cases. This sets the mechanical properties of the metallic powder as well as its physical properties (such as flow rate). The geometric form of the powder (as discussed in Section 3.7.2) will be “set” once an approved supplier is chosen. Assuming this has been audited, variation between batches should be minimal.

Internally the operator should maintain comprehensive data on the **powder state**, including material history and age. As discussed in Section 3.7.2 most powder is recycled over a number of builds, though it is sieved to remove the largest particles the powder can change mechanically and chemically over time. It is also possible that factors such as humidity can change during the storage of the powder (either in or out of the machine). If powder is not monitored these changes can cause changes to parts. Though this is not technically a setting itself, a trained engineer can provide limits to both of these variables. This may be considered as “setting” the limits for both, so that the SLM process can produce optimum parts with the raw material it is using.

Consideration must also be made with regard to the process setting measures applied to ensure the attainment of material-related product characteristics. Part properties, such as the desired surface finish, yield and ultimate strength, density and numerous geometric parameters will be controlled by the settings applied. These will need to be aligned with the specific part requirements which in turn will need to be carefully considered if they are to be met. **Powder properties** such as thermal conductivity, melting temperature, material absorptivity, material viscosity and shrinkage ratio will need to be assessed when setting the process parameters. This will most often involve a combination of operator know-how, embedded OEM expertise and trial and error. This will usually have been based upon the production of “test pieces” to establish control.

3.8.2 Digital information

It is likely that a number of individual parts will be “nested” within the build volume to reduce production costs. This process to produce the **build file** should involve the consideration of the requirements of each part as well as the whole build. This will involve careful consideration of the **part design for manufacture**, for the specific build-machine combination being considered. **Part location** and the subsequent model **data transformation** require setting by the operator before the manufacturing process can start. The operator needs to decide where the parts should be built on the build bed. This includes the setting of orientation, position, proximity and the overall build density. This process will be underpinned by knowledge of the effect on part qualities of variations in process parameters, such as laser focus and gas flow. Software can be used to set-up the build in a virtual setting. Currently these programs do not provide solutions for best utilisation of the build volume, but they do offer suggestions to make the decisions easier for the operator.

The decisions made at this level will include process settings to achieve the required part accuracy and geometric features for each part in their designated position in the build. In this context, overhangs will need to be supported and part features and surface finishes will need to be managed. This will be attempted using part orientation and laser path optimisation. Internal details will need to be considered with regard to supports, lattices etc. These considerations are shown in the SLM work flow diagram in Figure 3-12 as part of Phase 1, where the 3D CAD model is simulated and made fit for SLM manufacture. Some degree of intelligent decision making will be involved, which is difficult to represent, and more importantly difficult to capture for subsequent operations.

3.8.3 SLM machine

Once the build-specific part location is defined the operator is able to set the driving process parameters to control the manufacturing cycle by managing the associated process variables. This will require the understanding of a number of complicated relationships between the machine sub-systems, the manufacturing environment, the parts being produced and process parameters, as depicted in the **SLM machine** branch in Figure 3.16.

The features of the **laser** will need to be considered when producing laser path programs. These will include characteristics such as its type, power (and any age related reductions), wavelength, frequency, velocity and other measures of laser beam quality. These will usually be assumed to be fixed, with updates applied in annual or unscheduled maintenance operations. These characteristics will be represented by applicable attributes, such as laser offset and spot size, to enable the setting of process parameters. Thus laser parameters including scan speed, spacing, overlap and pulse rate can be set to provide appropriate conditions for optimum part production. Much of this setting is enabled by OEM provided controls that simplify operator inputs by building in the known parameters and establishing design for manufacture procedures.

Consideration will be applied to manage the **build chamber environment**. This is again challenging as numerous variables can be identified, including those related to the powder melting process, the shield gas properties and gas flow and to the properties and state of the powder bed. Understanding how these may be managed is beyond the capabilities of most operators and management is therefore usually enacted by embedded OEM functions. These aim to provide control over variables such as oxygen levels, humidity and powder compaction. Control is achieved via the setting of parameters including chamber pre-heating and process temperature, fan speed, gas pressure and power input as managed by the laser settings.

The actual SLM process will be enacted within the build chamber upon the powder bed. It is therefore essential that systems and elements undertaking functions within this process are fully defined and controlled. The **build bed** will need to be correctly heated, requiring control over the temperature and duration of the pre-heat cycle and knowledge of the material and dimensions of the build plate. The **re-coater and dosing** system will need to be properly set-up to provide the required powder layer thickness and compaction. This will depend upon the blade assembly and speed of the procedures involved. Finally, the **powder bed conditions** will need to be

managed using measurements of bed and chamber temperature to indicate that the anticipated powder melting process is being performed, the “science” behind this process is beyond the control of the machine operator. The powder bed conditions are dependent upon inputs related to the powder, its condition and the SLM machine elements performing their functions and can be anticipated and integrated into the machine program by the OEM.

To this point this section has considered process setting requirements that are largely defined by OEM based understanding of how their SLM machine can be deployed to produce specific parts using specified materials by supporting controlled manufacturing cycles. It may well be the case however, that the **operator** will be required to modify a process should they feel it necessary to do so. This can be the result of know-how related to particular builds, parts and/or materials previously enacted. It is inevitable that this will be the case, and it is important that such knowledge is shared and retained for future applications.

3.9 In-Process Control

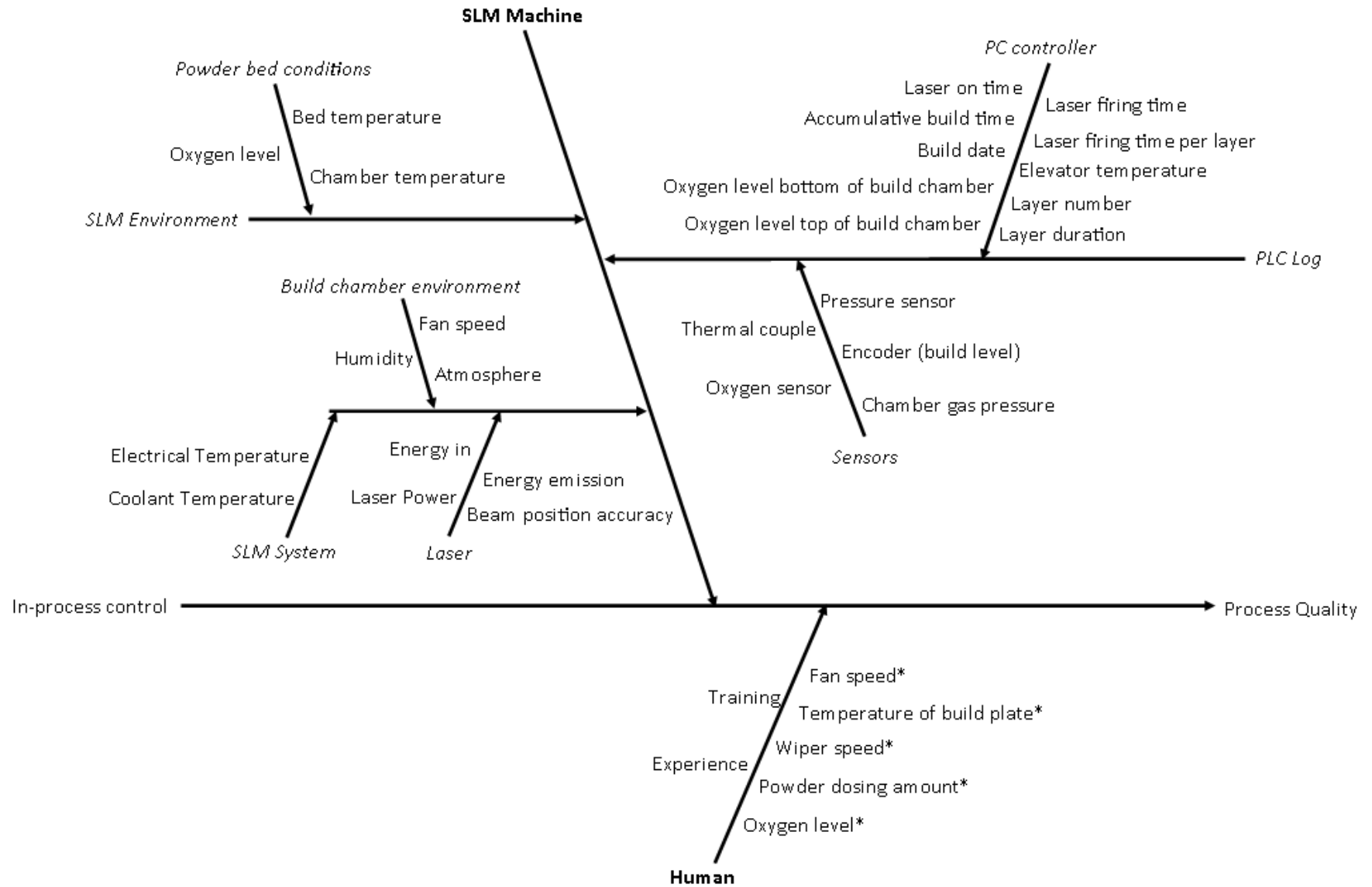
In-process control focusses on the identification and elimination of the sources of variation that are inherent to the manufacturing process. Currently most control systems in SLM machines provide defined in-process control functions to manage specific variables and communicate any perceived errors or unexpected events mainly using process alarms which are used to instigate actions by the operator. Figure 3-17 provides the fishbone diagram for current in-process control. There is a widely accepted need to introduce more intuitive closed loop control systems which reduce the reliance on the operator’s knowledge. This requires more sensors, integrated software and tested algorithms to allow the manufacturing process to auto-correct and/or compensate when the monitoring systems identifies changes in the build process that are unusual.

3.9.1 Operator

The **operator** can change or adjust settings on the control panel of the **SLM machine** and can alter powder dosing amount, oxygen level, wiper speed, temperature of the build plate, and the fan speed which circulates the inert gas in the build chamber. The evaluation of all aspects of these actions is carried out visually through the build chamber window or on the SLM’s digital display. The machine used in this project had audible alarms to notify the operator if the oxygen level, chamber pressure, or

humidity exceeded a pre-set threshold. An additional alarm sounds if the powder runs out in the hopper, or if there is a failure in the laser cooling system.

The actions taken by the operator will depend upon the perceived situation's specific requirement and the response will be conditioned by operator experience and training, as such their responses may not be consistent and thus processes themselves may not be repeatable. There may not be any recorded details of the specific adjustments made. Evidence that any problems occurred may be recorded but there may be quality issues associated with the loss of control that remain hidden. This situation threatens the long-term application of the SLM manufactured parts in safety-critical applications. This is well understood by OEMs who are seeking to advance the level and appropriateness of in-process control functionality on their machines.



* Denotes that the operator can change these options during the process.

Figure 3-17 In-process control Ishikawa fishbone diagram

3.9.2 SLM Machine

The SLM Machine control systems are engineered to provide levels of control appropriate to the tasks being undertaken. They can be complicated, as in the laser controller which manages the positioning, movement and firing of the laser using a combination of electro-mechanical systems. As such the **laser system** is often treated as a “black box” which can be managed with the appropriate inputs of desired process requirements. Performance can be monitored using measurements including laser power, efficiency (energy in versus energy emission) and beam position accuracy. Other systems within the SLM machine, such as the **build chamber** may be managed to produce required temperature, atmosphere and humidity related settings using the limited controls available. The **powder bed conditions** are subject to similar measures.

Unexpected events should also be taken into consideration such as wiper blade crashes, power outages and software errors. The solutions for some of these problems have already been integrated in SLM machines. For example, some machines are fitted with sensors that monitor the power usage on the motor that drives the blade back and forth over the build bed. If the power required to move the blade increases a problem may be flagged; the extra power being drawn would indicate greater resistance and therefore an obstruction in the build bed area. The increased resistance suggests that the part may have curled, cracked or snapped away from the support and be protruding through the powder.

3.9.3 In-process Monitoring: Quality appraisal.

It is helpful at this point to illustrate the level and purpose of the instrumentation embedded within a “typical” SLM machine; in this case the AM250 used in this research. Currently these **sensors** provide information in-process for layer duration, coolant temperature, chamber temperature, electrical temperature, layer number, laser power, powder level, oxygen level, fan speed, gas pressure, build temperature, humidity, and build level. For the AM250 this information is stored in the programmable logic controller (PLC) log. A representative extract of the log is shown in Table 3-1 .

Table 3-1 Part of the AM250 process Log (PLC log) from a build cycle

Plc To Pc – layer Number	Current layer number	75	76	77	77
	Accumulative Time (s)	1666	1686	1706	1721
	Time per layer (s)	35	20	20	
Plc To Pc – Oxygen Bottom Level	Recirculation circuit oxygen sensor value (ppm)	3549	3549	3542	3542
Plc To Pc – Oxygen Top Level	Vent point oxygen sensor value (ppm)	4967	4967	4967	4958
Plc To Pc – Gas Pressure	Chamber gas pressure (mBar)	9	9	9	9
Plc To Pc – Vacuum Temp	Vacuum chamber temperature (°C)	24	24	24	24
Plc To Pc – Elevator Temp	Elevator temperature (°C)	45.2	45	45	45.1
Pc To Plc – Laser Time On	Laser on time (s)	66610119	66610137	66610158	66610173
Pc To Plc – Laser Time Firing	Laser firing time (s)	11132538	11132547	11132558	11132569
	Firing time per layer (s)	26	9	11	

The AM250 software cycles through the sensor feedback every five seconds and uses that information to populate the **PLC log**. If, during this cycle, a value relating to the oxygen level, gas pressure or temperature changes the new value is recorded in the process log file. Currently this process log is not utilised for any automatic and/or intelligent adjustment to the manufacturing process, but it will enable an alarm if a value is outside the allowable process parameters. The information from the PLC log is both indirect and high-level, meaning that inferring relevant problems is challenging. Major problems that occurred can be identified and time specified, but it is not always possible to identify minor variations in the build process. It is also the case that this cannot be considered during the process currently, and thus is mostly applied post-process.

Next generation machines now include more sensors and/or systems using existing sensors that have been embedded to control functions. These include those sensors which can be used to monitor the laser, considered to be the most influential part of the machine in regards to part quality. Digital information that needs to be processed to complete this task will be at the terabyte level. Processing this in real time is thus a huge challenge. Current implementations can provide the operator with the capability to review the process as it is proceeding but more work is needed if the system is to operate as a truly in-process monitoring function.

3.10 Post-process Monitoring: Informative inspection

This is the top layer of the PPP which is the most commonly used in conventional manufacturing processes. This normally involves checking the part to verify that the process has performed as expected. It is usually deployed in conjunction with a computer controlled manufacturing process, wherein the production of parts is automated and consistent. Critical stages of production cycle can be assessed as required. Correctly used it can provide confidence that the manufacturing process is running as expected. The concern in applying this approach to SLM production, where parts are literally built in one operation, is that quality problems may not be apparent from features that can be measured post-process.

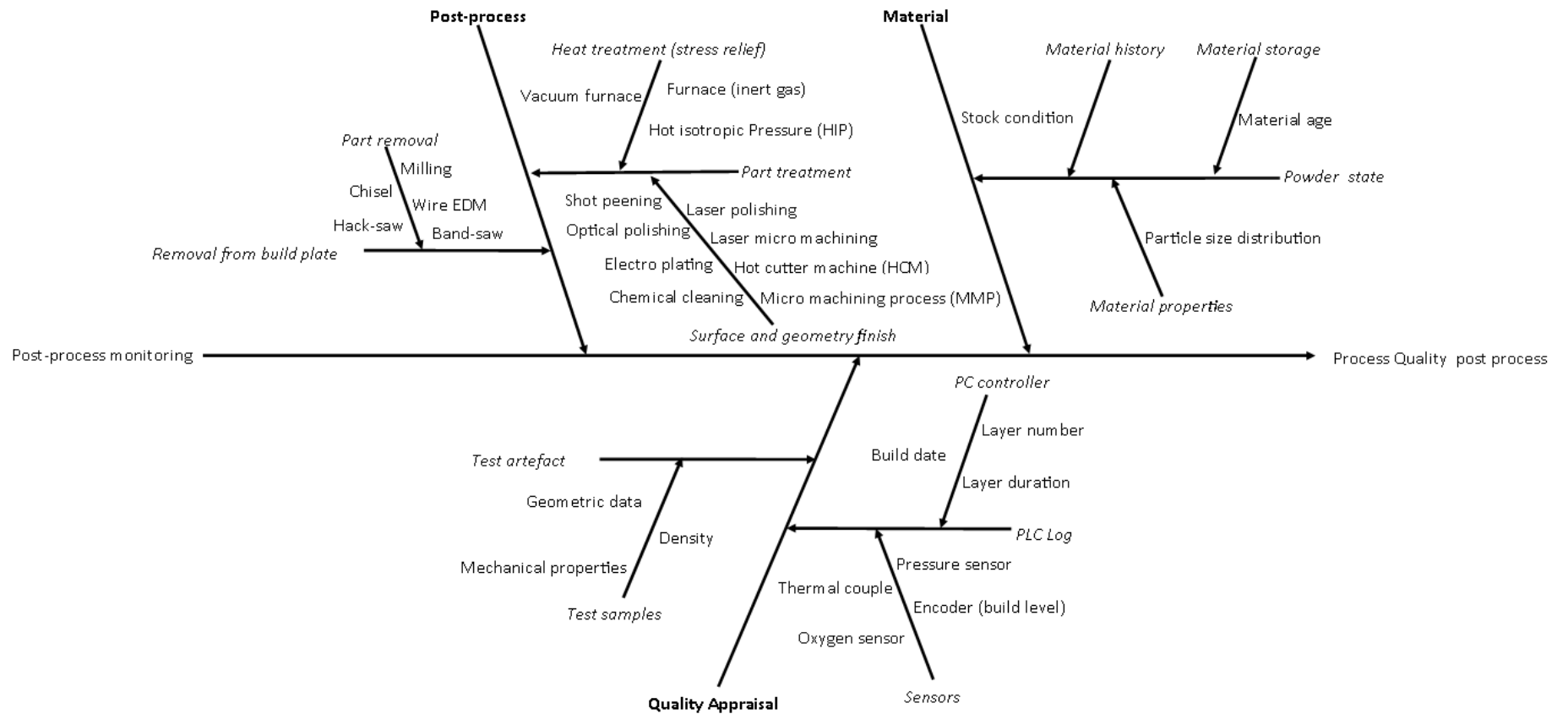


Figure 3-18 Post-process monitoring Ishikawa fishbone diagram

3.10.1 Quality Appraisal

Figure 3-18 shows the information that can inform post-process **quality appraisal**. The most basic methods appraise the **parts** using direct measurements, typically from a CMM, to check that the geometric dimensions and tolerances are correct. Other quality appraisal information, such as part density and mechanical properties cannot be assessed by directly appraising the part. This may be impractical due to the time and effort required, and the limitations of the available measurements. A more structured approach may consider the design and manufacture of a **test artefact**.

Test artefacts can be used to identify problems with the production process. Artefacts can be designed so that they assess a singular aspect of the manufacturing process or a number of aspects. For instance, density cubes can be manufactured to check that the manufacturing process is producing fully dense parts, or parts that match the density required by the customer. Other artefacts can be designed to assess surface finish, mechanical strength and/or geometry. The results of the assessment carried out on these artefacts have the potential to provide feedback into the SLM machine to improve the process. In this way the information associated with the production of a test artefact can be used to inform the process foundation layer and/or the process setting layer of the PPP. Using artefacts carefully it is possible to assess the state of a machine and investigate potential problems. These may be resolved and after the adjustments are carried out and the machine can be run again; the artefacts can be assessed to see if the changes have influenced the process in the required way.

Operators and engineers should be aware of the potential impact that **post processing** has on the results. Although post processing may be considered to be a separate process because it is not carried out in the SLM machine. Post processing using another process to create the final product can significantly influence the final product. Indeed, its main purpose may be to improve part features by the application of heat treatment or other mechanical processes. Engineers may be tempted to assess a part immediately after the build process, however there is no evidence to suggest that this is good practice and in some cases could even be classed as bad practice.

3.10.2 Material

Following the completion of a manufacturing cycle it becomes possible to establish the changes to **material properties** that have been caused as a consequence of the process. This will enable the material-related data to be updated to establish characteristics such as stock condition, material age and history. This may also

require off-machine inspection and/or measurement of powder quality and related material conditions. This is vital information for the next process to be enacted on the machine, thus feeding back into the earlier stages of the next cycle.

3.10.3 Post-Processing

As mentioned in Section 3.10.1 post-processing can change the physical and/or geometrical attributes of the parts produced using SLM. All parts manufactured using an SLM machine will require some level of post processing which would be based on the final part requirements. The least amount of post-processing required is **part removal from the build plate**. There are a number of different techniques that can be used to remove parts from the build plate which impact differently on the parts being removed. Parts can be removed by using a wire electrical discharge machine (EDM), band-saw, hack-saw, milling, or chisel, this is not an exhaustive list, but are the most common removal processes. Each of the processes can affect the parts in different ways due to the physical interaction between the cutter and the material being cut. For instance, the EDM cut will provide the most precise and smooth cut out of the five mentioned because it melts or vaporises the material being cut. A band saw uses a blade that cuts by shearing material away from the surface and the band-saw speed, teeth size, shape, and pitch will affect the roughness of the cut surface. Using a band-saw that is not set up to cut the parts off the build plate correctly can snag and bend parts. The crudest way of removing the parts would be to use a chisel, doing so can cause damage if care is not taken and the removal will create a very uneven finish.

Heat treatment is required primarily to stress relieve the parts. The stress relieving process is usually carried out when the parts are still attached the build plate because the build plate should be restraining the parts in the correct shape (geometry). The plate can be heat treated using a furnace (with an inert gas to prevent oxidisation), a vacuum furnace, or hot isotropic pressure (HIP). HIP increases part density by applying a constant pressure on the work-piece forcing voids to reduce through a combination of plastic deformation, creep and diffusion bonding.

As well as reducing the possibility of warping due to internal stresses there are a number of process available to **improve surface and geometry finishes**. Shot peen SLM parts to remove excess and/or un-melted powder is a minimum requirement. Shot peening is a cold work process used to finish metal parts to prevent fatigue and stress corrosion failures, for work hardening to improve wear characteristics, straightening distortions and surface texturing. Other processes that improve surface

finish and geometry are, optical polishing, electro plating, chemical cleaning, laser polishing, laser micro machining, hot cutter machine (MCH), and micro machining process (MMP). These can all be used once the parts have been removed from the build plate.

3.11 Summary

This chapter identifies over 175 sources of variation within the SLM process (Appendix 2 fully populated Ishikawa fishbone diagram for the SLM process). These sources of variation have been categorised using the PPP. The PPP has been adapted in this work for application to SLM. The four layers of the PPP have been streamlined to enable operators and engineers to easily identify where sources of variation are likely to occur.

In completing this chapter, it has been noted that the SLM build process is reliant on the experience or knowledge of operators and engineers to produce optimal parts. Currently the SLM process and software has no capability for intelligent or independent automation. Although the aim is to make SLM systems fully automated and traceable, this is not yet fully achievable. Early adopters of this technology are not fully aware of the number of variables within the SLM process. Some attempt to control the process by only using one layer of the PPP and do not consider the interaction of subsequent layers or interactions of post processes.

It has been identified that the process foundation and the process setting layers are primarily the responsibility of the machine operator but are guided by knowledge from the OEM. In-process control has been shown to have significant potential for future application of the process, however, this is currently limited by the capability of the available technologies. Due to the necessity for post-processing, post-process inspection will always be required. It has been shown that post process inspection has the capability to inform earlier process stages. SLM specific parts can be produced in set locations and evaluated after the build has been completed. The data from these parts can feed back into the process setting stage to improve either precision or accuracy. Additionally, geometric data can inform process settings (including laser power, position and strategy) or can be used to complement in-process control giving context to PLC log data.

Chapter 4: Establishing the validity to the approach of measurement

4.1 Chapter Overview

As discussed in Chapter 2 research has identified that validating the measurement system is a critical step which needs to be completed before any process can be evaluated. This chapter reviews the correct tactile probing procedure set out in guides and standards before introducing the test artefact used in this study. The need to establish the efficacy of CMM-based measurement approaches in SLM applications is not widely appreciated. Within the sector however it is of great concern, as demonstrated by the organising of international meetings to consider in detail such requirements. A paper laying out the approach to be adopted in this research (O'Regan, P. et al. 2018) was presented at the American Society for Precision Engineering Summer Topical Meeting: Advancing Precision in Additive Manufacturing. Discussions and presentations at this meeting highlighted the problems associated with the measurement of the complicated forms of AM parts and the influence of often very poor surface finish on CMM measurements. This was followed by the consideration of a timely review of the state of the art recently published (Leach et.al 2019 a & b) which clearly demonstrated that the approach being utilised in this research was suitable and of value within the sector.

The CMM used is subjected to a Gauge Repeatability and Reproducibility (GR&R) study to validate its suitability and the measurements it provides are appropriate for the set tasks. The term “gauge” is used in this context to represent any measurement system, and is applied herein to represent the CMM. It should be noted that the GR&R analysis will be applied to compare and confirm the efficacy of the different procedures used to measure the same features on the same CMM.

4.2 Feature measurements

A feature measurement is usually obtained using a minimum specified number of measurement points. For every feature such as a straight line, circle, plane, cylinder, cone and sphere there are a minimum number of contact points that must be used to fit the feature to a geometry. For example, two points can define a straight line and three points can define a circle. Just using three points to create a circle will give no information on form error and can thus falsely represent the feature. Therefore BS 7172 – 1989 Guide to assessment of position, size and departure from normal form

of geometry (British Standards Institution 1989), recommends the minimum number of points per feature.

Figure 4-1 shows that two different diameters can be measured when only using the minimum number of touch points. The wavy line shown in Figure 4-1(B.) represents the outline of a hole. Two sets of three touch point have been made on the outline indicated by three blue dots and three red dots. A best fit line is applied to each of the corresponding coloured points and an arc is created and extrapolated to create a circle. Though the touch points are on the same outline their proximity and position provide different diameters when extrapolated. Spreading these touch points out and increasing the number of points taken can improve the accuracy of the measurement.

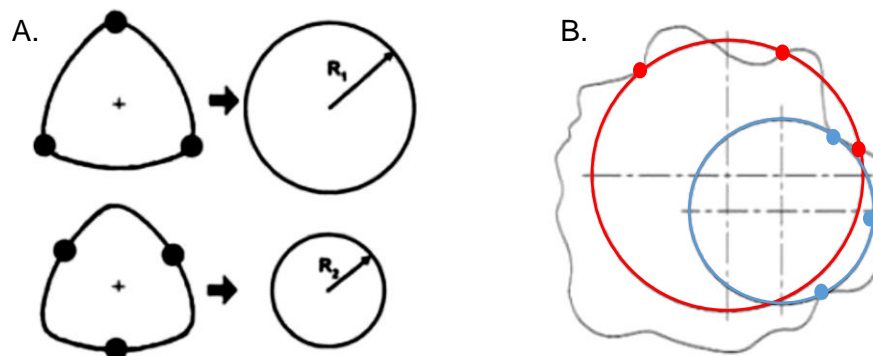


Figure 4-1 Wrong results because of A. Number of points used and B. Measuring strategy. Reproduced from (Chajda et al. 2008)

It can be shown to be important to use more than the mathematical minimum number of points so that geometric error can be determined. The points taken should also not be equally spaced, but taken with a suitable spread to ensure adequate coverage as this prevents or minimises the chance that systematic or periodic deformation in a geometry is missed. These requirements can be illustrated using a very simple example of a type of periodic distortion known as “lobbing”. Assuming that six points are taken equally on a 3-lobed “circle” it can be the case that the resulting circle may not detect the lobbing (see (A.) Figure 4-2). However, applying an alternative strategy and taking seven points on such a lobed circle means that the assessment will detect 79% for the amplitude of the lobbing (see (B.) Figure 4-2). It should be noted however that this remains an inadequate measure of the circular form being measured.

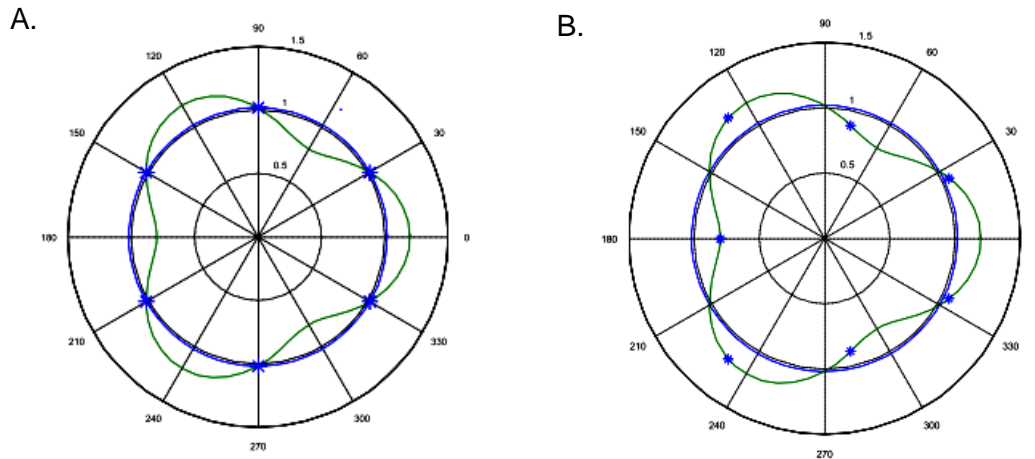


Figure 4-2 A. Six uniformly spaced points (*) with failure to identify lobbing. B. Seven uniformly spaced points (*) with 79% of the lobbing detected. Reproduced from (Flack 2001)

By using more than the mathematical minimum number of points to gather geometric data, more information regarding the part being measured can be interpreted, allowing the estimation of form related features, such as circularity. Circularity is normally expressed as a 2-dimensional tolerance that controls the form of a circle. It is used to describe how close an object is to a true circle. It is measured by taking a cross section of the object and assessing the roundness of the resulting shape. Cylindricity is a 3-dimensional tolerance that controls the overall form of a cylindrical feature using a tolerance that specifies the zone bound by two concentric cylinders within which the measured surface must lie. These characteristics are combined into one number, which represents the radial distance between two coaxial cylinders which are the boundaries that enclose the scanned surface. These features can then be evaluated based on their position. True position is the exact coordinate, or location defined by basic dimensions or other means that represent the nominal value.

Two of the most important concepts used in metrology are accuracy and precision. In this context accuracy relates to the closeness of agreement between a measured value to a standard or a known value or a reference value. The reference value may be taken from a traceable artefact feature or may represent an agreed true value of what is being measured. To be used a measurement gauge must be in a state of statistical control, otherwise the specified accuracy of the gauge has no meaning. If using a gauge to measure a particular feature of a traceable artefact produces a difference between the mean of repeated measurements and the true measurement, then this difference can be expressed as the bias. In this context bias expresses the systematic error in the measurement system (Barbato et al. 2010). It forms the contribution to the total error and it comprises of all the sources of variation, known

and unknown. Once a bias in a measurement is identified it can be accounted for, as long as it follows a known distribution and is not random.

Precision can be taken to represent the net effect of discrimination, sensitivity and repeatability over the operation range of the gauge. It is defined by the closeness of agreement between the values from a series of test results. For any measurement process high precision is a desirable characteristic, but it does not mean that the instrument is accurate. A measurement system is improved when the average value of a group of measurements gets closer to the target and the variation in the measurement is reduced.

4.3 Gauge Repeatability and Reproducibility

A GR&R study considers the combined estimate of the measurement system repeatability and reproducibility. All measurement systems can be affected by different sources of variation. This means that any part can be measured using the same system multiple times and the measurements produced may not yield the same results. Analysis of this variation in the context of a measurement system represents the gauge repeatability. The measurements will vary due to common and special causes. Common cause variations arise due to factors which are part of the measurement process. These are independent of each other and result in the random distribution of the output around the mean, their origin can usually be traced to the key elements of the system in which the process operates e.g. material, machine, environment and methods. If only common causes of variation are present, the output of the process forms a distribution that is stable over time.

Special cause variation results from an event which leads to an unexpected change in the measurement process output. The effects are intermittent and unpredictable, this means that overall the process is not stable and over time it will not be predictable. Analysis of this variation in the context of a measurement system represents the gauge reproducibility. These special causes of variation must be identified, detected and removed.

Figure 4-3 shows, using an Ishikawa diagram, the possible contributors to the CMM measurement system variability. These contributing factors must be considered when developing a new test piece to assess the capability of any SLM machine. In this investigation it is known that the CMM, environment and appraisers are all fixed variables. The CMM has been calibrated and validated to the appropriate standards so that the measurements taken are traceable. The laboratory environment is

controlled using a climate conditioning unit (temperature set to 20°C ±1°C) and in this study the same appraiser (the author) and equipment (the CMM) was used to provide consistency in the set up. The cause of most variation in this study can come from the test piece because of the manufacturing process and post-processing requirements. The test piece developed in this study satisfies all causal variations mentioned in the test piece branch, apart from cleanliness. Cleanliness for some SLM parts is more difficult than others dependant of the geometric design. In this case the geometry was designed to minimise cleaning issues, but due to the part size, there are physical restrictions in the cleaning process.

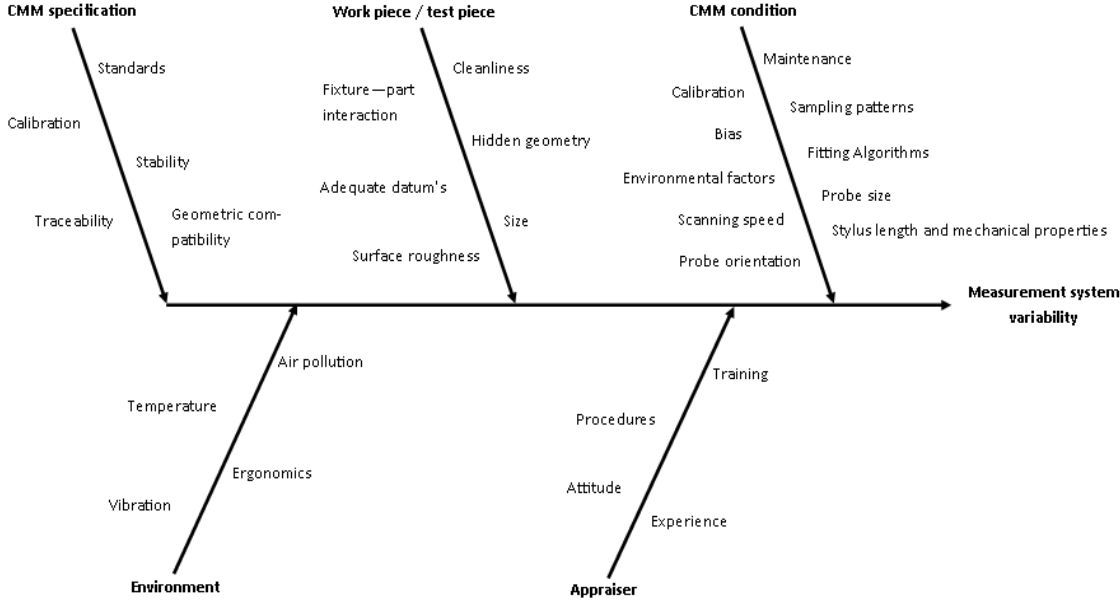


Figure 4-3 Measurement system variability Ishikawa diagram

4.3.1 GR&R using the Average and Range method

The calculation of measurement system variation is based upon the assessment of five contributions:

Equipment Variation (EV): assesses repeatability. This represents the variation in measurements taken when the same appraiser used the same gauge to measure the same characteristic on a part a number of times. When the measurement conditions are defined and fixed the variation in the measurements should be free from random error.

Appraiser Variation (AV): assesses reproducibility. This is conventionally assessed to indicate the variability between appraisers. In this case the CMM equipment was computer controlled and thus the actual measurement cycle was deemed free from appraiser related variation. However, to allow for potential variation in the setting up

of the test piece, measurement cycle enactment and related factors, sets of measurements were taken on different days. These were conducted using the same set up and procedures to measure the same characteristic on the same part. The results of the three measurements sets are compared and the variation between conditions is then taken to represent the conventionally assessed appraiser variation in the measurement process reproducibility.

Part variation (PV): is the variability between different components (part-to-part). In this study PV represents the variation between each test piece.

Repeatability and Reproducibility (R&R): represents the measurement system variation. This is calculated as the square root of the sum of the squares of the equipment variation and of the appraiser variation.

Total variation (TV): represents all three sources of variation and is calculated as the square root of the sum of the squares of the equipment variation, appraiser variation and part variation.

4.3.2 Development and use of a SLM test piece

The use of a test piece is a proven way to evaluate a manufacturing machine's ability to produce accurate and precise parts under pre-defined conditions. Specifications and standards exist for such test pieces for reductive manufacturing processes (British Standards Institution 2014). Currently there are no pre-defined test pieces developed for metal SLM. It is very likely that this deficiency will require that a similar approach to that used in reductive manufacturing be developed so that standard procedures can be used in future work to evaluate the process capabilities of the machine being used. One critical aspect of this work is to establish the suitability of available measurement systems to be used in support of this approach.

In this initial phase a method based upon the adoption of a simple geometric test piece, herein called a "bridge", was developed. This test piece was adopted in this research as there was an established body of work within the company in dental-related applications. The novel use of the test piece in this research related to the positioning of up to 12 such pieces around the build plate. The research also introduced the application of CMM based measurements to establish the dimensions and form of the various features embedded within the test piece. The bridge is made up of seven cylindrical elements each with an associated top plane, called "top-hats". Figure 4-4 shows the seven top-hat bridge test pieces printed on an AM-250 machine, removed from build plate and the corresponding computer aided design (CAD)

drawing of the bridge. The test piece developed in this study was created for the use in dental implant production. The shapes used are similar in shape and size to a large dental framework having features such as closed cups and connectors. It is not a test piece that will suit every component produced using a SLM machine. Such features could be used to evaluate spot compensation, X-Y scale factor, shrinkage and scan field error. The depth change in the cylinders could be used to assess height variation in the Z-axis and to provide datum so that the top-hat artefact is measured in the same direction.

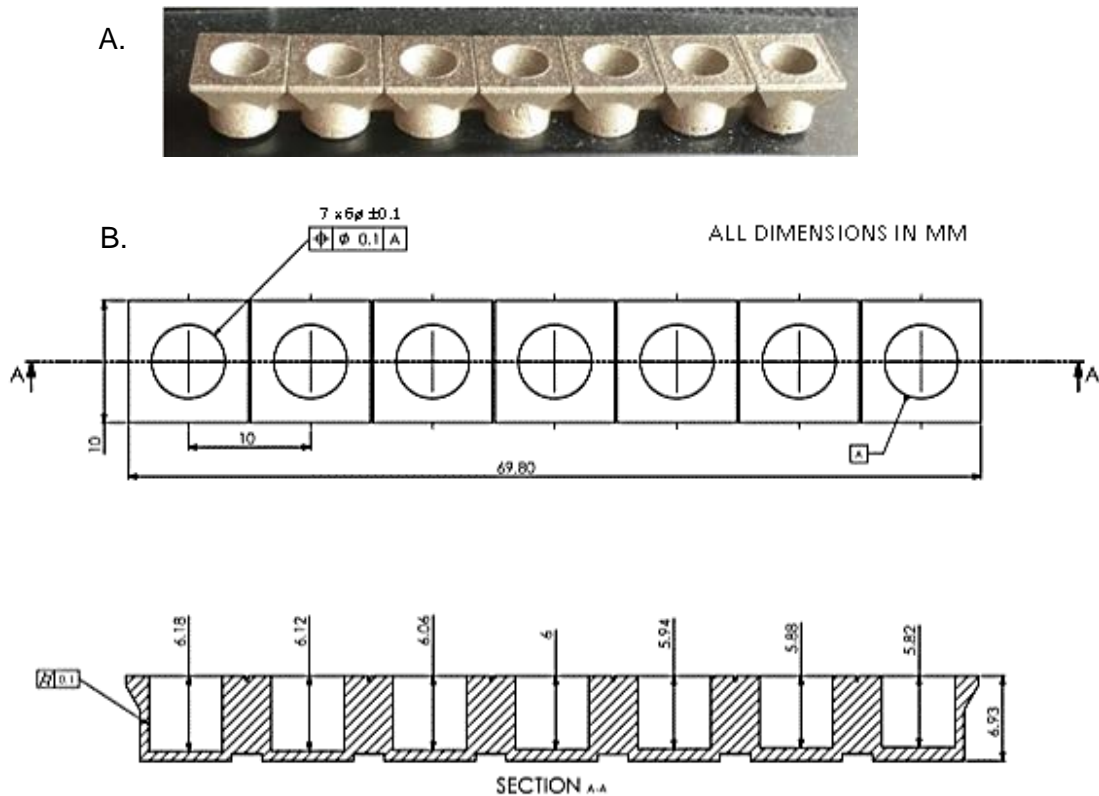


Figure 4-4 (A): A bridge made up of seven top hats (artefact) which has been removed from build plate, (B): CAD drawing of the bridge (artefact/test piece)

The test piece consists of seven cylinders of 6mm diameter each located within a 10mm square shaped plane positioned in a row. The depths of the cylinders vary from 5.82 to 6.18 mm and the centre of each cylinder is located 10 mm away from the adjacent cylinder. The test piece was produced with these incremental top-hat depths (which here represent +/- 3% in 1% increments) to provide the basis for subsequent analysis of the capability of the measurement system to identify that such changes

have been made. This step was necessary to enable more advanced R&R analysis on the varying depths (as described in Section 4.5).

The drawing of the test piece is shown in Figure 4-4 indicating the dimensions and tolerances of interest. The location of the twelve top-hat assemblies on the build plate are shown in Figure 4-5.

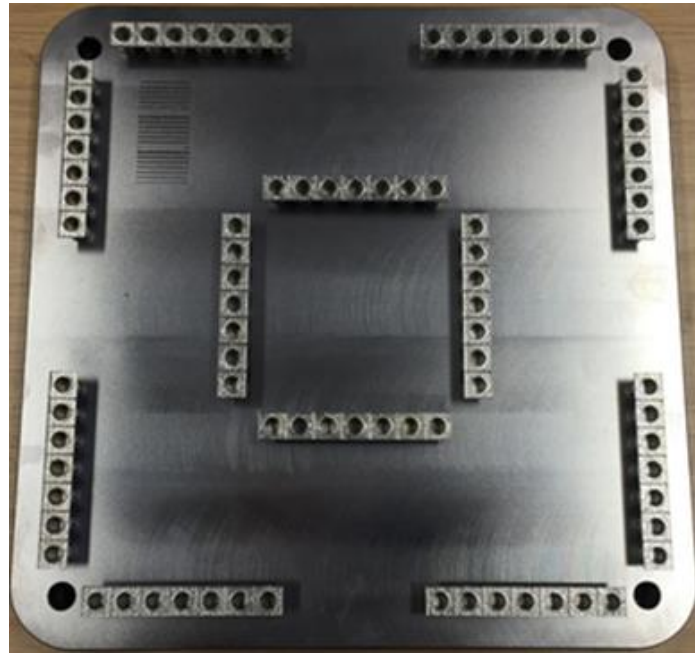


Figure 4-5 12 stainless steel top-hat assemblies on build plate

4.3.3 SLM top-hat manufacturing settings

The top-hats identified in Figure 4-4 were produced using the Renishaw AM250. The material used was stainless steel 316L-0410 powder, with a particle size range from 15-45 μ m, requiring a laser power of 200W (Appendix 3). This employs a modulated ytterbium fibre laser with a wavelength of 1.071 μ m, the nominal diameter of the focussed laser spot is 75 μ m. The scanning strategy employed for this study was meander, with a rotation angle between each adjacent layer of 67 $^\circ$ to eliminate the chance of scan lines repeating themselves directly on top of each other. The layer thickness of the deposited powder was set to 50 μ m (Renishaw Plc 2017). In a build volume of 250mm x 250mm x 300mm. The machine set up information used to produce all the parts on the plate is given in Table 4-1.

Table 4-1 AM250 fixed manufacturing settings for the production of a top-hat

Parameter	Value/Setting	Units
Layer thickness	50	µm
Shrinkage XY	-	%
Shrinkage Z	-	%
External support parameters		
Speed	150	mm/s
Power output	200	W
Focus offset	0	mm
Point distance	50	µm
Exposure time	90	µs
Meander-30 hatch style		
Layer path organisation	Inside to outside	
Volume border		
Speed	150	mm/s
Power output	110	W
Focus offset	0	mm
Point distance	20	µm
Exposure time	100	µs
Volume offset hatch		
Speed	150	mm/s
Power output	200	W
Focus offset	0	mm
Point distance	60	µm
Exposure time	80	µs
Volume area		
Speed	150	mm/s
Power output	200	W
Focus offset	0	mm
Point distance	85	µm
Exposure time	80	µs
Spot compensation	0.035	mm
Volume offset		
hatch offset space	0.0	mm
Volume area		
hatch space	0.11	mm
contour space	0.09	mm

The plate manufactured underwent a heat treatment process to stress relieve the part. The plate was heated to 1050-1120°C, held for an hour and cooled to room temperature under inert conditions using Argon. In this study the top-hat was measured once removed from the build plate.

4.4 Measurement process

The top-hat artefact in this study was measured using a Mitutoyo Euro Apex CMM fitted with a Renishaw REVO2. This study utilises a RSP3-3 probe fitted with a 2mm ruby and 100mm extension. The probe and REVO2 utilise a magnetic contact interface allowing the CMM to change probes using a rack situated in the machine volume. This is a fully automated procedure which minimises variation during setup. The CMM is controlled using MODUS a software application developed by Renishaw that communicates with the CMM using the dimensional measuring interface standard (DMIS) 5.2 standard (Consortium for Advanced Manufacturing - International 2004).

4.4.1 Set up and alignment

The key elements and associated statements of the MODUS program are outlined below. The full program is not shown here but it is included in Appendix 4. The intention of this section is to introduce the measurements taken and explore what information they can provide.

Firstly, the CMM environment is defined and the required probe is called and selected:

```
SNSET/APPRCH,0.5 $$Minimum approach distance for probe tip.
SNSET/RETRCT,0.5 $$Minimum clearance distance for probe tip.
D(0)=DATSET/MCS $$Re-calls and sets machine co-ordinate system.
T(CORTOL_X1)=TOL/CORTOL,XAXIS,-0.1,0.1 $$Sets axis tolerance for X.
T(CORTOL_Y1)=TOL/CORTOL,YAXIS,-0.1,0.1 $$Sets axis tolerance for Y.
T(CORTOL_Z1)=TOL/CORTOL,ZAXIS,-0.1,0.1 $$Sets axis tolerance for Z.
T(DIAM_1)=TOL/DIAM,-0.1,0.1 $$Diameter tolerance.

RECALL/SA(RSP3-3_SH25_3A_2x14.1.20.2.A0.0-B0.0) $$Loads probe build
into memory.
SNSLCT/SA(RSP3-3_SH25_3A_2x14.1.20.2.A0.0-B0.0) $$Selects the probe
if already in sets it.
```

Then the part is located using a manual alignment. To do this requires that the reference features are identified:

\$\$ Manual Alignment \$\$

```
MODE/MAN
F(PLN002)=FEAT/PLANE,CART,0,0,9.9,0,0,1 $$Defines the plane. (Top
surface of bridge)
MEAS/PLANE,F(PLN002),4 $$Take four points to define the plane.
ENDMES
F(CIR001)=FEAT/CIRCLE,INNER,CART,30,0,10,0,0,1,6 $$Defines the first
circle (top-hat hole 1)
MEAS/CIRCLE,F(CIR001),3 $$Take three points to define the circle.
ENDMES
F(CIR002)=FEAT/CIRCLE,INNER,CART,-30,0,10,0,0,1,6 $$Defines the
second circle (top-hat hole 7)
```

```
MEAS/CIRCLE,F(CIR002),3 $$Take three points to define the circle.
ENDMES
```

It is worth noting that by requesting the operator to “take” measurements some element of variation will arise in this process. Even the same operator is unlikely to take exactly the same points each time. Next a line is constructed bound by the centre points of circle 1 and circle 2:

```
F(LINE001)=FEAT/LINE,UNBND,CART,0,0,0.1,-1,0,0,0,0,1 $$Define the
line feature.
CONST/LINE,F(LINE001),BF,FA(CIR001),FA(CIR002) $$Construct the line
using the circle 1 and circle 2.
```

Lastly the part is located by defining the Part Co-ordinate System (PCS):

```
DATDEF/FA(PLN002), DAT(B) $$Plane 2 is datum B.
DATDEF/FA(LINE001), DAT(C) $$Line 1 is datum C.
DATDEF/FA(CIR001), DAT(D) $$Circle 1 is datum D.
D(2)=DATSET/DAT(B),ZDIR,ZORIG,DAT(C),XDIR,DAT(D),XORIG,YORIG
$$Setting PCS. So location of plane 2 defines the origin of Z the
normal to plane 2 defines the direction of positive Z. Line 1 defines
the direction of positive X. The centre of circle 1 defines the X and
Y origins.
```

The manual alignment produces an initial PCS which is essential to locate the part for subsequent CMM measurements. This location is then optimised by including a programmed computer numerical control (CNC) alignment. This procedure is enacted by the CMM controller and is repeatable and does not depend upon any actions taken by the operative.

```
$$ CNC Alignment $$
```

```
MODE/PROG,MAN $$Puts the CMM in programmed mode.
F(PLN003)=FEAT/PLANE,CART,30,0,0,0,0,1 $$Defines the plane. (Top
surface of bridge)
MEAS/PLANE,F(PLN003),4 $$Take the defined four points included in this
measurement block.
PTMEAS/CART,-4.092,4.052,0,0,0,1
PTMEAS/CART,-4.05,-4.06,0,0,0,1
PTMEAS/CART,64.009,-4.082,0,0,0,1
PTMEAS/CART,64.058,4.033,0,0,0,1
ENDMES $$End of this measurement block.
```

```
GOTO/CART,0,0,10 $$This is an automatic absolute machine movement.
```

This process is repeated for the other defined features (circles 1 and 2) introduced in the manual alignment. The PCS is then re-defined using the newly measured plane and circle features. At this point the part will be set-up within the CMM environment with respect to a defined datum.

4.4.2 Measurement of features

Measurement of the top and the bottom planes are separately defined using touch points as illustrated in Figure 4-6.

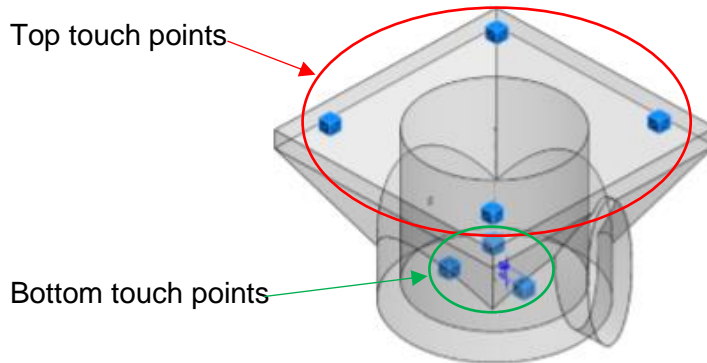


Figure 4-6 Planes defined with touch points on the top surface and bottom of cylinder

These are defined using the following DMIS code:

```
MODE/PROG,MAN $$Puts the CMM in programmed mode.
F (PLN001)=FEAT/PLANE,CART,60,0,-5.9,0,0,1 $$Defines the plane.
(Bottom surface of top-hat)
MEAS/PLANE,F (PLN001),3 $$Start of measurement block (3 points).
PTMEAS/CART,60.868,1.574,-5.9,0,0,1 $$Point 1
PTMEAS/CART,61.0,-1.048,-5.9,0,0,1 $$Point 2
PTMEAS/CART,59.913,-0.062,-5.9,0,0,1 $$Point 3
ENDMES $$End of this measurement block.
```

This has measured three points on the surface located at the bottom of the cylinder.

```
GOTO/CART,60,0,10 $$This is an automatic absolute machine movement.

F (PLN005)=FEAT/PLANE,CART,30,0,0.1,0,0,1 $$Defines the plane. (Top
surface of top-hat)
MEAS/PLANE,F (PLN005),4 $$Start of measurement block (4 points).
PTMEAS/CART,62.928,3.257,0.1,0,0,1 $$Point 1
PTMEAS/CART,56.574,3.543,0.1,0,0,1 $$Point 2
PTMEAS/CART,56.309,-3.723,0.1,0,0,1 $$Point 3
PTMEAS/CART,63.349,-3.484,0.1,0,0,1 $$Point 4
ENDMES $$End of this measurement block.
```

Each of the top-hat cylinders were measured using three different techniques. The first used nine individual point touches around the internal bore at the three different heights, illustrated in Figure 4-7 .

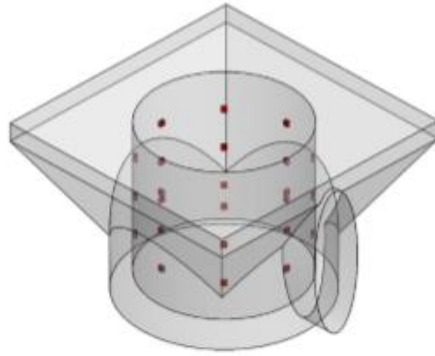


Figure 4-7 Cylinder defined with touch points

Where the corresponding DMIS instructions for one of the circles (7.1P) at one of the three heights (-0.5mm):

```
MODE/AUTO,PROG,MAN $$Puts the CMM in automatic mode.
F(CIR7.1P)=FEAT/CIRCLE,INNER,CART,60,0,-0.5,0,0,1,6 $$Defines inner
circle by diameter and centre co-ordinates.
MEAS/CIRCLE,F(CIR7.1P),9 $$Measure the circle taking 9 points.
ENDMES $$End measurement block.
```

The second utilised three circular scans around the circumference of the bore at three set heights, shown in Figure 4-8.

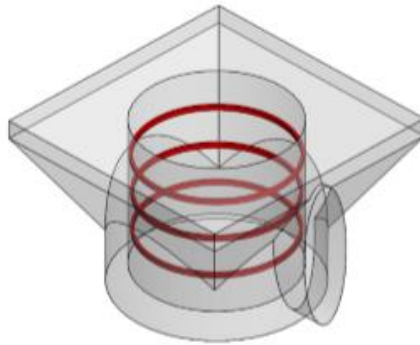


Figure 4-8 Cylinder defined with three circular scans and corresponding DMIS instructions for one of the three heights

Where the corresponding DMIS instructions for one of the three sweeps (7.1S) again at the first height (-0.5mm) is:

```
MODE/PROG,MAN $$Puts the CMM in programmed mode.
P(PArc4)=PATH/ARC,CART,60,0,-0.5,0,0,1,3,0,360,1,0,0 $$Defines the
scan path of the inner circle by radius, centre co-ordinates and angle
of rotation.
F(CIR7.1S)=FEAT/CIRCLE,INNER,CART,60,0,0.1,0,0,1,6 $$Defines inner
circle by diameter and centre co-ordinates.
MEAS/CIRCLE,F(CIR7.1S),9 $$Start of measurement block.
PAMEAS/DISTANCE,0.5,SCNVEL,MMPS,10,P(PArc4),-1,0,0 $$Measure the path
taking points every 0.5mm.
```

```
ENDMES $$End measurement block.
```

The last inspection employed a helical arc to scan the inside of the bore of the cylinder starting and stopping 1mm from the bottom and the top illustrated in Figure 4-9.

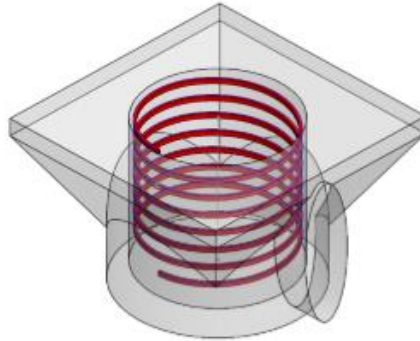


Figure 4-9 Cylinder defined with helix scan

Where the corresponding DMIS instructions for the helix scan is:

```
MODE/PROG,MAN $$Puts the CMM in programmed mode.  
P(PH1x2)=PATH/HELICAL,CART,50,0,-4.9,0,0,1,3,0,3600,1,0,0,0.4,0  
$$Defines the scan path of the inner circle by radius, centre co-  
ordinates with excess angle of rotation to give multiple sweep.  
F(CYL006)=FEAT/CYLNDR,INNER,CART,50,0,0.1,0,0,1,6,-6 $$Defines inner  
circle by diameter and centre co-ordinates.  
MEAS/CYLNDR,F(CYL006),6 $$Start of measurement block.  
PAMEAS/P(PH1x2),-1,0,0 $$Measure the path.  
ENDMES $$End measurement block.
```

4.4.3 Measurement output

Once all the features described in Section 4.4.2 have been measured the program outputs all the data into a .CSV file and .DAT file for evaluation. Below is an example of the DMIS extract showing the construction of a top-hat cylinder using the circles measured using points. Cylinders using sweeps are constructed in the same way. Nothing is needed for the helix scans as the data already represents a cylinder.

```
$$ CONSTRUCTING CYLINDER FROM CIRCLES  
F(CYL1P)=FEAT/CYLNDR,INNER,CART,-0.013,0.006,-  
2.495,0.01,0.002,1,5.805 $$Defining cylinder feature.  
CONST/CYLNDR,F(CYL1P),BF,FA(CIR1.1P)[1,9],FA(CIR1.2P)[1,9],FA(CIR1.3  
P)[1,9] $$Constructing the cylinder feature using the measured  
circles.
```

Here cylinder “1P” is being constructed using the three circles (1.1P, 1.2P and 1.3P) taken using the 9 points method.

After the cylinders are constructed the tolerances can be defined and printed for each named feature.

```
T(DIAM_1)=TOL/DIAM,-0.1,0.1 $$This defines the tolerance in this case +/- 0.1mm for the dia.  
T(1)=TOL/CYLCTY,0.1 $$This defines cylindricity where 0.1mm is the difference between the max-min cylinders.  
T(2)=TOL/POS,2D,0.1 $$This defines 2D true position.  
T(4)=TOL/CORTOL,ZAXIS,-0.1,0.1 $$This defines the distance in Z between the two planes.  
  
OUTPUT/FA(CYL001),TA(DIAM_1),TA(1),TA(2) $$This outputs the above for each named feature. (In this example printing diameter, cylindricity, and True position for cylinder 1.)  
OUTPUT/FA(PLN001),TA(4) $$Output the tolerance for each plane. (depth/height of cylinder)
```

The intention of using these different procedures was to establish the appropriateness of the measurement approach and compare the GR&R of each. It should be noted that these offer different solutions to the measurement of the cylinder. The helix scan is a direct measurement procedure in which a sequence of 133 points are used to produce a best fit of the associated constructed cylinder. The scanned circles indicate the form of the cylinder based upon a procedure that constructs the cylinder using the three scanned circles. Each circle is measured at a set height and is automatically constructed using 33 points generated around the circumference. No information can be acquired regarding the sections of the cylinder between these set heights. The touch point measurements were based upon acquiring the data relating to 9 points defined and measured around a similar set of three circles. In addition to providing no information regarding the sections of the cylinders between these heights, no information can be acquired regarding the sections of the circles between these points. This was an important element of this work as it provides evidence of potential impacts upon the measurement of future parts produced. To execute this operation a 2mm diameter ruby-tipped probe was utilised. This was carried out in the metrology laboratory that was environmentally controlled. The measurements were taken at a temperature of 20°C +/-1°C. The number of touch points and scan points were derived following established recommendations (British Standards Institution 1989) and (Flack 2001).

4.5 Conducting the GR&R

Before completing a GR&R study the resolution of the gauge needs to be assessed. It is generally accepted that the measurement system must have a resolution (RE) of $\%RE \leq 5\%$ of the characteristics specified tolerance in order to be able to reliably determine and observe measurement values. The measurements selected in this study are the diameter, cylindricity and true position of each cylinder and the position of the top and bottom planes of the artefact and the depth of the inclusions of the holes.

The reference figure (RF), or the specified tolerance (T), for the test piece elements was set to 0.2mm so the required indication of 5% of tolerance was equal to 0.01mm. The resolution of the CMM was taken as 0.001mm as stated by the equipment OEM. Given this information the %RE is calculated as 0.5% and the CMM was deemed to be able to provide the appropriate resolution.

Table 4-2 gives sample measurements from the GR&R study for the diameter of the top-hats. The top-hat diameters shown were calculated using the helix scan measurement explained previously (Section 4.3.4). Table 4-2 shows the results from 20 trials and the average ($\bar{X}_{a,b,c}$) and range ($\bar{R}_{a,b,c}$) for one measurement set for the first cycle. Also included are the part averages (\bar{X}) and average ranges (\bar{R}) for all three cycles in effect these three cycles correspond to the process required within this R&R procedure. Each cycle was performed from the start, with the part location in the fixture and the CMM alignment procedure being performed in each case. The intention was to replicate the actions of three appraisers within this set of computer controlled procedures. This provides all the information needed to complete the GR&R calculations. The information produced by the CMM for each feature and each measurement process was tabulated in a standard format and assessed. This was completed using Minitab and checked using Excel. As the results were similar Minitab was utilised for the remainder of the study as it is a specific designed statistical software.

Table 4-2 Prerequisite GR&R data for top-hat helix scan diameters for Appraiser 1 (A1) and A&R values for Appraisers 2 and 3 (A2, A3)

Trial	Part (mm)							Average (mm)
	1	2	3	4	5	6	7	
1.1	5.794	5.799	5.801	5.794	5.797	5.797	5.803	5.7979
1.2	5.794	5.798	5.801	5.794	5.797	5.797	5.802	5.7976
1.3	5.794	5.798	5.801	5.793	5.797	5.797	5.802	5.7974
1.4	5.794	5.798	5.801	5.794	5.797	5.798	5.802	5.7977
1.5	5.794	5.798	5.801	5.794	5.797	5.797	5.802	5.7976
1.6	5.794	5.798	5.801	5.794	5.797	5.798	5.802	5.7977
1.7	5.794	5.798	5.801	5.794	5.797	5.797	5.802	5.7976
1.8	5.794	5.798	5.801	5.794	5.797	5.797	5.802	5.7976
1.9	5.794	5.798	5.801	5.794	5.797	5.798	5.802	5.7977
1.10	5.794	5.798	5.801	5.794	5.797	5.798	5.802	5.7977
1.11	5.795	5.798	5.801	5.794	5.797	5.798	5.802	5.7979
1.12	5.794	5.798	5.801	5.793	5.797	5.797	5.802	5.7974
1.13	5.794	5.798	5.801	5.794	5.797	5.797	5.802	5.7976
1.14	5.794	5.798	5.801	5.794	5.797	5.797	5.802	5.7976
1.15	5.794	5.798	5.801	5.794	5.797	5.797	5.802	5.7976
1.16	5.795	5.798	5.801	5.793	5.797	5.797	5.802	5.7976
1.17	5.794	5.798	5.801	5.793	5.797	5.797	5.802	5.7974
1.18	5.794	5.798	5.8	5.794	5.797	5.798	5.802	5.7976
1.19	5.794	5.798	5.801	5.794	5.797	5.798	5.802	5.7977
1.20	5.794	5.798	5.801	5.793	5.797	5.798	5.802	5.7976
A1 Average	5.7941	5.7981	5.8010	5.7938	5.7970	5.7974	5.8021	$\bar{X}_a = 5.7976$
A1 Range	0.001	0.001	0.001	0.001	0.000	0.001	0.001	$\bar{R}_a = 0.0009$
A2 Average	5.7937	5.7982	5.8017	5.7938	5.7970	5.7975	5.8031	$\bar{X}_b = 5.7978$
A2 Range	0.0010	0.0010	0.0010	0.0010	0.0020	0.0010	0.0010	$\bar{R}_b = 0.0011$
A3 Average	5.7937	5.7980	5.8012	5.7936	5.7967	5.7971	5.8026	$\bar{X}_c = 5.7976$
A3 Range	0.0010	0.0000	0.0010	0.0010	0.0010	0.0010	0.0010	$\bar{R}_c = 0.0009$
Part Average	5.7938	5.7981	5.8013	5.7937	5.7969	5.7973	5.8026	$\bar{X} = 5.7977$
								$R_{\bar{p}} = 0.0088$
								$\bar{R} = 0.0010$
								$R_{\bar{X}} = 0.0003$
								$R_{\bar{R}} = 0.0003$

4.5.1 Average and Range method for GR&R

The steps required to complete the average and range method for GR&R are indicated below. This considers the information provided in Table 4-2 from the first run, designated as Appraiser 1 (A1), which uses the diameter of the top-hat holes measured using the data acquired from the helix scan measurements. The measurement results for Appraisers 2 and 3 (A2 & A3) are provided in Appendix 5.

The first step is to calculate the average and range for each cycle and appraiser. The average range for the three appraisers is calculated by:

$$\bar{\bar{R}} = \frac{\bar{R}_a + \bar{R}_b + \bar{R}_c}{3} \quad (4-1)$$

The difference between the maximum appraiser average and the minimum appraiser average:

$$\bar{X}_{Diff} = \bar{X}_{App Max} - \bar{X}_{App Min} \quad (4-2)$$

The range of the part averages (R_p) is the largest part average minus the smallest part average:

$$R_p = \bar{X}_{Part Max} - \bar{X}_{Part Min} \quad (4-3)$$

The individual contributors to the measurement system variation can now be calculated:

Equipment Variation (EV):

This measures the variation arising for one appraiser when measuring the same part (and same characteristic) using the same gauge. It is given by;

$$EV = \frac{\bar{\bar{R}}}{d_2} \quad (4-4)$$

Where:

\bar{R} = the average variation range of the repeated measurements for all parts.

d_2 = correction factor for values. This is linked to the distribution of average variation taken from Table A4 Appendix 6.

Appraiser Variation (AV):

This is the variation in the average of the measurements made by the different appraisers when measuring the same characteristic on the same part. It is given by;

$$AV = \sqrt{\left(\frac{\bar{R}_{diff}}{d_2}\right)^2 - \left(\frac{EV^2}{(n)(r)}\right)} \quad (4-5)$$

Where:

$$\bar{R}_{diff} = |\bar{R}_{max} - \bar{R}_{min}| \quad (4-6)$$

\bar{R}_{max} = largest arithmetical average within the acquired measurement sets.

\bar{R}_{min} = smallest arithmetical average within the acquired measurement sets.

n = number of trails, r = number of parts

$d_2 = d_s^*$. Where d_2 is determined by cross-referencing three appraisers (m) against the one range calculation (g). See Table A4 in Appendix 6.

Part variation (PV):

This represents the part to part variability between different components. It is calculated using:

$$PV = \frac{R_p}{d_2} \quad (4-7)$$

Where:

R_p = the variation range from the measurement of arithmetic mean of the individual repeats for the individual subgroups of the parts.

d_2 = is dependent on the 7 parts (m) and the 1 range calculation (g) (see Table A4 Appendix 6).

Reliability and Reproducibility (R&R):

The measurement system variation for repeatability and reproducibility (R&R) is calculated by adding the square of the equipment variation and the square of the appraiser variation and taking the square root.

$$R\&R = \sqrt{EV^2 + AV^2} \quad (4-8)$$

Once each of the above factors have been determined they can be compared to the tolerance (T). This tolerance is set by the process requirements pertaining to this artefact. In this case this is set to 0.2mm. It should be noted that this is not representing the general capability of the CMM, but is applying the R&R analysis to this artefact. Consideration of the CMM capabilities would be associated with the investigation of the absolute displacement measurement error, which lies outside the scope of this thesis. The nature of the R&R analysis lends itself to such process specific considerations. This is demonstrated in relation to ALM artefacts by Leach et al. (2019a). The percentage R&R, EV, AV and PV can be calculated using equation 8, by replacing each instance of R&R with the appropriate term. %R&R includes both EV and AV. Where %EV is the percentage of the tolerance attributed to the equipment variability and %AV is the percentage of the tolerance attributed to the operator. %PV is the percentage of the tolerance attributed to part-to-part variation.

$$\%R\&R = 100 \left(\frac{GRR}{T} \right) \quad (4-9)$$

These indicate the results when using data from Table 4-2, A1 and A2. The tolerance represents +/- 3 standard deviations and is therefore divided by six because EV, AV and PV only represent one standard deviation. Table 4-3 shows the average and range GR&R results for all measurement techniques.

The outcome for the average and range method helps engineers make informed decisions regarding their gauge. Whether it is acceptable, conditionally acceptable or not acceptable based on the results of the %R&R. If the %R&R is < 10% then the measurement system provides reliable information about process changes. If the

%R&R is 10% - 30% the measurement system can be used for some situations, but would rely on the operator understanding the limitations of the gauge. If the %R&R is > 30% the measurement system is not acceptable and is unable to provide reliable information about the process changes.

4.5.2 GR&R Results and Analysis

Table 4-3 shows the gauge variation as a percentage of the tolerance for all of the GR&R procedures. Each entry in this table represents the completion of a procedure produced using data similar to that included in Table 4.2 and Appendix 7. The data used to perform this analysis is too large to be included in this thesis and is available by request from the author's supervisors. The GR&R is composed of the equipment and the appraiser variation (explained fully in Section 4.4.1). Where GR&R percentages (Table 4-3) are less than 10% the gauge may be deemed to be capable of providing reliable information about the process changes and thus the gauge is acceptable to inspect the top-hats to a tolerance of 0.2mm. Where percentages are between 10-30% (highlighted in Table 4-3) the top-hat can be measured to a tolerance of 0.2mm, but the information has to be used carefully and in context. Here the consideration of this context has to include both the measurement process and the measured part. Both have potentially high levels of uncertainty due to surface roughness, un-melted powder, and size of ruby due to access. These uncertainties may contribute to the marginal process capability observed for cylindricity and true position. Considering the measurement of cylindricity it is possible to state that the form measurement is based upon an initial acquisition of scanned data, which allows the definition of the centre (X and Y position) and Z-axis around which the ideal cylinders may be constructed. Herein, only the helix scan attempts to directly measure the cylinder, both the circular scan and touch point methods rely upon procedures to construct and assess the measured cylinders. The measured cylinder is then fitted between two such ideal cylinders, the difference between which are used to define cylindricity. This is a convoluted procedure which can be affected by the process of establishing best fits to establish the axis and cylinders needed. No results are above the upper threshold (30%) for the EV, AV, and GR&R therefore the measurement system being used is suitable (Barbato et al. 2010).

Table 4-3 The results of the average and range method for all the scan strategies mentioned in Section 4.3 in relation to the tolerance

Measurement process	Feature	% to Tolerance			
		EV	AV	GR&R	PV
Helix scan	Diameter	0.84	0.48	0.97	9.51
	True Position	14.88	9.86	17.85	648.45
	Cylindricity	7.15	0.93	7.21	15.51
Circular scans	Diameter	0.99	2.97	3.13	11.96
	True Position	12.09	8.44	14.74	74.46
	Cylindricity	4.90	1.83	5.23	36.43
Touch Points	Diameter	3.06	4.20	5.19	8.57
	True Position	14.73	0.00	14.73	61.22
	Cylindricity	10.67	3.38	11.19	30.59
Top Plane		8.80	9.74	13.12	52.18
Bottom Plane		8.68	11.20	14.17	345.85
Depth		0.96	1.58	1.85	384.51

It is noted that the results for the PV range from 8.57-648.45. These are an indication of high process variability and not the variability of the gauge. As the measurements are compared to a given process tolerance, a high PV indicates that the given tolerance is too narrow, and the process is not capable of meeting it. It should also be noted, however, that a higher PV will arise when there is variation designed into the process. An example of designed variation would be the depth measurements. Nevertheless, if designed variation is outside of the requested tolerance, then the requested tolerance should be reviewed. The high PV values indicate that there is, for some cases, significant process variation. As all of the GR&R results are either acceptable or marginal, the process should be investigated further, however, the CMM (according to Table 4-3) would be suitable as an enabling technology for this.

4.5.3 Measurement analysis X-bar R charts process capability

To present the results obtained from the processing of these GR&R measurements in a more meaningful way and to support further analysis, a series of X-bar and R charts were produced using Minitab17. Figure 4-10 shows the chart for the top-hat diameters derived from the helix scan, circular scans and touch points. In each case this data is formed from three cycles of sets of twenty repeated measurements of the same test piece. Adopting this style of presentation makes it possible to consider how the measurement variations are represented within the acquired results. The mean subgroup measurements ($\bar{\bar{X}}$) indicate that the helix scan and the circular scans have the same mean (5.798mm), but different data ranges (0.011mm versus 0.013mm). The diameter derived from the touch points has an increased mean (5.801mm) and greater range (0.014mm). This represents a shift of 3 μm , shown in Figure 4-10, when comparing the diameter derived from the helix scan or the circular scans to the diameter derived from the touch points.

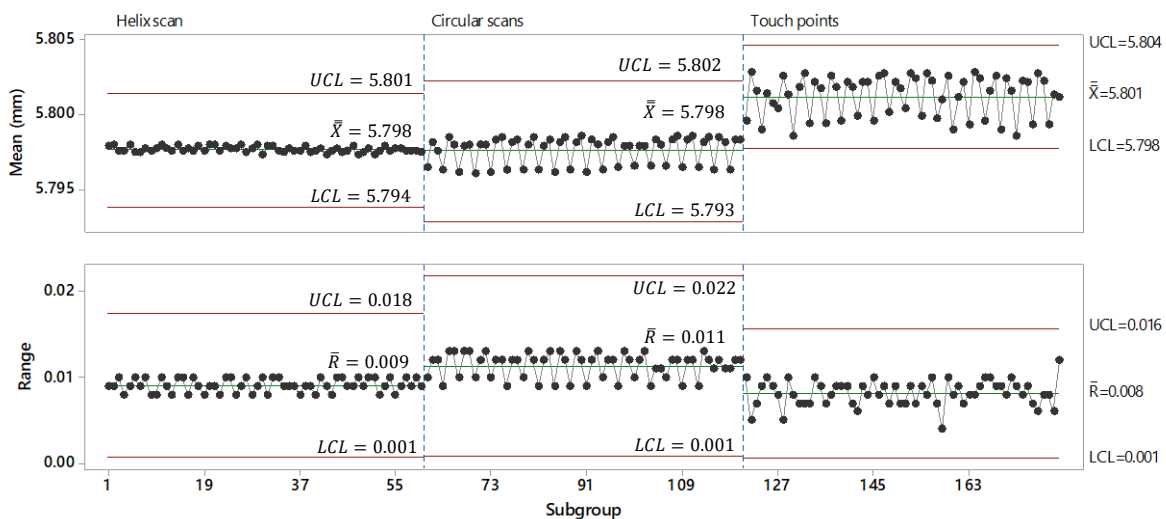


Figure 4-10 X-bar R chart for the top-hat diameters derived from helix scan, circular scans and point measurements. Made up of 60x7 subgroups (produced using Minitab17)

Figure 4-11 shows an X-bar R chart for the top-hat cylindricity measurements derived from the helix scan, circular scans and touch point measurements. In this case the point measurements resulted in a smaller mean (0.052mm) versus the helix scan and the circular scans measurements (0.064mm). The largest range was produced by the touch points (0.008mm) compared to the circular scans (0.004mm) and the helix scan (0.006mm).

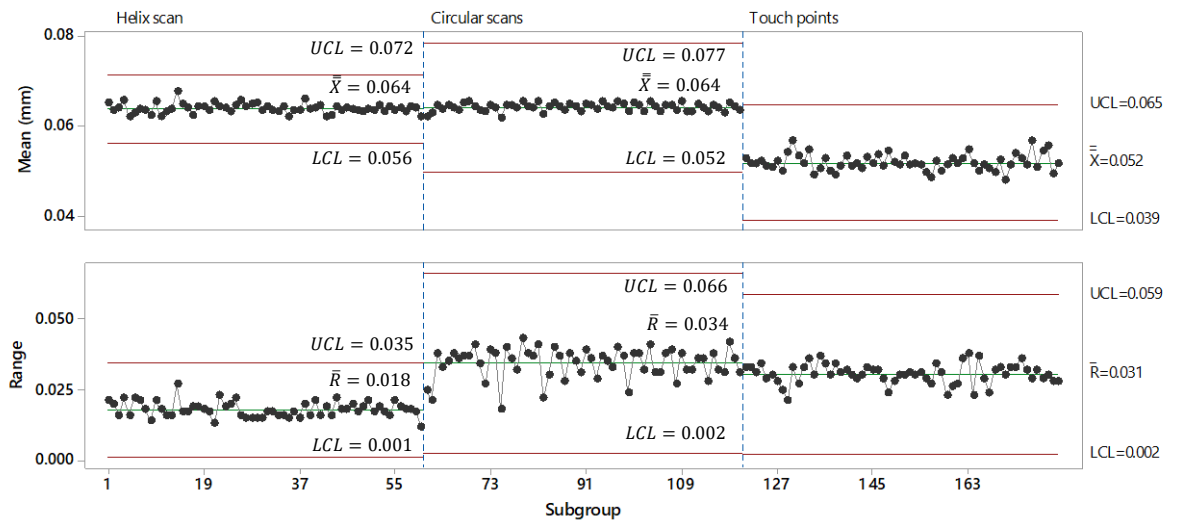
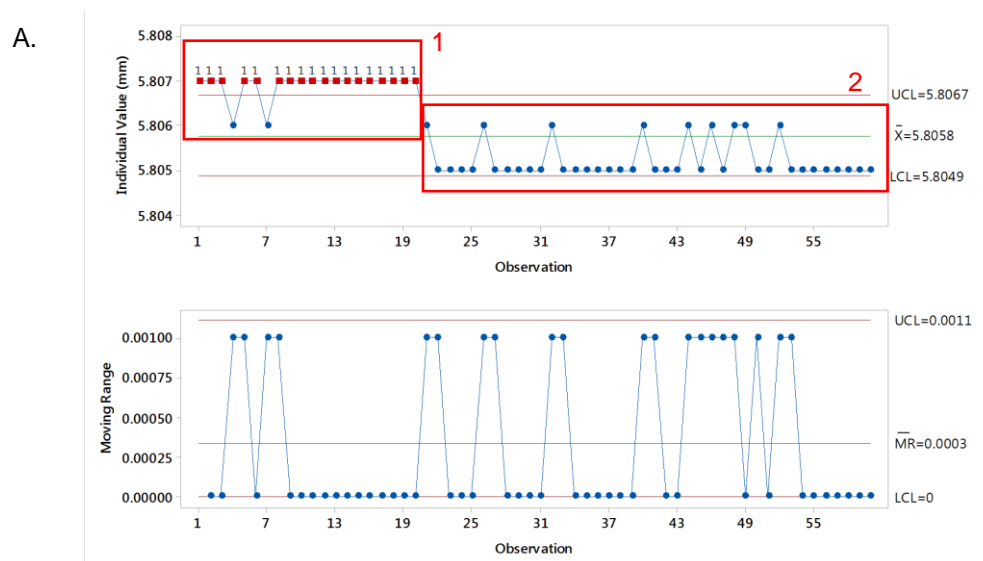
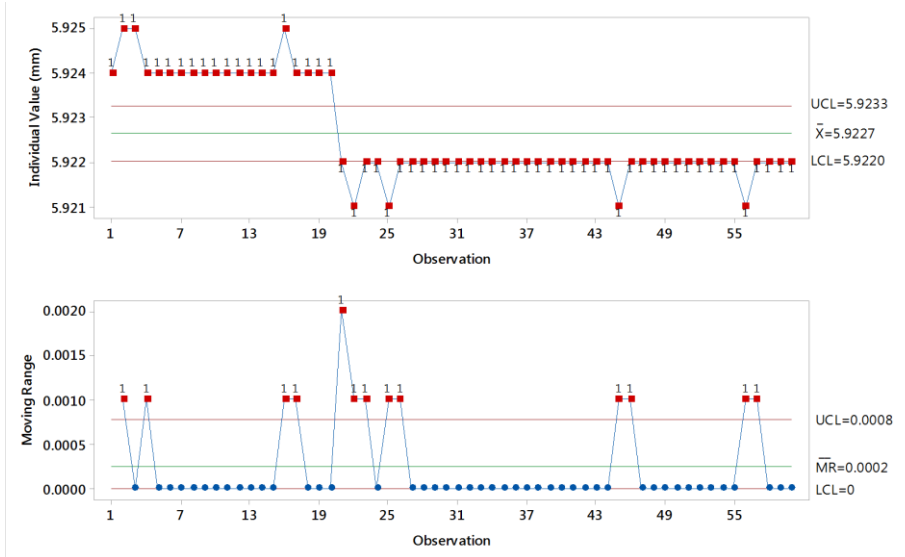


Figure 4-11 X-bar R chart for the top-hat cylindricity derived from helix scan, circular scans and point measurements. Made up of 60x7 subgroups (produced using Minitab17)

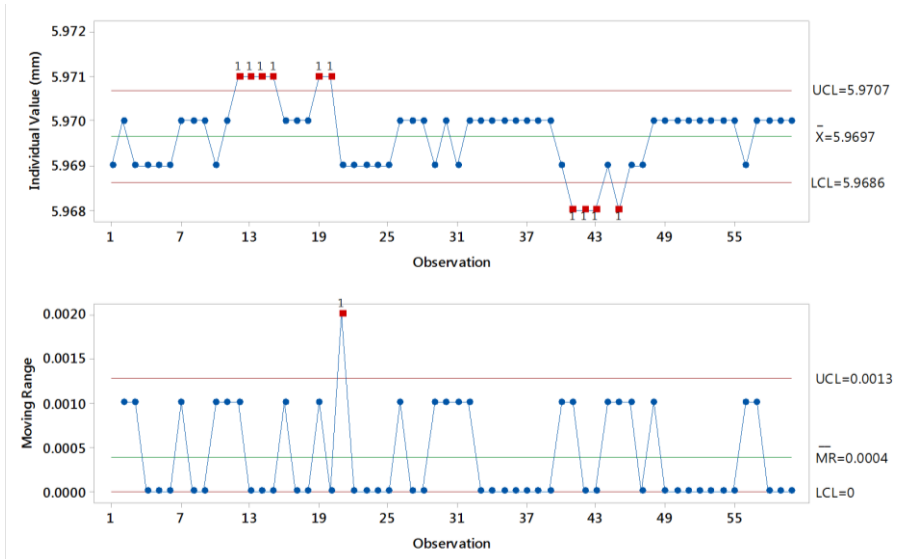
Figure 4-12 shows individual value and moving range (I-MR) charts for all the top-hat depths across a bridge. The mean average for each of the depths are: A. 5.806mm, B.5.923mm, C. 5.970mm, D. 6.003mm, E. 6.063mm F. 6.136mm, and G. 6.169mm. Most of the charts (except for A and B) indicate that the depths derived from the top plane and bottom plane are within the upper and lower control limits. There is also a distinct shift between the measurements taken by appraiser one (Figure 4-12A. region 1) compared to appraiser two and three (Figure 4-12A. region 2). Excluding Figure 4-12B. and Figure 4-12C., it is observed that the measurements are under control. The distinct measurement shift will be discussed in Section 4.5.



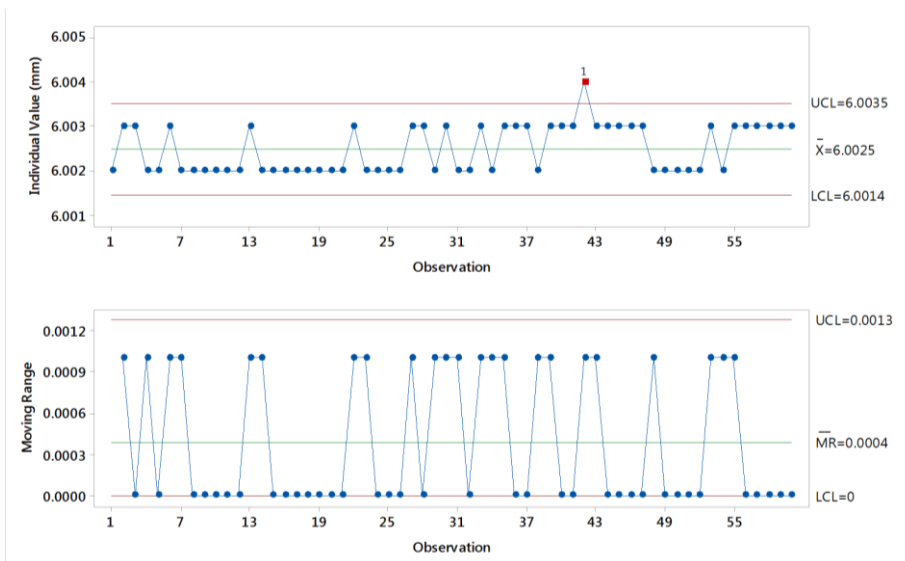
B.



C.



D.



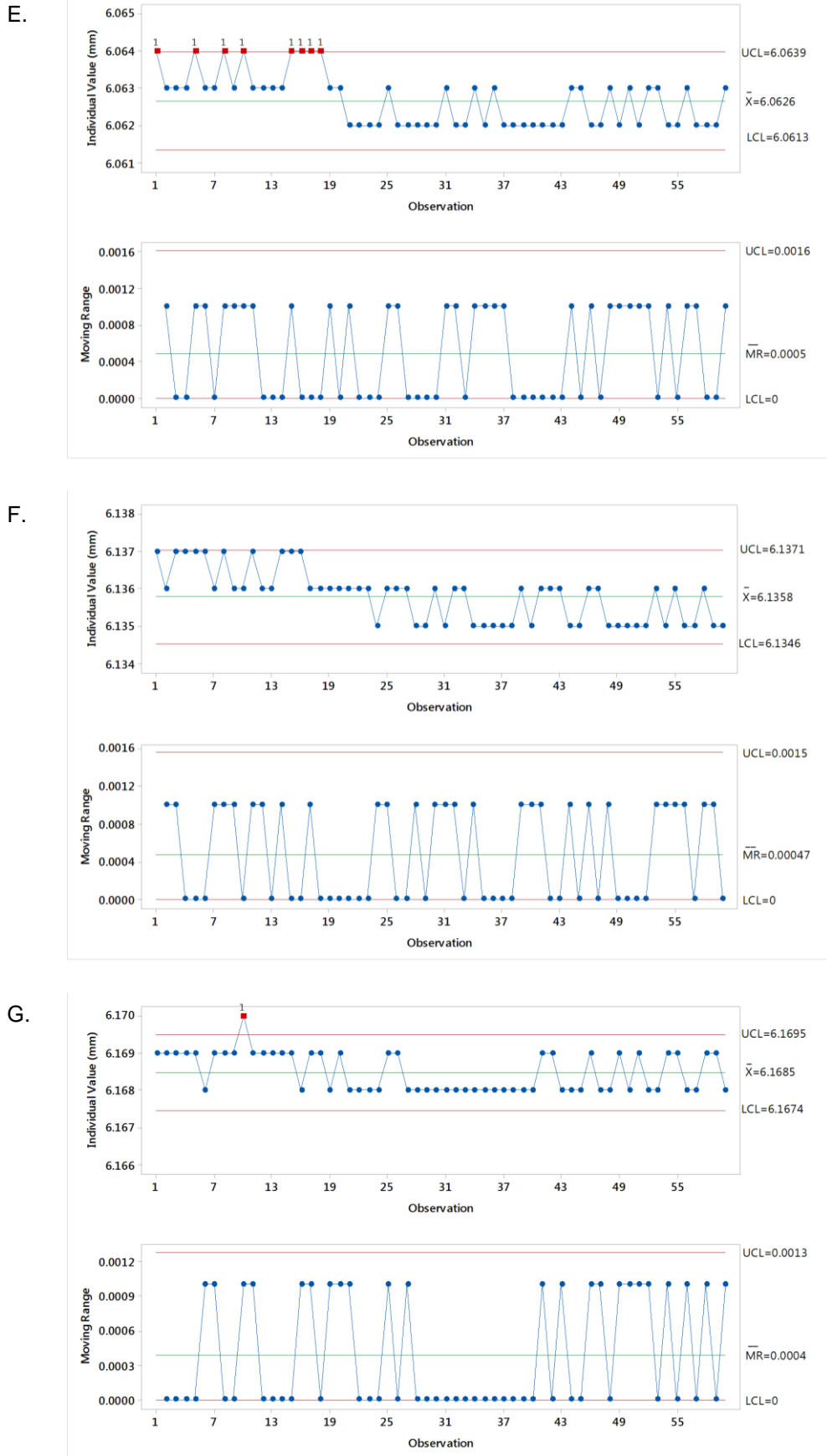


Figure 4-12 I-MR charts showing the top-hat depths across a bridge for: (A.) top-hat one (B.) top-hat two (C.) top-hat three (D.) top-hat four (E.) top-hat five (F.) top-hat six (G.) top-hat seven

4.6 GR&R discussion

When practitioners and researchers decide to create or use an artefact to set up their process, in this case an SLM machine, they must think carefully about how they are going to measure that artefact. The artefact presented may appear simple, but the analysis is not. SLM is capable of producing complex three dimensional shapes, but using these complex shapes to complete a gauge study would be extremely difficult and may not provide information that can be trusted.

The GR&R used in this study was the Automotive Industry Action Group (AIAG) GR&R study. The AIAG GR&R study was chosen because it is the study described in (International Organization for Standardization 2011) “selective illustrations of gauge repeatability and reproducibility studies”. Alternative GR&R approaches, such as the study created by Donald J. Wheeler (Wheeler 2009) could also be applied to the measurements taken in this study. The AIAG GR&R study was developed by the automotive industry to identify if the gauge being used is capable of identifying geometrical change in critical features on parts produced during different production runs. It is intended as a tool to identify the source of measurement variation, whether from the gauge used or from the production process.

The development of the test piece in this study allowed the gauge evaluation to be carried out with only one part, rather than taking multiple parts from different batch runs. To ensure that variation between parts could be identified the test piece was produced with incremental top-hat depths (+/- 3% in 1% increments (Section 4.4.3)). The GR&R identified that the depths were distinctly different and that the gauge could identify the variation in the top-hat depths. This indicates that the gauge could identify when a feature changes by 60µm. The GR&R results showed that the depths are precise to 0.002mm, which is 100 times better than the required tolerance of 0.2mm. As discussed in Section 4.4.2 this is smaller than 5% of the feature tolerance and is an indication that variation in the manufacturing process can be observed.

As well as identifying which features were important, this study also considered different CMM tactile probing techniques (Section 4.3.4). The results indicated (Section 4.4.3) that the number of points contributes greatly to the precision of the measurement. This confirms information previously published (Flack 2001). The diameter results indicate the gauge was suitable for all techniques when using the manufacturing tolerance. Using a tolerance provides the measurements with context and defines the boundary of what is acceptable. Results suggest that preference should be given to circular scans or helix scan measurement techniques. The

measurements derived using helix scan or circular scans for the diameter of each top-hat indicated that the gauge precision is 131 greater than the required tolerance of 0.2mm compared to 26 times when using touch points. Although the nine-point strategy was found to be less precise in this study it is still a viable measurement technique for this test piece.

The cylindricity measurements indicated a similar pattern to the diameter measurements in that the performance is shown to improve with more points. There was a distinct shift in the mean from 0.052mm for 9 points to 0.064mm when using the circular scans and the helix scan. The helix scan records 133 points circumferentially from the bottom to the top of each cylinder and the circular scans strategy takes 99 points at three different heights within the cylinder (refer to Figure 4-7 to Figure 4-9). Using these measurement strategies provides more information about the form of the cylinder and will include more of the surface features. With the increased number of points Modus is able to accommodate variations associated with surface localised peaks and troughs. This results in a better representation of the radial distance between two coaxial cylinders, which are the boundaries that enclose all the scanned points.

Though the top and bottom planes used close to the mathematical minimum number of points to derive the feature being measured they appear susceptible to marginal GR&R. The measurements for the top and bottom planes were precise to 0.029mm, which is 6.8 times better than the required tolerance of 0.2mm. Due to the number of points taken these measurements may be susceptible to error. The number of points used for the bottom plane measurements was the mathematical minimum (3 points). The marginal GR&R in this case could be due to the tactile probe not being able to return to the exact same touch point when measuring the bottom plane. This could be caused by the surface friction and/or the surface finish at the bottom of the holes. Other research has suggested that using the largest viable probe diameter may be effective in reducing uncertainty due to surface roughness. However, as a large probe diameter acts as a mechanical low pass filter, a systematic deviation is to be expected for such measurements. It is interesting to note that a conflict may arise between the suggestion that a larger diameter probe can be used to improve repeatability and the requirement to measure features with restricted access. Due to the access restrictions in this study, neither increasing the number of points taken nor increasing the probe diameter was possible for the bottom plane measurements.

The top-hat depths measured were all within 16µm of the target value apart from top-hat 2 which varied by 43µm. Despite the top and bottom plane measurements being marginal, the depth measurements are well within the tolerance of the part. The run charts indicate a difference between appraiser one and appraiser two and three. In this case the variation in top-hat 2 (Figure 4-12 B) was found to be caused by partly-melted powder sitting at the bottom of the cylinder. Having been detected this was dislodged before subsequent measurement cycles. This is an interesting point that should be considered carefully. In effect, the presence of the residual powder may be taken as a “special cause” and its effect carefully noted. Attention could be drawn to the need for an improved cleaning treatment but it is of course very difficult to detect such instances. It could be argued that any related effect should not be included in the measurement assessment.

The critical features of the top-hats (diameter and depth) have shown a large redundancy in the capability of the gauge when measuring to the current tolerance. This redundancy is important to ensure that the gauge is still capable when considering tighter tolerances. With the improvement in manufacturing process control and the development of advanced technologies this is inevitable.

4.7 Chapter summary

A test piece has been developed (top-hat) that allowed a gauge evaluation to be carried out with only one part, rather than taking multiple parts from different batch runs. The AGIG GR&R study was used and also considered the information presented in X-bar R charts and I-MR charts. The Gauge evaluation proved that the CMM based measurement system used in this study is capable, when used with caution, of being applied to the measurement of form based elements. This was expanded to consider three tactile probing techniques (helix scan, circular scans and touch points). It was shown that all three tactile probing techniques are capable, however, results suggested that preference should be given to circular scans or helix scan based measurement techniques.

The critical features of the top-hats (diameter and depth) have shown a large redundancy in the capability of the gauge when measuring to the current tolerance. There is no doubt that given the tolerance used in this study the gauge can measure the developed SLM top-hat, nevertheless it is accepted that most parts produced using SLM are one-off components and completing a GR&R on such components is difficult, especially if they have very complex geometries and high values of surface finish.

This study has therefore provided the ability to assess and evaluate the capability of the SLM process using the top-hat with confidence that gauge variation is not significant.

Chapter 5: Artefact appraisal and use in process assessment

5.1 Chapter Overview

The CMM measurement process has been validated using the GR&R method shown in Chapter 4. This chapter will consider the use of the artefacts to confirm the appropriate enactment of the SLM process. Current quality assurance procedures require the direct measurement of the often complicated parts produced in each build. This is often very challenging and potentially time consuming and expensive. The intention underpinning this research is that the adopted test piece can be included within all builds and assessed to confirm that the build process was enacted correctly. The intention is that by adopting such a procedure more knowledge can be established as each build is undertaken, in effect forming a set of data appropriate to each individual machine. The knowledge thus generated will also be of potential use across users who operate similar machines. Users of other machines may adopt this approach to produce similar levels of knowledge for their own applications. Before evaluating each cycle of the SLM process and thereby affirming its capability, it is necessary to determine at which stage the artefacts should be measured. There are three stages at which measurements can be taken after the parts have been produced. This chapter will evaluate these and identify which one provides the most suitable measurement opportunity.

5.2 Artefact Condition

This study is designed to provide a structured approach which can be used and improved over time to evaluate an SLM process. With this knowledge, it is important to consider this study in an industrial setting. Knowing when to evaluate a part is an important consideration in any manufacturing process. Finding the optimal point for evaluation will save time and money on further manufacturing processes. SLM parts, as discussed previously, need one or more post-processes for mechanical and/or geometric reasons (Chapter 3).

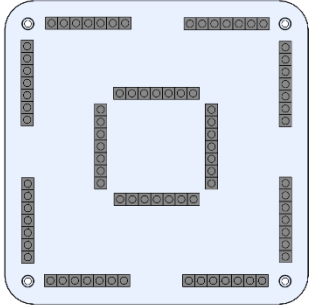
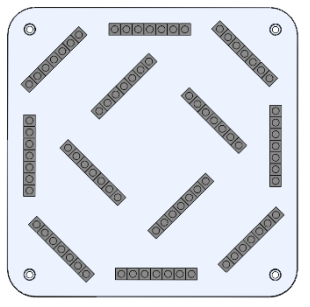
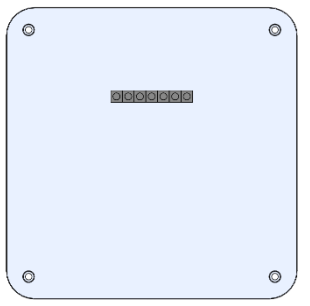
In this study the artefacts are measured at three stages of the post-process. When the parts have been produced they are removed from the AM250 machine and firstly cleaned using a brush; the build plate and artefacts are then shot peened to remove any remaining partly melted powder. A by-product of the shot peening is a “smoothing” of all external surfaces. This condition (stage) will be referred to in the

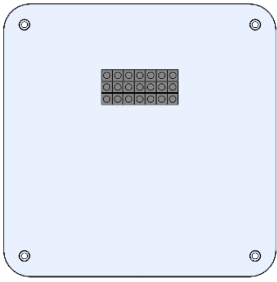
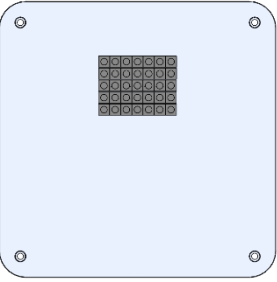
rest of this work as “pre”. After the build plate and artefacts have been measured in the “pre” state they undergo heat treatment (which is explained in more detail later in this section). The build plate and artefacts are then shot peened again to remove any oxidation. This new condition (stage) is referred to as “post” and, once complete, new measurements are taken. The third condition (stage) is “off” which represents that the artefacts have been removed from the build plate using a band-saw and then measured.

It is important to understand how these processes influence the geometry of the part. Knowing this can reduce the number of measurements required therefore saving valuable time when assessing the capability of the SLM process. To do this, a set of significance tests will be carried out to quantitatively assess the geometry of the artefacts in each of the three conditions.

During the life of this study, 14 plates have been produced under the same conditions, using the same material and with the same process settings. Alternative layouts were used to support related masters level studies being conducted under the supervision of the author within this laboratory. A modified arrangement of the 12 test pieces at different locations was applied in plate 4. This was not formally considered in this research. Plates 5,6 and 7 were formed as part of a related project investigating the influence of build densities. These plates were also not formally considered in this research. In both studies no discernible effects arose from the changes made, and thus the work was not developed further in this research. Table 5-1 provides an overview of these 14 plates providing a layout diagram and observations that occurred during the full process. In this chapter, plates 1-3 and 8-12 will be of interest. These plates all have the same layout and have been built using the same machine settings, (see Table 4.1) were exposed to the same post-processes, but were built at different times over the duration of this research.

Table 5-1 Build plate layout and process observations.

Plate number	Build layout	Observations
1		<ul style="list-style-type: none"> • Problems with heat treatment. • Parts cut off and the bottom of the top hats removed. • Version 1 of the modus program.
2	See plate 1	<ul style="list-style-type: none"> • Problems with heat treatment. • Half the parts cut off and had the bottom of the top hats removed. • Version 2 of the modus program.
3	See plate 1	<ul style="list-style-type: none"> • AM250 was subject to a yearly calibration carried out by Renishaw. • Argon failure during heat treatment.
4		<ul style="list-style-type: none"> • Different orientation with overlapping holes to see if diameters changed when the part was rotated by 45 degrees. • Argon failure during heat treatment.
5		<ul style="list-style-type: none"> • Builds 5, 6, and 7 were completed for another project looking at the density of parts and the effect of proximity on geometry. • One top hat made in the 12 o'clock position.

6		<ul style="list-style-type: none"> • Three top hats built adjacent to each other with the centre top hat being in the 12 o'clock position.
7		<ul style="list-style-type: none"> • Five top hats built adjacent to each other with the centre top hat being in the 12 o'clock position.
8	See plate 1	<ul style="list-style-type: none"> • AM250 was subject to a yearly calibration carried out by Renishaw. • Some supports around the sides and back of plate failed to be produced.
9	See plate 1	<ul style="list-style-type: none"> • Some supports around the sides and back of plate failed to be produced.
10	See plate 1	<ul style="list-style-type: none"> • No significant observations regarding the process.
11	See plate 1	<ul style="list-style-type: none"> • No significant observations regarding the process.
12	See plate 1	<ul style="list-style-type: none"> • AM250 was subject to a yearly calibration carried out by Renishaw. • New plate made with 12 top hats for a base line test before amending the CAD models for plates 13 and 14. • No significant observations regarding the process.
13	See plate 1	<ul style="list-style-type: none"> • Inside and outside cylinder diameter increased to account for observed bias. • No significant observations regarding the process.
14	See plate 1	<ul style="list-style-type: none"> • Inside cylinder diameter increased to account for observed bias. • No significant observations regarding the process.

The material used was Renishaw's 316L-0410 austenitic stainless steel alloy. This is composed of iron alloyed with chromium (of mass fraction up to 18%), nickel (up to 14%) and molybdenum (up to 3%), along with other minor elements. The material specification sheet for this powder is included as Appendix 3 to this thesis.

All the build plates were heat treated in accordance to Renishaw's heat treatment procedure for 316L 0410 stainless steel. The annealing process to stress-relieve the stainless steel build plate and parts was carried out using a Nabertherm N41/H annealing and hardening furnace. This process used a control program, Controltherm 5.55, to conduct the required heat treatment. The furnace programme used in the 316L procedure is represented in Figure 5-1. The program heated the furnace up to 1085°C and held the temperature for 1 hour. The full details of the heat treatment cycle are provided in Appendix 8.

It should be noted that this heat treatment cycle was adopted as standard practice within Renishaw's SLM stainless steel part production procedure. No additional consideration was applied in this research to phase change related effects. The parts thus treated were found to be consistent and it was therefore reasoned that if any such effect was occurring it was not evident from the geometry-based measurement processes being tested here. The build plate was then allowed to cool under inert conditions using argon gas to saturate the chamber's environment and displace the oxygen to prevent the oxygenation of the parts. The black line on Figure 5-1 represents the programmed heat treatment. The red line on the graph represents the temperature recorded by the thermocouple situated inside the furnace chamber. Figure 5-1 is representative of all the heat treatments carried out throughout the duration of this research.

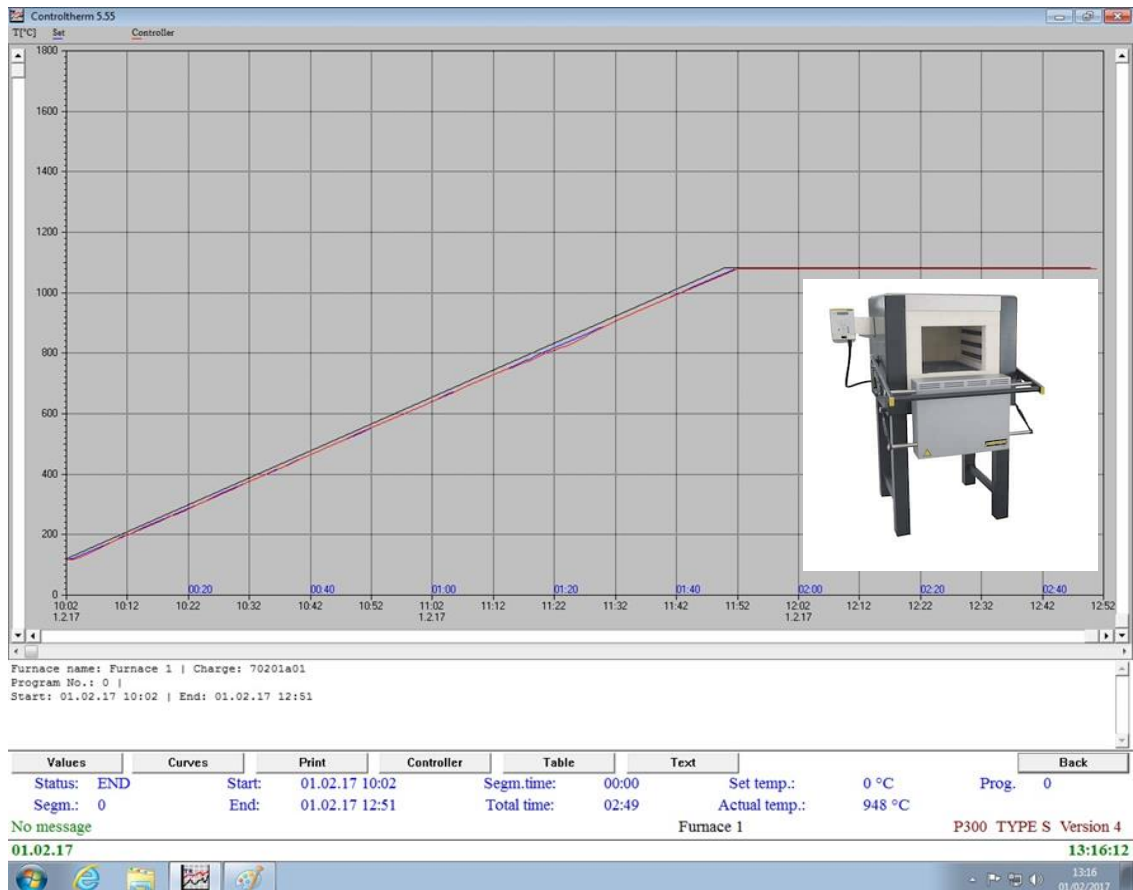


Figure 5-1 Screen shot of furnace program with tracked temperature read out.

5.3 Variation in artefact condition

It is important to understand how the heat treatment and the removal of the artefact from the build plate can influence its dimension and form. This section will investigate how the five attributes (diameter, cylindricity, true position, top plane and depth (identified in Chapter 4 Section 4.5)) change between process conditions. To provide evidence of the effect of the heat-treatment and removal processes, Figure 5-2 indicates the part diameters measured for each part on plate 8 between the pre (A), post (B) and off (C) conditions. The intention is to investigate the development of a methodology that can confirm the nature of the relationship between changes in the parts occurring at each of the stages. The intention here is to demonstrate the potential of the methodology rather than to fully investigate the differences arising between builds. Such an investigation will clearly require many more builds than could be envisaged in this research. In this case this will be considered initially using Plate 8 data.

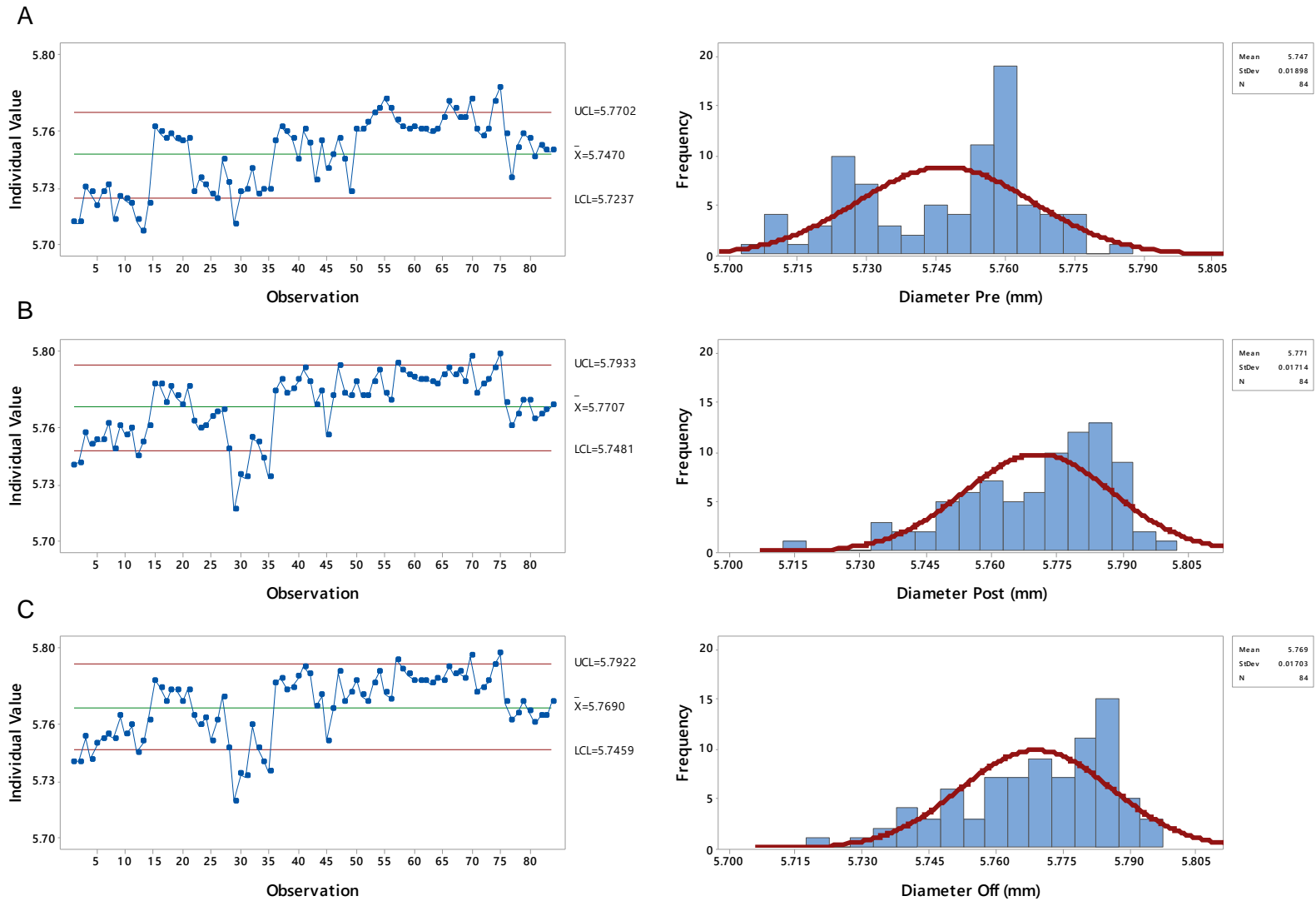


Figure 5-2 A. Run chart of all hole diameters from all top hats on plate 8 pre heat treatment (left) Histogram of all hole diameters on plate 8 with a fitted normal distribution curve pre heat treatment (right) B. Run chart of all hole diameters from all top hats on plate 8 post heat treatment (left) Histogram of all hole diameters on plate 8 with a fitted normal distribution curve post heat treatment (right) C. Run chart of all hole diameters from all top hats on plate 8 cut off build plate (left) Histogram of all hole diameters on plate 8 with a fitted normal distribution curve cut off build plate (right)

The left hand side of Figure 5-2 show run charts for each of the 84 parts (formed from 7 holes in each of the 12 test pieces) in the three conditions. These run charts provide too much information to make any informed decision regarding the optimum stage in which the parts should be measured. The histograms on the right hand side of the figure provide similar information, but allow an easier comparison between process conditions. The histograms can be overlaid to aid further comparison. Figure 5-3 shows the pre, post, and off histograms for plate 8.

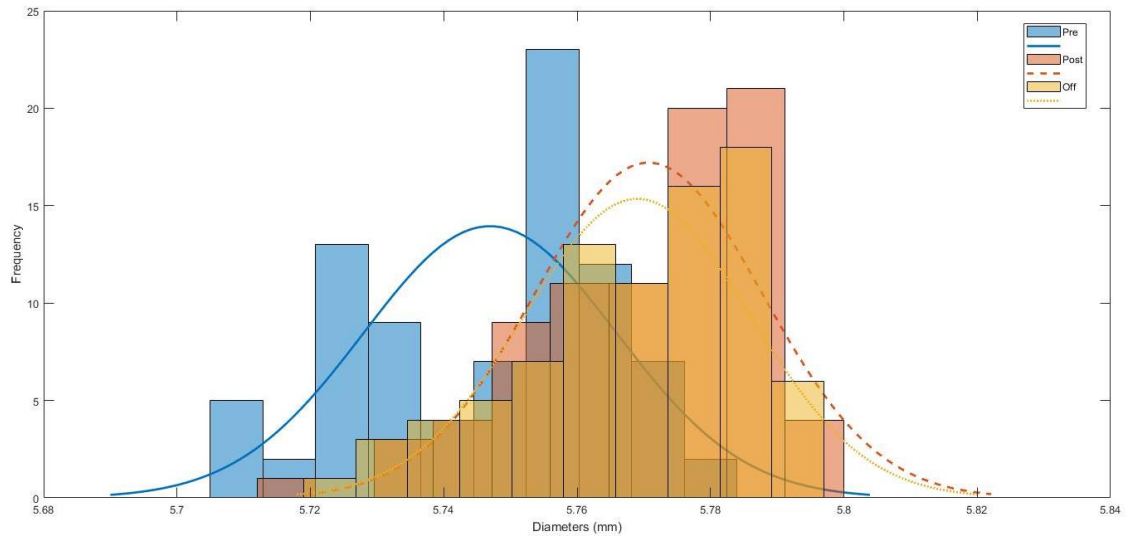


Figure 5-3 Histograms of all hole diameters for pre post and off with normal distribution curve fitted.

By overlaying the three histograms it becomes possible to observe that there is a visible difference between pre, post, and off. This difference is clarified by the introduction of the normal distribution curves for each data set. It is noted that without the normal distribution curves it would be hard to discern the shift in the diameters. This method for presenting the data is therefore shown to be suitable for one plate. Considering the necessity to compare multiple plates it is apparent that, even deploying the approach indicated in Figure 5-3, the information presented would become overwhelming. Figure 5-4 shows the same information as Figure 5-3, but as an interval plot. The relative simplification of the plot style allows for more information to be presented together. It is thus adopted for the remaining phases of this investigation.

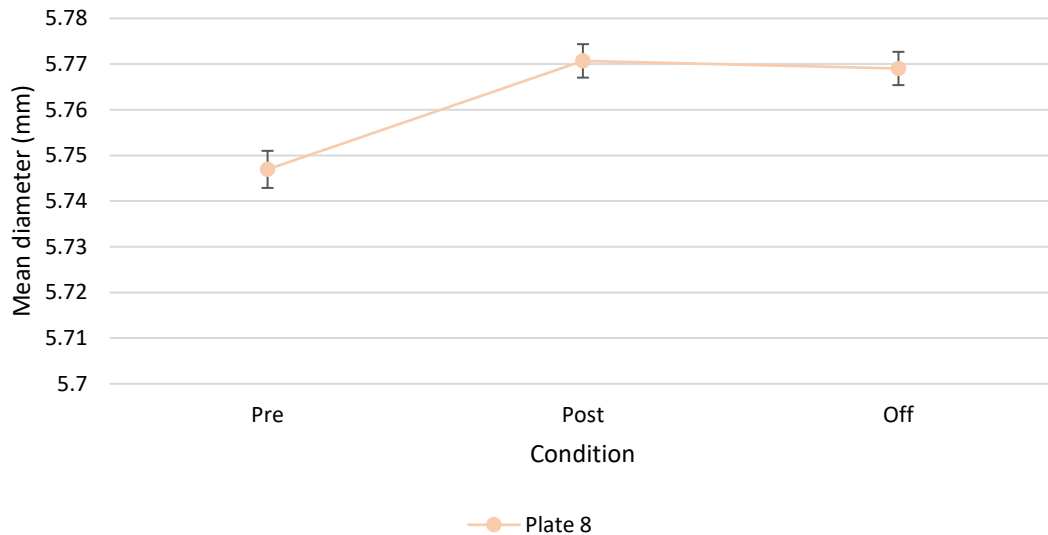


Figure 5-4 Interval plot of plate 8 mean diameters pre, post, and off.

Figure 5-4 shows the shift in the mean diameters for plate 8 for pre, post, and off and also includes the upper and lower confidence intervals shown as error bars for each condition (Easton and McColl's 1997). The confidence level was calculated using;

$$\bar{x} \pm z * \left(\frac{\sigma}{\sqrt{n}} \right) \quad (5-1)$$

Where:

n = sample size

z = is the standard normal distribution (95%) which is 1.96

σ = standard deviation

The confidence intervals for each condition can be used to identify whether the shift between conditions has statistical significance. This is expanded upon later in this section. Figure 5-5 shows the nine plates that were produced with the same layout as plate 1 in Table 5-1.

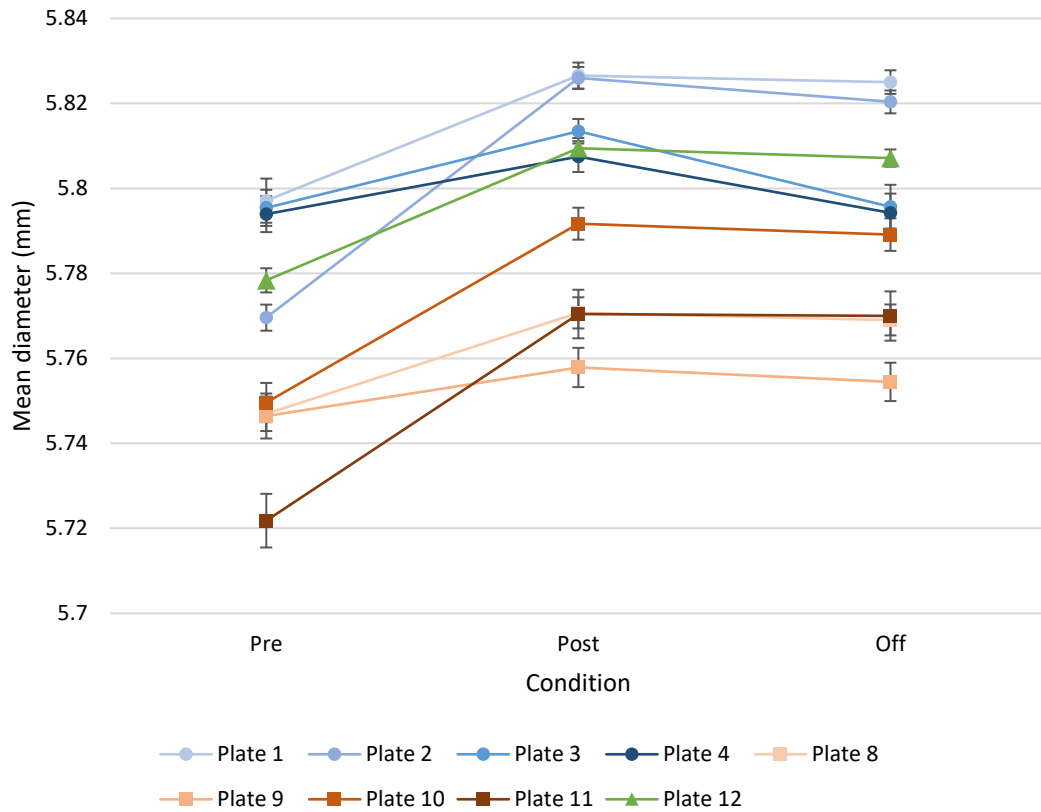


Figure 5-5 Interval plot of all mean diameters for all plates pre, post and off.

Figure 5-5 shows the mean diameters for the “normally” (i.e. laid out as plate 1) manufactured plates for pre, post and off. The plots are grouped based on the calibration of the AM250 machine by the OEM. Plates 1, 2, 3 & 4 are shown in blue with circle markers, these represent builds that occurred after the installation of the machine and the first set-up calibration in 2015. Plates 8, 9, 10 & 11 are shown in orange with square markers, these represent builds that occurred after the second calibration in 2016. Plate 12 (green with triangular markers) was built after the third calibration in 2017. This colour key and plate grouping has been maintained for the other interval plots in this section. From Figure 5-5 it is observed that parts manufactured between the second and third calibrations had an increased and had moved further from the nominal diameter, compared to the plates manufactured after the initial installation and set-up calibration of the AM250 machine. Following the third calibration the bias visibly reduces. The calibration could, in part, be responsible for these shifts. The differences within and between the groupings was investigated. It was found that the difference between groupings was statistically significant P-Value = 0.003 (calculated probability using ANOVA (Minitab)). It was also found that the differences within groups were statistically significant. It is evident from Figure 5-5

that plates 2 and 11 pre heat treatment do not start in the same position as their counterparts. However, since the significance is eliminated post heat treatment, this difference is not investigated further.

The interval plots for the majority of the plates show an increase in diameter between pre and post diameters, with minimal change between post and off. Plates 3, 4, and 9 do not show the same change in bias, this is highlighted in Table 5-2 (orange). For these three plates the mean diameters for pre and off appear to be similar. This effect and possible causes for the change in pattern it represents is investigated further below.

Table 5-2 Mean and standard deviation results for diameter distributions.

Plate	Pre Mean (SD)	Post Mean (SD)	Off Mean (SD)
1	5.797 (0.024)	5.827 (0.014)	5.825 (0.013)
2	5.770 (0.014)	5.826 (0.012)	5.820 (0.013)
3	5.795 (0.020)	5.813 (0.013)	5.795 (0.024)
4	5.794 (0.020)	5.807 (0.017)	5.794 (0.021)
8	5.747 (0.019)	5.807 (0.017)	5.795 (0.017)
9	5.746 (0.025)	5.758 (0.022)	5.754 (0.021)
10	5.750 (0.022)	5.792 (0.018)	5.789 (0.018)
11	5.722 (0.030)	5.770 (0.027)	5.770 (0.027)
12	5.778 (0.013)	5.809 (0.011)	5.807 (0.009)

Table 5-2 shows that the mean diameters vary between pre, post and off. The statistical difference needs to be investigated. It is also noted that the standard deviations vary, which implies that the variance is not equal across each condition. Monitoring the variance is essential to any manufacturing and quality evaluation because a reduction of process variance increases the precision and reduces the number of defects. If there is not an equal variance in the data sets being evaluated the Welch’s method should be applied to the One-Way analysis of variance (ANOVA) (Minitab 2015). Table 5-3 identifies that equal variance cannot be assumed this was identified by using Bonett test (Banga and Fox 2013). Where the P-values are above 0.05 in Table 5-3 equal variance can be assumed, as there are a number of values that are below 0.05 (highlighted in orange) equal variance cannot be assumed and therefore the Welch’s method is applied.

Table 5-3 P-values for diameter equal variance test comparison.

Plate	Pre versus Post P-value	Post versus Off P-value	Pre versus Off P-value
1	0.000	0.380	0.000
2	0.063	0.710	0.148
3	0.000	0.000	0.069
4	0.067	0.049	0.528
8	0.308	0.955	0.252
9	0.142	0.801	0.077
10	0.016	0.832	0.025
11	0.194	0.863	0.261
12	0.262	0.290	0.010

Table 5-4 presents the difference between the mean diameters for each condition. It is hypothesized that the mean diameter for two given conditions are the same. Table 5-4 indicates the actual difference (shift in mm) between the given conditions and provides the statistical significance of that shift. The significance level $\alpha = 0.05$ (5%)

Table 5-4 Two-sample T-test results for sample means

Plate	Pre versus Post P-value (Shift in mm)	Post versus Off P-value (Shift in mm)	Pre versus Off P-value (Shift in mm)
1	0.000 (0.029)	0.468 (0.001)	0.000 (0.028)
2	0.000 (0.056)	0.004 (0.005)	0.000 (0.051)
3	0.000 (0.018)	0.000 (0.018)	0.933 (0.000)
4	0.000 (0.014)	0.000 (0.013)	0.928 (0.000)
8	0.000 (0.024)	0.528 (0.002)	0.000 (0.022)
9	0.002 (0.011)	0.306 (0.003)	0.025 (0.008)
10	0.000 (0.042)	0.349 (0.003)	0.000 (0.040)
11	0.000 (0.049)	0.911 (0.000)	0.000 (0.048)
12	0.000 (0.031)	0.152 (0.002)	0.000 (0.029)

For more than half of the built plates a statistically significant shift is observed between pre to post and pre to off. Post to off measurement variation is indicated to be not statistically significant.

Plate 2 is observed to have a statistically significant shift between all conditions. Pre versus post and pre versus off both have a shift that is ten times that of post versus

off. It is considered that the shift between post and off is only significant because of the relatively small variance of the distributions (refer back to Table 5-2).

Plates 3 and 4 have no statistically significant shift between pre and off. There is a significant shift between pre and post as well as post and off. This indicates that the top hat measurements changed during the heat treatment process, but returned to their original measurements following the removal from the plate. Plate 9 followed a similar pattern to plates 3 and 4, however the parts on plate 9 do not completely return to the pre heat measurements following removal from the plate.

The behaviour of this “sub-set” of plates 3, 4 and 9 was first flagged-up in Table 5.2, where they were highlighted. Further investigation, conducted at the time of their manufacture, indicated that there was an issue with the heat treatment process. It is noted that, for plates 3 and 4 (which were heat treated together) the argon required was exhausted during the heat treatment process. This caused excessive oxidisation, as shown in Figure 5-6, to the parts and therefore likely to be preventing effective stress relief. In the heat treatment of plate 9 it was noted that the argon flow through the system was restricted.



Figure 5-6 Plate 3 before removal from furnace showing excessive oxidisation

Although adding an element of complication to the analysis of the experiments the problems related to heat treatment were identified and the differences caused were highlighted. This process was then carried forward for the remaining part features;

cylindricity, true position, top plane and depth. These are analysed using the same method as the diameter because it was proven to be effective.

Figure 5-7 shows the interval plots for all the mean cylindricity measurements. From initial observations of the graph, it can be observed that the same relationship between the measurements acquired for the pre, post and off stages is largely maintained. The cylindricity measurements generally improve (here that means they reduce towards zero) apart from plates 3, and 4 in which the values increase. Plate 1 appears to be unchanged through the three stages.

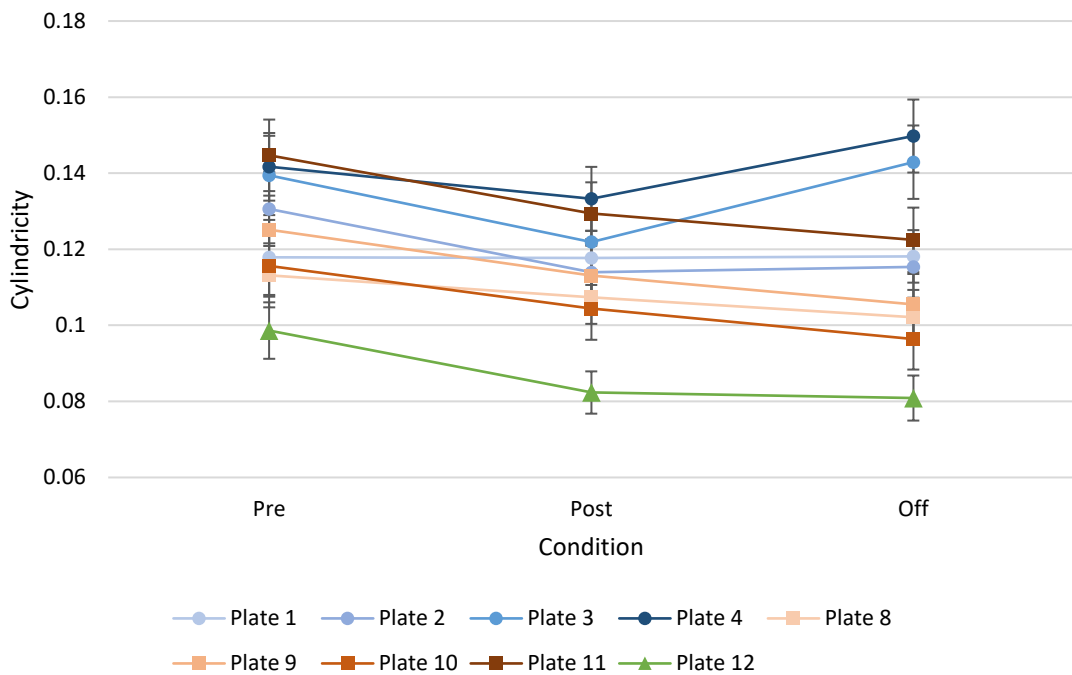


Figure 5-7 Interval plot of all mean cylindricity measurements for all plates pre, post and off. The mean and standard deviation for the cylindricity measurements are presented in Table 5.5.

Table 5-5

Plate 1 measurements confirm that there is no change in the mean measurements, but there is a reduction in the standard deviation showing that there was a reduction in the spread of cylindricity values. Plates 3 and 4 return to their original state after being removed from the plates showing that the form measurement followed the same variation/pattern as the diameter measurements.

Table 5-5 Mean and standard deviation results for cylindricity distributions.

Plate	Pre Mean (SD)	Post Mean (SD)	Off Mean (SD)
1	0.118 (0.046)	0.118 (0.033)	0.118 (0.032)
2	0.131 (0.045)	0.114 (0.041)	0.115 (0.038)
3	0.139 (0.049)	0.122 (0.042)	0.143 (0.045)
4	0.142 (0.042)	0.133 (0.039)	0.150 (0.045)
8	0.113 (0.039)	0.107 (0.033)	0.102 (0.034)
9	0.125 (0.042)	0.113 (0.037)	0.106 (0.037)
10	0.116 (0.038)	0.104 (0.039)	0.096 (0.038)
11	0.145 (0.044)	0.129 (0.038)	0.122 (0.040)
12	0.099 (0.035)	0.082 (0.026)	0.081 (0.028)

Table 5-6 shows the two-sample T-test results for cylindricity comparing pre versus post, post versus off, and pre versus off. This confirms that the plate 1 cylindricity measurements do not statistically change between the three conditions. Analysis of the data for plates 3 and 4 show that there is a statistically significant change when comparing pre versus post and post versus off. Pre versus off does not significantly change, confirming that the parts return to their original geometry. The T-test also identifies that all the other plates conform to the same pattern as the diameter measurements. As diameter and cylindricity measurements are linked, the similarities in relation to the changes are reassuring.

Table 5-6 Two-sample T-test results for cylindricity sample means

Plate	Pre versus Post P-value (Shift)	Post versus Off P-value (Shift)	Pre versus Off P-value (Shift)
1	0.982 (0.001)	0.934 (0.001)	0.965 (0.001)
2	0.013 (0.017)	0.820 (0.001)	0.019 (0.016)
3	0.013 (0.017)	0.002 (-0.021)	0.631 (-0.004)
4	0.180 (0.009)	0.012 (-0.017)	0.227 (-0.008)
8	0.306 (0.006)	0.304 (0.005)	0.053 (0.011)
9	0.049 (0.012)	0.189 (0.007)	0.002 (0.019)
10	0.060 (0.012)	0.172 (0.008)	0.001 (0.020)
11	0.017 (0.016)	0.247 (0.007)	0.001 (0.023)
12	0.001 (0.017)	0.726 (0.001)	0.000 (0.018)

True position was the next measurement to be observed. It should be stated that true position is specified by the calculated difference between the required and measured centre of the cylinder. Figure 5-8 shows the interval plots for all the mean true positions of the cylinder measurements. There is a distinct difference between plates made in 2015 (after the initial installation of the AM250 machine) and those produced from 2016 onwards (after the first calibration). Plates 1-4 have an average true position mean of 0.211 versus 0.084 for plates 8-12. The average standard deviation for plates 1-4 is 0.110 versus 0.056 for plates 8-12. These indicate that plates 1-4 have a mean 2.5 times greater than plates 8-12 and a standard deviation 1.96 times greater. It is also evident from Figure 5-8 that the true position plots for plates 8-12 are more tightly grouped compared to plates 1-4.

The top-hats manufactured pre 2016 show that between pre, post, and off the position bias increases (tends further away from 0). For the majority of the plates manufactured after 2016, Figure 5-8 indicates that the position bias improves between pre, post, and off. Two exceptions are plates 8 and 9 for which true position appears to remain consistent.

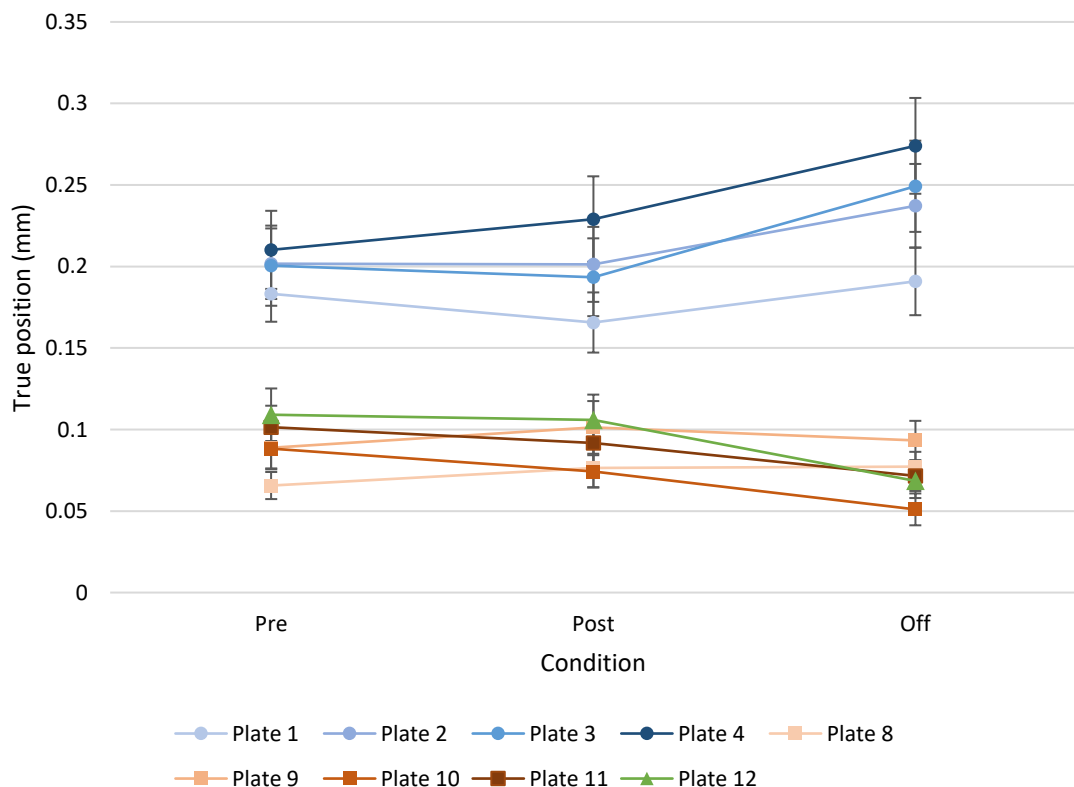


Figure 5-8 Interval plot of all mean true positions of cylinders measurements for all plates pre, post and off.

Table 5-7 show the two-sample T-test and shift in the mean for the true position mean measurements. Plate 1, 8, and 9 show no statistically significant shifts between pre, post and off. This implies measuring the true position post or off would give you the same result, but in reality this could be up to a 25µm different. The remainder of the plates shows a statistically significant change between post and off, this implies that the top-hats have changed significantly when they have been removed from the plate. Plates 2, 3, and 4 show a relatively large shift (up to 64µm). Figure 5-8 shows that this shift is away from zero and therefore the true position had degraded. Plates 10, 11, and 12 show smaller shift (up to 40µm), however Figure 5-8 shows that this is towards zero therefore indicating that the plates are improving.

Table 5-7 Two-sample T-test results for true position mean measurements

Plate	Pre versus Post P-value (Shift)	Post versus Off P-value (Shift)	Pre versus Off P-value (Shift)
1	0.174 (0.017)	0.077 (-0.025)	0.574 (-0.008)
2	0.982(0.001)	0.043 (-0.036)	0.040 (-0.035)
3	0.685 (0.007)	0.003 (-0.056)	0.011 (-0.049)
4	0.300 (-0.019)	0.027 (-0.045)	0.001 (-0.064)
8	0.145 (-0.01)	0.910 (-0.001)	0.066 (-0.011)
9	0.235 (-0.012)	0.437 (0.008)	0.617 (-0.004)
10	0.092 (0.014)	0.001 (0.023)	0.000 (0.037)
11	0.300 (0.009)	0.013 (0.02)	0.000 (0.029)
12	0.776 (0.003)	0.000 (0.035)	0.000 (0.04)

Figure 5-9 shows the interval plots for the mean top plane measurements, for all top hats pre, post, and off. Plates 1 and 2 are the obvious anomalies in these measurement sets. These were identified to arise from the part alignment process for plates 1 and 2 pre and plate 1 post (highlighted in red). The MODUS program was improved as a solution. Due to these issues the top plane measurements for Plates 1 and 2 are not considered further.

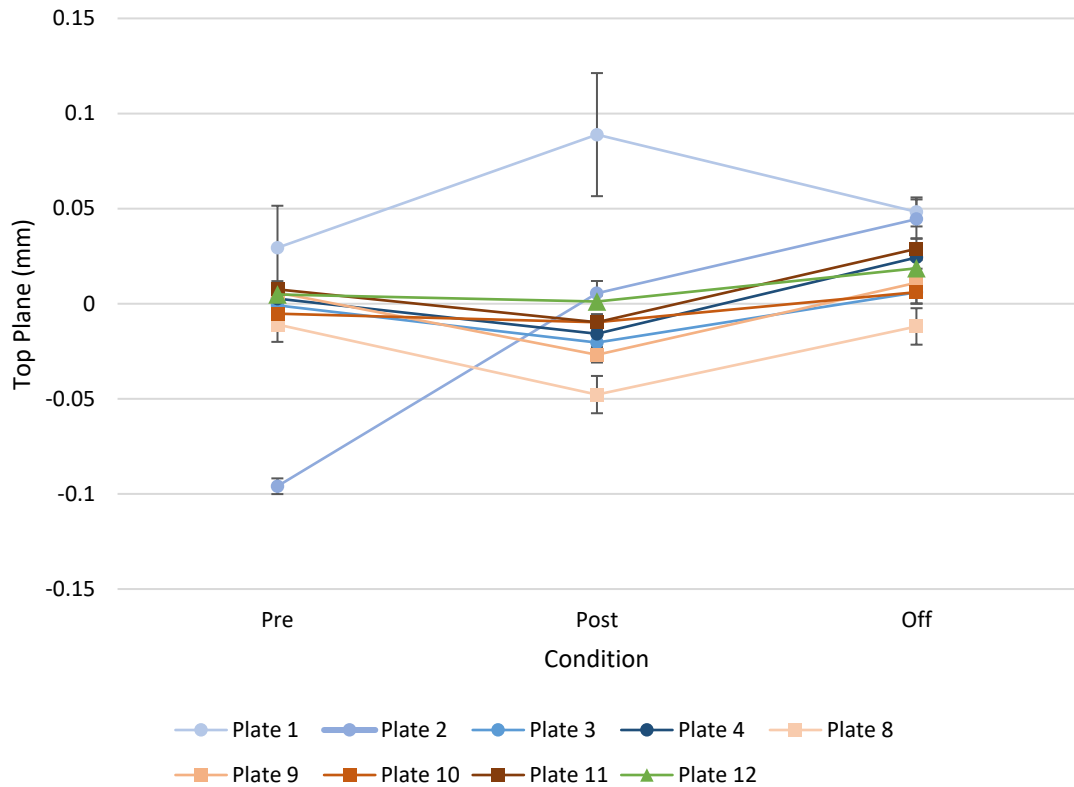


Figure 5-9 Interval plot of all mean top plane measurements for all top hats pre, post and off.

All the other plates are closely grouped together and show similar geometric changes. Table 5-8 show the mean and standard deviation results for all top plane measurements. The data range for the top plane is 0.0243mm, where the largest variation occurs in plate 4 (0.040mm) highlighted in orange and the smallest in plate 10 (0.016mm) highlighted in green.

Table 5-8 Mean and standard deviation results for top plane measurements.

Plate	Pre Mean (SD)	Post Mean (SD)	Off Mean (SD)
1	0.029 (0.103)	0.089 (0.151)	0.048 (0.036)
2	-0.096 (0.019)	0.006 (0.030)	0.044 (0.048)
3	-0.001 (0.027)	-0.020 (0.026)	0.006 (0.028)
4	0.003 (0.019)	-0.016 (0.024)	0.024 (0.028)
8	-0.011 (0.043)	-0.048 (0.046)	-0.012 (0.045)
9	0.006 (0.019)	-0.027 (0.019)	0.011 (0.019)
10	-0.005 (0.021)	-0.010 (0.019)	0.006 (0.027)
11	0.008 (0.020)	-0.010 (0.020)	0.029 (0.026)
12	0.005 (0.014)	0.001 (0.015)	0.019 (0.020)

Table 5-9 shows that for all the plates when the bridges are removed, they exhibit an (statistically significant) increased top plane measurement. This would need to be considered in more detail to see if this shows warping in the bridge once it was removed from the plate.

Table 5-9 Two-sample T-test results for top plane mean measurements

Plate	Pre versus Post P-value (Shift)	Post versus Off P-value (Shift)	Pre versus Off P-value (Shift)
1	0.000 (-0.119)	0.019 (0.041)	0.911 (-0.001)
2	0.000 (-0.102)	0.000 (-0.039)	0.000 (-0.141)
3	0.000 (0.020)	0.000 (-0.026)	0.111 (-0.007)
4	0.000 (0.019)	0.000 (-0.040)	0.000 (-0.022)
8	0.000 (0.037)	0.000 (-0.036)	0.880 (0.001)
9	0.000 (0.033)	0.000 (-0.038)	0.081 (-0.005)
10	0.140 (0.005)	0.000 (-0.016)	0.003 (-0.011)
11	0.000 (0.017)	0.000 (-0.039)	0.000 (-0.021)
12	0.098 (0.004)	0.000 (-0.017)	0.000 (-0.014)

In the final element of this initial work the average depths of the cylinders were considered. Figure 5-10 shows the interval plot of all the mean depths for all top hats from pre, post, and off. Unfortunately, when the plate 1 bridges were removed from the build plate they were cut at the wrong height. This had the unwanted effect of removing the cylinder bottoms. This also occurred for some of the bridges on plate 2. These measurements will not be reliable and therefore will not be considered further.

Table 5 10 shows that the standard deviation for the depth measurements is substantial because of the forced depth variation built into the bridges, this was discussed in Chapter 4. The average depth should be 6mm, plates 10, 11, and 12 average close to this target value, but plates 3, 4, 8, and 9 indicate on average shallower depths. Due to the substantial standard deviation for all plates, there is no statistically significant variation in depth between pre, post and off.

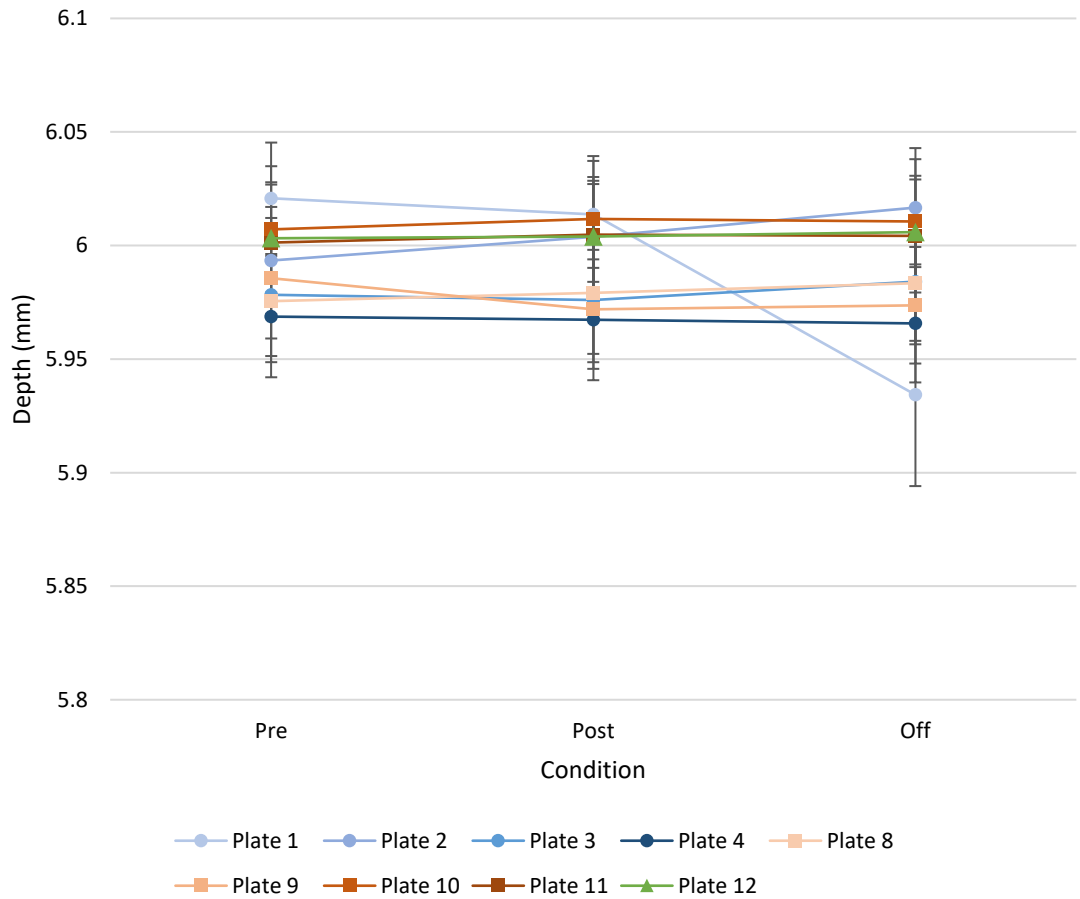


Figure 5-10 Interval plot of all mean top hat hole depths for pre, post and off.

Table 5-10 Mean and standard deviation results for all top hat hole depths for pre, post, and off.

Plate	Pre Mean (SD)	Post Mean (SD)	Off Mean (SD)
1	6.021 (0.115)	6.014 (0.110)	5.934 (0.188)
2	5.993 (0.110)	6.004 (0.109)	6.017 (0.123)
3	5.978 (0.126)	5.976 (0.128)	5.984 (0.123)
4	5.969 (0.125)	5.967 (0.124)	5.966 (0.122)
8	5.976 (0.126)	5.979 (0.125)	5.983 (0.126)
9	5.986 (0.124)	5.972 (0.123)	5.974 (0.120)
10	6.007 (0.130)	6.012 (0.130)	6.011 (0.128)
11	6.001 (0.119)	6.005 (0.119)	6.004 (0.116)
12	6.003 (0.115)	6.004 (0.115)	6.006 (0.116)

5.4 Discussion

The information presented in this section has shown that the heat treatment of the build plate and artefacts cause a statistically significant geometric change. This change reduces any measurement difference towards the target value, improving the geometric form of the parts. This would indicate that where it has been determined that parts need to be heat treated the geometric check (measurement) should occur after this process has been completed. For example, if a component is manufactured with an off-set based on the pre measurement data the significant geometric change that heat treatment introduces will result in the final part being significantly different to the intended form/dimensions. The artefacts can either be measured in the post condition or in the off condition, after they have been removed from the build plate. Deciding which of these two points is best to measure the artefact one must consider the work carried out in Chapter 4 and how traceability can be best maintained for future use.

Chapter 4 considered in detail at the repeatability and reproducibility of measurements using a bridge to assess the capability of the CMM. This enabled the reliable measurement of the forms and features considered in this chapter. One of the largest contributing factors to repeatability is the ability to carry out the measurement process in exactly the same way time and time again. Removing the bridge from the build plate will mean that a fixture would be required to ensure that the measurement process remains repeatable. This fixture would need to be designed so that the bridge was held in exactly the same position each time a measurement cycle was carried out. Each bridge would need to be measured in turn, presumably using the same fixture. This would also rely heavily on the competency of the operator to making sure that the bridge is correctly inserted, located and held in the fixture. It is also necessary to assure that the measurement process is carried out in exactly the same way each time. It would therefore appear that measuring the artefacts on the build plate would help to eliminate the need for specially designed fixtures and the knowledge of how to use them. By keeping the artefacts on the build plate it is possible to maintain traceability and the ability to better relate parts to process parameters. The counter case for the removal of the bridge can be made based on the continued utilisation of the build plate for this purpose. These are expensive specially manufactured components and their use for this process must be justified. It is acceptable to utilise a build plate for the measurement cycle, but, to maintain traceability, it is important that the test pieces are retained for reference.

Keeping a build plate long-term with the bridges in place would not be practical, and sets of removed test pieces would offer a more sensible long-term solution.

This chapter has highlighted that the failure of the heat treatment may be identified when parts have been cut off the build plate. Diameter and cylindricity measurements showed that when the bridges were removed from the build plates, plates 3 and 4 indicated that the heat treatment failed due to an issue with the argon supply. The measurements for these plates returned to pre heat treatment values. This can only be identified if measurement occurs after the parts are removed from the build plates. However, this requires comparative measurements either pre or post to identify the relative shifts.

The implication of this is that post process measurements are most appropriate because post processing significantly affects the geometric form of the components being produced. In terms of assuring the correct enactment of any post processing (such as heat treatment) this eliminates pre-measurements from consideration as the best and/or most viable measurement state. It is also identified that cutting components off the build plate harms the repeatability of the measurements unless increased investment is made in training and fixtures. It was highlighted that off the plate measurements are needed to assess the success of the heat treatment, but would be in addition to post process measurements. It is argued that if the manufacturer is concerned that the heat treatment has failed an additional measurement cycle for off the build plate components could be implemented.

5.5 Summary

This chapter has identified that post processing introduced statistically significant changes to a build and therefore any measurements aimed at assuring the process should be taken after the parts have been post processed. It was shown that, for the purpose of establishing that the process foundation phase has been properly completed, the optimum time to assess components is post process, whilst all twelve test pieces are still located on the build plate. This simplifies the CMM measurement cycle and removes the potential for any variations arising due to fixturing and related measurement cycle variations. This supports the assessment of the test pieces as they are produced by the SLM process but not subject to any changes due to their removal from the plates. It is thus able to map changes arising within the SLM process. Chapter 6 expands on the results considered in this chapter to assess the build capability of the AM250 machine. This will exclusively consider post process components still attached to the build plate.

Chapter 6: Artefact evaluation and its use in process foundation

6.1 Artefacts and the process foundation fishbone

Chapter 3 identified many variables that contribute to the overall process quality. Though it would be impossible to cover all of these variables, some are explored in this chapter. This chapter discusses the links between geometric information and the process variables that occur in the process foundation fishbone (see Chapter 3 Figure 3-14). The features discussed in Chapter 4 and 5 are used to explore manufacturing variation within the AM250 machine.

This phase of the research considers the application of the twelve test pieces to investigate the enactment of the SLM process. This approach is believed to be the first to use multiple test pieces in this manner. In this procedure the influence of build location, orientation, position, and top hat cylinder depth will be explored. These manufacturing details can be explored and linked to variables in Figure 3-14. The questions posed in this section are:

1. Does build location affect the geometry of an artefact?
2. Is there variation across the build bed, if so what pattern does it show?
3. If there is variation is it consistent (is it repeatable plate to plate)?
4. Does orientation in the x or y direction show any difference?
5. Is there any difference in the Z build depth from plate to plate?

6.2 Build plate evaluation and analysis

Chapter 5 identified that post heat treatment was an optimum time to evaluate the artefacts on the build plate. Using Plate 8 as an example in this condition one can now look at how the five attributes discussed in Chapters 4 and 5 (diameter, cylindricity, true position, top plane, and depth) can be evaluated to assess the build quality of the AM250 machine. Plate 8 has been chosen as an example in this section because it was the first plate manufactured after the calibration. The individual and moving range chart (Figure 6-1) shows all top hat diameters for plate 8. These are numbered from 1 to 84 to represent the twelve sets of seven top hats produced on each plate.

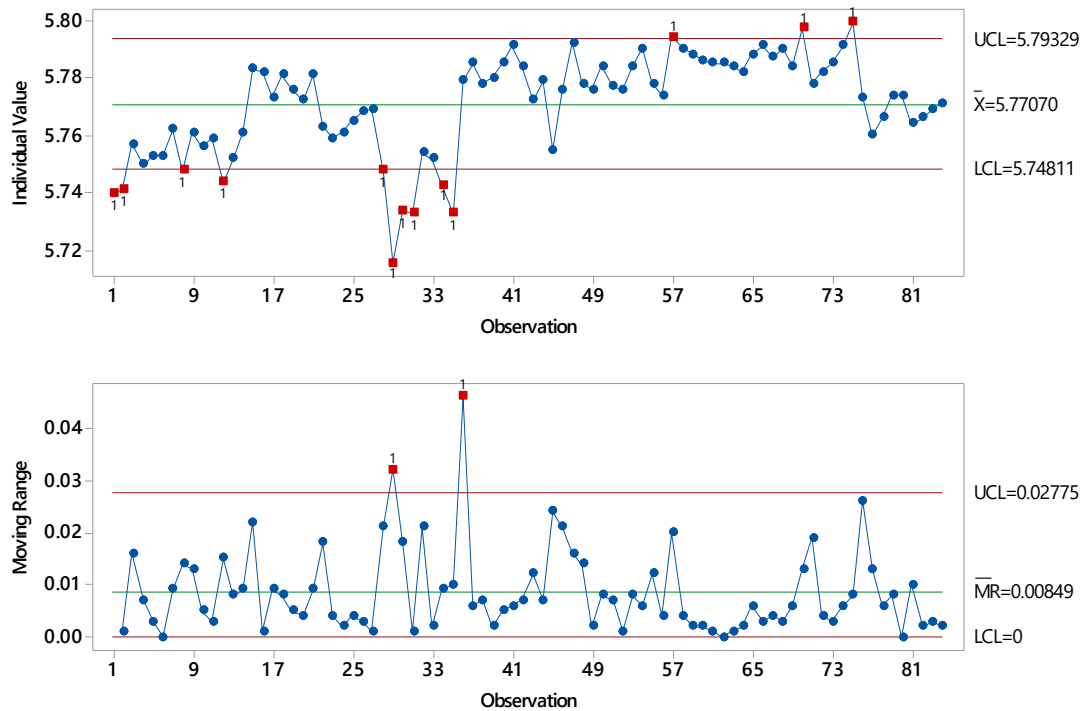


Figure 6-1 I-MR run chart for all top hat diameters on plate 8

The run chart provides a great deal of information, however, though it is informative, important details can be lost or hidden. The run chart shows that the mean diameter is 0.23mm smaller than the target 6mm and all measurements are outside of the ± 0.2 mm tolerance. No attempt was made at this stage to modify the program since this element of work was aimed at establishing the control needed to achieve the accurate manufacture of parts. However, when using the run chart, it is difficult to identify which positions within the plate are “better” (closer to the nominal) or “worse” (further away from the nominal) because no quick/easy comparisons can be made between different bridges. One way to compare the relative condition of different bridges is to consider outliers. These are highlighted in Figure 6-1 and are given in Table 6-1. Although this starts to identify locations on the plate that could be worse than other locations, it does not indicate which locations are better.

Table 6-1 Plate 8 statistical outliers from Figure 6-1 run chart

Bridge	Outliers
1	1, 2
2	8, 12
4	28
5	29, 30, 31, 34, and 35
9	57
10	70
11	75

In an effort to identify which bridges are better each bridge is averaged and presented in Figure 6-2.

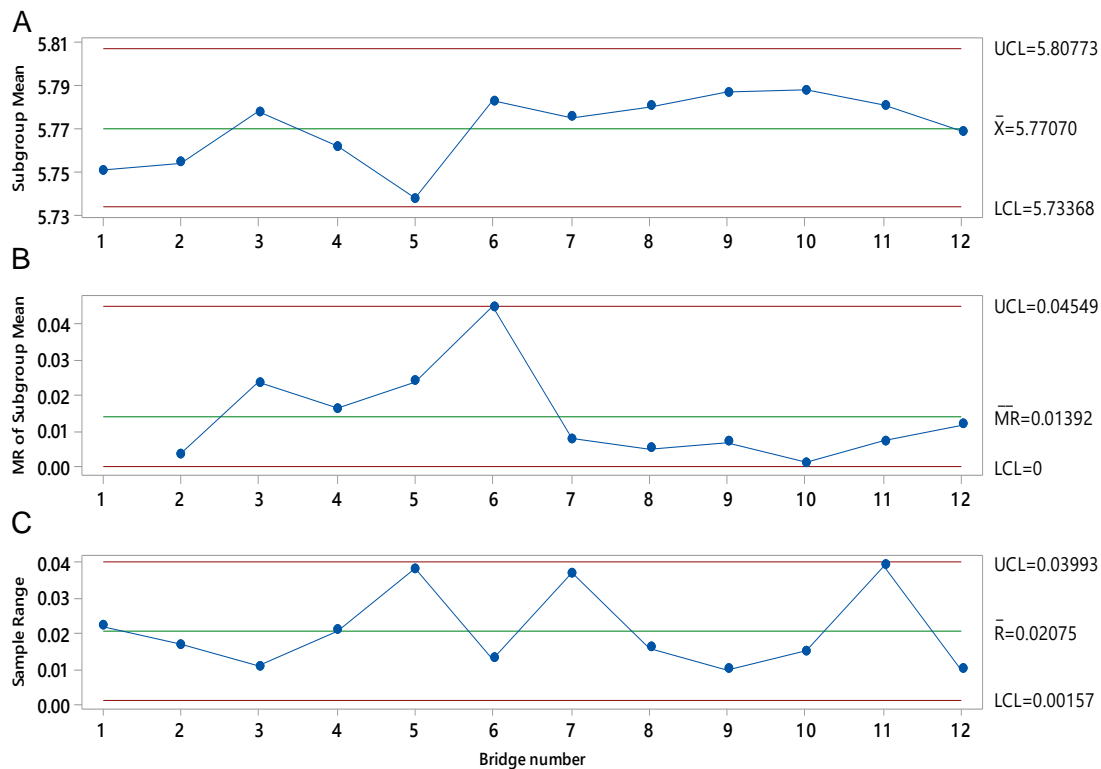


Figure 6-2 I-MR-R/S (Between/Within) for all bridge diameter measurements on plate 8

The first observation is there are no outliers. The outliers still exist, but because the data has been averaged over each bridge extreme measurements are reduced and the data is smoothed. This is in contrast to Figure 6-1 and Table 6-1, which show numerous outliers. It can still be observed that bridge 5 is the “worst” position (Figure 6-2 (A.)). By inspection Figure 6-2 (C.) further confirms that bridge 5 is poor and indicates that bridges 7 and 11 are also poor. This is despite Figure 6-1 showing no

obvious abnormalities for bridges 7 and 11, other than a single outlier at position 75 (see also Table 6-1). Again no bridge can be identified as being the “best”, and there are no obvious trends or patterns across the plate. The initial assessment of the quality of the bridges motivated the author to better define the relative quality of each bridge. This is explored later in this section with the adoption of the assessment based upon Equation 6.1.

The run charts have identified where measurements deviate further from the mean, but cannot infer patterns or trends relating to the build location. A different approach should be considered to complement the run charts to see if more information can be extracted from the data available. In this case, the starting point was to plot the diameters of the top hats grouping them based on position. Knowing that the laser in the AM250 machine is calibrated in the middle of the build plate (Appendix 1) it was sensible to explore if the influence of position could be investigated by grouping the bridges into two sets. The bridges built near to the centre of the build plate could be plotted as one set of data and the bridges built around its perimeter as a second set of data. Figure 6-3 is a line plot showing all the top hat diameters for bridges manufactured on the perimeter of the build plate (e.g. positions 1, 2, 4, 5, 7, 8, 10, and 11). Figure 6-4 shows the remaining top hat diameters (3, 6, 9, and 12). The UCL and LCL have been included for reference.

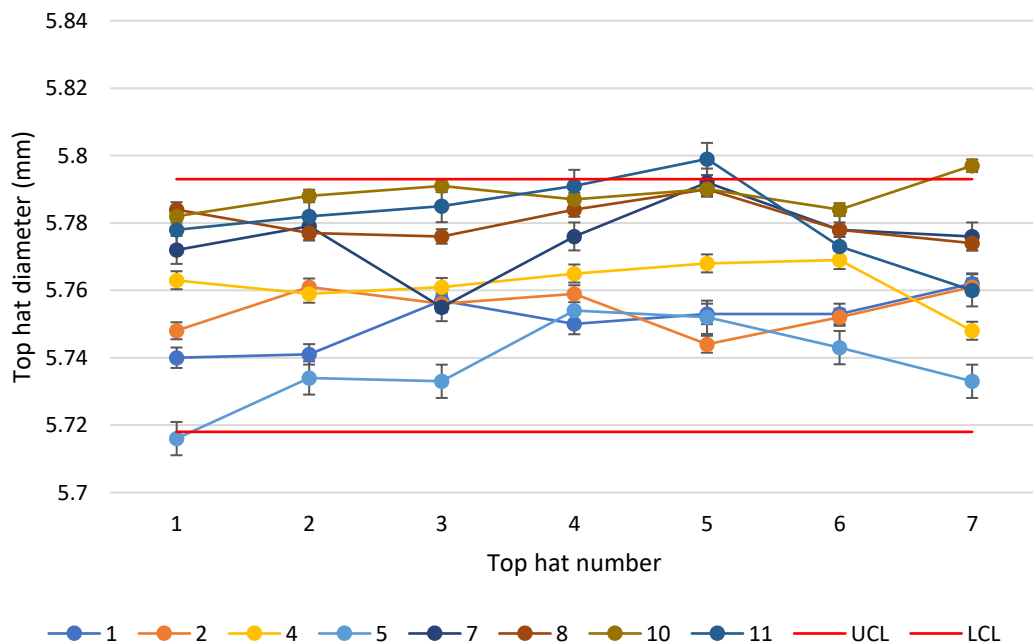


Figure 6-3 Top hat diameter plot for bridges manufactured on the outside edge of the build plate. (The legend indicates the bridge number where a bridge is made up of seven top hats.)

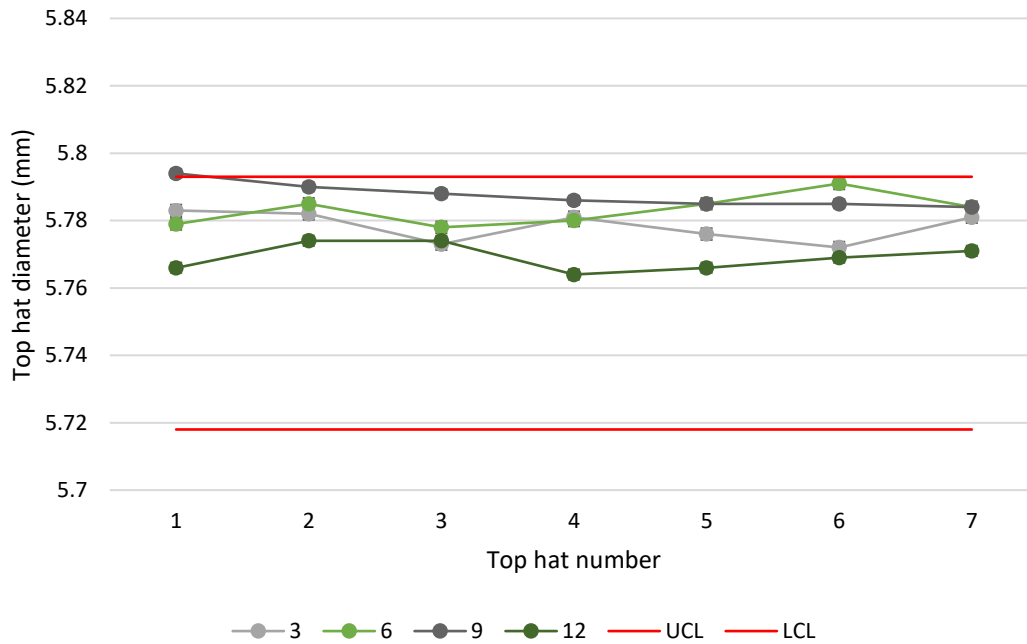


Figure 6-4 Top hat diameter plot for bridges manufactured near to the centre of the build plate. (The legend indicates the bridge number where a bridge is made up of seven top hats.)

The top hat diameters plotted in Figure 6-4 have a smaller range than the bridge top hat diameters built around the perimeter of the build plate (Figure 6-3). The average diameter measurement in the centre of the plate is 5.779mm and the average diameter measurement around the outside of the plate is 5.766mm, a difference of 0.013mm. The range of the outside bridge diameters is 0.083mm and the range of the bridges manufactured in the centre of the plate is 0.027mm. The variation of a top hat diameter on the perimeter of this build plate is three times larger than the variation in the centre. Considering the GR&R results, these measurements can be attributed to definite variation in the process and between the respective parts because variation from the gauge is only $\pm 0.002\text{mm}$ (refer to Chapter 4).

When manufacturing, part bias (accuracy) and variation (precision) are two important factors. The aim is to get as close as possible to the target value with minimal variation around that figure. The point at which these two criteria are met relative to the data being used will be considered the “best” position on the build plate. Conversely, the position for which the plate shows the highest variation and the largest bias will be considered the “worst” position on the build plate. These terms do not infer that either position is in or out of tolerance and is purely a comparative statement. Using a line plot to do this would be time consuming so a ranking system was developed using these two attributes.

Each bridge was summarised using two descriptive values for each attribute. For diameter the most important consideration was how far each top hat diameter was from the target value. Each top hat diameter was subtracted from the target value of 6mm to produce a bias. The absolute of these values was averaged to give the first descriptive value for the bridge. The second descriptive value was the standard deviation of each top hat bias averaged across the bridge. These two values describe the overall bias for an individual bridge and the variation within that bridge. For cylindricality, true position, and top plane the first descriptive value is the mean value averaged across the bridge. The second descriptive value was the standard deviation of each top hat averaged across the plate. Lastly the depth was adjusted to account for the step change in each top hat (see Figure 4-6b.). The absolute of these values was averaged to produce the first descriptive value and the standard deviation for all top hats within the bridge was used for the second descriptive value. Equation (6-1) expresses how the raw measurement data is combined. This has been adapted from (Kreyszig 1979),

$$Y_{Descriptive} = \left(\left(\frac{X_1 - X_1bar}{X_1sd} \right) + 100 \right) * \left(\left(\frac{X_2 - X_2bar}{X_2sd} \right) + 100 \right) \quad (6-1)$$

Where,

X_i = Individual descriptive value (bridge)

$X_i\bar{}$ = Mean of all descriptive value (plate)

$X_i\text{sd}$ = Standard deviations of all descriptive values (plate)

i = denotes which descriptive value (first or second)

+100 = is an arbitrary shift which is used to ensure that the entire distribution is greater than zero.

$Y_{Descriptive}$ is the combination of the two descriptive values X_1 and X_2 and indicates the relative quality of each bridge. $Y_{Descriptive}$ can then be ranked using the RANK.EQ formula built into Excel. The rank is displayed on a matrix, shaded in monochrome (green) to help indicate where on the build plate is best (ranked as 1) and where it is worst (ranked as 12). A monochrome colour system was used to minimise the interpretation of patterns that may not exist, but may look like they do when two different colours are used. Using two different colours such as green and red can infer information subconsciously (Rogowitz et al. 1996; Borland and Li 2007). For example, if a colour scale was implemented which used green to red anyone just glancing at the information without reading what these colour represent may

automatically assume anything shaded in green is correct (in tolerance) and anything shaded in red is incorrect (out of tolerance), therefore misinterpreting the results and the information.

The matrix is grouped into a five by five square grid; the shaded squares represent regions within which bridges were built, the other squares were left intentionally blank since they are not related to the position of any of the bridges. Creating a matrix in this way helps visualise the information in relation to the positions on the build plate. Although Figure 6-1 – Figure 6-4 indicate the same information as the matrices, they do not spatially correspond to the build plate, therefore working out which plots to analyse can be extremely time consuming. The matrices of shaded squares, on the other hand, help show changes across the build plate in a simple and effective manner.

This can be demonstrated with reference to Figure 6-5. Here Figure 6-5 (A.) shows the build quality matrix for plate 8 diameter measurements, Figure 6-5 (B.) shows the bridge location and the numbering convention used to maintain traceability. The direction of gas flow is indicated and the argon inlet and outlet positions are shown in Figure 6-5(B). The location and form of these inlet and outlet ports are also shown within the build chamber in Figure 3-2.

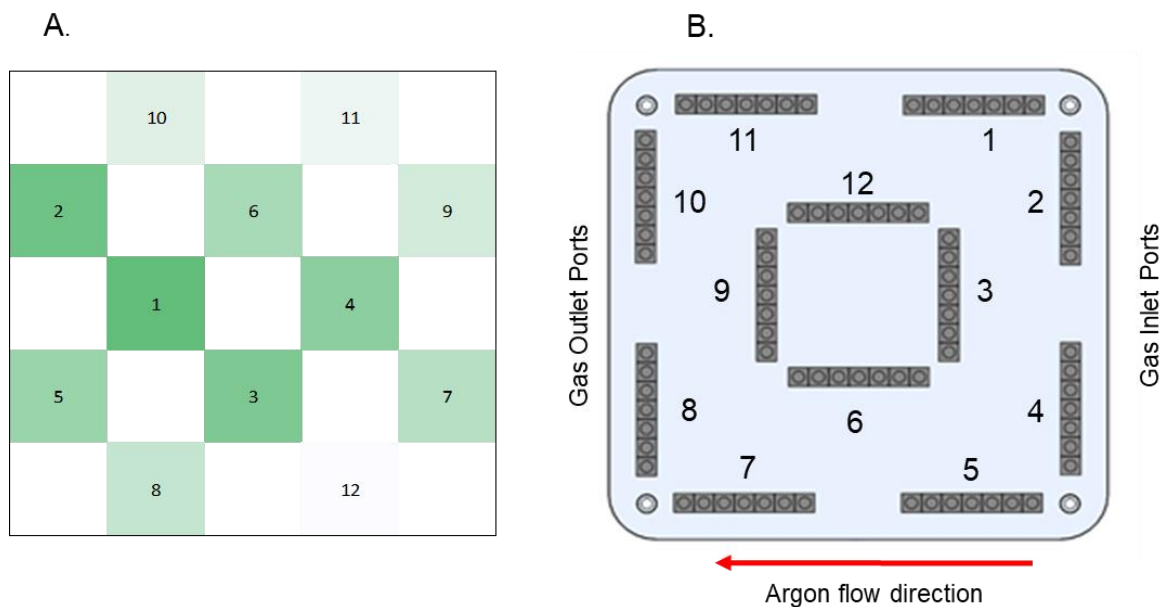


Figure 6-5 A. Build quality matrix for plate 8 presenting a quality ranking based on average bridge diameter measurements and variance of measurements. B. Bridge location and numbering convention.

In Figure 6.5 (A) the square corresponding to bridge 9 is labelled “1” and shaded darkest to indicate that it was ranked as the “best” position on build plate 8 for diameter. This implies a combination of the average top hat diameters within bridge 9 being closest to the target value of 6mm and that there was a low level of variation within this bridge. Conversely Figure 6.5 shows that bridge 5 is in the “worst” position on the build plate, with the corresponding square being lightly shaded and labelled as “12”. This implies an average top hat diameter that is further from the target value of 6mm combined with a higher level of variation within this bridge. This information can then be used to compare both positions, referring back to Figure 6-3 and Figure 6-4. Figure 6-6 shows these measurements for bridge 5 and 9.

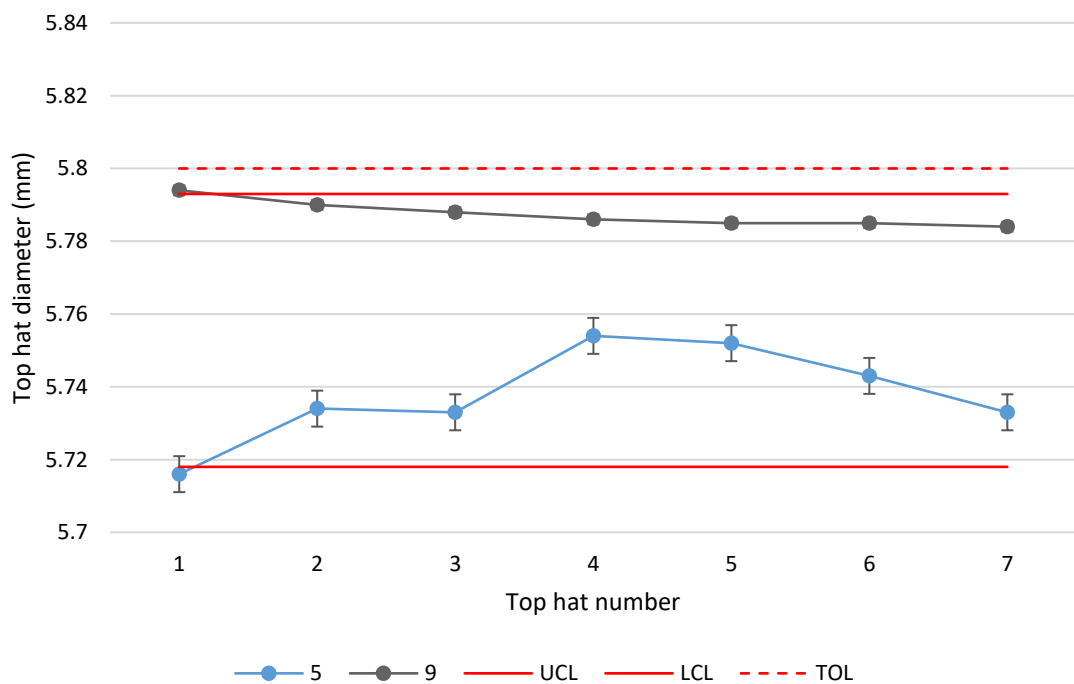


Figure 6-6 Top hat diameter plot for bridges 5 and 9.

Figure 6-6 confirms that bridge 9 is on average closer to the target diameter of 6mm than bridge 5 and shows less variation within the bridge. It also indicates that all bridges manufactured on plate 8 are out of tolerance. The dashed red line on the plot shows the lower tolerance limit and though the data is mostly within the upper and lower statistical control limits it is outside of the 0.2mm process control tolerance. This analysis can be extended to consider the other attributes of cylindricity, true position, top-plane and depth, shown in Figure 6-7 A, B, C and D respectively. It should be noted that cylindricity is a composite form measurement representing the circularity, straightness, and taper features of a cylinder. Cylindricity can be used to indicate how

close the measured cylinder is to a theoretical perfect cylinder, i.e. a cylinder that is perfectly circular, straight and has no taper. All three characteristics are combined in one number (here in measured in mm), which represents the radial distance between two coaxial cylinders which are the boundaries that enclose all the scanned points. The resulting measure of cylindricity allowed the quality of the cylinders to be ranked.

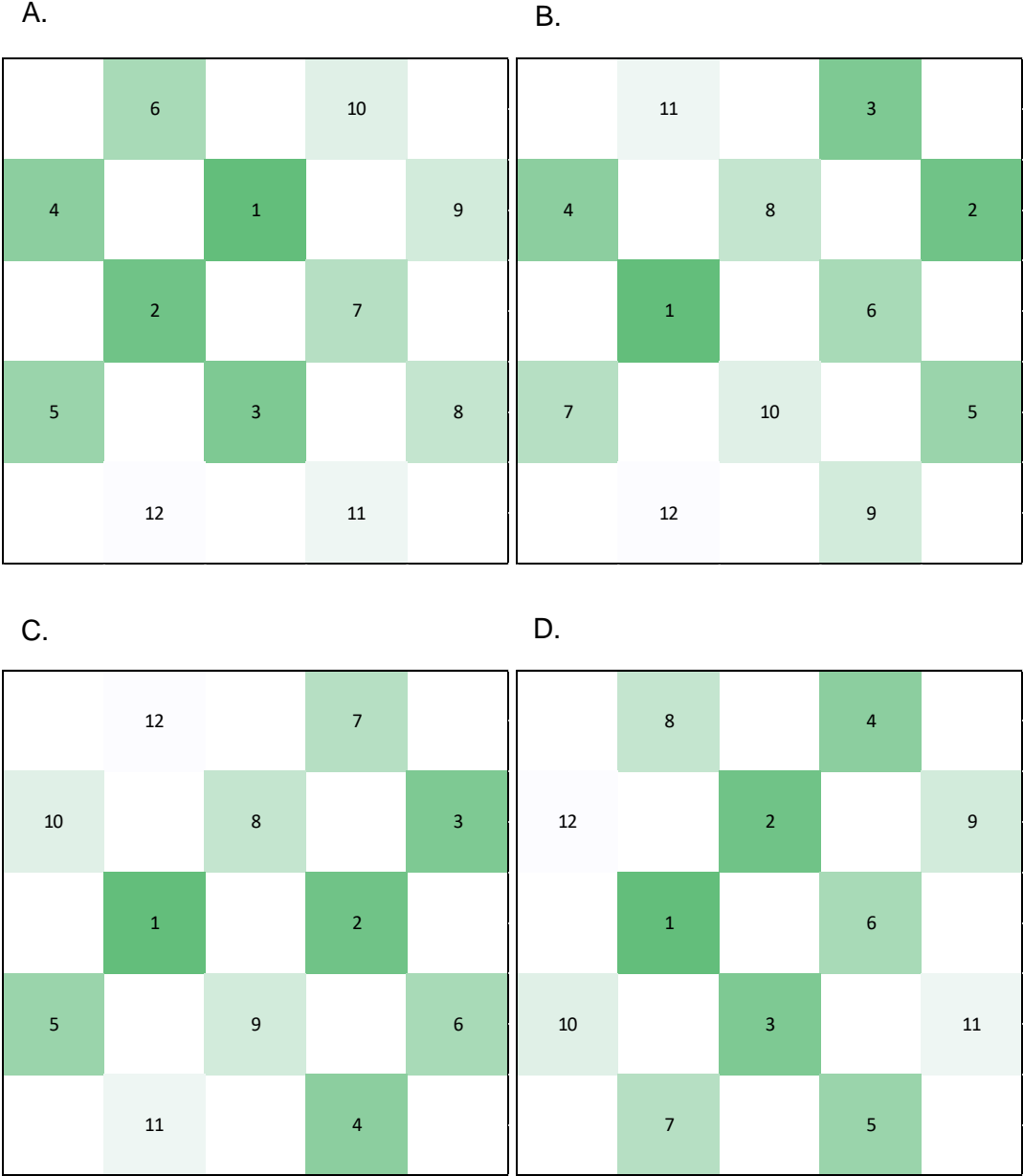


Figure 6-7 Build quality matrix for plate 8 presenting a quality ranking for; A. Average cylindricity measurements and variance, B. Average true position measurements and variance, C. Average top plane measurements and variance, and D. Average depth measurements and variance across the build plate.

The “best” and “worst” bridges for each attribute are explicitly compared in Figure 6-8.

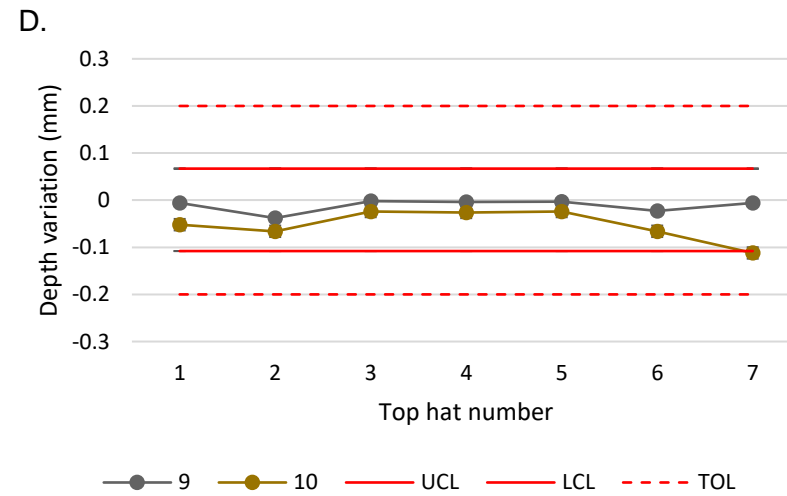
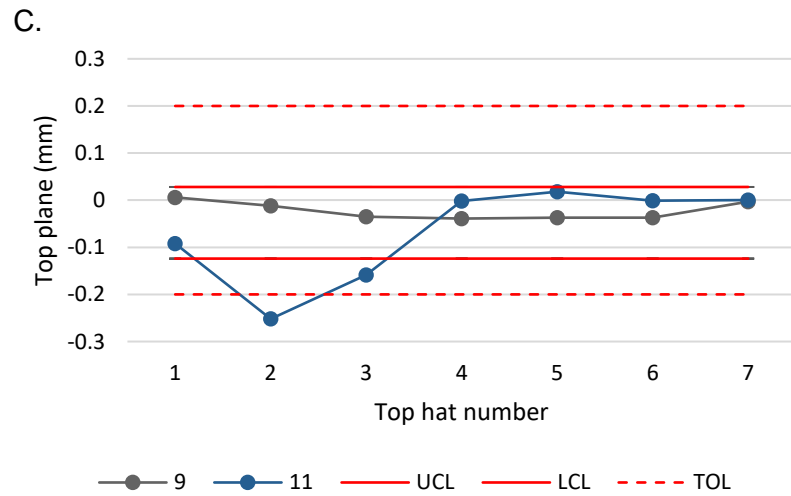
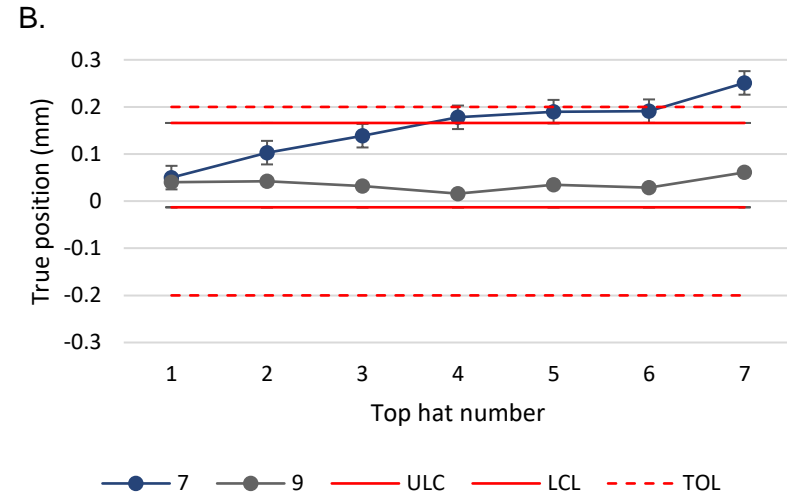
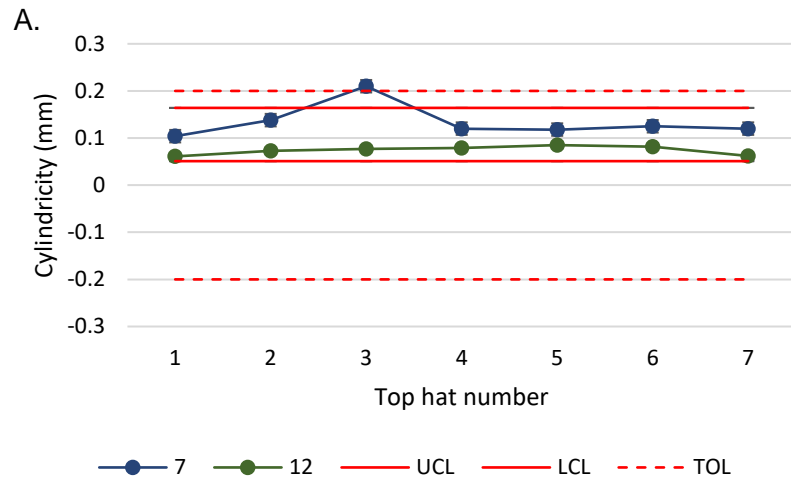


Figure 6-8 Line plots showing the best and worst bridges for A. Cylindricity, B. True position, C. Top plane variation, and D. Depth variation.

Across four of the five attributes, bridge 9 is ranked the “best” and is ranked in the top two for all attributes. The “worst” bridge varies, but is repeatedly on the outer edge of the build plate. Figure 6-8 also shows that the “worst” position for cylindricity, true position, and top plane have measurements that are out of tolerance and lay outside of the upper and lower statistical control limits. The depth variation measurements are the only data set, which lay between the process tolerance limits and just inside the statistical upper and lower limits. (Using the combination of line plots and the matrices, engineers can use this geometric information to improve the process. This will be looked at in more detail in Chapter 7)

The five attributes can be combined to create a new matrix, which rank their sums. Table 6-2 show the combined attribute ranking (shaded in green) for plate 8.

Table 6-2 All attributes and combined attribute ranks for all bridges on plate 8.

Bridge number	Diameter	Cylindricity	True position	Top plane	Depth	Total	Combined rank
1	11	10	3	7	4	35	8
2	9	9	2	3	9	32	5
3	4	7	6	2	6	25	2
4	7	8	5	6	11	37	9
5	12	11	9	4	5	41	10
6	3	3	10	9	3	28	4
7	8	12	12	11	7	50	12
8	5	5	7	5	10	32	5
9	1	2	1	1	1	6	1
10	2	4	4	10	12	32	5
11	10	6	11	12	8	47	11
12	6	1	8	8	2	25	2

Combining all the attributes together creates a new matrix Figure 6-9 which indicates the most optimum build location for this plate.

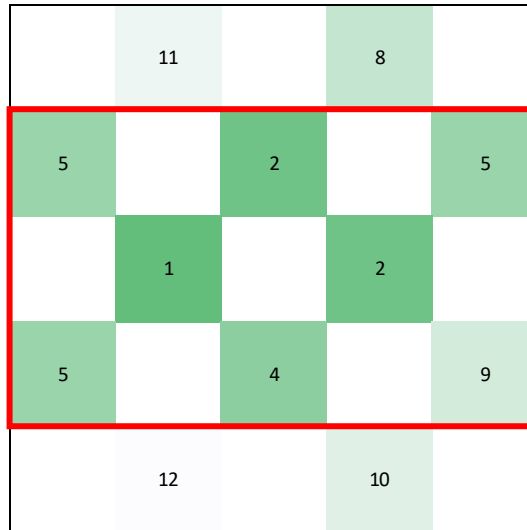


Figure 6-9 Build quality ranking matrix for all attributes on plate 8, indicating best region.

Figure 6-9 show that some regions on the plate are better than others. One example being that the inner bridges are significantly better than the outer bridges. The matrix can be grouped into different sections and each of these sections can be compared using the sum of the rankings (Table 6-3). This can indicate which regions of the plate are better.

Table 6-3 Section sum comparisons for Plate 8

Section	Bridges included	Sum
Inner	3, 6, 9, and 12	9
Outer	1, 2, 4, 5, 7, 8, 10, and 11	65 (33)
Top	1, 2, 10, 11, and 12	31
Bottom	4, 5, 6, 7, and 8	40
Left	7, 8, 9, 10, and 11	34
Right	1, 2, 3, 4, and 5	34
Vertical (bridges built in Y)	2, 3, 4, 8, 9, and 10	27
Horizontal (bridges built in X)	1, 5, 6, 7, 11, and 12	47
Forward diagonal top (\)	1, 2, 3, 4, 11, and 12	37
Forward diagonal bottom (/)	5, 6, 7, 8, 9, and 10	37
Backward diagonal top (/)	1, 8, 9, 10, 11, and 12	32
Backward diagonal bottom (\)	2, 3, 4, 5, 6, and 7	42
Top Quadrant	1, 11, and 12	21
Right Quadrant	2, 3, and 4	16
Bottom Quadrant	5, 6, and 7	26
Left Quadrant	8, 9, and 10	11

Figure 6-9 indicates that bridges built in the centre of the build plate exhibit less bias and less variation, considering all attributes, when compared to the outer bridges. Table 6-3 confirms this with a sum of 9 vs 65 for inner vs outer rankings. It is noted that there are only 4 inner bridges compared with 8 outer bridges, however even the adjusted sum of 33 still indicates that the inner region of the plate is significantly better than the outer regions of the plate.

Considering further regional comparisons allows the plate to be considered holistically. Top vs bottom indicates a marginal improvement in bridges built at the top of the plate vs bridges built at the bottom. Left vs right show no difference in the sum of the rankings, despite Figure 6-9 appearing (implied in the shading) to be better on the right side of the plate. Horizontal vs vertical indicates a potential issue with horizontal bridges, with a sum almost double that of vertical bridges. Grouping the plate from top left to bottom right proves that the sum of ranks for both regions are identical, however grouping the plate from bottom left to top right indicates marginally better bridges built in the top left. Further grouping the plate into four quadrants shows that the left and right quadrants are significantly better than the top and bottom quadrants.

All the regional comparisons indicate that the build quality matrices presented are useful; however, they present different information visually than they do numerically due to the monochromatic shading. For plate 8 the comparison of all the sections show that the central two thirds of the build plate contain bridges that are closest to the target value and have least measurement variation. Plate 8 needs to be compared to the other plates built in the same calibration window to see if they show the same quality trends.

It is noted that all the parts are out of tolerance for plates 8-11 based on their diameter. This would need to be addressed before any further assessments of the parts are made. In a manufacturing environment parts that are out of tolerance would be scrapped and the process immediately adjusted to bring it back into tolerance. The bias is addressed Section 6.4.

6.3 Comparing build sections across builds

Section 6.2 showed that the best build section on plate 8 was the central section across the build plate. Applying the same ranking system, plates 9-11 were investigated. Table 6-4 shows the section sum comparisons for plates 8 - 11.

Table 6-4 Section sum comparisons for plates 8-11

Section	Bridge numbers	Sum (Plate 8)	Sum (Plate 9)	Sum (Plate 10)	Sum (Plate 11)
Inner	3, 6, 9, and 12	9	13	19	17
Outer	1, 2, 4, 5, 7, 8, 10, and 11	65 (33)	63 (32)	58 (29)	60 (30)
Top	1, 2, 10, 11, and 12	31	29	31	27
Bottom	4, 5, 6, 7, and 8	40	41	37	39
Left	7, 8, 9, 10, and 11	34	25	18	30
Right	1, 2, 3, 4, and 5	34	44	47	41
Vertical (bridges built in Y)	2, 3, 4, 8, 9, and 10	27	42	35	35
Horizontal (bridges built in X)	1, 5, 6, 7, 11, and 12	47	34	41	42
Forward diagonal top (\)	1, 2, 3, 4, 11, and 12	37	40	47	38
Forward diagonal bottom (/)	5, 6, 7, 8, 9, and 10	37	36	29	39
Backward diagonal top (/)	1, 8, 9, 10, 11, and 12	32	28	26	27
Backward diagonal bottom (\)	2, 3, 4, 5, 6, and 7	42	48	50	50
Top Quadrant (Q)	1, 11, and 12	21	13	19	15
Right Quadrant (Q)	2, 3, and 4	16	27	28	23
Bottom Quadrant (Q)	5, 6, and 7	26	21	22	27
Left Quadrant (Q)	8, 9, and 10	11	15	7	12

Figure 6-11 shows the same regional comparisons considered in Table 6-3 and Table 6-4. The magnitude of the shift indicates a stronger difference between regions; however, the direction of the shift indicates if the attribute is better or worse and is the more significant aspect of the plot. Individual rank sum values are not important as they are purely comparative.

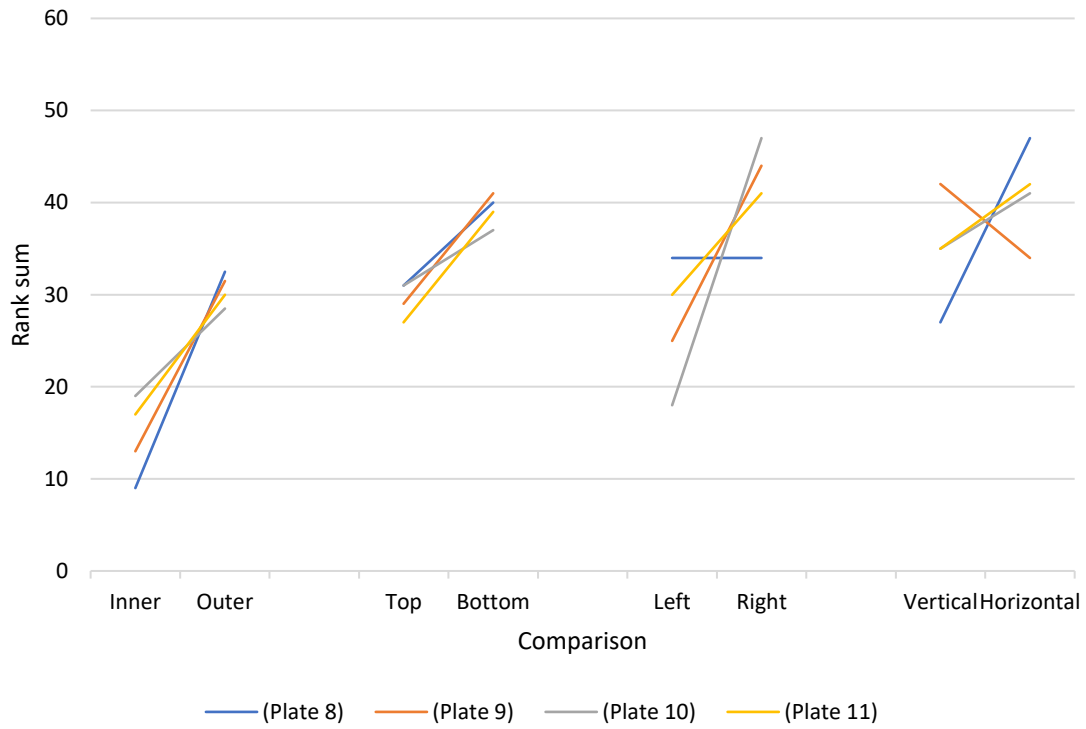


Figure 6-10 line graph showing regional comparisons for plates 8-11

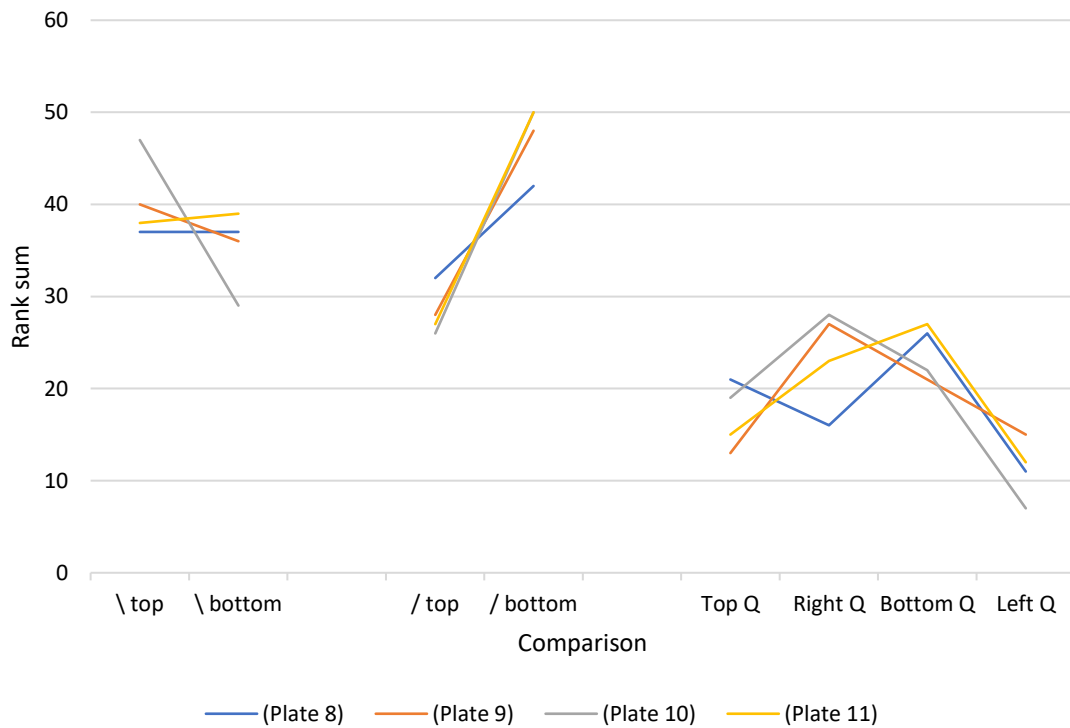


Figure 6-11 line graph showing regional comparisons for plates 8-11

Figure 6-11 shows that for inner vs outer, top vs bottom, and backward diagonal top vs backward diagonal bottom all four plates indicate similar directional differences between regions. This implies a 43% match (three matches out of seven comparisons). Comparing left vs right and quadrant comparisons, three of the plates indicate similar directional differences, but plate 8 differs. Comparing vertical vs horizontal indicates that three of the plates show similar directional differences, but plate 9 differs. Forward diagonal top vs forward diagonal bottom shows no overall similarity between the plates. This analysis indicates that for the aforementioned regions, plates within this calibration indicate a 71% match.

The analysis of specific regions is inherently high-level and is only useful in situations where an operator is concerned with fixed build regions. For example, the operator could choose to either put the part on the top half of the build plate if only considering the top vs bottom comparison, or in the centre of the build plate if only considering the inner vs outer comparison. One could combine the information to identify the optimum position, but that would rely on the operator successfully interpreting the information. Therefore, an approach is required that provides similar information about which region is best, yet also accounts for variation between different builds. This information represents the transition from process foundation to process setting.

Comparing the plates using the quality matrices one can visually show which areas on the build plate are the best and how they alter with the introduction of further builds. Figure 6-12 shows the combined attribute ranking for each individual plate across the top matrices. The bottom matrices show the accumulative ranked average.

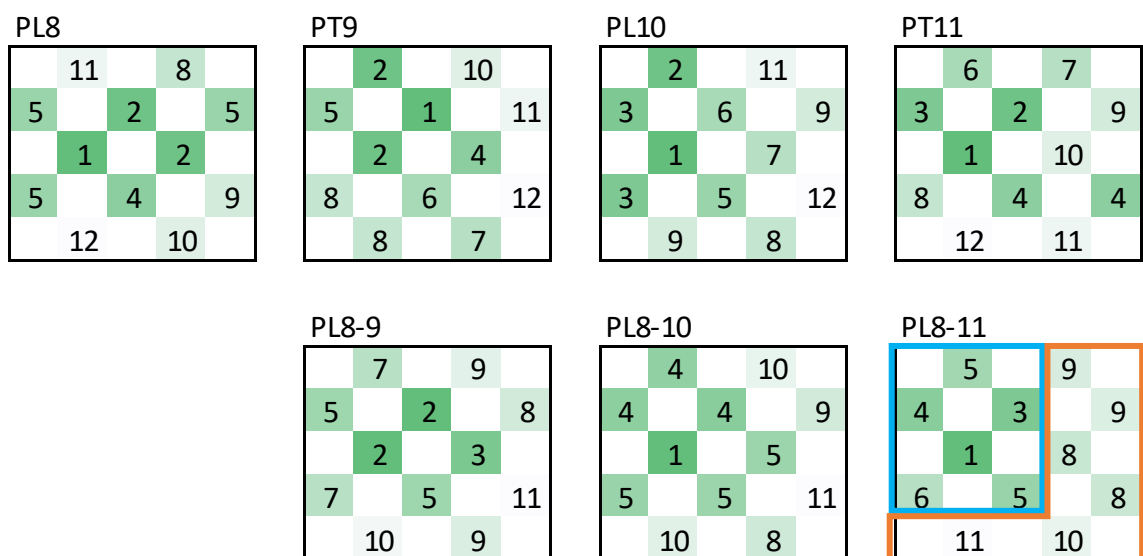


Figure 6-12 Combined attributes ranking for each individual build plate (top), build plate accumulative ranked average (bottom)

Observing the accumulative ranked average for PL8-11, it is identified that the top left section of the plate produces the best parts on average (highlighted by a blue box). The bottom right sections of the build plate produce the worst parts (highlighted by an orange “L” shaped box). The top row of matrices can be used to compare patterns within each individual plate with the accumulative average. It can be seen that plates 9, 10, and 11 correspond strongly to the overall average, but plate 8 does not appear to conform to this pattern.

Introducing the first three build plates it can be observed that they exhibit similar patterns to the average of plates 8-11. Despite there being slightly more variation within plates 1-3, the general trend appears to be the same. The variation is likely to be due to natural variation caused when beginning a new manufacturing process. This is highlighted in Figure 6-13 as “preliminary builds”. Plate 8 seems to be an anomaly as the pattern observed differs to the others (as pointed out previously). As more than half of the plates show strong similarities, the overall pattern is unaffected by plate 8. The top left remains the best section, the bottom right remains the worst.

Without producing hundreds of build plates with these test samples, it is difficult to check if this is the true plate variation or the consequence of random variations associated with the enactment of this limited set of build processes. The contribution made by this research is in the engineering of the structured approach enabling the acquisition, analysis and representation of the test piece quality. This can support further detailed assessments of the relationship between location and quality and separate this from the stochastic variations that will arise during the natural enactment of the SLM process. This is also necessary to determine whether plate 8 is unique or is a repeating anomaly.

To bring the plates into tolerance the next section will explore the top hat diameters. This was carried out following a second calibration process.

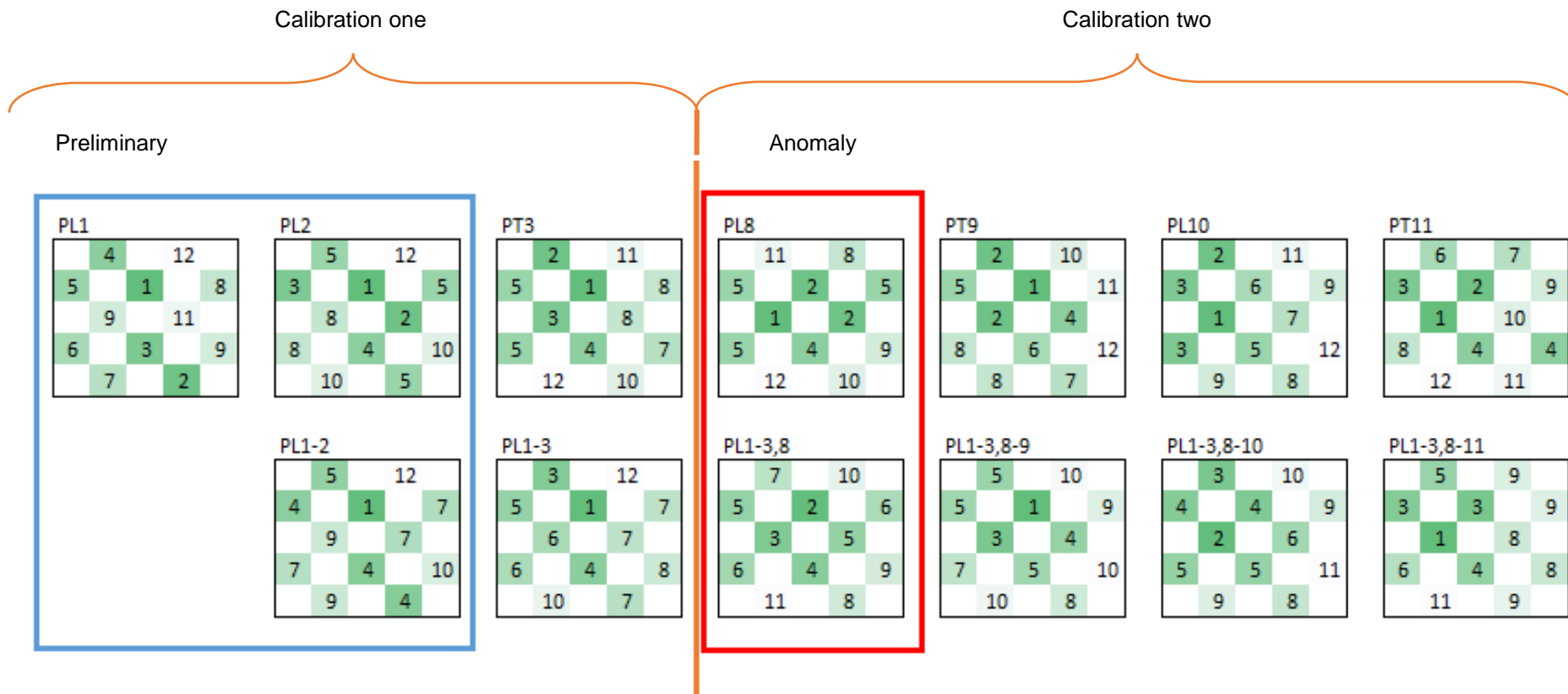


Figure 6-13 build plates 1-11 combined ranking (shown on top row) and build plate accumulative average ranking (bottom row)

6.4 Artefact diameter adjustment

Though five attributes are measured, diameter and depth were classed as critical attributes and can be broken down and evaluated individually. As discussed in Section 6.2, it was identified that the diameters of the top hats were out of tolerance (Figure 6-6). These diameters needed to be adjusted to bring them back into tolerance and bring them closer to the nominal value of 6mm. The values for depth and flatness lay in tolerance so were not in need of adjustment.

There is observable variation across the build plate (see Section 6.3), however the engineer/operator has limited scope to change calibration setting to improve this. For this reason in this thesis this step is taken here, in the process foundation section, as opposed to the process setting phase, where it may also have been placed. As there is no significantly repeatable pattern identified in this small study, one is unable to apply a change at individual positions around the build plate to eliminate/mitigate the inherent process variation that occurs. As the operator cannot make significant changes to the AM250 machine, changes to the CAD model are the best option. General changes can be made to the CAD model to improve accuracy and to bring the parts manufactured back into tolerance (mitigating the bias). Before working out the changes that need to be applied, a base line build is needed to check that the third calibration had not changed the general trend in variation across the build plate. Figure 6-14 provides the matrices for all build plates manufactured (1-3 and 8-12) including when a calibration took place. The top matrices show the combined attribute ranking for each individual build plate. The matrices on the bottom line show the average ranking change over time based on each new build.

It can be seen that the introduction of plate 12 has shifted the “best” and “worst” regions slightly, but, in general, bridges 6, 7, 9, 10, 11, and 12 are still the preferred place positions to build parts. Bridge positions 1, 2, 3, 4, 5, and 8 are still the “worst” positions. As there is no major shift across the build plate an offset can be applied to the top hat diameters. It would be possible to apply different offset to different zones to maximise the improvement and reduce variation in the top hat artefacts, but the aim at this stage is to get all top hat diameters in tolerance by applying one offset to the CAD model. Further refinements could be applied in the future to reduce variation.

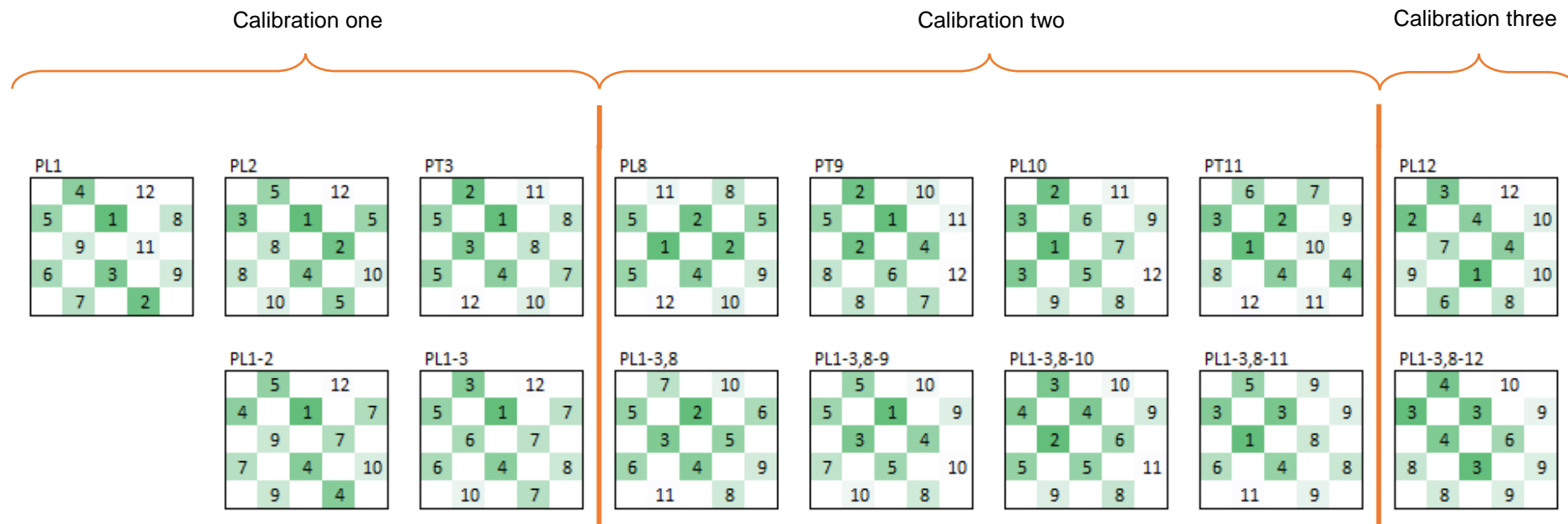


Figure 6-14 build plates 1-12 combined ranking (shown on top row) and build plate accumulative average ranking (bottom row)

Figure 6-15 shows the average diameters for plates 1-3 and 8-12. The average for all the plates shown as a red line is 0.204mm (± 0.002 mm). The error bars indicate the range in the average bias measurements across each plate. It is observed that plate 12 is closest to the mean bias with an average bias of 0.191mm and the measurement range has decreased across the build plate by 0.039mm compared to plates 8-11 which were built in the previous calibration. This indicates that there is more variation in plates 8-11 compared to plate 12.

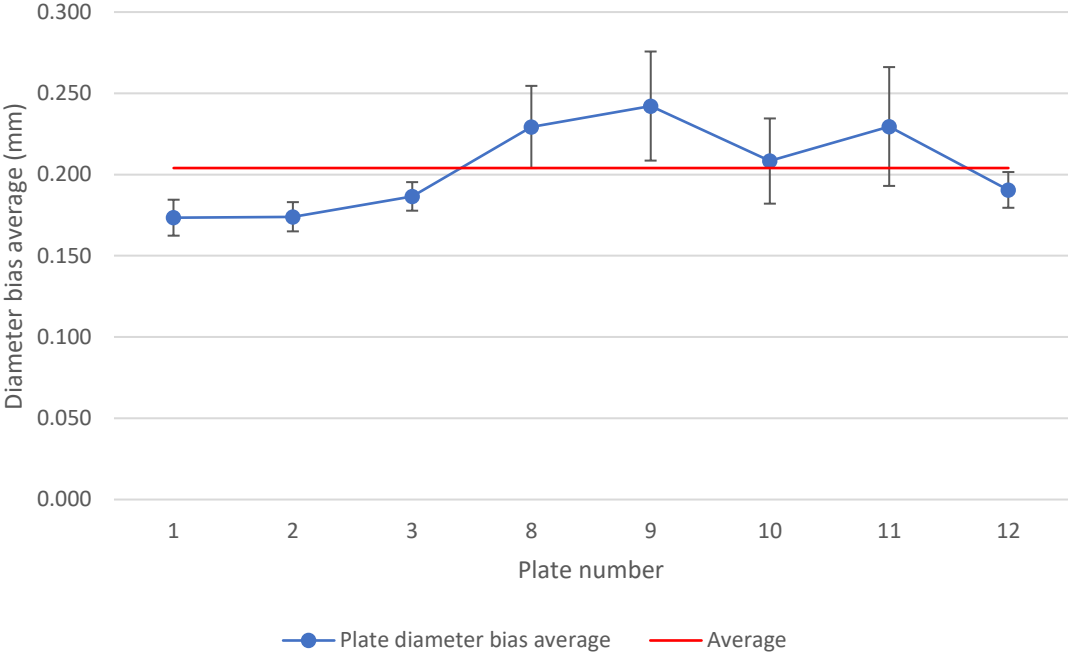


Figure 6-15 Line plot of diameter bias average for plates 1-3 and 8-12

To consider the manufacture of an improved set of test pieces the CAD drawing for all the top hats was changed, increasing the hole diameter by the mean bias identified in Figure 6-15, rounded to one significant figure (0.2mm). The outer diameter of each top hat was also increased so that the wall thickness of the cylinder was maintained. Plate 13 was then produced.

Figure 6-16 shows the top hat diameter plot for the bridges manufactured on build plate 13. It is observed that all the diameters are now closer to the target value of 6mm, so the planned change could be said to have been successful. However, the measurement range on the build plate is 0.091mm, an increase of 0.007mm over plate 12. The increase of 0.007mm is close to the CMM variability of 0.002mm discussed previously and therefore close to the limitations of the gauge used in this study (see the GR&R Chapter 4).

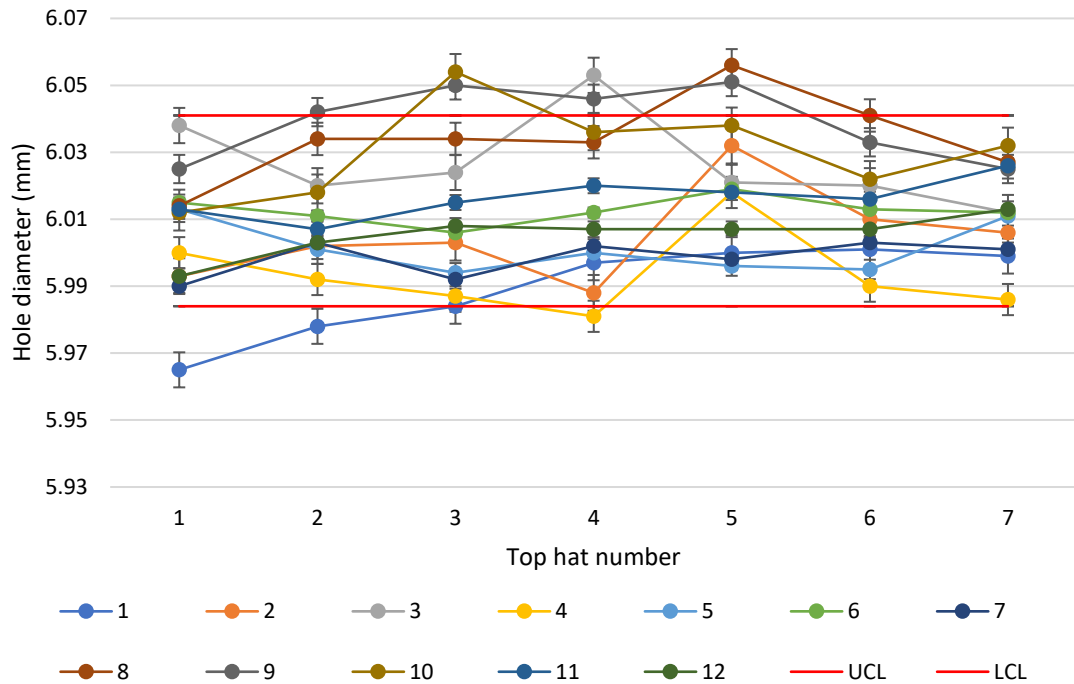


Figure 6-16 Top hat diameter plot for all bridges manufactured on build plate 13. (The legend indicates the bridge number where a bridge is made up of seven top hats.)

Figure 6-17 shows the “best” position alongside the “worst”, identified using the quality matrices (Figure 6-14). Bridge 7, on average, was the best with an average bias of 0.002mm (5.998mm diameter) and a standard deviation of 0.005mm. The worst bridge was number 10 with an average bias of 0.030mm (6.030mm) and standard deviation of 0.013mm. All parts now lay between the required tolerance limits.

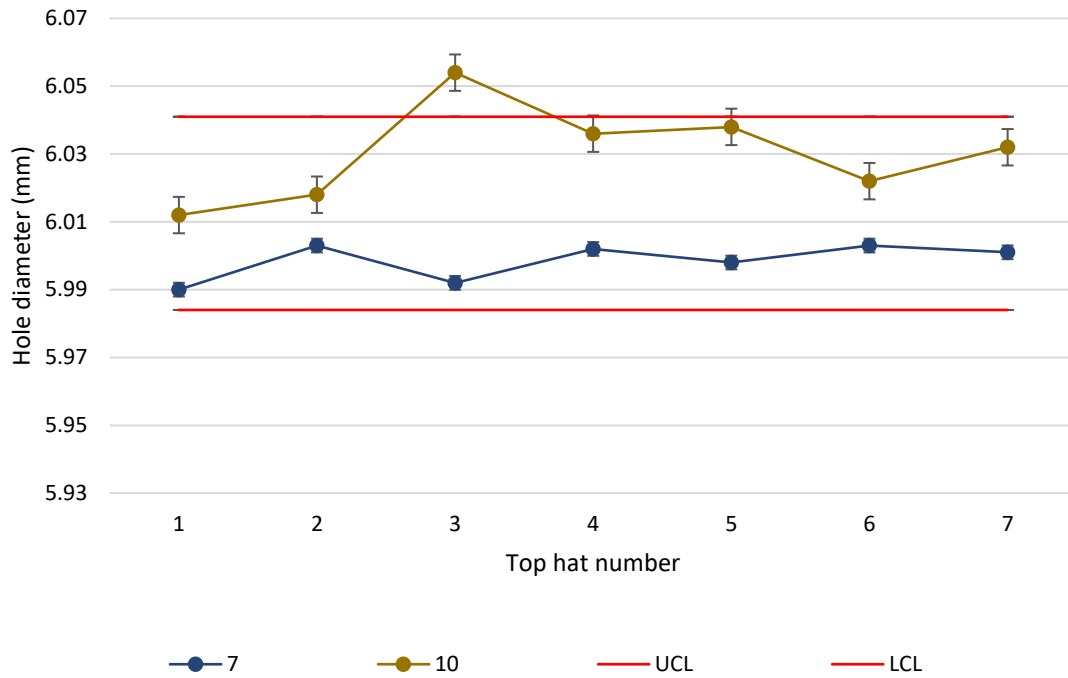


Figure 6-17 Top hat diameter plot for bridges 7 and 10

6.5 Cylindricity investigation

In the previous section it was confirmed that the part diameter accuracy was improved by increasing the top hat cylinder diameter. The improvement was achieved by increasing the inner and outer cylinder diameters on the CAD model by 0.2mm. In this section the cylindricity measurements will be explored, as cylindricity is linked to the diameter measurement, but relates to the cylinder form, rather than to, the feature size. Figure 6-18 shows the cylindricity measurement for all top hats on plates 12 and 13.

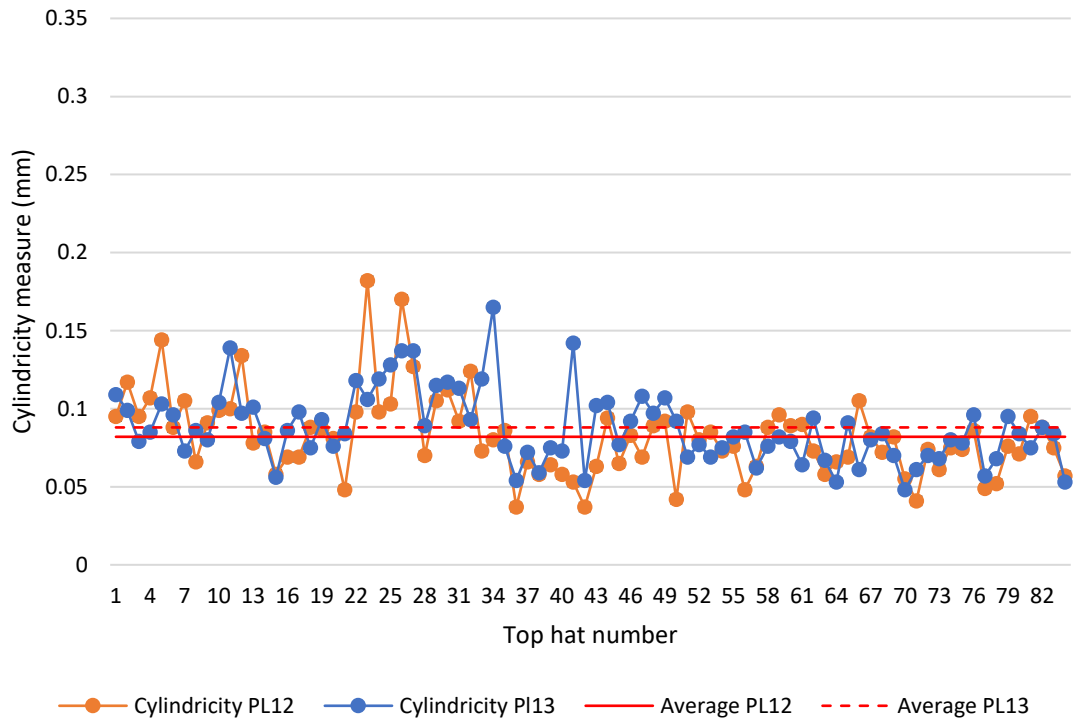


Figure 6-18 Cylindricity measurements for all top hat on plates 12 and 13

The cylindricity measurement for plates 12 and 13 should be comparable because the parts were similar, the wall thickness for the cylinders being the same. The cylindricity measurements for plates 12 and 13 indicated no significant difference when compared using a T-test, with a P-value of 0.159. The average value for plate 12 being 0.082mm and plate 13 being 0.088mm Figure 6-18. The alterations made between plate 12 and 13 assumed that the external cylinder diameter was not a critical feature, meaning that it could be altered to maintain the wall thickness manufactured for plates 1-3 and 8-12. If, however, the external cylinder dimensions were critical and could not be changed, only an increase of the inner diameter would be possible. This would reduce the wall thickness from 0.75mm to 0.65mm and may adversely affect the cylindricity measurement. To investigate this possibility an extra build, Plate 14, was completed to investigate if the change in wall thickness caused a statistically significant change in the cylindricity measure.

Plate 14 was produced under the same build conditions as plates 12 and 13. The top hats manufactured on plate 14 had an altered CAD model that had an inner cylinder diameter of 6.2mm and an outer cylinder diameter of 7.5mm as per the original artefacts. This produced a wall thickness of 0.65mm and the cylindricity was compared to that of plate 12 and 13 (Figure 6-19).

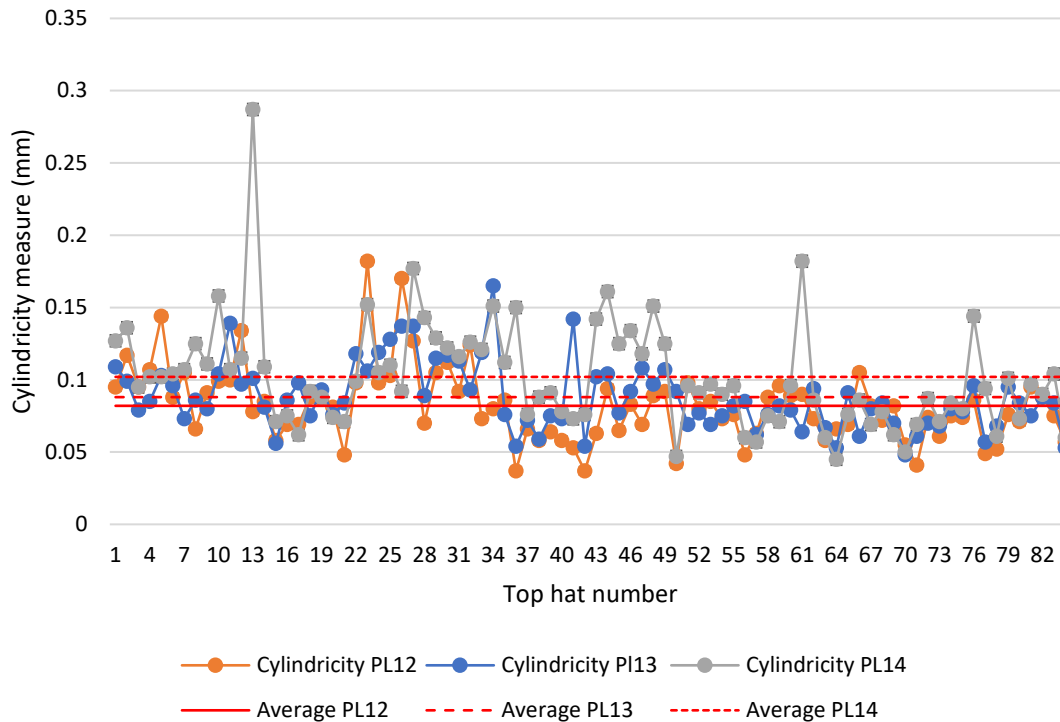


Figure 6-19 Cylindricity measurements for all top hat on plates 12 – 14

Plate 14 shows an increase in the mean cylindricity (0.102mm) and has a Kurtosis value (6.599) which is much higher than both plate 12 and plate 13 (2.958 and 0.908 respectively). The higher Kurtosis for plate 14 cylindricity indicates a higher risk of outlier measurements. A T-test comparison indicated that for cylindricity neither plate 12 nor plate 13 were statistically the same as plate 14, with a P-value of 0.000 for plate 12 versus 14 and a P-value of 0.003 for plate 13 versus 14.

This initial investigation implies that a thinner cylinder wall in the top hat geometry results in a worse cylindricity measurement. However, the top hat is designed to have a thin wall. This implies that the design should be reviewed and thicker walls implemented, unless the cylindricity is not a critical. Further investigation is required and is outside of the scope of this thesis.

6.6 A quantitative approach

Section 6.3 showed that each build plate can be grouped into two distinct regions by considering the average accumulative rank across plates. By grouping the build plate into the best and worst regions one can compare how much better the “best” section is compared to the “worst”. This assessment must be set against the required levels of quality associated with each feature. In each case, with the exception of the

diameters, the features were consistently achieving an acceptable level of quality. Figure 6-10 and Figure 6-11 indicated that bridges 1-5 and 7 were in the worst region and are inferior to bridges 6 and 8-12 which were situated in the best region. It is noted that bias was corrected for in Section 6.4 and is hence not considered in this section.

Figure 6-20 shows the probability distributions for the best half of the build plate (blue distribution) and the worst half of the build plate (orange distribution). These distributions consider the accumulated $Y_{\text{Descriptive}}$ measures explained in Section 6.2 as a measure of the bridge quality. Lower values indicate a higher bridge quality. It is noted that these numbers are perhaps arbitrary and only represent the relative difference between the “worst” bridge and the “best” bridge.

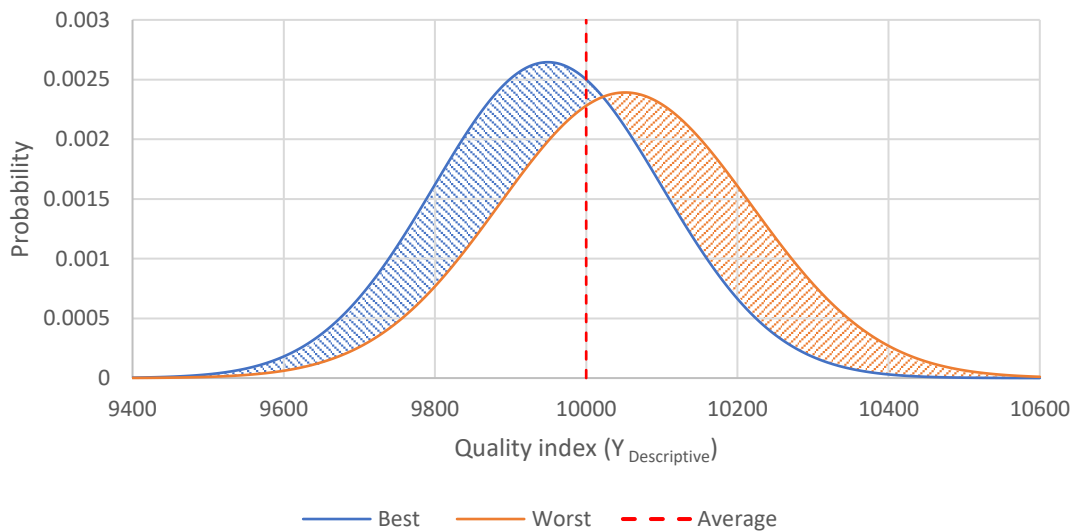


Figure 6-20 Normal distributions for the “Best” and “Worst” areas on the build plate

The “Best” distribution includes bridges 1-5 and bridge 7 and has an average bridge quality of 9949.31 with a standard deviation of 150.80. The “Worst” distribution includes bridge 6 and bridges 8-12 and has an average bridge quality of 10051.46 with a standard deviation of 166.79. The average across both distributions is 10000.39 with a standard deviation of 158.79. Each hatched region indicates how different each distribution is from the other. The hatched areas are equal to 25.51%. This may be taken to represent that the best region is 25.51% better than the worst region.

Using the tolerance provided by Renishaw, it is possible to apply true measurements to the quality index for each attribute that was measured. This will inform about the

process and state the tolerances that can be achieved according to the data that has been collected to date. For each bridge, on all plates, the average standard deviation was calculated by considering all the five attributes (diameter, cylindricity, true position, top plane, and depth). This resulted in 12 standard deviations per plate (Table 6-5).

Table 6-5 Average standard deviations for all attributes per bridge

Position	PL1	PL2	PL3	PL8	PL9	PL10	PL11	PL12	PL13	PL14
1	0.039	0.040	0.044	0.018	0.025	0.022	0.018	0.027	0.031	0.019
2	0.034	0.031	0.063	0.020	0.025	0.018	0.022	0.025	0.033	0.034
3	0.032	0.031	0.042	0.021	0.021	0.019	0.029	0.023	0.026	0.019
4	0.032	0.034	0.038	0.022	0.029	0.024	0.017	0.024	0.023	0.029
5	0.026	0.030	0.040	0.024	0.029	0.018	0.025	0.022	0.024	0.023
6	0.024	0.030	0.033	0.024	0.032	0.024	0.026	0.028	0.037	0.034
7	0.032	0.040	0.046	0.047	0.022	0.022	0.027	0.017	0.016	0.018
8	0.028	0.033	0.034	0.018	0.023	0.015	0.036	0.024	0.023	0.024
9	0.036	0.031	0.036	0.012	0.022	0.018	0.023	0.022	0.023	0.030
10	0.030	0.030	0.039	0.019	0.016	0.014	0.028	0.016	0.022	0.024
11	0.030	0.030	0.034	0.042	0.025	0.013	0.019	0.023	0.017	0.019
12	0.029	0.028	0.032	0.019	0.027	0.022	0.027	0.026	0.026	0.026

To represent an entire plate, the second highest value from all 12 positions was taken as the “representative deviation”. To consider the best and worst regions of a plate, the second highest value from positions 6 and 8-12 was taken as the “representative deviation” for the best region, whilst the second highest value from positions 1-5 and 7 was taken as the “representative deviation” for the worst region. The second highest value was explicitly considered to reduce the risk of artificially high values arising from plate anomalies (Sindhumul et al. 2016). The build plates can then be evaluated against the acquired standard deviations (representative deviations) to identify how

much of the measurement data can be contained within the representative deviation, or equally how many representative deviations are needed to contain all the measurement data.

Firstly, the total representative deviation was set at 0.2mm to represent the design tolerance for the entire plate, this was equal to 4.35 times the representative deviation of 0.046mm (see Table 6-6). It is observed that 100% of the diameters were within tolerance, but cylindricity, true position, top plane and depth had a number of measurements that were out of tolerance. Of all 4200 measurements, 185 were identified as out of tolerance, indicating a reject rate of 4.40% across the whole plate. The “best” and “worst” regions of a plate were also be assessed in a similar manner (the results are provided in Table 6-6). It is noted that a reject rate of 3.76% for the best region of the build plate indicates an improvement over the plate average, compared to a reject rate of 5.14% for the worst region of the build plate (higher than the plate average).

Table 6-6 Build tolerance analysis

		Diameter	Cylindricity	True Position	Top plane	Depth
FULL PLATE	Rep. dev. (rDev)	0.046	0.046	0.046	0.046	0.046
	No. rDev	4.35	4.35	4.35	4.35	4.35
	In count	840	832	680	824	839
	Tot count	840	840	840	840	840
	% in	100.00%	99.05%	80.95%	98.10%	99.88%
	TOL ±	0.200	0.200	0.200	0.200	0.200
BEST	Rep. dev. (rDev)	0.036	0.036	0.036	0.036	0.036
	No. rDev	5.56	5.56	5.56	5.56	5.56
	In count	420	419	345	419	420
	Tot count	420	420	420	420	420
	% in	100.00%	99.76%	82.14%	99.76%	100.00%
	TOL ±	0.200	0.200	0.200	0.200	0.200
WORST	Rep. dev. (rDev)	0.046	0.046	0.046	0.046	0.046
	No. rDev	4.35	4.35	4.35	4.35	4.35
	In count	420	413	335	405	419
	Tot count	420	420	420	420	420
	% in	100.00%	98.33%	79.76%	96.43%	99.76%
	TOL ±	0.200	0.200	0.200	0.200	0.200

The method can be extended to find the smallest achievable tolerance for across the plate and for the “best” and “worst” regions individually (Table 6-7). This can be achieved by finding the minimum total representative deviation (TOL) that encompasses 100% of the measurement data. This is applied to each of the attributes individually.

Table 6-7 Build tolerance analysis showing new tolerances

		Diameter	Cylindricity	True Position	Top plane	Depth
PLATE	Rep. dev. (rDev)	0.046	0.046	0.046	0.046	0.046
	No. rDev	2.1	6.3	10.1	13.5	9.3
	In count	840	840	840	840	840
	Tot count	840	840	840	840	840
	% in	100.00%	100.00%	100.00%	100.00%	100.00%
	TOL ±	0.097	0.290	0.465	0.621	0.428
BEST	Rep. dev. (rDev)	0.036	0.036	0.036	0.036	0.036
	No. rDev	1.6	7.8	11.3	7.1	3.3
	In count	420	420	420	420	420
	Tot count	420	420	420	420	420
	% in	100.00%	100.00%	100.00%	100.00%	100.00%
	TOL ±	0.058	0.281	0.407	0.256	0.119
WORST	Rep. dev. (rDev)	0.046	0.046	0.046	0.046	0.046
	No. rDev	2.1	6.3	10.1	13.5	9.3
	In count	420	420	420	420	420
	Tot count	420	420	420	420	420
	% in	100.00%	100.00%	100.00%	100.00%	100.00%
	TOL ±	0.097	0.290	0.465	0.621	0.428

Taking the diameter measurements as an example, it can be observed that the tolerance can be improved to 0.1mm (a change of 50%) across the entire plate. For the “best” region of a plate, the tolerance improves to 0.06mm, whilst the “worst” region of a plate results in an achievable tolerance of 0.1mm. The difference between the “best” and “worst” regions for diameter on the plate is 40%. It was previously identified that the overall improvement across the plate is 25.51% (see Figure 6-20), but this indicates a greater improvement in the “best” and “worst” for diameter. It is noted that most of the other attributes result in a recommended tolerance higher than

0.2mm, but to achieve this the process needs to be set up correctly and the CAD model correctly defined.

6.7 Discussion

At the beginning of this chapter five questions were posed, these questions were explored and answered. It was identified that build location does appear to affect the geometry of the top hats. However, more runs are needed to properly ascertain trends/patterns in the measurement data. It is important to stress that the work carried out in this thesis is only a small sample and to make it representative of the process at least 100 plates would need to be produced once the machine was brought into tolerance. Following this structured approach the new data could then be collected and used to identify if patterns were evident and repeatable. If patterns were identified they could then be related to the AM250 machine used to manufacture the parts. By adopting the same approach, using the same test piece and test piece arrangement other AM250 machines could be subjected to this structured approach. By adopting a similar approach, using equivalent test pieces, any SLM machine could be subjected to the structured approach, thus improving its operation. It is therefore the structured approach that can be viewed as a research contribution.

It was also shown in Sections 6.2 and 6.3 that some sections of the build plate are better than others. It was also evidenced that the AM250 machine produces the artefact better in positions 6, 8, 9, 10, 11, and 12 (see Figure 6-12 and Figure 6-14). This seems to be consistent from the builds built after the preliminary set up (Figure 6-13). There is evidence that plate 8 is different from the other build plates based on the matrices in Section 6.3. The best build locations for plate 8 are bridges 2, 3, 6, 8, 9, 10, and 12 which only matches 50% of the “best” bridges from the other builds. There is no obvious reason for why this build was different and it could simply be down to the cleanliness of the machine or an unidentified fluctuation in production parameters as there is no definitive evidence for either of these it can be classed as a one off event (random).

The matrices and regional comparison graph (Figure 6-9 and Figure 6-11) showed that orientation does have an impact on geometry. To investigate this further one would need to look at .dat file data produced from the CMM. These files can be used to produce a point cloud that can be examined. The different section of the .dat file can be compared to see how the form changes from one cylinder to another, this could then be related to the build direction. If the cylinders in one direction are more oval in shape it could be that the encoders on mirrors need recalibrating or software

updating. Processing the .dat files would be time consuming and complex as machine co-ordinates would need to be matched with part co-ordinates. As there is no way of checking where the laser fires during a build, matching the two with the data available would be very difficult and could be independently studied.

Lastly, there is evidence of build variation for cylinder depth, however the matrices show when depth is isolated, the build quality for each bridge location is similar (See Appendix 9). Though there is variation this may not be solely due to the build process, but also the measurement process. As discussed in Chapter 4 Section 4.5 the top and bottom planes used to derive this feature are susceptible to measurement variation due to the size restriction of the cylinder, so this variation must be assessed with caution. Further work would be needed to improve the measurement process for depth. If this measurement variation is ignored and the depths considered as per the measurements taken, because the general trend is the same across all plates, the variation can/could be isolated to a manufacturing process. Based on experience from operating the AM250 machine depth variation could be due to; the elevator encoder error, the build plate not being fixed securely to the elevator plate, the recoater blade being over tightened which can cause the rubber blade to flex and bulge producing different size gaps along its length therefore changing the powder distribution on the build bed, or over melting of the powder. These could all be evaluated and tested once the machine was brought under control (in tolerance).

The introduction of the quality matrices helps engineers and operators visualise the best and worst regions of the build plate quickly and can be used to consider either individual or all attributes. When a machine is optimised the matrix can be used in conjunction with the tolerance analysis to locate parts that need to be made to a set precision, by locating it in the best area on the build plate.

The matrices have limitations, in that the information contained only relates to the bridge locations and does not provide information between artefacts. Also, the matrix does not indicate if any of the attributes are out of tolerance; the engineer would have to look at run charts to check although, as identified in Section 6.2, the individual attribute matrix would show the engineer which measurements to look at i.e. the “best” and “worst”. To further improve this tool, research would need to be carried out to see if variation extrapolation can be made between the bridges built around the edge of the build plate and the ones built in the middle.

Over time the matrix can be used to provide a unique “finger print” for the machine. At critical stages, for instance following a calibration or other maintenance action, if

the matrix (fingerprint) changes (similar to plate 8 in Figure 6-13) then the set up could be evaluated. It would also be possible to use this approach to identify if any enacted process changes have affected the build quality around the build plate.

The AM250 machine allows users to change a number of parameters, but as identified in this chapter once the calibration by the OEM is completed, there is no easy way of improving the process other than amending the CAD model. This chapter identified that most of the top hat diameters were out of tolerance after the first calibration of the ALM machine. As none of the parameters nor the CAD model were changed this had to be a result of the OEM's calibration. The implication of this is that the laser was not firing in the required position on the build bed. The fix was to change the CAD model to bring the top hats back into tolerance by altering the bias (increasing the cylinder diameters by 0.2mm). In one case however, by making this change to the CAD model, a cylindricity issue occurred. Increasing the internal diameter of the cylinder reduced the wall thickness causing the cylindricity to degrade. If the wall thickness was a critical component to the build and the external dimensions were constrained, amending the CAD model would not be an option and the OEM would have to revisit the machine. This shows that the calibration currently performed could be improved by running 12 bridges on a plate and using the information they provide to set up the AM250 machine to suit.

Section 6.6 showed that the attributes measured could be compared to the OEM's tolerances. Using the tolerance and the measurements taken for all attributes across all plates the reject rate could be calculated. This could also be used to identify which attributes needed to be improved so that the reject rate can be reduced or eliminated. Engineers can use this information to further improve the manufacturing process if they are able to adjust the setting currently locked by the OEM. From the diameter evaluation it is evident that all the attributes could be further improved and the tolerance reduced. True position in this instance had the worst tolerance of 0.465mm compared to the best which was diameter 0.097mm. Based on this small study, OEM could provide different tolerances based on different attributes. Though one can tighten the manufacturing tolerances one must consider where the line is drawn, just because you can does not always mean you should. 0.2mm seems to be a considerable tolerance for a modern manufacturing process and to be on par with traditional manufacturing processes, the tolerance will need to be improved.

6.8 Summary

This chapter has identified that location does affect geometry and it was observed that the AM250 machine in this study had less variation when parts were manufactured in the top left hand corner of the build plate. The matrices are a useful tool for identifying where the best and worst locations are, but it is not clearly defined. As Section 6.6 shows there is still a small probability that parts built in the best section of the plate can have attributes that measure below the build plate average. The quality of parts is highly dependent on the OEM's calibration, but CAD model changes can be implemented to improve accuracy.

Chapter 7 will consider artefacts which are cut off the plate to see if they retain the same information as the bridges measured on the plate. Lastly the in-process log data will be looked at to see if the variation identified on the matrices can be attributed to a change in build environment.

Chapter 7: Discussion; of the use of the artefact across all four layers of the process pyramid

7.1 The use of the artefact in process foundation

This chapter will discuss the use of the artefact in the four stages of the process pyramid. The first section of the chapter relates to process foundation stage. The work presented in Chapters 5 and 6 considered how the artefact can be used to set up the AM250 machine or to check that a calibration has been carried out correctly so that parts can be manufactured accurately. In this chapter plate 12 will be initially subjected to the same analysis as plates 1-3 and 8-11, shown in Chapter 5 and 6 for all three conditions (pre, post, and off). Plate 12 will then be used to represent the knowledge acquired from all previous plates produced on the AM250. During this project, 3 machine calibrations have been undertaken. All the plates have been produced without changing any settings and used to show that the process foundation layer of the pyramid is stable. Table 7-1 shows the sum comparison for all three conditions, for all plates.

Table 7-1 Sum comparisons for plates 1-3, 8-11, and 12

Section	Bridge numbers	Average sum (Plates 1-3)	Average sum (Plates 8-11)	Sum (Plate 12)
Inner	3, 6, 9, and 12	23	15	16
Outer	1, 2, 4, 5, 7, 8, 10, and	27	31	30
Top	1, 2, 10, 11, and 12	37	30	31
Bottom	4, 5, 6, 7, and 8	29	39	34
Left	7, 8, 9, 10, and 11	34	27	27
Right	1, 2, 3, 4, and 5	31	42	44
Vertical (bridges built in Y)	2, 3, 4, 8, 9, and 10	40	35	42
Horizontal (bridges built in	1, 5, 6, 7, 11, and 12	38	41	34
Forward diagonal top (\)	1, 2, 3, 4, 11, and 12	37	41	43
Forward diagonal bottom	5, 6, 7, 8, 9, and 10	40	35	33
Backward diagonal top (/)	1, 8, 9, 10, 11, and 12	45	28	37
Backward diagonal bottom	2, 3, 4, 5, 6, and 7	33	48	39
Top Quadrant (Q)	1, 11, and 12	21	17	19
Right Quadrant (Q)	2, 3, and 4	16	24	24
Bottom Quadrant (Q)	5, 6, and 7	17	24	15
Left Quadrant (Q)	8, 9, and 10	24	11	18

The plate 12 entries in Table 7-1 were compiled following the in-depth analysis of each feature on every bridge using the build plate evaluation and analysis procedure detailed in Section 6.2. To simplify the comparison, the plates were combined according to the calibration window within which they were produced. Plates 1-3 were first combined and averaged, as were plates 8-11, this allowed for easy comparison with plate 12.

The sum comparisons for plate 12 mostly fall between the other two calibration averages. Ten of the comparisons lie between, or are the same as, the sum comparisons for the other manufactured plates. The remaining six comparisons are different and have been highlighted in green and orange. Green represents the comparisons that indicate an improvement over the previous plates, orange represents those that are worse.

Figure 7-2 illustrate the information provided in Table 7-1. The direction of each comparison is the most significant aspect of the plots and indicates where the preferred region is in the comparison. Individual rank sum values are not in themselves seen as being important as they used for comparative purposes.

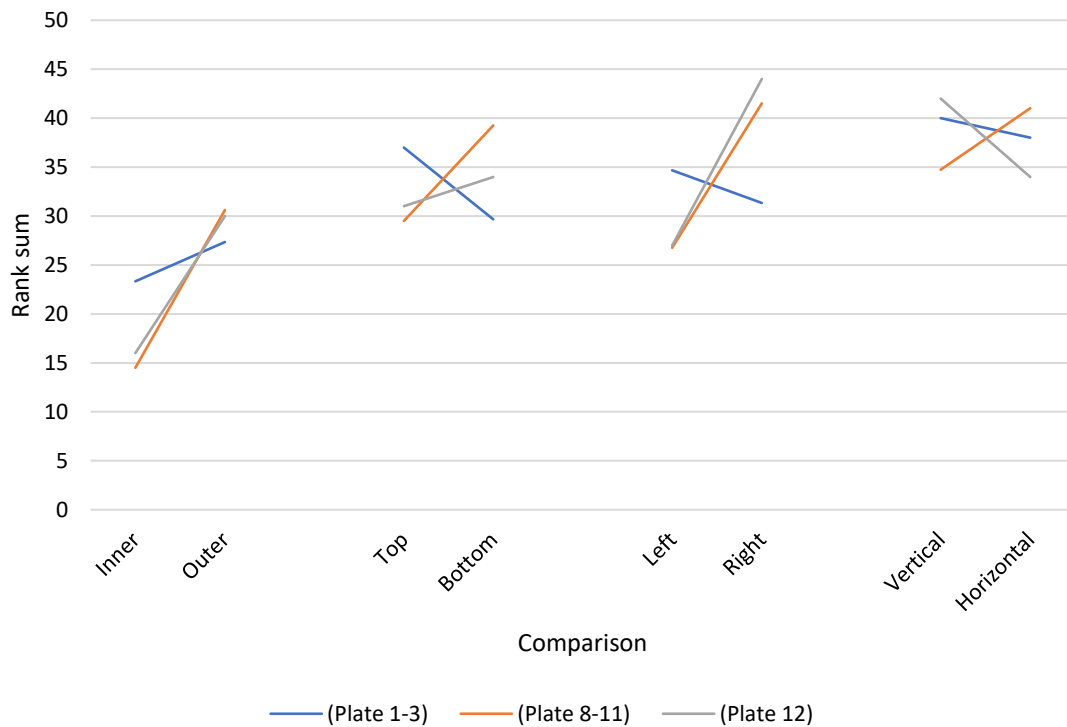


Figure 7-1 line graph showing regional comparisons for plates 1-3, 8-11, and 12

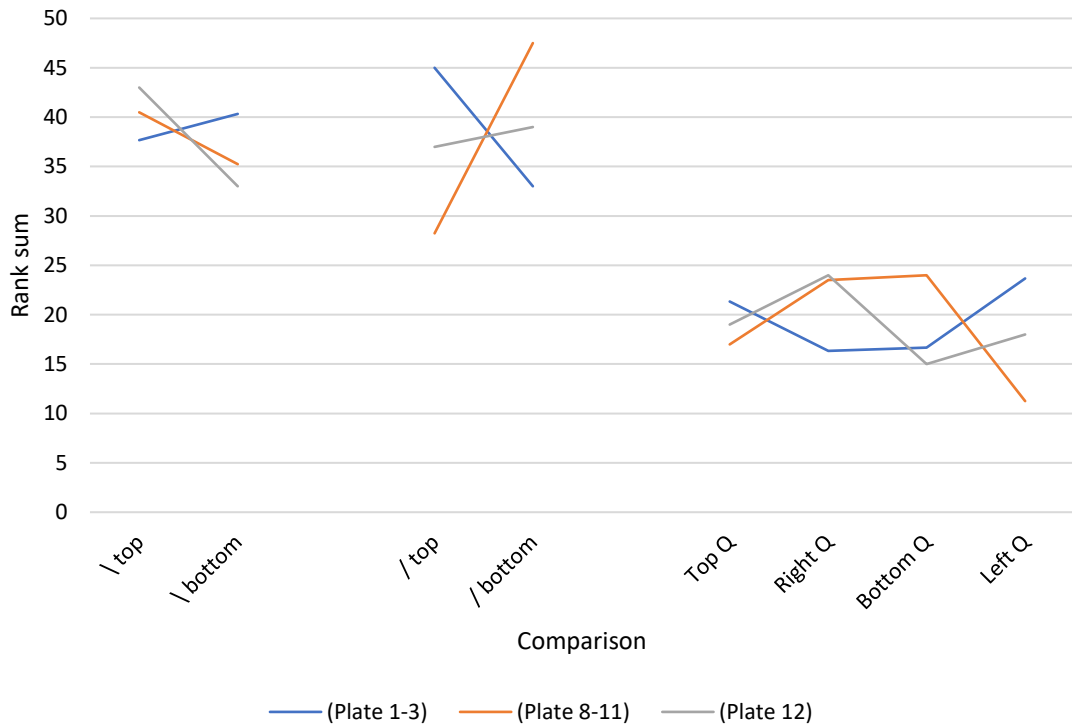


Figure 7-2 line graph showing regional comparisons for plates 1-3, 8-11, and 12

Figure 7-1 and Figure 7-2 indicate that plate 12 shares most of the characteristics associated with both of the previous build calibrations. Not all the plates conform in the same way, but plate 12 shows a 71.4% similarity to plates 8-11. As discussed in Section 6.3, more credibility should be given to plates 8-11 as they were manufactured after learning how to set-up and use the AM250. Plates 1-3 were manufactured during the learning phase and, as explained in Section 6.3, the results from these plates should be utilized with care. Combining the information using the matrices developed in Chapter 6, one can see the overall change in the plate accumulative ranked average. Figure 7-3 shows the matrix for plate 12, the accumulative rank average for all plates prior to plate 12, and the accumulative rank average for all plates including plate 12.

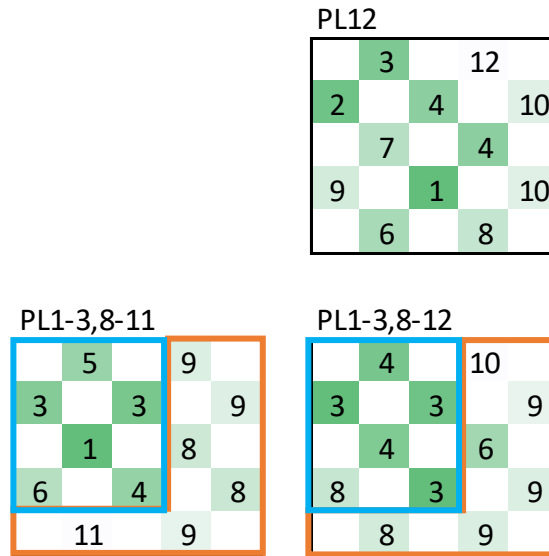


Figure 7-3 Combined attributes ranking for plate 12 (top) and build plate accumulative ranked average (bottom)

The matrices indicate no major changes, with plate 12 appearing to support the previous manufacturing build patterns. Using the developed artefact and the rank comparisons (Table 7-1, Figure 7-1, and Figure 7-2) has confirmed the continuity of the process foundation. Therefore, plate 12 is suitable for considering the potential for using the artefact to support the rest of the process pyramid. It should be noted that the above analysis is representative of the approach enabled by this method. As with any such process monitoring and management approach more stability will be achieved with time; as the number of plates manufactured increases the information becomes less prone to change by individual plate details, but making it easier to identify changes when they do occur. As machine calibrations are undertaken, sets of twelve artefacts will be manufactured. The data acquired would be added to the relevant information about the machine. This information can be made into a generic database, which could then be supplied with all the machines manufactured; in essence, giving the client the expectation of how the machine should perform.

7.2 The use of the artefact in process setting

It was established in the previous chapter that some of the process foundation information overlaps with the process setting section of the process pyramid. The fishbones for process foundation and process setting developed in Chapter 3 (Figure 3-14 and Figure 3-16) also indicated a considerable crossover between the two.

The AM250 is unusual because the machine is designed to accept different metallic materials. Therefore, process foundation and process setting present a greater

challenge compared to single material AM machines. Preparing the machine to undertake processes for a single material will make the process easier to use and simpler to manage. The key process parameters for the AM250 machine are provided in Table 7-2. This table classifies the parameters into ‘controllable’ and ‘predefined’ Controllable parameters can be altered at the start and during the build cycle. ‘Predefined’ parameters are fixed at the start of the build and are either already built into the software running the AM machine or fixed by the operator during the start of the build.

It is noted that some of the fixed variables provided in this table may, on other machines, be controllable in-process. Table 7-2 also informs which of these parameters are monitored throughout the build and are recorded in the programmable logic controller (PLC) log during a build cycle. The PLC log will be considered further in Section 7.3.

Table 7-2 Summary of key process parameters in AM250 machine

	<u>Parameter</u>	<u>Description</u>	<u>Controllable or predefined</u>	<u>AM Plc Log</u>
<u>Feed Stock</u>				
1	Bulk density (ρ_b)	Material density, limits maximum density of final component	Predefined	-
2	Thermal conductivity (k_b)	Measure of material’s ability to conduct heat	Predefined	-
3	Heat capacity ($c_{p,b}$)	Measure of energy required to raise the temperature of the material	Predefined	-
4	Latent heat of fusion (L_f)	Energy required for solid-liquid and liquid-solid phase change	Predefined	-
5	Melting temperature (T_m)	Temperature at which material melts; for alloys, the difference between the liquidus and solidus temperature is typically of greater interest	Predefined	-
6	Boiling temperature (T_b)	Temperature at which material vaporizes; may only be important in certain process conditions	Predefined	-
7	Vapor pressure (p_v)	Measure of the tendency of material to vaporize	Predefined	-
8	Heat (enthalpy) of reaction (H_r)	Energy associated with a chemical reaction of the material (e.g., oxide formation), not always relevant	Predefined	-
9	Material absorptivity ($A_{b,m}$)	Measure of laser energy absorbed by the material, as opposed to that which is transmitted or reflected	Predefined	-
10	Particle morphology (A_R , f_{circ} , f_{elong} , etc.)	Measures of shape of individual particles and their distributions, e.g., aspect ratio, circularity, and elongation	Predefined	-
11	Surface roughness (R_A)	Arithmetic mean of the surface profile	Predefined	-

12	Particle size distribution	particle sizes, usually diameter, is a powder sample	Predefined	-
13	Contamination	Ill-defined factor describing change in properties of powder due to reuse as dust and other particles added to powder	Predefined	-
<u>Build environment</u>				
14	Shield Gas	Usually Ar or N2, but may also be He, or something else	Predefined	Yes
15	Oxygen level (O ₂ %)	Most important environmental parameter; oxygen can lead to oxide formation in metal, change wettability, energy required for welding	Controllable	Yes
16	Shield gas molecular weight (MW _g)	Influences heat balance, diffusivity into and out of part	Predefined	-
17	Shield gas viscosity (μ _g)	May influence free surface activity of melt pool, convective heat balance	Predefined	-
18	Thermal conductivity (k _{c,g})	Term in heat balance	Predefined	-
	Heat capacity of gas (C _{p,g})	Term in heat balance	Predefined	-
19	Pressure (p)	Influence vaporization of metal as well as oxygen content	Controllable	Yes
20	Gas flow velocity (v _g)	Influences convective cooling, removal of condensate	Controllable	Yes
21	Convective heat transfer coefficient (h _c)	Convective cooling of just melted part by gas flowing over the surface	Predefined	-
22	Ambient temperature (T _∞)	Appears in heat balance, may impact powder preheat and residual stress	Controllable	Yes
23	Surface free energy (γ _{gl})	Between liquid and surrounding gas influence melt pool shape	Predefined	-
24	Density (ρ _p)	Measure of packing density of powder particles, influence heat balance	Predefined	-
25	Thermal conductivity (k _p)	Measure of powder bed's ability to conduct heat	Predefined	-
26	Heat capacity (c _{p,p})	Measure of energy required to raise the temperature of the powder bed	Predefined	-
27	Absorptivity (A _p)	Measure of laser energy absorbed, dependent on A _b and state of powder bed	Predefined	-
28	Emissivity (ε)	Ratio of energy radiated to that of black body	Predefined	-
29	Deposition system parameters	Re-coater velocity, pressure, re-coater type, dosing	Controllable	-
30	Layer thickness (L)	Height of a single powder layer, limiting resolution and impacting process speed	Controllable	Yes
31	Powder bed temperature (T _p)	Bulk temperature of the powder bed	Controllable	Yes
<u>Laser</u>				
32	Average power (P _L)	Measure of total energy output of a laser	Controllable	-
33	Mode	Continuous wave or pulsed	Predefined	-

34	Peak power (P_{peak})	Maximum power in a laser pulse	Predefined	-
35	Pulse width (PW)	Length of a laser pulse when operating in pulsed mode	Predefined	Yes
36	Frequency (f)	Pulses per unit time	Predefined	-
37	Wavelength (λ)	Distance between crests in laser electromagnetic waves	Predefined	-
38	Polarization	Orientation of electromagnetic waves in laser beam	Predefined	-
39	Beam quality (M_2)	Related to intensity profile and used to predict how well beam can be focused and determine minimum theoretical spot size (equal to 1 for a Gaussian)	Predefined	-
40	Intensity profile I (x,y,t)	Determines how much energy added at a specific location	Predefined	-
41	Spot size (d_x and d_y)	Length and width of elliptical spot (equal for circular spots)	Controllable	Yes
42	Scan velocity (v)	Velocity at which laser moves across build surface	Controllable	Yes
43	Scan spacing (S_s)	Distance between neighbouring laser passes	Controllable	Yes
44	Scan strategy	Pattern in which the laser is scanned across the build surface (hatches, zigzags, spirals, etc.) and associated parameters	Controllable	Yes
<u>Melt pool</u>				
45	Melt pool viscosity (μ)	Measure of resistance of melt to flow	Predefined	-
46	Coefficient of thermal expansion (α)	Measure of volume change of material on heating or cooling	Predefined	-
47	Surface free energy (γ_{sl})	Free energy required to form new unit area of solid-liquid interfacial surface	Predefined	-
48	Solubility (S)	Solubility of solid material in liquid melt, unlikely to be significant	Predefined	-
49	Melt pool shape	Length (in scan direction), depth, width, and area	Controllable	-

It was outside the scope of this thesis to consider in depth the controllable process parameters to see how alteration on the AM machine would affect the artefact due to external constraints. Instead the CAD model was altered to improve the accuracy of the artefacts being produced (Chapter 6). Monitoring and changing process parameters could improve the precision of the process but would need to be investigated on a machine that was under control.

The design of the bridges on plates 13 and 14 will be considered in this section as they have had process settings changed. In order to achieve the specified cylinder dimensions changes were made to the CAD files. Figure 7-4 and Figure 7-5 show details from the revised CAD information for the two altered top hats. Figure 7-4 shows the first revision in which there was an increase in cylinder diameter from 6.00

to 6.20 mm for each cylinder. This change was applied to determine whether it was then possible to achieve a set of test pieces with 6.00 mm diameter cylinders. Increasing just the internal bore measurement in this manner produces a reduction in wall thickness. This could have an impact on the cylinder measurements. Therefore, a second plate of top hats was produced with the external cylinder diameter increased to maintain the wall thickness as for previous builds. Figure 7 5 shows the second revision with the same increased inner diameter of 6.20mm and an increased outer cylinder diameter, from 7.50 to 7.70 mm. Plates 12, 13 and 14 were built within the same calibration window and therefore will be compared in this section.

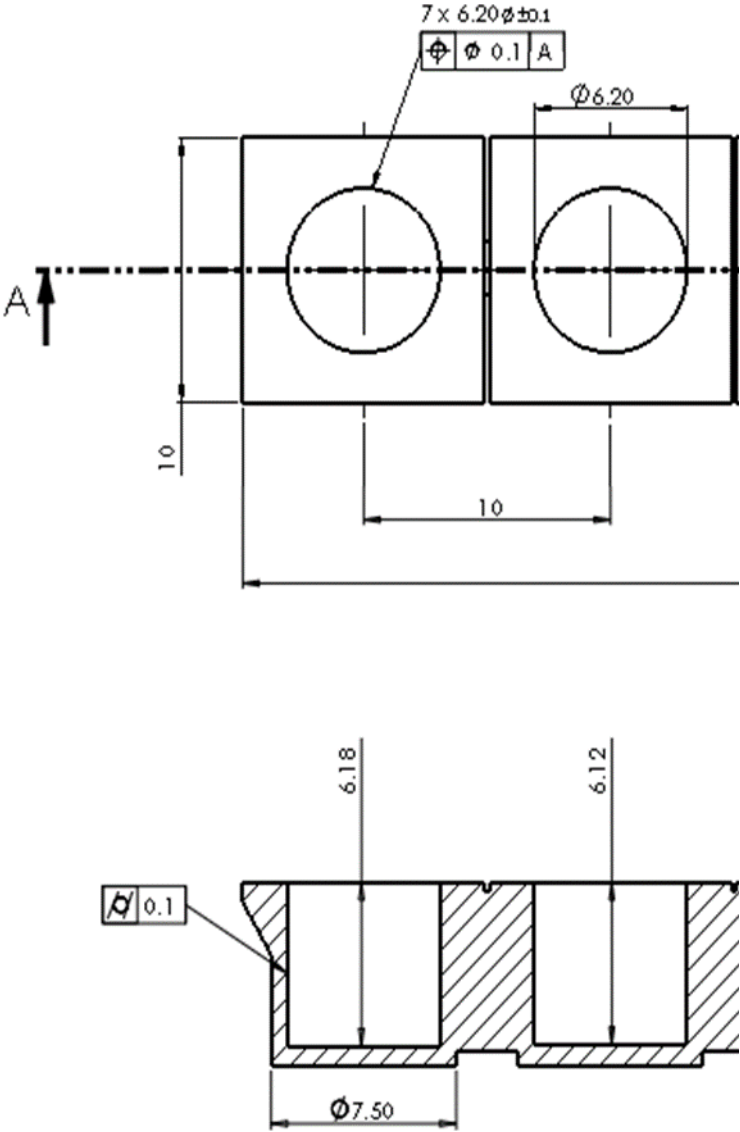


Figure 7-4 Extract from the amended CAD drawing of the bridge with and increased inner diameter

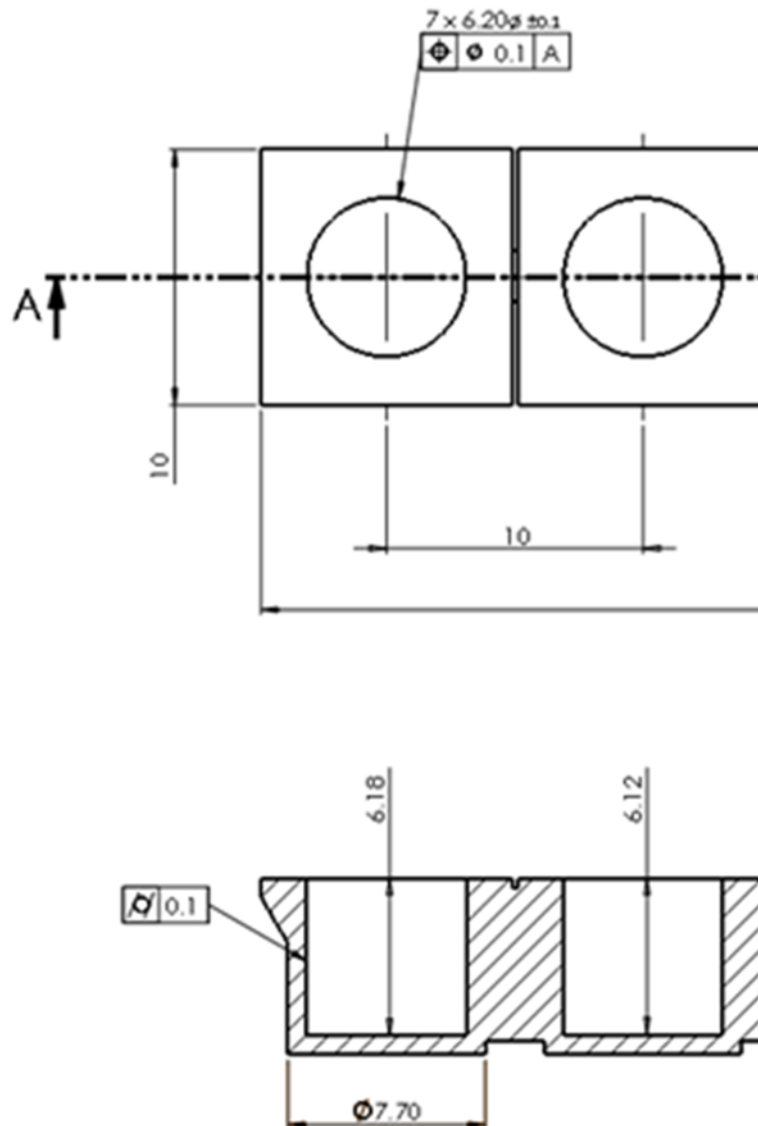


Figure 7-5 Extract from the amended CAD drawing of the bridge with an increased inner diameter and external cylinder diameter

In considering the above changes it was identified that the artefact being produced by the AM250 machine had cylinder diameters that were close to the limit or out of the tolerance provided by the OEM. Therefore, the artefacts needed to be adjusted to bring them within tolerance and to make them more accurate. To achieve this the CAD model was adjusted to increase the cylinder diameters by 0.2mm. This action was the result of the analysis of the level of deviation from the required diameter previously measured. It is outside of the remit of this research to fully investigate why such deviations occurred. It is common practice to modify parts in this way to allow

for such deviations, perhaps indicating the relative newness of the SLM technology being deployed. The objective here was to observe the effect of the change on the process, rather than testing the accuracy of the parts produced. In future applications it is envisaged that the OEM may be able to re-calibrate the machine to achieve similar improvements.

This was shown to achieve the desired effect, with plates 13 and 14 having diameters closer to 6mm. The detailed analysis and discussion of the information provided by the results achieved with this approach are presented in Section 7.4.

Before carrying out any changes to the CAD model of any part that was to be produced it would be sensible to manufacture a set of artefacts to check important dimensions while running the machine on the standard settings. These are then checked, with settings changed if required to improve the manufactured parts. Initially any changes should be completed by an engineer overseeing the production process. Subsequent changes made to the CAD model could be completed by the operator if they have knowledge of CAD and have been trained to understand the information provided by the artefact. The operator would only need to learn specifically how to assess the artefact, rather than potentially complex builds. It should be possible to develop a structured set of guidelines to inform how the build should be adjusted during process setting, to account for problems with past builds, by using observations from the artefact. In this way the artefact can be used as an audit to identify when issues have arisen, and what adjustments were necessary to maintain process integrity.

The information gathered from the initial artefact run can inform changes to the CAD file if there is a dimensional error, as discussed previously. Further scrutiny of the part can inform other parameter changes. One such observation may be that the artefact has over-melt, indicating that the power or speed of the laser may need to be explored. However, for some parameters and some complex builds the artefact developed in this work may not be suitable. For example, several of the parameters (Table 7-2) would require an investigation into the mechanical properties in order to inform the setting of those parameters. In those situations, this specific artefact may not be optimal.

Nevertheless, the top hat used in this work could inform end-users of the machine that their calibration and/or process setting change has been successful. This is useful to both the OEM during the calibration, and the operator after the calibration. However, when used by the OEM the process would be considered part of process

foundation, whereas when used by an operator it would be to inform process settings. The overlap between process foundation and settings will shift as operators become more familiar with the machines, they will be more confident to change the process foundation element.

7.3 The use of the artefact in-process control

In-process control within the AM250 machine is enacted using functions embedded within the controller. Access to the information generated is limited, even with full access to the PLC. The PLC log provides an overview of the build environment during a build, but at the start of this project it was only available for analysis after a build was completed. This limited the potential for in-process control, more realistically, in-process monitoring. In any practical application it should be possible to relate the information provided during the manufacture of a 12 artefact build plate to the acquired process information, and then to check for differences. This of course is unrelated to any actual manufacturing cycle, wherein a single artefact could have been included for quality management purposes. The application of single artefacts to process management is discussed in Section 7.4. At this stage it is worth pointing out that, due to the layer-by-layer nature of the build process, it is not currently feasible to isolate the data associated with the production of a single part.

The OEM provided direct access to the PLC so that monitoring could happen in a slightly delayed format. In this format the PLC log can be utilised as an in-process monitoring tool. Direct access to the raw PLC log is not available to current AM250 owners, but during the life of this project the OEM has provided an online portal called InfiniAM Central (Renishaw Plc 2017). This allows users to access a cloud-based repository providing real-time information on the condition of any AM250 machine they own, if connected to the internet. This provides an interface that can be used to view some of the information stored in the PLC log.

The raw data file produced by the PLC log was a long string text file that needs to be processed so that the data recorded during a build process can be extracted. The PLC log records 228 fields of information of which 93 contain the message “unknown alarm”. These were ignored because no information could be gathered to explain what they related to, leaving 135 fields of information. Of the remaining fields, 116 contained predefined parameters, which include settings set by the operator. The remaining 19 fields contain actual feedback recorded by the sensors in the machine.

To present the nature of the process monitoring information available it is helpful to consider that, for an individual build containing all 12 top hats, just under one million data entries are recorded in the PLC log. However, only 23% of that information relates directly to the build environment and can be explored for the purpose of in-process monitoring. Figure 7-6 - Figure 7-8 show some of the most useful information from a PLC log. Figure 7-6 shows the build layer duration and the accumulative layer number (plcToPc-layerNumber).

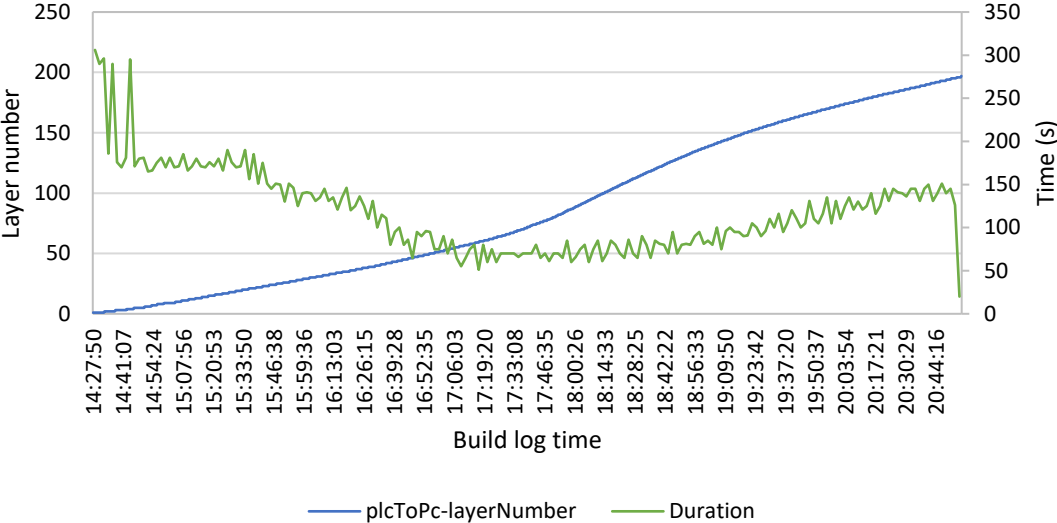


Figure 7-6 line graph showing layer duration (Green) and layer number (Blue) for plate 1

This graph can be used in conjunction with the build file produced using QuantAM (Renishaw Plc 2015). The build file has an estimated layer build time, which can be compared to the actual build time to identify any disparities. To create this graph, the raw data must be processed to work out the time each layer takes to build. The PLC is programmed to record information from the SLM machine every 5 seconds, unless one of the sensors indicates a change in the process. These need to be combined so that the total layer build time is available to plot against the correct layer number. This graph can be used to identify prolonged periods of inactivity, which could be related to operator interference or a machine fault. Overlaying the layer number on the same graph means that if the layer time shows an extended period of time spent on one layer the engineer can cross reference the long period of processing time with the layer number. These two numbers can be cross-referenced against the estimated build time for that layer and if they are different further investigation can take place. For instance, the part once removed can then be examined paying closer attention to the layer, or layers, which took longer than expected to manufacture.

The limitation of the PLC log in this instance is that the recorded data may not relate to the layer indicated in the log because of the acquisition rate. The log does not count a new layer starting as a time to record the current environment. This means that a new layer may have started 4.9 seconds prior to the next data recording or 0.1 seconds before. Also, further PLC log data would need to be cross referenced to see what exactly the AM250 machine was doing during the prolonged time spent on a single layer. The first check would identify if the operator requested to pause or stop the build manually. If this did not happen then further investigation would be needed, which could include checking the laser log. If the laser was active during the extended build time the time estimation for the layer may be wrong or there could be an issue with one of the servo-motors moving the mirror and further investigation could be carried out.

Figure 7-7 shows the elevator build bed temperature (plcToPc-elevatorTemp) and the accumulative layer number (plcToPc-layerNumber). The AM250 machine evaluates the elevator build bed temperatures using TD thermal LTD SEN-106-090-001 thermal couples. The thermal couples used have a precision of $\pm(0.3 + 0.005[t])^{\circ}\text{C}$ (so at a reading of 100°C the actual reading is $\pm 0.8^{\circ}\text{C}$). This error increases the hotter the build chamber gets.

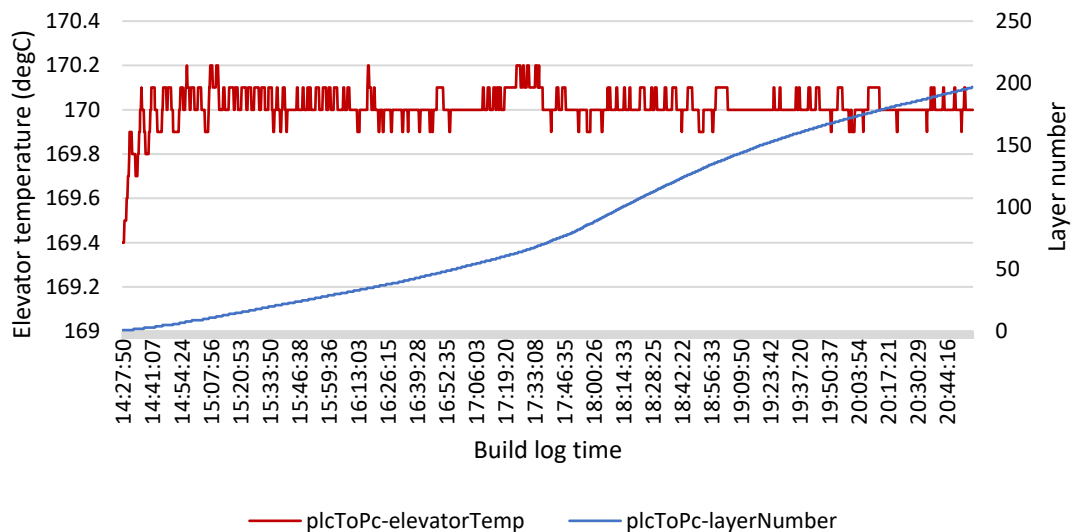


Figure 7-7 Line graph showing elevator temperature and Layer number for plate 1

Monitoring the elevator build plate temperature is important as, for some materials, it is critical for the build plate to be pre-heated and for the set temperature to be maintained. This helps materials such as titanium to adhere to the build plate and

prevents cracks from forming. The temperature sensor that provides the build bed temperature is not directly measuring the build plate, but the temperature under the elevator plate where the heating pad is situated. The temperature of the actual build plate is therefore inferred. The temperature output can be easily misinterpreted by the end-user. The AM250 does not have the ability to measure the temperature of the layer that is being manufactured as the other temperature sensor situated in the machine indicates the chamber environment temperature and does not provide any direct temperature measurements of the manufactured parts.

Figure 7-8 shows the oxygen level at the top and bottom of the build chamber. Minimising the oxygen levels during a build is critical to the quality of the part being manufactured for mechanical and geometric reasons. Oxidisation in the part can produce parts that are mechanically and geometrically inferior. Controlled levels of oxygen in the system are critical because some of the powders used in metal ALM are highly explosive when exposed to normal atmosphere. The upper safe limit for metal powders is 5000ppm of oxygen (O₂).

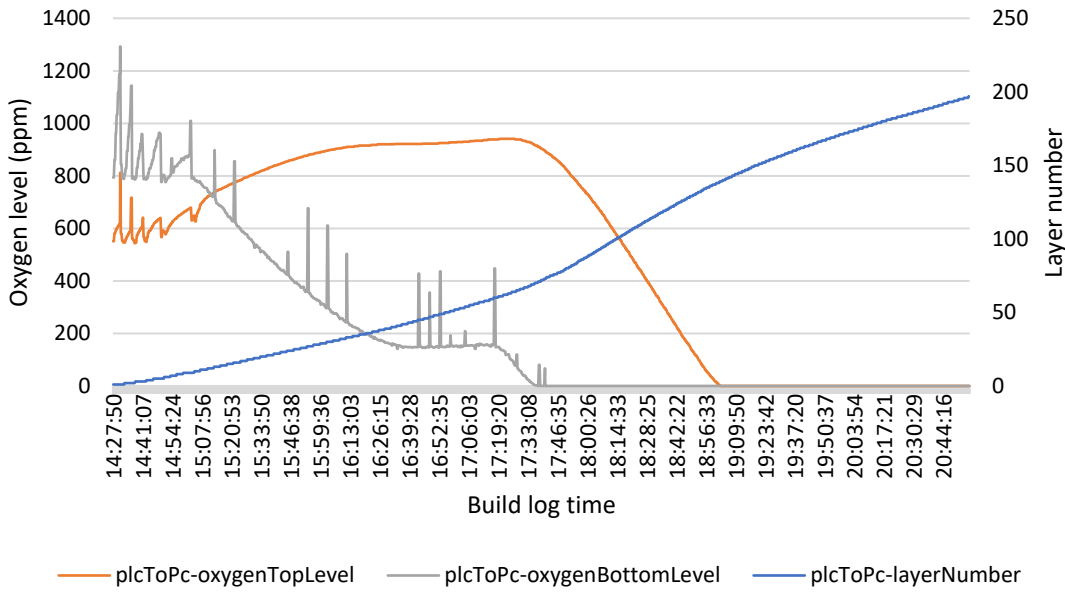


Figure 7-8 Line graph showing top and bottom oxygen levels and layer number for plate 1

Figure 7-8 shows the top and bottom oxygen sensors for the first build carried out in the AM250. The graph indicates that the system took a long time to purge the system fully of oxygen. For all the builds, the default oxygen level was set to zero with an alarm set to sound when the oxygen levels exceeded 1000ppm. The bottom oxygen level did not get under 1000ppm until layer 107 which meant that 5.35mm of the top

hat assemblies were built before the chamber displaced the required amount of oxygen, meaning 41% of the build had been completed. In a manufacturing environment the parts would need to be examined to check if this exposure to oxygen causes any adverse mechanical problems. The top oxygen level sensor recorded oxygen levels of less than 1000ppm after layer 72, though being at the top of the build chamber this saturation is less critical. This is very much in contrast with one of the latest builds completed (Plate 12). Figure 7-9 shows the same information as Figure 7-8, but for Plate 12 the oxygen sensor at the bottom of the build chamber recorded zero oxygen content for the complete build. The oxygen sensor at the top of the build chamber recorded a zero reading from layer 11 onwards, but the process started with a diminishing oxygen content of just over 600ppm. The AM250 in this case completed 0.55mm of the build, which was the supports for the top hats and constitutes only 4.2% of the complete build. Technically, because only the top sensor registered oxygen and the bottom was free from oxygen, the build was completed in an inert atmosphere reducing the chances of oxidisation.

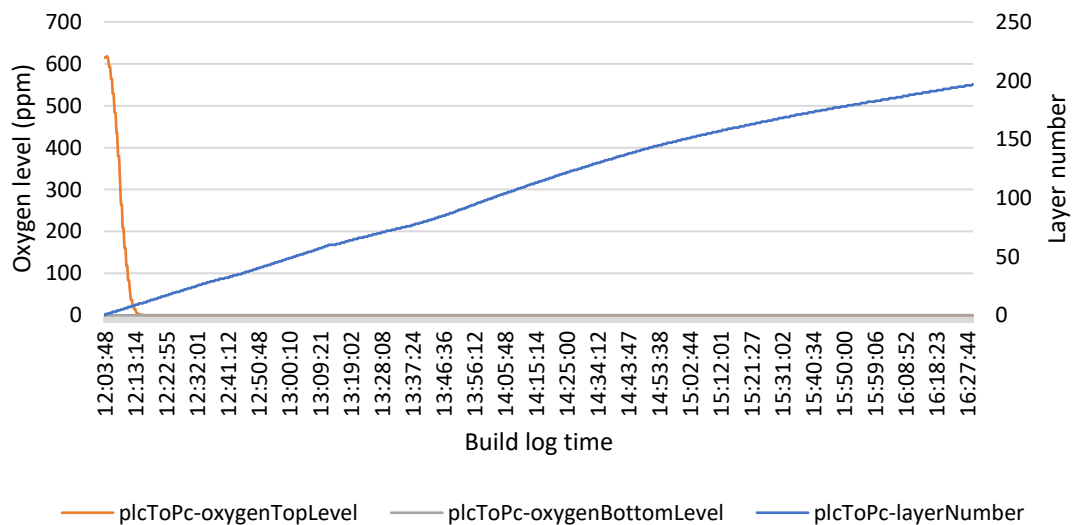


Figure 7-9 Line graph showing oxygen levels and layer number for plate 12

Over the length of this research, learning how the AM250 machine works has impacted on the quality of the builds. More knowledge has meant more control over the system. This would support arguments that the process is still heavily reliant on the operator for consistent and high-quality parts.

The PLC log can, in theory, be used to monitor a build, however, it is better suited to post process analysis. The PLC provides feedback for the entire build chamber environment and the AM250 machine settings. The resolution of the information is too low to identify what is happening at a set point in time for each part being

manufactured in each region of the build plate. The data capture interval means that some data cannot be correlated to an exact point in time, such as specific layers, as previously discussed. Some of the sensors are also indirect, meaning that the information obtained from them may not indicate exactly what is happening at the point indicated by the name of the sensor in the log. It is impossible to isolate a part within the build process using just the PLC log on its own, knowing this the OEM has developed the next step in in-process monitoring with InfiniAM Spectral (Renishaw PLC 2018).

InfiniAM Spectral was not available on the AM250 machine used in this research, but during the latter stages some data was made available for a build containing 12 top hats. The information provided allows an operator or engineer to visualise the energy sent from the laser module to the powder bed and, using visible and invisible light spectrums, work out how much of that energy is absorbed and returned to the photodiodes along the laser path. It can be used to identify when the laser fires, its location on the bed and if there are any anomalies within the laser melting part of the process. The limitation with this process is that it is pixel-based and, until further research is completed, outputs are not clearly understood. Currently it is only a retrospective process, as with the information provided by the PLC log. This will change in time with further research.

Using failure fault analysis one can use information gathered by InfiniAM Spectral to see what causes a fault within a part being produced. The analysis could be used to program software to identify when these events are in process for future builds. The program can then either alert the engineer or be programmed to evaluate the problem in-process and change the process in-situ to correct the issue.

Where the PLC log is unable to isolate a part on the build bed because of its lack of resolution, InfiniAM Spectral has the potential to isolate individual parts. Considering the artefacts, one could be isolated within a standard cycle to confirm the integrity of the build. This could be beneficial in reducing the computational requirements. InfiniAM Spectral creates huge data files – one plate with 12 top hats has a file size of 1TB for all the raw data collected. If this was reduced to just one artefact for in-process evaluation, it could be used in real time without taking up as much memory (85GB), therefore reducing the hardware requirements needed for data processing.

7.4 The use of the artefact in post-process monitoring

It has been discussed within this thesis that post build processes are, in effect, part of the overall process, therefore it is sensible that post process monitoring should take place once these are completed. This would include the removal of the parts from the build plate. To ensure repeatable measurements these parts need to be suitably restrained. During this project it was identified that generic fixing kits were not suitable as they did not restrain the parts effectively and tended to cover surfaces that needed to be measured. This resulted in poor repeatability and reproducibility. A specialist fixture was developed to improve the repeatability and reproducibility of the gauge. Figure 7-10 shows the development of the specialist jaws designed to be assembled into a standard machine vice, as shown in Figure 7-10 B and C.

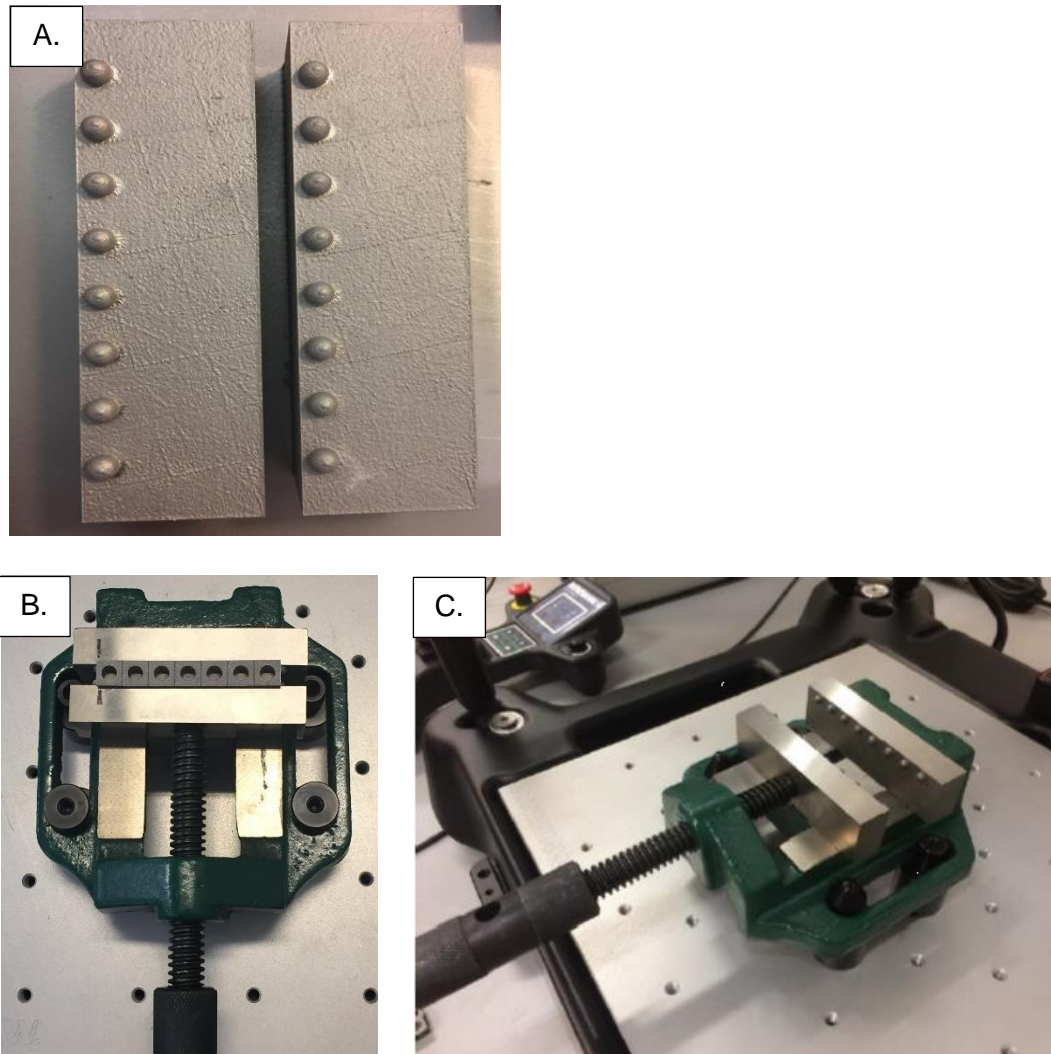


Figure 7-10 (A.) Specialist stainless steel vice jaws made using AL250 machine after post processing, (B.) Machine vice with stainless steel vice jaws fitted holding top hat, (C.) Machine vice with stainless steel jaws fitted

The initial design and development of the jaws was carried out using a fused deposition modelling machine (commonly known as a 3-D printer). A number of designs were trialled until the stainless-steel specialist jaws were developed. The stainless-steel jaws were manufactured using the ALM250, heat treated and shot peened to ensure they were not distorted or had any over-melt on the surface of the jaws. This was completed so that the top hats could be positioned precisely and held securely. Once in place the jaws would maintain a suitable gripping force. One limitation of the design is a lack of control over the orientation of the top hats. The top hats are marked on the outside with a unique identifier to indicate their original position on the plate. These markings are always on the same side of the top hats to ensure repeatable measurement processes. However, operator error can result in the top hats being fixed in the vice differently each time (they can be rotated 180 degrees and therefore, without due consideration, have a 50% probability of being measured in the correct orientation). The use of the markings is currently the primary method to ensure that the top hats are measured in the same orientation. The correct orientation of the top hats can be checked following the measurement process, using the forced depth variation shown in previous chapters. As shown in Section 4.4 using this fixture had no effect on the measurement process R&R and therefore the measurements can be applied to the off the plate analysis.

To commence this analysis, it is important to confirm that removing the artefact from the plate had no consequences for their dimension and form. Figure 7-11 shows the shift in the mean diameters for plates 12 – 14 for post and off and includes the upper and lower confidence intervals shown as error bars for each condition.

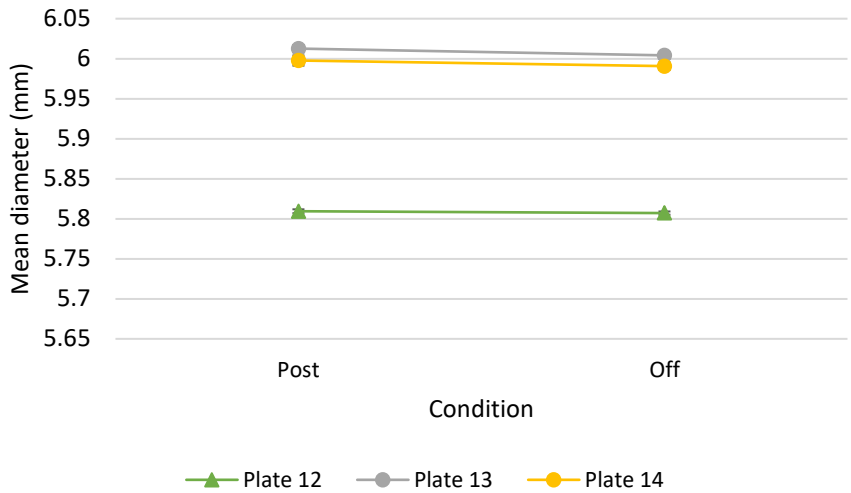


Figure 7-11 Interval plot for plates 12, 13, and 14 for mean diameters for post and off

Plate 12 had no changes made to the CAD file and was built to check that the recent calibration had not significantly changed the manufacturing process (see Chapter 6). Plate 12 can thus be used to compare subsequent builds to see if any changes had been made. From Figure 7-11 it is evident that plates 13 and 14 are different from plate 12. The mean diameter has shifted from 5.8mm for plate 12 to 6mm for plates 13 and 14. The changes from post to off seems similar in all cases from the interval plot but will be analysed after all the attribute plots to see if the visual interpretation is statistically correct.

Figure 7-12 shows the interval plots for all the mean cylindricity measurements for plates 12-14 for post and off conditions.

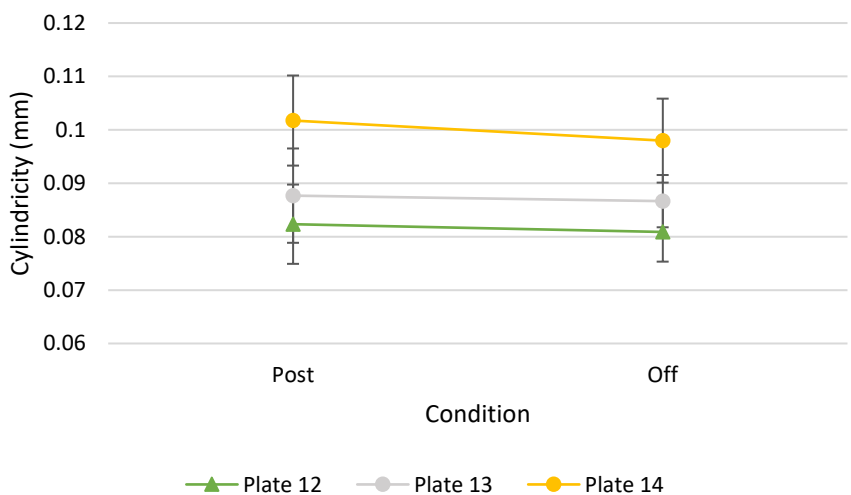


Figure 7-12 Interval plot for plates 12, 13, and 14 for cylindricity measurements for post and off

It can be observed that plates 12 and 13 show more similarities to one another, than to plate 14. Plate 14 indicates a cylindricity of 0.1mm, which is slightly worse than both plate 12 and plate 13 (0.08 and 0.09mm respectively). Although the difference in cylindricity is very small, it is representative of the changes made to the CAD model. It should be noted that plate 14 was changed so that the cylinder wall thickness was thinner than the original builds. It is possible therefore that it would be more susceptible to form variation. Although Figure 7-12 indicates a slight difference in the cylindricity measurements, care needs to be taken to draw correct conclusions from these differences. The cylindricity measurements recorded for previous top hat builds show that, even with equal cylinder wall thicknesses, the cylindricity measurements can vary between 0.1 and 0.15 mm. Based on that information it would be challenging to justify the introduction of the thinner wall, if all builds were considered in the evaluation.

Additionally, plates 12 and 13 may be investigated to identify which parameters were changed to result in the improved cylindricity measurements. Figure 7-14 show the post and off measurements for true position for plates 12-14. The interval plot indicates that the position bias improved between post and off, following the same pattern as plates 8-11.

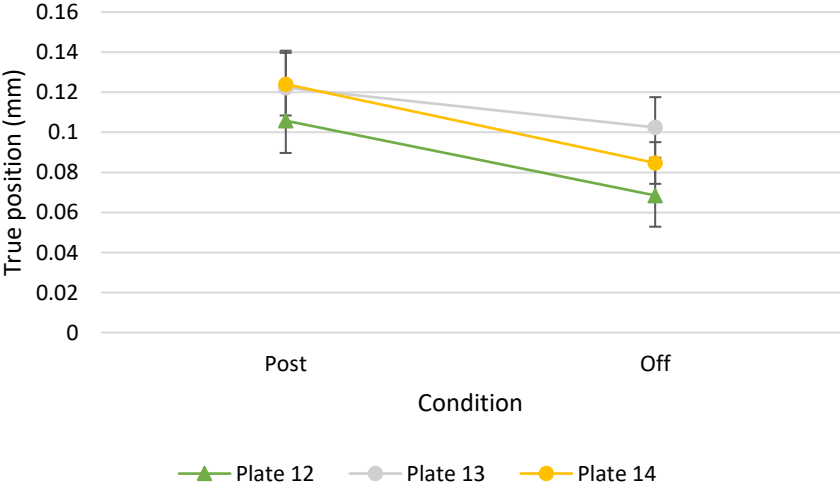


Figure 7-13 Interval plot for plates 12, 13, and 14 for true position for post and off

Figure 7-14 shows the interval plots for the mean top hat top plane measurements, for plates 12-14, post to off.

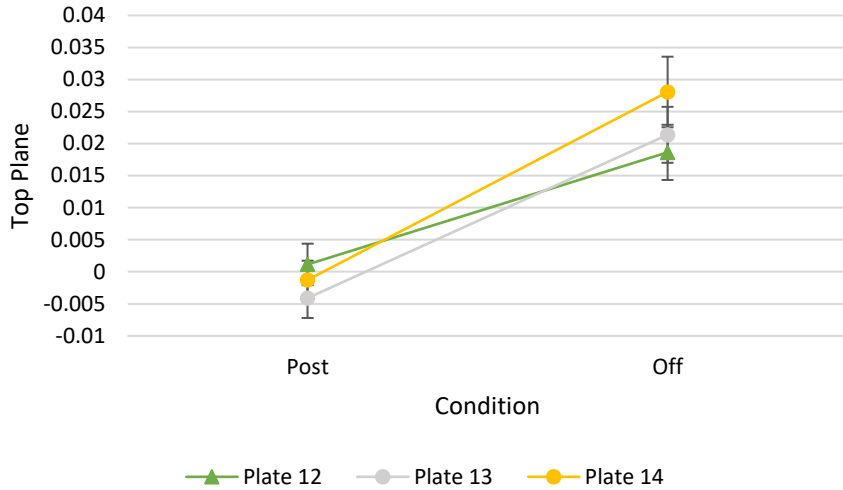


Figure 7-14 Interval plot for plates 12, 13, and 14 for top plane measurements for post and off

As per the other plates (3, 8-11) the top plane measurements for plates 12-14 are closely grouped. The spread of the measurements for plates 12-14 are inside the measurement spread taken for plates 1-3 and 8-11 (-0.05mm – 0.05mm). This shows that there is no significant difference between the top plane measurements for plates 12-14 compared to the previous plates.

Figure 7-15 shows the mean depths for each top hat position, adjusted to account for their designed offset to centre them around 6mm. The line plot shows the post and off measurements for plates 12-14.

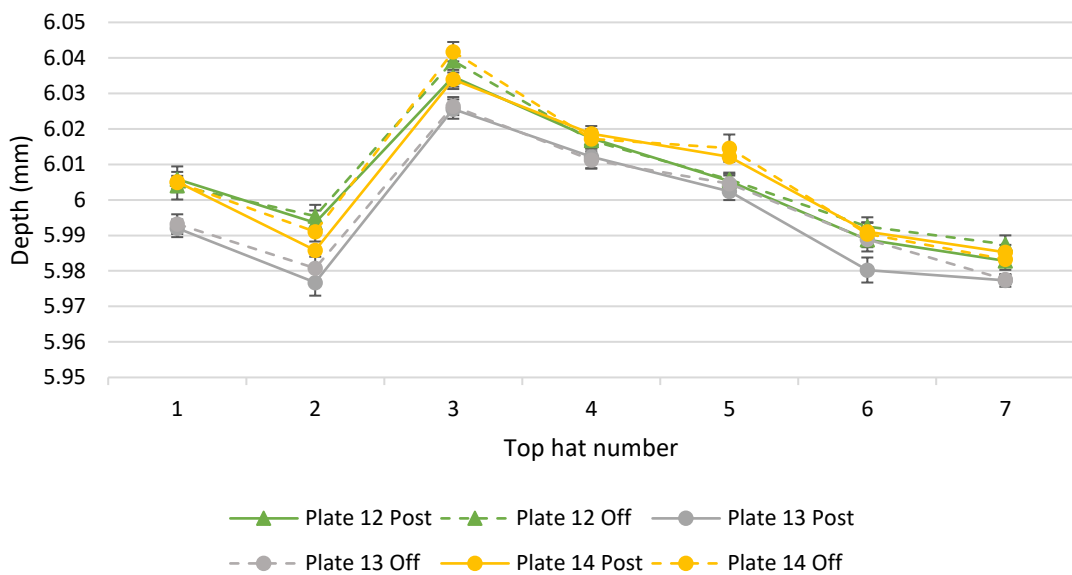


Figure 7-15 Interval plot for plates 12, 13, and 14 for mean depths for post and off

In this case there does not seem to be any major differences between the depths of the top hats. If after depth correction, there was an obvious difference in one of the measurements, further investigation could be carried out on the artefact. This would include checking for any over melted section that would provide a significantly different measurement than the others on the artefact. If a repeatable pattern is found in the depths it may be necessary to examine the operation of the encoders controlling the movement of the elevator. Currently, plates 12-14 replicate that which was observed on plates 3, 8-11 and variation at this point seems random. Within these three plates there are only three locations that indicate that the post and off measurements are potentially different. These indicate an 8.33% difference between depths measured post versus off. When completing a one-way ANOVA test all the depths across the plate are found to be statistically the same (see Table 7-3).

Table 7-3 show the results of a one-way ANOVA test for each of the attributes measured showing post versus off measurements for plates 12-14.

Table 7-3 One-way ANOVA results for plates 12-14 for all attributes measured

Attribute	Plate 12 Post versus Off (p-value) (shift in mm)	Plate 13 Post versus Off (p-value) (shift in mm)	Plate 14 Post versus Off (p-value) (shift in mm)
Diameter	0.152 (0.001)	0.001 (0.007)	0.032 (0.004)
Cylindricity	0.726 (0.002)	0.784 (0.003)	0.491 (0.004)
True position	0.000 (0.024)	0.104 (0.020)	0.000 (0.040)
Top plane	0.000 (0.017)	0.000 (0.025)	0.000 (0.029)
Depth	0.918 (0.002)	0.900 (0.002)	0.930 (0.002)

The results given in Table 7-3 indicate some similarities to previous plates manufactured using the AM250 machine. Cylindricity and depth results for plates 12-14 show similarities to all previous plates manufactured, when comparing artefacts post with artefacts off. However, the cylinder diameters vary, with one of the plates (12) showing statistical similarity and the other two plates (13 and 14) showing more significant variation (highlighted in orange on Table 7-3). The artefact could be used

to explore this further by considering the heat treatment cycle (as discussed in Chapter 5) or by considering other significant changes to the build process such as the change made to the CAD model. It should, however, be noted that the observed variation may be a result of any improvement in the precision of the process, hence smaller margins resulting in a “statistically significant shift”.

Figure 7-16 shows that plates 12-14 do not change dramatically post heat treatment. The worst regions of the build plate continue to be positions 1, 2, 3 and 8. The off-plate rankings indicate that the worst parts are in similar positions.

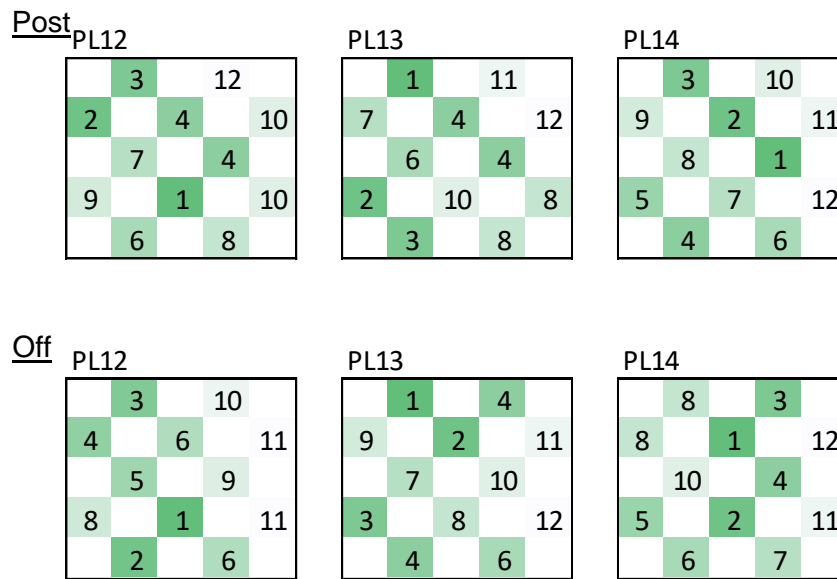


Figure 7-16 Matrices for post heat treatment on the build plate (top) and top hats cut off the build plate (bottom) plates 12-13

It has been shown that the AM250 builds can be shifted within tolerance simply by altering the CAD models for the included parts. This is of interest to the end-user of the machine as the change requires little intimate knowledge of the machine itself. It has also been shown that there is minimal difference between artefact measurements immediately post heat-treatment and artefact measurements following their removal from the build plate. Differences tend to occur when issues have arisen post process, however, the true cause of any variations would, in practice, require enough further investigation to determine the cause (if the variation is outside the process tolerance).

Evidence indicates that there should be no preference in when the artefact should be measured (post or off). However, when performing a test involving the manufacture of a 12 artefact test build, if possible, the artefacts should be measured after each condition. Carrying out a measurement cycle after post will inform the user about only the manufacturing process. Measuring after off will inform the user; if the heat

treatment was successful, the build was within tolerance, and whether the removal process affected the artefact. However, it would be difficult to isolate each entity. The optimum approach would be to measure both post and off. This would enable the comparison of the measurements and hence the user could isolate whether variations are caused by the build, the post process, or the removal of the artefact from the plate.

The use of the developed artefact for post-process monitoring gains the most benefit when a single artefact, rather than multiple artefacts, is employed for the evaluation of the manufacturing process capability. The manufacture of twelve artefacts would be beneficial for benchmark builds, especially following maintenance, or calibration of the machine, because it provides the most complete picture of the plate. However, there would be limited room on the plate to manufacture any medium or large parts if the plates contained test pieces set out as previously described (Chapter 5; Table 5-1).

The most economical build would only include one artefact in regular builds for use in post process monitoring and to be used to assure the build process. Use of a single artefact should be possible if the benchmark builds are regularly completed following machine maintenance and/or calibrations, providing a comparison for subsequent builds. At present a sensible requirement would be that the individual artefact would need to be built in the same location as one of the 12 positions detailed in Table 5-1. This would allow for a direct comparison. However, as more parts are produced this could be strengthened. Position 2 was found to be consistently the worst location on the plate for all builds. Using this position as a location for the artefact to be built is beneficial because it prevents users building parts in positions that result in lower quality outcomes. The artefact appraisal will indicate that the process was performed under control and that no common causes were detected. This cannot rule out special causes of variation that may have affected some of the parts on the build plate.

For many manufacturing companies access to a CMM or a CMM lab is limited or expensive. Additionally, the time and expense of sending a complete build plate out for evaluation after each manufacturing process would be impractical. Assessing an artefact after it has been removed from the build plate would be the most practical approach. As the parts should be fit for purpose after their removal, this would be the optimum time for the artefacts to be assessed. It is possible that a dedicated measurement system, such as the Equator gauge, could be deployed to enable the economic local enactment of this measurement process.

7.5 Summary

This chapter has discussed the use of an artefact for assessing each of the four layers of the PPP. It has identified that an artefact can be used post and off the plate and that changes in process settings can be identified by measuring the changes in the artefact.

Building twelve artefacts and assessing them for process foundation confirms that the calibration carried out on the machine has either changed the accuracy or kept it consistent to previous calibrations. The twelve top hat artefacts can be used to build up a picture of the machine over time, creating the machine's "fingerprint" making it easier to identify when the process has changed. In this chapter, it was identified that the calibration carried out prior to the production of plate 12 did not change the process significantly (Figure 7-3) and the same regions on the build plate were identified as being "best" and "worst". It has been discussed that the top hat artefact is not optimal for complex builds, as these may require the verification of mechanical properties. Either another artefact needs to be included (such as a density cube) next to the top hat that is designed for such a purpose, or the top hat needs to be re-designed to incorporate extra requirements. In a single material machine such change may not be needed as the OEM should be able to calibrate the machine to process the material being used with the most optimum settings the machine has to offer. If, as in this project, the machine could process multiple materials, an artefact which can be used to assess mechanical properties should be considered.

As discussed in process setting (Section 7.2), there is a blurred line between that which constitutes process foundation and process setting. In a multi-material machine this differentiation is harder to identify because the operator must change the set up to account for using different materials with distinct material properties. Different materials will interact differently with some of the SLM machines processes. It is clear, in this instance, that changing the CAD model did have the desired effect on the artefact, producing cylinder diameters with a nominal diameter of 6mm.

Although there is in-process feedback, the AM250 machine is still open loop and the PLC log can only be considered as a tool for monitoring and is not yet a closed loop in-process control. The information available from the PLC log can be used to comment on the build environment and is limited by design. It can provide high-level feedback, but one is unable to identify individual builds on the build plate. It was discussed that the integration of InfiniAM Spectral (Renishaw PLC 2018) can improve

the resolution of the feedback and potentially individual parts can be assessed; the use of both will have great potential in the future, when further research is completed.

It has been shown that an individual artefact can be used to confirm the build geometry integrity if it is built in a known position that can be compared to the initial full plate build. The assessment can be carried out after the artefact has been removed from the plate and should indicate (if built in the worst position) that as far as we can tell the process was enacted correctly. It was shown that the artefact can be assessed when off the build plate, but specialist tools are required to guarantee measurement repeatability and reproducibility (full R&R provided in Chapter 4). The main source of operator error for off-plate measurements was identified as orientation, because the top hat bridge can be put into the vice in two separate ways. This error could be identified due to the known changes in depth and either compensated by the “soft” realignment of the part or by a repeated measurement cycle.

Identifying manufacturing improvements in both the PLC log and artefact highlights that build quality is influenced by the operator’s knowledge of the manufacturing process and set-up. Ways to mitigate this interaction should be investigated and implemented to minimise the operator’s influence on quality.

Chapter 8: Conclusions, Research Contributions and Future work

8.1 Conclusion

The review of the current state-of-the-art for the SLM manufacturing process clearly indicated that quality control and management must be better understood to support the effective use of SLM processes. This research has investigated methods that can be applied by adapting and using the established Renishaw PPP approach.

The research in this thesis identified the SLM process variables that can influence parts being manufactured. Based upon the deployment of the in-house AM250 machine a total of 175 sources of variation have been identified. To represent clearly the challenges faced, these sources of variation have been categorised within the four layers of the PPP (process foundation, process setting, in-process control, and post-process monitoring). Fish bone diagrams have been developed for each of these four layers and may be built upon and refined as more information is acquired. Currently, these diagrams have been adopted internally by Renishaw and are being used to improve the development of future SLM systems.

An existing bridge artefact, intended to be used in dental related builds, was adopted by this research to help assure process integrity. The use and arrangement of the 12 artefacts on a SLM build plate was specifically engineered for this project. It was decided that the measurement processes to be deployed should be based upon CMM tactile probing. The requirements for, and specification of, the necessary gauge evaluation was investigated and no SLM process-related standard could be identified and little previous research found. The suitability of selected methods to measure the features and form related parameters of the test piece was evaluated and the specified measurement process was validated and assured.

A repeatability and reproducibility (R&R) analysis was carried out to confirm that the tactile probing method adopted and deployed on the CMM was capable of measuring the artefacts manufactured on the AM250 machine. The gauge evaluation process was engineered, developed and tested. It was then applied to prove that the CMM based measurement system used in this study is capable, when used with caution, of the measurement of form and feature based test piece elements. The measurement of the test piece features was assessed in the context of the nature of the measurement being taken. The CMM was shown to provide the accuracy and

precision required in the context of the measurement of the test piece features; the cylinder diameters, depth, true position and the top and bottom planes. It was also found to be capable of the measurement of the cylindrical form.

The first in-depth element of this research considered the Process Foundation layer. The application of the 12 test piece build plate to this layer was fully investigated. A novel method of combining the various measurements taken into an understandable format was engineered and tested. The resulting quality ranking matrix method was shown to be capable of representing the quality of the test pieces produced. The method was then applied to establish build plate position related to quality performance. This method was then adopted and utilised to inform the remaining research undertaken.

The Process Foundation layer must be primarily the responsibility of the OEM. The existing calibration process for the AM250 was found to be fairly basic. It is recommended that the 12 test piece build plate layout is manufactured during the calibration and used to set up machines. At least 10 plates should be made on every new machine and the data taken from these ten plates can form the process foundation information. It is proposed that the quality matrix should in effect establish the fingerprint of the machine. These plates can be assessed for repeatability and reproducibility and this information can then be used to compare later calibrations.

The Process Setting layer is primarily the responsibility of the machine owner/operator. The number and nature of the inputs into this layer have been considered. It is recommended that the use of the 12 test piece build plate is adopted, particularly in the initial stages of process setting. This is particularly relevant to the AM250 machine when used in its multi-material mode. The application of the quality matrix approach to assure process quality in this context has been demonstrated. It is apparent that there is considerable overlap with process foundation considerations, and any test pieces manufactured will add to the existing machine related information.

The in-process monitoring layer of the PPP has been considered but not fully investigated. The data acquisition, processing and management elements of this activity are very challenging and best suited to research by the OEM, such research is known to be on-going. It can be suggested that, each time a 12 top hat build plate is manufactured, the information can be used to inform the process monitoring. Each plate can add to the process monitoring information acquired and this information can be evaluated. It is possible that any found defects in test pieces can be related back to the process monitoring information.

It has been established that for process foundation purposes the optimum time to assess components is post process, whilst still on the build plate. In this condition it is possible to place the entire build plate into the CMM and conduct the measurement cycle. However, this is clearly not a viable solution for post-process monitoring. It was recognised that it is not possible to make 12 artefacts each a time build cycle is completed for use in post-process monitoring, as doing so would reduce valuable manufacturing space. Due to the need for post-processing, including heat treatment and part removal, the off the plate condition was adopted and the measurement of a single artefact was considered. The design and deployment of a suitable part fixture was undertaken and the resulting part measurements acquired. The single artefact, if built in the same position as one of the 12 artefacts, can be evaluated after it has been removed from the build plate and be compared to that equivalent position on a 12 artefact build. It is clear that the location on the build plate does affect geometry. The data from these parts can feed back into the process setting stage to improve either precision and/or accuracy.

It was shown that the individual artefact can be used to understand that the process used to make that artefact has been enacted correctly. The assumption must then be made that the other parts produced during the same cycle have had no variation due to common cause. Some process monitoring can be used to check that nothing untoward has happened during the cycle. If discrepancies are found in the manufacturing process of the artefact, it could be presumed that there may be irregularity with the manufacturing process of other parts being produced in the same cycle. Appropriate quality measures could be carried out to assess the build.

8.2 Research contributions

- As a result of this work, quality control and management are better understood and can better support the effective use of SLM processes.
- The fish bone diagrams have been developed for each of the four layers of the PPP. These are being used by Renishaw to improve the development of future SLM systems.
- The use and arrangement of the 12 artefacts on a SLM build plate was specifically engineered for this project. The requirements for, and specification of, the necessary gauge evaluation was investigated and the specified measurement process was validated and assured.
- The gauge evaluation process was engineered, developed and tested. The CMM was shown to provide the accuracy and precision required in the context

of the measurement of the test piece features, which had not been previously proven.

- The quality ranking matrix is a novel method of combining the various measurements taken into an understandable format. It was engineered and tested and this method was then adopted and utilised to inform the remaining research undertaken. The 12 test piece build plate can be combined with the quality matrix approach to assure process quality.
- SLM specific parts can be produced in set locations and evaluated after the build. Data from these parts can feed back into the process setting stage to improve either precision or accuracy. The individual artefact can be used to understand that the process used to make the artefact has been enacted correctly.

8.3 Future Work

More work needs to be completed to establish control over the SLM process. This work can be underpinned by the adoption and deployment of the 12 bridge build layout approach. Each of the other three existing layers where this has been tested can be further developed for the role of process monitoring. The next step in this process would be to combine both measurement data with the in-process PLC log to build up a catalogue of information. This information could be used to identify when a build is carried out correctly or when a build has deviated from the normal, based on historic data (special cause variation). This information should be then cross referenced with InfiniAM Spectral so that a layer by layer assessment of the build can occur allowing engineers to assess individual parts in greater detail.

List of Appendices

The list of appendices below can be found on the accompanying CD.

Appendix 1: SLM calibration information

Appendix 2: Fully populated Ishikawa fishbone diagram showing all SLM variables discussed in thesis

Appendix 3: H-5800-1104-01 SS-316L-0410 material data sheet

Appendix 4: CMM MODUS program

Appendix 5: Measurement results for appraiser 2 and 3 for Section 4.5.1

Appendix 6: d_2 correction factor values Table 4A

Appendix 7: GR&R raw data and processing excel spreadsheet

Appendix 8: Renishaw heat treatment procedure for stainless steel

Appendix 9: Excel spread sheet showing accumulative matrices for post and off the plate measurements

Appendix 10: All sorted raw measurement data from CMM Plates 1-14

Appendix 11: Minitab processed data

The information is also available on request from Paul Prickett (Prickett@cardiff.ac.uk).

References

- 3D Systems, 2019. 3D Systems. Available at: <https://uk.3dsystems.com/on-demand-manufacturing/stereolithography-sla> [Accessed: 28 August 2019].
- 3DSIM, 2016. exaSIM. Available at: <http://3dsim.com/product/exasim/> [Accessed: 17 October 2016].
- Achamfuo-Yeboah, S.O., Light, R.A., and Sharples, S.D. 2015. Optical detection of ultrasound from optically rough surfaces using a custom CMOS sensor: *Journal of physics: Conference series* 581. doi: 10.1088/1742-6596/581/1/012009.
- Additiveworks, 2016. Simulation and process software for additive manufacturing. Available at: <https://additive.works/> [Accessed: 17 October 2016].
- Alimardani, M., Toyserkani, E., Huissoon, J.P., and Christ, P.P. 2009. On the delamination and crack formation in a thin wall fabricated using laser solid freeform fabrication process: An experimental–numerical investigation: *Optics and lasers in engineering* 47(11), pp. 1160–1168.
- Angelo, P.C. and Subramanian, R. 2008. *Powder metallurgy: Science, technology and applications*. 2nd ed. New Delhi: PHI Learning Private Limited.
- ASTM International 2013. F2792 - 12a. *Standard terminology for additive manufacturing technologies* (withdrawn). United States: ASTM International.
- Autodesk, 2016. NetFabb. Available at: <https://www.netfabb.com/> [Accessed: 17 October 2016].
- Banga, S.J. and Fox, G.D. 2013. *Bonett' s method*. Available at: https://support.minitab.com/en-us/minitab/18/Bonetts_Method_Two_Variiances.pdf. [Accessed: 21 October 2017].
- Barbato, G., Vicario, G., Levi, R. 2010. *Measurement system analysis*. In: *Statistical practice in business and industry*. 4th ed. Chichester, UK: John Wiley & Sons, Ltd.
- Barneveld van, J. and Jansson, T. 2017. *Additive manufacturing: A layered revolution*. <http://www.technopolis-group.com/wp-content/uploads/2018/08/wpfomeef18002.pdf>. [Accessed: 21 October 2017].

- Van Belle, L., Boyer, J., and Vansteenkiste, G. 2013. Investigation of residual stresses induced during the selective laser melting process: *Key engineering materials* 554–557, pp. 1828–1834. doi: 10.4028/www.scientific.net/KEM.554-557.1828
- Benda, J.A. 1994. *Temperature-controlled selective laser sintering: Proceedings of the solid freeform fabrication symposium*. pp. 277–284. East Hartford: United Technology Research Centre.
- Boillot, J.P., Cielo, P., Begin, C., Michel, C., Lessard, M. et al. 1985. Adaptive welding by fibre optic thermographic sensing: An analysis of thermal and instrumental considerations: *Welding Journal* 64, pp. 209–217.
- Bollig, A., Man, S., Beck, R., and Kaierle, S. 2005. Use of optical technologies to control the laser beam welding process: *Automotion technology*, pp. 513–521.
- Borland, D., Taylor, R., and Taylor, M. 2007. Rainbow colour map (still) considered harmful: *IEEE Visualization* (April), pp. 14–17.
- Botsch, M., Kobbelt, L., Pauly, M. et al. 2010. *Polygon mesh processing*. Boca Raton: Taylor & Francis Group.
- British Standards Institution. 1989. BS 7172:1989 *Guide to assessment of position, size and departure from nominal form of geometric features*. London: BSI.
- British Standards Institution. 2013. BS ISO/ASTM 52921:2013 *Standard terminology for additive manufacturing - Coordinate systems and test methodologies*. London: BSI.
- British Standards Institution. 2014a. BS ISO 10791-7:2014 *Test conditions for machining centres Part 7: Accuracy of finished test pieces*. London: BSI.
- British Standards Institution. 2014b. BS ISO 17296-3:2014 *General principles Part 3: Main characteristics and corresponding test methods*. London: BSI.
- British Standards Institution. 2014c. BS ISO 17296-4:2014 *Additive manufacturing - General principles Part 4: Overview of data processing*. London: BSI.
- British Standards Institution. 2015a. BS ISO/ASTM 52900:2015 *Additive manufacturing - General principles - Terminology*. London: BSI.
- British Standards Institution. 2015b. BS ISO 17296-2:2015 *Additive manufacturing - General principles Part 2: Overview of process categories and feedstock*. London: BSI.

British Standards Institution. 2015c. Draft BS ISO 20195 *Standard practice - Guide for design for additive manufacturing*. London: BSI.

British Standards Institution. 2017. BS EN ISO/ASTM 52915:2017 *Specification for additive manufacturing file format (AMF) Version 1.2*. London: BSI.

British Standards Institution. 2018. BS ISO/ASTM 52910:2018 *Additive manufacturing - design - requirements, guidelines and recommendations*. London: BSI.

Brückner, F., Lepski, D., and Beyer, E. 2007. Modelling the influence of process parameters and additional heat sources on residual stresses in laser cladding: *Journal of thermal spray technology* 16(3), pp. 355–373. doi: 10.1007/s11666-007-9026-7

Calignano, F., Lorusso, M., Pakkanen, J., Trevisan, F., Ambrosio, E. P. et al. 2017. Investigation of accuracy and dimensional limits of part produced in aluminium alloy by selective laser melting: *International journal of advanced manufacturing technology* 88(1–4), pp. 451–458. doi: 10.1007/s00170-016-8788-9.

Campbell, I., Diegel, O., Kowen, J., and Wohlers, T. 2018. *Wohlers report 2018: 3D printing and additive manufacturing state of the industry: Annual worldwide report*. Fort Collins. Available at: <https://wohlersassociates.com/2018report.htm>. [Accessed: 26 September 2019]

Carter, L.N., Martin, C., Withers, P. J., Attallah, M. M. 2014. The influence of the laser scan strategy on grain structure and cracking behaviour in SLM powder-bed fabricated nickel superalloy: *Journal of alloys and compounds* 615, pp. 338–347. doi: 10.1016/j.jallcom.2014.06.172.

Castillo, L. 2005. *Study about the rapid manufacturing of complex parts of stainless steel and titanium*. Amsterdam, TNO. Available at: http://www.lasercusing.nl/files/bestanden/binding_mechanisms_SLM_SLS.pdf.

[Accessed: 26 September 2019]

Chajda, J., Grzelka, M., Gapinski, B., Pawłowski, M. Szelewski, M. et al. 2008. *Coordinate measurement of complicated parameters like roundness, cylindricity, gear teeth or free-form surface: 8th International Conference in Advanced Manufacturing Operations*, pp. 225–231.

Consortium for advanced manufacturing - International 2004. *Dimensional measuring interface standard*, p. 682. Available at: http://linuxdaq-labs.com/demo/dmis/DMIS_5.0.pdf [Accessed: 26 September 2019]

- Cooke, A.L. and Soons, J.A. 2010. *Variability in the geometric accuracy of additively manufactured test parts. The 21st annual solid freeform fabrication symposium: An additive manufacturing conference*. August 9-11, 2010 Gaithersburg, NIST.
- Craeghs, T. Clijsters, S., Yasa, E., Bechmann, F., Berumen, S. et al. 2011. Determination of geometrical factors in layerwise laser melting using optical process monitoring: *Optics and Lasers in Engineering* 49(12), pp. 1440–1446. doi: 10.1016/j.optlaseng.2011.06.016
- Dinwiddie, R.B., Dehoff, R. R., Lloyd, P. D., Lowe, L. E., Ulrich, J. B. 2013. Thermographic in-situ process monitoring of the electron-beam melting technology used in additive manufacturing: *Thermosense: Thermal infrared applications XXXV* 8705, p. 87050K. doi: 10.1117/12.2018412.
- Easton, V.J. and McColl's, J.H. 1997. *Confidence intervals*. Available at: <http://www.stat.yale.edu/Courses/1997-98/101/confint.htm> [Accessed: 26 September 2019]
- Eriksson, I. Powell, J., Kaplan, A. F.H. 2010. Signal overlap in the monitoring of laser welding: *Measurement science and technology* 21(10). doi: 10.1088/0957-0233/21/10/105705.
- Flack, D. 2001. *Good practice guide No.41 CMM Measurement Strategies*. Teddington, NPL. Available at: <https://www.npl.co.uk/resources/gpgs> [Accessed: 26 September 2019]
- Gardan, J. 2016. Additive manufacturing technologies: State of the art and trends: *International journal of production research*. 7543, pp. 149–168. doi: 10.1201/9781315119106
- Geonx and LPT, 2016. Geonx. Available at: <http://www.geonx.com/> [Accessed: 17 October 2016].
- Gibson, I., Rosen, D., Stucker, B. 2015. *Additive manufacturing technologies: 3D printing, rapid prototyping, and direct digital manufacturing*. 2nd ed. New York: Springer.
- Hague, R., Reeves, P., and Jones, S. 2016. Mapping UK research and innovation in additive manufacturing. Available at: <http://www.imeche.org/news/news-article/innovation-additive-manufacturing>. [Accessed: 26 September 2019]

Hammett, P.C., Guzman, L. G., Frescoln, K. D., Ellison, S. J. et al. 2005. *Changing automotive body measurement system paradigms with 3D non-contact measurement systems: SAE 2005 world congress & exhibition*. SAE international. February 2016. Available at: <https://www.sae.org/content/2005-01-0585/>. [Accessed: 26 September 2019]

Han, Q. 2017. *Selective laser melting of an advanced Al-Al₂O₃ nanocomposite*. PhD Thesis. Cardiff University.

Hirsch, M., Patel, R., Li, W., Guan, G., Leach, R. K. et al. 2017. Assessing the capability of in-situ non-destructive analysis during layer based additive manufacture: *Additive Manufacturing* 13, pp. 135–142. doi: 10.1016/j.addma.2016.10.004

Hitzler, L., Hirsch, J., Merkel, M., Hall, W., and Öchsner, A. 2017. Position dependent surface quality in selective laser melting. *Materialwissenschaft und werkstofftechnik* 48(5), pp. 327–334. doi: 10.1002/mawe.201600742

Hocken, R.J. and Pereira, P.H. 2011. *Coordinate measuring machines and systems*. 2nd ed. Boca Raton: CRC press. Available at: <https://www.crcpress.com/Coordinate-Measuring-Machines-and-Systems/Hocken-Pereira/p/book/9781138076891>.

[Accessed: 26 September 2019]

Huang, Y., Leu, M. C., Mazumder, J., Donmez, A. 2015. Additive manufacturing: Current state, future potential, gaps and needs, and recommendations: *Journal of Manufacturing Science and Engineering* 137(1), p. 014001. doi. 10.1115/1.4028725

International Organization for Standardization 2011a. ISO-TR12888:2011 *Selected illustrations of gauge repeatability and reproducibility studies*. Geneva: ISO.

International Organization for Standardization 2011b. Standards catalogue ISO/TC 261 *Additive manufacturing*. Geneva: ISO.

International Organization for Standardization 2016. Business Plan ISO/TC 261 *Additive manufacturing*. Geneva: ISO.

International Organization for Standardization 2017. ISO 1101:2017 Geometric Product Specifications (GPS) – Geometrical Tolerancing - Tolerances of Form, Orientation, Location and Run-out. Geneva. Switzerland.

International Organization for Standardization 1989. ISO 2768-2:1989 General Tolerances – Part 2: Geometrical Tolerances for Features Without Individual Tolerance Indications. Geneva. Switzerland.

International Organization for Standardization. 2018. ISO/ASTM 52902 (2018) Additive Manufacturing – Test artefacts – Standard guideline for geometric capability assessment of additive manufacturing systems. Geneva. Switzerland.

Jing, L., Connor, M., Billy, W. 2016. *The current landscape for additive manufacturing research: A review to map the UK's research activities in AM internationally and nationally*. Available at: <https://spiral.imperial.ac.uk/handle/10044/1/39726>. [Accessed: 26 September 2019]

Kniepkamp, M., Fischer, J., Abele, E. 2016. *Dimensional accuracy of small parts manufactured by micro selective laser melting: Proceedings of the 26th Annual International Solid Freeform Fabrication* August 10 - 12 2015, pp. 1530–1537.

Koester, L. Taheri, H., Bond, L. J., Barnard, D., Gray, J. 2016. *Additive manufacturing metrology: State of the art and needs assessment: AIP conference proceedings*, p. 130001. Available at: <http://aip.scitation.org/doi/abs/10.1063/1.4940604>. [Accessed: 17 July 2017 2019]

Köhler, H., Jayaraman, V., Brosch, D., Hutter, F. X., Seefeld, T. 2013. A novel thermal sensor applied for laser materials processing: *Physics Procedia* 41, pp. 502–508. doi: 10.1016/j.phpro.2013.03.107

Kranz, J., Herzog, D., Emmelmann, C. 2015. Design guidelines for laser additive manufacturing of lightweight structures in TiAl6V4: *Journal of laser applications* 27(S1), p. S14001. doi: 10.2351/1.4885235

Krauss, H., Zeugner, T., Zaeh, M.F. 2014. *Layerwise monitoring of the selective laser melting process by thermography: 8th International Conference on Photonic Technologies* 56, pp. 64–71. 2014.

Kreyszig, E., Kreyszig, H., Norminton, E.J. 1979. *Advanced engineering mathematics*. 10th ed. USA:John Wiley & Sons, Inc.

Kruth, J.-P., Vandenbroucke, B., Van Vaerenbergh, J., Naert, I. 2007. Rapid manufacturing of dental prostheses by means of selective laser sintering / melting: *Journal of dental technology* (2), pp. 24–32.

Kruth, J., Vandenbroucke, B., Van Vaerenbergh, J., Mercelis, P. 2005. *Benchmarking of different SLS/SLM processes as rapid manufacturing techniques: International conference polymers & moulds innovations*. Gent. 2005.

Kruth, J., Deckers, J., Yasa, E., Wauthle, R. 2012. Assessing and comparing influencing factors of residual stresses in selective laser melting using a novel analysis method: *Journal of engineering manufacture*. 226(6), pp. 980–991. doi: 10.1177/0954405412437085.

Leach, R.K., Bourell, D., Carmignato, S., Donmez, A., Senin, N. et al. 2019a. *Geometrical metrology for metal additive manufacturing: CIRP Annals - Manufacturing technology*. May 2019. doi: 10.1016/j.cirp.2019.05.004

Leach, R.K., Bourell, D., Carmignato, S., Donmez, A., Senin, N. et al. 2019b. Geometrical metrology for metal additive manufacturing: *CIRP Annals* 68(2), pp. 677–700. Available at: <https://doi.org/10.1016/j.cirp.2019.05.004>. [Accessed: 26 September 2019]

Low, S.C. and Ake, B.E. 2004. *Thermocouple control system for selective laser sintering part bed temperature control* US6822194B2 [Patent].

Mani, M., Lane, B., Donmez, A., Feng, S., Moylan, S., et al. 2015. *Measurement science needs for real-time control of additive manufacturing powder bed fusion processes*. Gaithersburg, MD: Taylor & Francis. Available at: <https://www.tandfonline.com/doi/full/10.1080/00207543.2016.1223378>. [Accessed: 28 August 2016]

Manvatkar, V., De, A., DebRoy, T. 2015. Spatial variation of melt pool geometry, peak temperature and solidification parameters during laser assisted additive manufacturing process: *Materials science and technology* 31(8), pp. 924–930. doi: 10.1179/1743284714Y.0000000701

Materialise, 2017. Materialise. Available at: <http://www.materialise.com>. [Accessed: 26 September 2017]

Minitab, 2015. One-Way ANOVA. Available at: https://support.minitab.com/en-us/minitab/18/Assistant_One_Way_ANOVA.pdf. [Accessed: 27 June 2017]

Moylan, S., De, A., DebRoy, T. 2013. *Lessons learned in establishing the NIST metal additive manufacturing laboratory*. Available at: <https://nvlpubs.nist.gov/nistpubs/TechnicalNotes/NIST.TN.1801.pdf>. [Accessed: 18 June 2016]

Moylan, S., Slotwinski, J., Cooke, A., Jurrens, K., and Donmez, A. 2014. An additive manufacturing test artefact: *Journal of research of the national institute of standards and technology* 119, p. 429. Available at:

<http://nvlpubs.nist.gov/nistpubs/jres/119/jres.119.017.pdf>. [Accessed: 26 September 2019]

Mumtaz, K.A. and Hopkinson, N. 2010. Selective laser melting of thin wall parts using pulse shaping: *Journal of materials processing technology* 210(2), pp. 279–287. doi: 10.1016/j.jmatprotec.2009.09.011

O'Regan, P., Prickett, P., Setchi, R., Hankins, G., Jones, N. 2016. *Metal based additive layer manufacturing: Variations, correlations and process control: Procedia computer science* 96, pp. 216–224. doi: 10.1016/j.procs.2016.08.134

O'Regan, P., Prickett, P., Setchi, R., Hankins, G., Jones, N. 2018. *Selective laser melting: the use of metrology to assure process integrity: ASPE and euspen summer topical meeting: advancing precision in additive manufacturing*. July 2018. pp. 143–149.

Peels, J. 2019. *Design guidelines for direct metal laser sintering, selective laser melting, laser powder bed fusion*. Available at: <https://3dprint.com/237866/design-guidelines-for-direct-metal-laser-sintering-selective-laser-melting-laser-powder-bed-fusion/> [Accessed: 26 September 2019]

Rebaioli, L. and Fassi, I. 2017. A review on benchmark artefacts for evaluating the geometrical performance of additive manufacturing processes: *International Journal of Advanced Manufacturing Technology* 93(5–8), pp. 2571–2598. doi: 10.1007/s00170-017-0570-0.

Renishaw Plc 2011. *Survival of the fittest - the process control imperative*. Available at: <https://resources.renishaw.com/en/details/white-paper-survival-of-the-fittest-the-process-control-imperative--35900> [Accessed: 26 September 2019]

Renishaw Plc 2015. *QuantAM build preparation software*. Available at: <https://www.renishaw.com/en/quantam-build-preparation-software--35455> [Accessed: 18 April 2019].

Renishaw Plc, 2016. *Ballbar testing in tandem with circle, diamond, square machining tests*. Available at: [http://resources.renishaw.com/details/White+paper%3A+Ballbar+testing+with+circle.+diamond.+square+machining+tests\(216293\)\(78857\)](http://resources.renishaw.com/details/White+paper%3A+Ballbar+testing+with+circle.+diamond.+square+machining+tests(216293)(78857)). [Accessed: 5 September 2016].

Renishaw Plc, 2017. *InfiniAM Central*. Available at: <https://www.renishaw.com/en/infiniam-central--39816> [Accessed: 5 September 2019].

Renishaw Plc, 2018. *Design for metal AM - a beginner's guide*. Available at: <http://www.renishaw.com/en/design-for-metal-am-a-beginners-guide--42652> [Accessed: 3 April 2019].

Renishaw Plc, 2018. *InfiniAM Spectral – Energy input and melt pool emissions monitoring for AM systems*. Available at: <http://resources.renishaw.com/en/details/data-sheet-renam-500q--99032> [Accessed: 1 September 2017].

Rivas Santos, V.M., Maskery, I., Sims-waterhouse, D., Thompson, A., Leach, R. et al. 2018. *Benchmarking of an additive manufacturing process: Proceedings - 2018 ASPE and euspen summer topical meeting: Advancing precision in additive manufacturing.*, pp. 138–142.

Roberts, I.A. 2012. *Investigation of residual stresses in laser melting of metal powders in additive layer*. PhD Thesis. University of Wolverhampton.

Rogowitz, B.E., Treinish, L. A., Bryson, S. 1996. How not to lie with visualization: *Computers in physics* 10(3), p. 268. doi: 10.1063/1.4822401

Ryan, M.J. and Eyers, D.R. 2016. *Sustainable design and manufacturing 2016: Smart innovation, systems and technologies*. UK:Springer

Sainte-Catherine, C., Jeandin, M., Kechemair, D., Ricaud, J.-P., and Sabatie, L. 1991. Study of dynamic absorptivity at 10.6 μm (co2) and 1.06 μm (nd-yag) wavelengths as a function of temperature: *Journal de Physique IV Colloque*, pp. 151-157. doi: 10.1051/jp4:199174

Savio, E., De Chiffre, L., Schmitt, R. 2007. Metrology of freeform shaped parts. *CIRP Annals* 56(2), pp. 810–835. doi: 10.1016/j.cirp.2007.10.008

Schild, L., Kraemer, A., Reiling, D., Wu, H., Lanza, G. 2018. *Influence of surface roughness on measurement uncertainty in computed tomography: 8th Conference on industrial computed tomography*, Wels, Austria (iCT 2018). pp. 3–10.

Schoeters, S. de Fromanoir, C., Boeckmans, B., Witvrouw, A., Dewulf, W. et al. 2018. *Geometrical design and assessment of an industrially relevant benchmark part for*

selective laser melting. In: *ASPE and euspem summer topical meeting: Advancing precision in additive manufacturing*. Raleigh, pp. 150–155.

Shishkovsky, I. V., Morozov, Y. G., Kuznetsov, M. V., Parkin, I. P. 2008. Surface laser sintering of exothermic powder compositions: A thermal and SEM/EDX study: *Journal of thermal analysis and calorimetry* 91(2), pp. 427–436. doi: 10.1007/s10973-007-8353-8.

Simufact, 2016. Simulation of manufacturing processes. Available at: <http://www.simufact.com/additive-manufacturing.html> [Accessed: 17 October 2016].

Sindhumol, M.R. Srinivasan, M.R., Gallo, M. 2016. Robust control charts based on modified trimmed standard deviation and Gini's mean difference: *Journal of applied quantitative Methods*, p. 18.

Smith, P. and Maier, J. 2017. *Additive manufacturing UK national strategy 2018 - 25*. Available at: <https://am-uk.org/project/additive-manufacturing-uk-national-strategy-2018-25/> [Accessed: 18 April 2019]

Spears, T.G. and Gold, S.A. 2016. In-process sensing in selective laser melting (SLM) additive manufacturing: *Integrating materials and manufacturing innovation* 5(1), p. 2. doi: 10.1186/s40192-016-0045-4

Strano, G., Hao, L., Everson, R. M., Evans, K. E. 2013. Surface roughness analysis, modelling and prediction in selective laser melting: *Journal of materials processing technology* 213(4), pp. 589–597. doi: 10.1016/j.jmatprotec.2012.11.011

Tapia, G. and Elwany, A. 2014. A review on process monitoring and control in metal-based additive manufacturing: *Journal of manufacturing science and engineering* 136(6), p. 060801-01-060801-10. doi: 10.1115/1.4028540

Taylor, C. 2004. Direct laser sintering of stainless steel: Thermal experiments and numerical modelling. PhD Thesis, University of York.

Teeter, M.G., Childs, T. 2015. Metrology test object for dimensional verification in additive manufacturing of metals for biomedical applications. Proceedings of the institution of mechanical engineers, Part H: *Journal of Engineering in Medicine* 229(1), pp. 20–27. doi: 10.1177/0954411914565222.

Thomas, D. 2009. *The development of design rules for selective laser melting*. PhD Thesis. University of Wales Institute, Cardiff.

- Tobergte, D.R. and Curtis, S. 2015. *Elevated region area measurement for quantitative analysis of laser beam melting process stability: Solid freeform fabrication symposium* 53(9), pp. 1689–1699. doi: 10.1017/CBO9781107415324.004.
- Todorov, E., Spencer, R., Gleeson, S., Jamshidinia, M., Ewi, S.M.K. 2014. America makes: national additive manufacturing innovation institute (NAMII) Project 1: Non-destructive evaluation (NDE) of complex metallic additive manufactured (AM) structures. Available at: <http://www.dtic.mil>. [Accessed: 18 April 2019]
- Toguem, S.-C.T., Rupal, B.S., Mehdi-Souzani, C., Qureshi, A.J., Anwer, N. 2018. *A review of AM artifact design methods: Proceedings - 2018 ASPE and euspen summer topical meeting: Advancing precision in additive manufacturing*. Raleigh, pp. 132–137.
- Triantaphyllou, A., Giusca, C. L., Macaulay, G. D., Roerig, F., Hoebel, M. et al. 2015. Surface texture measurement for additive manufacturing: *Surface Topography: Metrology and Properties* 3(2). doi: 10.1088/2051-672X/3/2/024002.
- UK Additive Manufacturing Steering Group 2016. *Additive manufacturing UK - Strategy positioning paper MTC*. Available at: <https://am-uk.org/project/strategy-positioning-paper-mtc/strategypositioningpapermtc/> [Accessed: 26 September 2019]
- Vallejo, D.D. 2014. *Spectroscopic investigations of plasma emission induced during laser material processing*. Germany: epubli GmbH.
- Vandenbroucke, B. and Kruth, J.-P. 2007. Selective laser melting of biocompatible metals for rapid manufacturing of medical parts: *Rapid Prototyping Journal* 13(4), pp. 196–203. doi: 10.1108/13552540710776142.
- Vasinonta, A., Beuth, J. L., Griffith, M. 2007. Process maps for predicting residual stress and melt pool size in the laser-based fabrication of thin-walled structures: *Journal of manufacturing science and engineering* 129(1), p. 101. doi: 10.1115/1.2335852.
- Vrancken, B. 2016. Study of residual stresses in selective laser melting. PhD Thesis. Ku Leuven.
- Wheeler, D. 2006. *An honest gauge R&R study: ASQ/ASA Fall technical conference*. Available at: <https://www.spcpress.com/pdf/DJW189.pdf> [Accessed: 26 September 2019]

Wohlers, T. and Gornet, T. 2014. *History of additive manufacturing 2014: Wohlers report 2014 - 3D printing and additive manufacturing state of the industry*, pp. 1–34. doi: 10.1017/CBO9781107415324.004.

Wu, A.S., Brown, D. W., Kumar, M., Gallegos, G. F., King, W. E. 2014. An experimental investigation into additive manufacturing-induced residual stresses in 316L stainless steel: *Metallurgical and materials transactions A* 45(13), pp. 6260–6270. doi: 10.1007/s11661-014-2549-x

Yadroitsev, I., Krakhmalev, P., Yadroitsava, I. 2014. Selective laser melting of Ti6Al4V alloy for biomedical applications: Temperature monitoring and microstructural evolution: *Journal of Alloys and Compounds* 583, pp. 404–409. doi: 10.1016/j.jallcom.2013.08.183

Yasa, E., Demir, F., Akbulut, G., Pilatin, S. 2014. *Benchmarking of different powder bed metal fusion processes for machine selection in additive manufacturing: Solid free form fabrication*. pp. 390–403.

Ye, D., Hong, G. S., Zhang, Y., Zhu, K., Fuh, J.Y.H. 2018. Defect detection in selective laser melting technology by acoustic signals with deep belief networks: *International journal of advanced manufacturing technology* 96(5–8), pp. 2791–2801. doi: 10.1007/s00170-018-1728-0.

Zaeh, M.F. and Branner, G. 2010. Investigations on residual stresses and deformations in selective laser melting: *Production engineering* 4(1), pp. 35–45. doi: 10.1007/s11740-009-0192-y

Zeng, K., Pal, D., Stucker, B.E. 2012. *A review of thermal analysis methods in laser sintering and selective laser melting: Proceedings of the solid freeform fabrication symposium*. pp. 796–814. Available at: <http://sffsymposium.engr.utexas.edu/Manuscripts/2012/2012-60-Zeng.pdf>

[Accessed: 26 September 2019]